

(A) REGION NUMBER (THRU)
 2 3
 (PAGES) (CODE)
 (NASA CR OR TMX OR AD NUMBER) (CATEGORY)

04682-1-T

THE UNIVERSITY OF MICHIGAN

COLLEGE OF ENGINEERING DEPARTMENT OF METEOROLOGY AND OCEANOGRAPHY

Technical Report

A Study of the Influence of Carbon Dioxide on Infrared Radiative Transfer in the Stratosphere and Mesosphere

CHARLES YOUNG

E. S. Epstein
 Project Director

Under contract with:

National Science Foundation
 Grant No. G-19131
 Washington, D. C.

N66-83718

(ACCESSION NUMBER) (PAGES)
 201
 (NASA CR OR TMX OR AD NUMBER)

(THRU) (CODE) (CATEGORY)
 Young

Administered through:

March 1964

OFFICE OF RESEARCH ADMINISTRATION • ANN ARBOR

Sd 35076

T H E U N I V E R S I T Y O F M I C H I G A N

COLLEGE OF ENGINEERING

Department of Meteorology and Oceanography

Technical Report

A STUDY OF THE INFLUENCE OF CARBON DIOXIDE ON INFRARED RADIATIVE
TRANSFER IN THE STRATOSPHERE AND MESOSPHERE

Charles Young

E. S. Epstein
Project Director

ORA Project 04682

under contract with:

NATIONAL SCIENCE FOUNDATION
GRANT NO. G-19131
WASHINGTON, D.C.

administered through:

OFFICE OF RESEARCH ADMINISTRATION ANN ARBOR

March 1964

This report was also a dissertation submitted in partial fulfillment of the requirements for the degree of Doctor of Philosophy in The University of Michigan, 1964.

ACKNOWLEDGMENTS

The author wishes to thank all who assisted him during the progress of this study. The advice and guidance of Professor Edward S. Epstein, Chairman of the Doctoral Committee, is particularly appreciated. The author is also grateful to Professors E. Wendell Hewson, Leslie M. Jones, and Donald J. Portman for serving as members of the Committee and for their willingness to help.

The constant interest and encouragement of my colleagues, particularly Mr. Carlton L. Mateer, Department of Meteorology and Oceanography, and Mr. S. Roland Drayson, High Altitude Engineering Laboratory, Department of Aeronautical and Astronautical Engineering, are greatly appreciated.

The author is grateful for financial support received from the National Science Foundation under Grant No. G-19131 to the Department of Meteorology and Oceanography and from the National Aeronautical and Space Administration under Contract No. NASr-54(03) to the Department of Aeronautical and Astronautical Engineering, High Altitude Engineering Laboratory.

TABLE OF CONTENTS

	Page
LIST OF TABLES	v
LIST OF FIGURES	vii
LIST OF SYMBOLS	viii
ABSTRACT	x
1. INTRODUCTION	1
1.1 Aim of the Study	1
1.2 Importance of Infrared Radiative Transfer in the Stratosphere and Mesosphere	1
1.3 Approach to the Problem	3
2. REVIEW OF RESEARCH ON THE INFLUENCE OF CARBON DIOXIDE ON RADIATIVE TRANSFER IN THE STRATOSPHERE AND MESOSPHERE	5
2.1 Preliminary Remarks	5
2.2 Preview of Earlier Work	5
3. THE BASIC EQUATIONS AND PARAMETERS RELEVANT TO THE PROBLEM OF RADIATIVE TRANSFER IN THE STRATOSPHERE AND MESOSPHERE	9
3.1 The Basic Radiative Transfer Equations	9
3.2 Relaxation of the Carbon Dioxide Molecule	15
3.3 The Radiative Transfer Equation for a Vibrationally Relaxing Gas	21
3.4 The Evaluation of the Absorption Coefficient for Various Atmospheric Pressures	28
3.4.1 Preliminary Remarks	28
3.4.2 Absorption Associated with Collisional Broadening	30
3.4.3 Absorption Associated with Doppler Broadening	34
3.4.4 Absorption Associated with Natural Broadening	36
3.4.5 Comparison of Line Half-Widths	37
3.4.6 Absorption Taking into Account Collisional, Doppler and Natural Broadening	38
3.4.7 Practical Determination of the Absorption Coefficient for Various Atmospheric Pressures	41

TABLE OF CONTENTS (Concluded)

	Page
3.5 Models for Molecular Band Absorption	48
3.5.1 Preliminary Remarks	48
3.5.2 The Quasirandom Model	50
3.6 Approximations Used in Solving the Radiative Transfer Equation	56
3.6.1 The Curtis-Godson Approximation	56
3.6.2 Approximate Methods for Performing the Angular Integration in the Flux Equation	62
4. EVALUATION OF THE TRANSMISSIVITIES AND FLUXES IN THE STRATOSPHERE AND MESOSPHERE DUE TO CARBON DIOXIDE	66
4.1 Transmissivity Determination Using the Quasirandom Model	66
4.1.1 Transmissivity Determination and Comparison with Experimental Measurements	66
4.1.2 Test of Approximate Methods for Performing the Angular Integration in the Flux Equation	75
4.1.3 Test of Validity of Using the Lorentz Line Shape at Pressures Lower than 20 mb	78
4.2 Evaluation of the Source Function for Vibrationally Relaxing Carbon Dioxide	80
4.3 Flux Determination	91
4.4 Cooling Rate Calculations	94
4.5 Discussion of the Problem of Cooling Rate Determination	102
5. CONCLUSIONS	104
6. SUGGESTIONS FOR FURTHER RESEARCH	107
APPENDIX A. Physical Details of the Carbon Dioxide Molecule	109
APPENDIX B. Calculation of the Line Positions and Intensities for the Carbon Dioxide Bands in the 15-micron Region of the Spectrum	116
REFERENCES	171

LIST OF TABLES

Table	Page
I. Values of radiative lifetime θ for various bands.	17
II. Theoretical and experimental values for the vibrational relaxation of CO_2 and $\text{CO}_2\text{-N}_2$ mixture.	18
III. α_D in cm^{-1} for various temperatures and frequencies.	36
IV. Half-widths for collisional, Doppler and natural broadening.	37
V. Comparison of absorption coefficients evaluated using various formulae at pressures lower than 50 mb.	42
VI. Evaluation of absorption coefficient for various atmospheric pressures.	46
VII. Comparison between values of $\int A_\nu d\nu$ calculated using the quasi-random model and experimentally measured by Burch et al. (1962b).	72
VIII. Values of I^* obtained using various approximations for the angular integration.	77
IX. Comparison between I^* evaluated using the Lorentz line shape and the Lorentz broadened Doppler line shape (the mixed line shape) at pressures below 20 mb.	79
X. Comparison between \bar{J}/\bar{E} and $\theta/(\theta+\lambda)$ for the U. S. Standard Atmosphere (1962).	89
XI. ΔF and F computed at several representative levels (U. S. Standard Atmosphere (1962)) for a cooling rate of 1°K day^{-1} .	96
XII. Cooling rates up to 30 km for the U. S. Standard Atmosphere (1962) over the frequency ranges 507.5 to 857.5 cm^{-1} and 630 to 715 cm^{-1} .	97

LIST OF TABLES (Concluded)

Table	Page
XIII. Cooling rates above 80 km for U. S. Standard Atmosphere (1962).	100
XIV. Values for $F(J'')$.	118
XV. Vibrational quantum numbers, band centers, band intensities and I_R factors for 14 bands in the 15-micron region for a temperature of 300°K	121
XVI. Rotational line positions and intensities for the 14 bands in Table XV for six temperatures from 175 to 300°K.	123
XVII. Comparison between computed line positions and intensities and Madden's experimental values ($T = 300^\circ\text{K}$).	170

LIST OF FIGURES

Figure	Page
1. Illustrating some basic quantities occurring in radiative transfer.	10
2. Calculated and experimental transmissivities versus frequency for different pressures and optical masses.	69
3. $\int A_\nu d\nu$ vs. optical mass for pressures of 1 and 0.2 atm.	73
4. \bar{J}/\bar{E} vs. pressure.	87
5. Temperature profile for warm mesosphere case, from Stroud <u>et al.</u> (1960).	88
6. Upward and downward fluxes for U. S. Standard Atmosphere (1962).	95
7. Possible vibrations for the carbon dioxide molecule and changes in electric moment.	109

LIST OF SYMBOLS

A_ν	absorptivity
c_p	specific heat at constant pressure
$E(\nu, T)$	black-body specific intensity
F_+	upward directed flux
F_-	downward directed flux
F	net flux
$I(\nu, \tau, \mu)$	specific intensity
$J(\nu, \tau)$	source function
k_ν	absorption coefficient
p	pressure
S	band strength
S_j	line strength
T	temperature
u	optical mass
z	altitude
α_D	Doppler half-width
α_L	Lorentz half-width
α_N	natural half-width
$\gamma_\nu(t, \tau)$	transmissivity
ϵ_ν	emission coefficient
Θ	zenith angle, radiative lifetime

LIST OF SYMBOLS (Concluded)

λ vibrational relaxation time

μ cosine of zenith angle θ

ν frequency (in cm^{-1})

ρ density

τ optical thickness

ABSTRACT

The main object of the study is to calculate cooling rates in the stratosphere and mesosphere due to the carbon dioxide vibration-rotation bands in the 12- to 18-micron spectral region. Carbon dioxide dominates the infrared radiative transfer in this region. Accurate values for atmospheric cooling rates are essential if the dynamics of the stratosphere and mesosphere are to be investigated in any detail.

The first step in the investigation is the calculation of the positions and intensities of the rotational lines belonging to the 14 strongest carbon dioxide vibration-rotation bands in the 12- to 18-micron region. The rotational line intensities are evaluated for 6 temperatures in the range 175 to 300°K. The results of the calculation are included in the study. The basic radiative transfer equations relevant to the problem are considered in detail. The influence of vibrational relaxation of carbon dioxide on the transfer equations is discussed. It is shown that, at low pressures such as occur in the upper mesosphere, the source function is not given by the black body specific intensity. This means that local thermodynamic equilibrium breaks down in the upper mesosphere. An approximate method for calculating the source function for vibrationally relaxing carbon dioxide is presented. The source function is calculated for vibrational relaxation times of 10^{-5} and 10^{-6} sec (at 1 atm) using the U. S. Standard Atmosphere (1962) temperature profile. The calculated source functions show that vibrational relaxation of carbon dioxide must be considered in radiative transfer calculations starting between 60 and 75 km.

The radiative transfer equation is integrated to give the upward and downward directed fluxes at various atmospheric levels. The cooling rates are obtained directly from the fluxes. The use of the quasi-random spectral band model permits integration of the transfer equations with a minimum of effort. A model allows the calculation of an average transmissivity for a finite frequency interval. An accurate knowledge of the absorption coefficient and its variation with pressure is essential for accurate transmissivity calculations. A scheme is presented whereby the absorption coefficient can be evaluated for any pressure. The Lorentz formula for the absorption coefficient is shown to be a poor approximation in flux calculations at pressure below 20 mb. This demonstrates that Doppler broadening must be taken into account once the pressure decreases to 20 mb.

The atmosphere from the surface to 100 km is divided into 24 layers, and the transmissivities are calculated for each of the layers using the

pressures and temperatures given by the U. S. Standard Atmosphere (1962). The Curtis-Godsen approximation is used in the troposphere allowing the choice of a small number of thick layers. The fluxes and cooling rates are then calculated for each layer.

Cooling rates from 0.4 to 5°K day⁻¹ are calculated for levels up to 35 km. Above 35 km the calculations give unrealistically large values of tens of degrees per day for the cooling rates. If only the spectral region around the 15-micron fundamental band is considered the maximum cooling rate is reduced to 35°K day⁻¹ at 55 km. This is probably too large a value. A vibrational relaxation time of 10⁻⁵ sec (at 1 atm) leads to a cooling rate of 15°K day⁻¹ in the vicinity of the mesopause while 10⁻⁶ sec (at 1 atm) results in a value about three times as great.

An examination of the basic equations shows that extremely accurate flux values are required for the calculation of cooling rates above 30 km. A spectral band model is not accurate enough for cooling rate calculations. Direct integration over the spectral region of interest is necessary for accurate flux determination. Further progress in this field requires experimental determination of accurate values for the vibrational relaxation time of carbon dioxide-air mixtures so that accurate cooling rates in the upper mesosphere may be calculated.

1. INTRODUCTION

1.1 AIM OF THE STUDY

The study deals primarily with the influence of carbon dioxide on infrared radiative transfer in the stratosphere and mesosphere. A great number of the problems arising are common to the whole field of infrared radiative transfer and not restricted to the carbon dioxide problem. Consequently, most of the techniques discussed in the following sections would be applicable to the more general problem.

The main objective of this study is to examine the feasibility of accurately determining cooling rates in the stratosphere and mesosphere. Accurate knowledge of atmospheric cooling rates is necessary if dynamical investigations of the stratosphere and mesosphere are to be undertaken in any detail.

1.2 IMPORTANCE OF INFRARED RADIATIVE TRANSFER IN THE STRATOSPHERE AND MESOSPHERE

Infrared radiative transfer in the earth's atmosphere is associated with the three molecules, water vapor, carbon dioxide and ozone. In the troposphere water vapor is the more important of the three. Once the stratosphere is entered the importance of water vapor diminishes. Carbon dioxide and ozone then become the main infrared active gases. Ozone unfortunately has a variable concentration and a complicated band structure. Consequently the infrared transfer problem for ozone is

somewhat more involved than for carbon dioxide. Carbon dioxide, on the other hand, has a somewhat simpler band structure than ozone. It also has an almost constant concentration with height up to around 95 km where dissociation into carbon monoxide and atomic oxygen takes place. Ozone is very important in infrared radiative transfer in the stratosphere and lower mesosphere to about 60 km. Above that level carbon dioxide becomes the important infrared active gas. This section contains a brief discussion of the importance of infrared transfer in the meteorology of the stratosphere and particularly the mesosphere.

This study was initially prompted by the problem of explaining the warm winter polar mesosphere observed at Fort Churchill using rocket borne instruments (cf. Jones, et al. 1959, Stroud, et al. 1960). Kellogg (1961) and Young and Epstein (1962) discussed the hypothesis that subsidence of atomic oxygen rich air from higher levels, with chemical energy being released by the formation of molecular oxygen from atomic oxygen, would provide the necessary energy source. Recent observations (Nordberg and Smith, 1963) at Wallops Island during the winter indicate that mesospheric warmings are not confined to the polar regions but are evident at more southerly latitudes.

If subsidence of atomic oxygen rich air is the primary mechanism for mesospheric warmings then, as discussed by Young and Epstein (1962), a knowledge of mesospheric cooling rates is essential for any estimation of the subsidence rate.

The study of the more general problem of the atmospheric circula-

tion in the stratosphere and mesosphere demands an accurate knowledge of the sources and sinks of radiative energy. Murgatroyd and Singleton (1961), using results of Murgatroyd and Goody (1958) on the disposition of the sources and sinks of radiative energy, calculated meridional circulations in the stratosphere and mesosphere neglecting eddy effects. Newell (1963) using the Meteorological Rocket Network data computed the zonal available potential energy generation and compared it with the kinetic energy for the 25 to 60 km layer. He took into account radiative energy sources and sinks using the results of Murgatroyd and Goody (1948), and Murgatroyd and Singleton (1961).

It is evident that an accurate knowledge of the sources and sinks of radiative energy is very desirable if any dynamical investigations of the stratosphere and mesosphere are to be pursued. One of the most important aspects of this problem is to determine the infrared cooling rates for the stratosphere and mesosphere.

1.3 APPROACH TO THE PROBLEM.

The basic objective of this study is to examine the feasibility of obtaining mesospheric cooling rates with reasonable accuracy. Unfortunately a devious route must be travelled before cooling rates can be estimated. As is common in scientific research, the problem turned out to be more involved than originally envisaged. It is impossible to separate the problem of infrared radiative transfer in the mesosphere from that in the stratosphere and troposphere. Also, other aspects of

infrared radiative transfer must be considered such as, line profile variation with pressure, spectral models for infrared bands, and so on.

The attitude adopted in attacking this problem has been to examine critically and check, whenever possible, the various relations and approximations generally accepted in the literature.

Section 2 is a rather brief survey of previous work in the field while Section 3 derives and critically examines the basic equations and parameters relevant to the problem. Necessarily the literature dealing with the particular aspect being studied is surveyed. Thus Section 3 is partly devoted to adding some detail to Section 2. In Section 4 are presented the main findings based on the techniques developed in Section 3. Again some of the relevant literature must be examined, particularly with respect to comparison of the values calculated in this study for transmissivities, fluxes, etc. Sections 5 and 6 are devoted to the conclusions and suggestions for further research.

It was decided to include some of the material in the form of appendices. Appendix A is a brief description of the carbon dioxide molecule, giving details of such things as its behavior in the infrared, allowed transitions, etc. In Appendix B the methods used to calculate the line positions and intensities of the carbon dioxide bands in the 15-micron region are described. Also included is a table of the line positions and intensities for 2080 rotational lines.

2. REVIEW OF RESEARCH ON THE INFLUENCE OF CARBON DIOXIDE ON RADIATIVE TRANSFER IN THE STRATOSPHERE AND MESOSPHERE

2.1 PRELIMINARY REMARKS

The review presented in Section 2.2 of earlier research on radiative transfer due to carbon dioxide in the stratosphere and mesosphere is rather brief. There are two main reasons for this brevity. One is that little effort seems to have been exerted in this direction compared to other areas of meteorological interest. The other reason is that in Section 3 where the basic equations and parameters relevant to the problem are derived and critically examined, it is necessary to review the previous research dealing with the particular item under consideration. Thus in Section 2.2 only a generalized picture will be presented with most of the detail being added in Section 3.

2.2 REVIEW OF EARLIER WORK

The earliest work drawing attention to the importance of radiative transfer in the stratosphere appears to have been carried out by Gold (1909) and Humphreys (1909). It is interesting to note that even at this early date in stratospheric and mesospheric research a fair amount of information was available and some quite accurate conjectures were made. This is all the more surprising since Teisserenc de Bort's balloon soundings extending from 1899-1904 were just making their mark on meteorology. Both Gold and Humphreys pointed out that ozone was probably of importance

in infrared radiative transfer in the stratosphere. Gold considered carbon dioxide, water vapor and ozone in the stratosphere. He used the absorptivity measurements of Ångström in his calculations. The main assumption in his work was that the various absorbing gases acted as black bodies for emission. Humphreys, however, noted that this assumption might not be correct. Gold's main result was that the stratosphere does not absorb enough radiation to induce convection. Humphreys' paper is mostly a review and contains some suggestions for further research.

After these two papers little effort was devoted to the problem until 1937 when Godfrey and Price investigated infrared radiation effects in the atmosphere above 100 km. They considered ozone, water vapor and oxygen. Unfortunately they did not consider the breakdown of local thermodynamic equilibrium due to the relaxation of the ozone and water vapor molecules. The importance of this had been noted by Milne (1930), who worked out the radiative transfer equation for a two-state relaxing gas. The neglect of relaxation invalidates Godfrey and Price's results.

In the period from 1909 to 1937, while little effort was being devoted to infrared radiation in the stratosphere, considerable progress was being made in understanding the structure of molecular bands and measuring the absorptivities of the various molecular bands of atmospheric interest in the laboratory. The University of Michigan was one of the leaders in the field producing three classic pieces of research. Martin and Barker (1932) investigated the infrared spectrum of carbon

dioxide and Randall, et al. (1937) studied the absorption of water vapor. On the theoretical side Dennison (1931) published a very important paper discussing the infrared spectra of polyatomic molecules.

The next study of the stratosphere was by Gowan (1947a,b) who investigated the influence of ozone on the radiation processes in the stratosphere. During the late forties and early fifties it was realized that carbon dioxide was a very important constituent of the stratosphere and mesosphere, probably more important than ozone, with respect to infrared radiative transfer.

Plass (1956a,b) investigated the effects of the 9.6-micron ozone band and the 15-micron carbon dioxide band on atmospheric cooling rates, basing his calculations on laboratory transmissivity measurements. He showed that carbon dioxide was more important than ozone for radiative cooling of the stratosphere. The problem of extending infrared radiative transfer calculations to higher levels where relaxation must be considered was attacked by Curtis and Goody (1956). They investigated the importance of vibrational relaxation in the mesosphere and derived a radiative transfer equation for a vibrationally relaxing gas. This equation should be used above 65 km. They applied their technique to the 15-micron carbon dioxide band and derived the cooling rates in the mesosphere due to this gas.

Studies of the radiation budget of the stratosphere and mesosphere were published by Ohring (1958) and Murgatroyd and Goody (1958). Ohring

considered carbon dioxide, water vapor and ozone. He used Callendar's (1941) empirical formulae for the carbon dioxide transmissivities between 12 and 18 microns. Murgatroyd and Goody considered only ozone and carbon dioxide but extended their calculations to higher levels in the mesosphere using the technique developed by Curtis and Goody (1956) to take account of vibrational relaxation. They, like Plass, found the cooling rates due to carbon dioxide to be greater than those due to ozone.

The next major contribution was by Hitschfeld and Houghton (1961) who looked at radiative transfer in the lower stratosphere due to the 9.6-micron ozone band. They determined the fluxes and hence the cooling rates by evaluating them for narrow regions of the spectrum and then combining these results to give estimates for the whole band. They did not use a spectral model but integrated directly over the narrow intervals to obtain the fluxes. Their results for the cooling rates due to ozone were about twice those of Plass (1956a,b) which makes the cooling rates due to ozone in the vicinity of 45 km close to those due to carbon dioxide. However, at higher and lower levels carbon dioxide is still the more important gas for infrared radiative transfer.

3. THE BASIC EQUATIONS AND PARAMETERS RELEVANT TO THE PROBLEM OF RADIATIVE TRANSFER IN THE STRATOSPHERE AND MESOSPHERE

3.1 THE BASIC RADIATIVE TRANSFER EQUATIONS

The basic equation appropriate to the transfer of radiation through a plane parallel atmosphere may be written

$$\mu \frac{dI(\nu, \tau, \mu)}{d\tau} = I(\nu, \tau, \mu) - J(\nu, \tau) \quad (3.1.1)$$

$I(\nu, \tau, \mu)$ the specific intensity

$J(\nu, \tau) = \epsilon_\nu / k_\nu$, the source function

ϵ_ν the emission coefficient

k_ν the absorption coefficient

$\mu = \cos \theta$

θ the angle which $I(\nu, \tau, \mu)$ makes with \vec{n}

\vec{n} the outward drawn normal to the plane parallel atmosphere

τ the optical thickness defined by $d\tau = -\rho k_\nu dz$

ρ the density of the gas (molecules per unit volume)

z the height measured from the earth's surface

Figure 1 illustrates the relation between some of the quantities defined above.

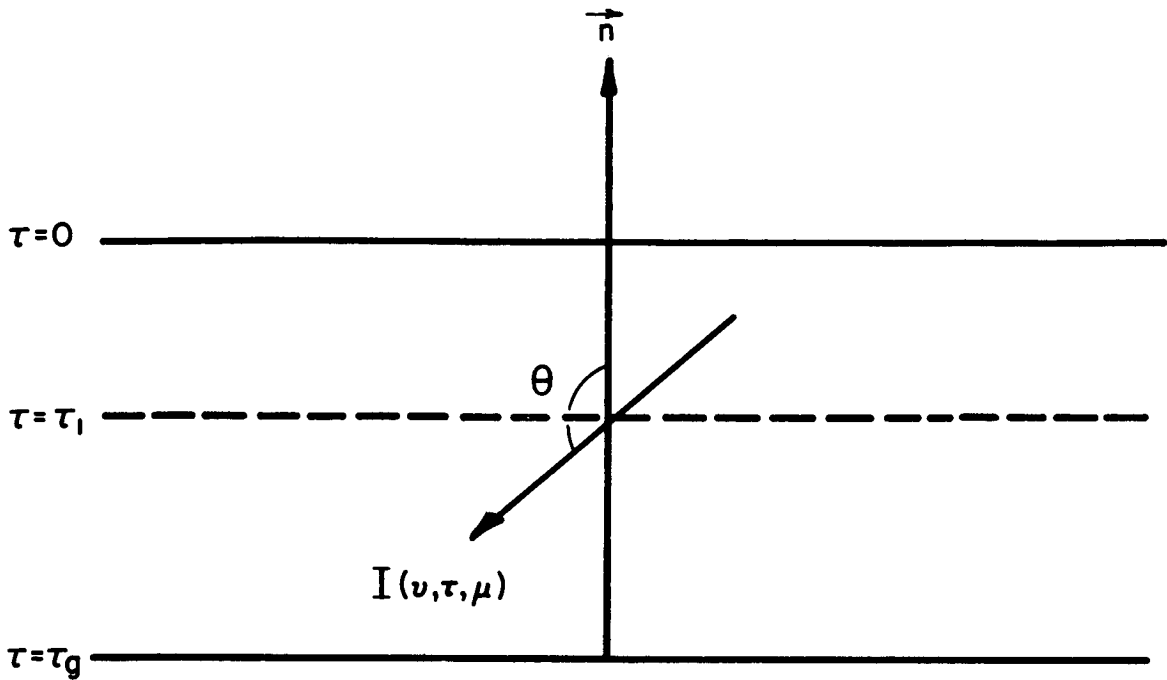


Fig. 1. Illustrating some basic quantities occurring in radiative transfer

It should be noted by definition that $\tau = 0$ at the top of the atmosphere and increases downwards reaching a maximum τ_g at the earth's surface.

For convenience angles are measured from \vec{n} , hence $+\mu$ means that a beam makes an acute angle with \vec{n} , and $-\mu$ that it makes an acute angle with $-\vec{n}$. Then $I(\nu, \tau, +\mu)$ denotes an outward directed beam and $I(\nu, \tau, -\mu)$ denotes an inward directed beam. In the above discussion it has been assumed that the specific intensity does not depend on the azimuthal angle ϕ .

It is easy to write a formal solution for Eq. (3.1.1) (Cf., Chandrasekhar 1960, Sobolev 1963),

$$I(\nu, \tau, +\mu) = I(\nu, \tau_g, +\mu)e^{-(\tau_g - \tau)/\mu} + \int_{\tau}^{\tau_g} J(\nu, t)e^{-(t - \tau)/\mu} \frac{dt}{\mu} \quad (3.1.2a)$$

$$I(\nu, \tau, -\mu) = I(\nu, 0, -\mu)e^{-\tau/\mu} + \int_0^\tau J(\nu, t)e^{-(\tau-t)/\mu} \frac{dt}{\mu} \quad (3.1.2b)$$

where $I(\nu, 0, -\mu)$ is the incident specific intensity at the top of the atmosphere $\tau = 0$ and $I(\nu, \tau_g, +\mu)$ is the specific intensity directed upwards at the base of the atmosphere where $\tau = \tau_g$. To obtain the upward and downward fluxes $F_+(\tau)$ and $F_-(\tau)$ respectively, Eqs. (3.1.2a) and (3.1.2b) must be integrated with respect to frequency and angle, viz.,

$$F_+(\tau) = \int_0^{2\pi} \int_0^{+1} \int_\nu I(\nu, \tau, +\mu) \mu \, d\nu \, d\mu \, d\phi \quad (3.1.3a)$$

$$F_-(\tau) = \int_0^{2\pi} \int_0^{+1} \int_\nu I(\nu, \tau, -\mu) \mu \, d\nu \, d\mu \, d\phi \quad (3.1.3b)$$

or,

$$F_+(\tau) = 2\pi \int_0^{+1} \int_\nu I(\nu, \tau, +\mu) \mu \, d\nu \, d\mu \quad (3.1.4a)$$

$$F_-(\tau) = 2\pi \int_0^{+1} \int_\nu I(\nu, \tau, -\mu) \mu \, d\nu \, d\mu \quad (3.1.4b)$$

The net flux at a level τ is thus given by

$$F(\tau) = F_+(\tau) + F_-(\tau)$$

The heating rate dT/dt , due to radiative transfer at the same level z ,

is then expressed by the flux divergence,

$$\frac{dT}{dt} = \frac{1}{c_p \rho} \frac{dF(\tau)}{dz} \quad (3.1.5)$$

where ρ and c_p are the density and specific heat at constant pressure of the air at height z .

Equations (3.1.2a) and (3.1.2b) are sometimes expressed in a different form. It is sometimes convenient to define a transmissivity $\gamma_v(t, \tau)$ by

$$\begin{aligned} \gamma_v(t, \tau) &= e^{-(t-\tau)/\mu} \\ &= \exp \left[-\frac{1}{\mu} \int_{z_t}^{z_\tau} N k_v dz \right] \end{aligned} \quad (3.1.6)$$

Thus (3.1.2a) and (3.1.2b) become

$$I(v, \tau, +\mu) = I(v, \tau_g, +\mu) \gamma_v(\tau_g, \tau) - \int_{\tau}^{\tau_g} J(v, t) \frac{\partial \gamma_v(t, \tau)}{\partial t} dt \quad (3.1.7a)$$

$$I(v, \tau, -\mu) = I(v, 0, -\mu) \gamma_v(\tau, 0) - \int_0^{\tau} J(v, t) \frac{\partial \gamma_v(\tau, t)}{\partial t} dt \quad (3.1.7b)$$

If local thermodynamic equilibrium prevails, then Kirchhoff's law is applicable, i.e.,

$$\epsilon_v/k_v = E(v, T) \quad (3.1.8)$$

where $E(\nu, T)$ is the blackbody specific intensity given by

$$E(\nu, T) = 2 hc^2 \nu^3 [\exp(h c \nu / kT) - 1]^{-1} \quad (3.1.9)$$

where h is Planck's constant, k Boltzmann's constant, c the velocity of light, T the temperature, and ν the wave-number (in cm^{-1}). Thus in the case of local thermodynamic equilibrium the source function $J(\nu, \tau)$ is equal to the black-body specific intensity $E(\nu, T)$. This is very convenient since $E(\nu, T)$ is a readily calculable quantity and is, moreover, isotropic. i.e., independent of the angle θ . The important question is to decide what regions of the atmosphere are in local thermodynamic equilibrium. This question will be taken up in detail in Section 3.2 where the relaxation of carbon dioxide will be considered. However, for the moment, it is sufficient to state that from the surface up to about 65 km the atmosphere is, to a good approximation, in local thermodynamic equilibrium.

Using Eqs. (3.1.4a) and (3.1.4b) the upward and downward directed fluxes may be written,

$$F_+(\tau) = 2\pi \int_{\nu} E(\nu, T_g) \int_0^{+1} e^{-(\tau_g - \tau)/\mu} \mu d\mu d\nu + 2\pi \int_{\nu} \int_{\tau}^{\tau_g} E(\nu, T_t) \int_0^{+1} e^{-(t - \tau)/\mu} \mu d\mu dt d\nu \quad (3.1.10a)$$

$$F_-(\tau) = 2\pi \int_{\nu} \int_0^{\tau} E(\nu, T_t) \int_0^{+1} e^{-(\tau - t)/\mu} \mu d\mu dt d\nu \quad (3.1.10b)$$

where it has been assumed that

$$I(\nu, 0, -\mu) = 0 \text{ and } I(\nu, \tau_g, +\mu) = E(\nu, T_g).$$

The first assumption is equivalent to neglecting solar radiation at long wavelengths (near 15 microns). The second implies that the earth's surface is black in the wavelength region being considered which, of course, is only approximately correct. The integration over angle in Eqs. (3.1.10a) and (3.1.10b) may be carried out to give

$$F_+(\tau) = 2\pi \int_{\nu} E(\nu, T_g) Ei_3(\tau_g - \tau) d\nu + 2\pi \int_{\nu} \int_{\tau}^{\tau_g} E(\nu, T_t) Ei_2(t - \tau) dt d\nu \quad (3.1.11a)$$

$$F_-(\tau) = 2\pi \int_{\nu} \int_0^{\tau} E(\nu, T_t) Ei_2(\tau - t) dt d\nu \quad (3.1.11b)$$

where

$$Ei_n(y) = \int_1^{\infty} e^{-yt} \frac{dt}{t^n} = \int_0^{+1} e^{-y/\mu} \mu^{n-1} \frac{d\mu}{\mu}$$

Extensive tables exist for the exponential integral ($Ei_n(y)$). Pagurova (1961) tabulates the function for $n = 1$ (1) 20 and for $y = 0$ (0.01) 2 (0.1) 10. However, the function may also be evaluated on the computer using one of a number of series expansions which are available (cf., Chandrasekhar 1960, Hastings 1955).

3.2 RELAXATION OF THE CARBON DIOXIDE MOLECULE

In the infrared a molecule such as CO_2 has three forms of energy, translational, vibrational, and rotational. The translational energy is unquantized and may be freely interchanged in collisions, the gas taking up or losing translational energy at a rate depending only on the molecular collision rate. The vibrational and rotational energies are both quantized and thus are not freely interchanged with translational energy in collisions. The probability of a transfer of energy between vibration or rotation and translation during a collision is less than one and thus a molecule will normally undergo a number of collisions before it gains or loses vibrational or rotational energy. At tropospheric pressures collisions are frequent enough to provide an effective transfer of energy from translation to vibration and rotation and vice versa. Thus thermodynamic equilibrium is attained with the energy levels of the various vibrational and rotational states following a Boltzmann distribution. If the pressure is lowered, then a point is reached when the collision rate becomes smaller than the radiative lifetime of the vibrational or rotational states. In this case thermodynamic equilibrium will not be attained and the vibrational or rotational energy levels will not have a Boltzmann distribution. Thus vibrational or rotational relaxation has occurred. To use the energy distribution of the vibrational or rotational levels as a means for determining the temperature of a gas at low pressures is improper, if the problem of vibrational or rotational relaxation is not considered.

If Z^* is the average number of collisions an excited molecule experiences before losing one quantum, and if Z is the total number of collisions per molecule per second, then the relaxation time λ is defined by

$$Z^* = Z\lambda \quad (3.2.1)$$

Z^* is a function of the level of excitation of the molecule and also the temperature. Thus if p_1 and p_2 are two pressures then, at a given temperature,

$$Z^* = Z_{p_1} \lambda_{p_1} = Z_{p_2} \lambda_{p_2}$$

giving

$$\lambda_{p_2} = \frac{Z_{p_1}}{Z_{p_2}} \lambda_{p_1}$$

however Z is proportional to the pressure, and therefore

$$\lambda_{p_2} = \frac{p_1}{p_2} \lambda_{p_1} \quad (3.2.2)$$

λ is usually given for a standard pressure, 1 atmosphere, and for various temperatures.

Curtis and Goody (1956) give a formula for determining the radiative lifetime of a vibration-rotation band, viz.,

$$\theta^{-1} = 8\pi \frac{\nu_0^2}{c^2} \int_{\nu} k_{\nu} d\nu \quad (3.2.3)$$

where θ is the radiative lifetime and ν_0 the frequency of the band center. In deriving Eq. (3.2.3) it has been assumed that the black-body specific intensity $E(\nu, T)$ does not vary much across the band, a reasonable approximation. Equation (3.2.3) may be written

$$\theta^{-1} = \frac{8\pi \nu_0^2 S}{c^2} \quad (3.2.4)$$

where S is the integrated absorption of the band. Table I lists values for θ for the various CO_2 bands in the 15-micron region based on band intensities given by Madden (1961) where available and otherwise, the values given by Yamamoto and Sasamori (1958) are used.

TABLE I
VALUES OF RADIATIVE LIFETIME θ FOR VARIOUS BANDS

Band Code*	Band Center (cm^{-1})	Band Intensity ($\text{cm}^{-2} \text{ atm}^{-1}$)	θ (sec)
1	667.40	194.	4.12 (-1)**
2	618.03	4.27	2.19 (1)
3	720.83	6.2	1.11 (1)
4	667.76	30.	2.66
5	647.02	1.0	8.51 (1)
6	791.48	0.022	2.59 (1)
7	597.29	0.14	7.14 (2)
8	741.75	0.14	4.63 (2)
9	668.3	0.85	9.39 (1)
10	544.26	0.0040	3.01 (4)
11	581.2	0.0042	3.01 (4)
12	756.75	0.0059	1.05 (4)
13	828.18	0.00049	1.06 (5)
14	740.5	0.014	4.64 (3)

*The band code is described in Appendix B.

**For typing convenience, in most of the tables powers of ten are enclosed in parentheses, e.g., $4.12 (-1) = 4.12 \times 10^{-1}$.

The vibrational relaxation time for the CO_2 fundamentals have been measured by numerous researchers using various techniques (cf., Herzfeld and Litovitz, 1959; Lambert 1962). Unfortunately, most of the measurements have been made for pure CO_2 or mixtures of CO_2 and H_2 or He. The relaxation time is greatly influenced by small amounts of water vapor, probably due to some catalytic effect. No reliable measurements appear to have been made for mixtures of CO_2 and N_2 or O_2 . Witteman (1962) measured the relaxation times for pure CO_2 . He obtained a value of 3.74×10^{-6} sec at 1 atm pressure and 440°K for the 15-micron fundamental. Extrapolating his results to 300°K a value of about 4.2×10^{-6} sec is obtained. Schwarz, Slawsky, and Herzfeld (1952), and Schwarz and Herzfeld (1954) have computed relaxation times for various gas mixtures. They consider that their estimates are only in error by a factor depending only on the geometry of the collisions. Their results relevant to this discussion are given in Table II.

TABLE II

THEORETICAL AND EXPERIMENTAL VALUES FOR THE VIBRATIONAL
RELAXATION OF CO_2 AND $\text{CO}_2\text{-N}_2$ MIXTURES

	λ (theory)	λ^* (experimental)
$\text{CO}_2\text{-CO}_2$	4×10^{-4} sec (288°K)	4.2×10^{-6} sec (300°K)
$\text{CO}_2\text{-N}_2$	7.5×10^{-4} sec (288°K)	---

*Witteman (1962).

The factor in the case of pure CO_2 is close to 100. Using this same factor for the $\text{CO}_2\text{-N}_2$ mixture gives a value for the vibrational relaxation time of 7.5×10^{-6} sec. Curtis and Goody (1956) suggest using a value of 15×10^{-6} sec at 220°K . They obtained this value using an argument similar to the one above but they used earlier experimental results. Due to the uncertainties involved in arriving at an accurate value for the relaxation time for CO_2 - air mixtures, it seems reasonable to assume that the value for the 15-micron fundamental lies between 10^{-5} and 10^{-6} sec at 1 atm for temperatures around 250°K . Thus calculations involving the relaxation time are carried out using these two approximate bounding values. Obviously the above state of affairs is highly unsatisfactory and more experimental measurements are badly needed. The situation with respect to the overtone and other CO_2 bands in the 15-micron part of the spectrum is even more unsatisfactory. No estimates of the appropriate relaxation times appear in the literature. However, as Table I shows, the radiative lifetime of all the bands is at least an order of magnitude greater than the fundamental and if band 4 is excluded, at least two orders of magnitude greater. Thus if the relaxation times for these bands are of the same order as for the 15-micron fundamental, then the relaxation would occur at higher levels in the atmosphere. For the 15-micron fundamental vibrational relaxation becomes significant between 65 and 75 km and if it is assumed that the same relaxation time holds for the other bands then it would be-

come significant for band 4 between 85 and 90 km, and above 100 km for the remaining bands. Witteman's (1962) results indicate that the relaxation time for the 4.3-micron fundamental (ν_3 - mode or valence mode) is at least one order of magnitude smaller than that for the 15-micron fundamental (ν_2 - mode or bending mode). This indicates that the bending energy follows the translational energy at a slower rate than does the valence energy. Since the other bands in the 15-micron region have different vibrational transitions than the fundamental, they might follow the translational energy at a faster rate and thus have a lower relaxation time. Thus it seems reasonable to assume that at the worst they have a relaxation time of the same order as that of the 15-micron fundamental. In this study it will be assumed that vibrational relaxation does not affect bands other than the 15-micron fundamental until 100 km is reached.

The 15-micron fundamental is by far the strongest band as can be seen by examining Table XIV. Thus by the time the height is reached at which vibrational relaxation becomes of importance, the optical mass of carbon dioxide has become so small that only the 15-micron band will have much influence on the radiative transfer.

The problem of rotational relaxation is somewhat simpler since rotational quanta are much smaller than vibrational quanta. Thus the probability of a translation-rotation energy transfer occurring in collisions is that much greater. Typical values for the rotational relaxation time appear to be around 10^{-9} sec at 1 atm (cf., Lambert,

1962) and thus rotational relaxation can be neglected.

3.3 THE RADIATIVE TRANSFER EQUATION FOR A VIBRATIONALLY RELAXING GAS

As discussed in Section 3.2 vibrational relaxation occurs when high enough levels of the atmosphere are reached, around 70 km. Thus local thermodynamic equilibrium is no longer attained and Kirchhoff's law is no longer applicable. This means that the source function is no longer equal to the black-body specific intensity. It is easy to see from physical considerations what form the source function should take. At fairly high pressures, as in the stratosphere and troposphere, the source function should be the same as the black-body specific intensity. As pressures decrease, ultimately the source function will be that for noncoherent scattering. In this case noncoherent scattering means that redistribution of frequency occurs within the particular molecular band under consideration, but no interchange of energy occurs between the various molecular bands due to vibrational relaxation. If the pressure is lowered until rotational relaxation sets in, then there will be no redistribution of frequency over the band only over the individual rotation lines. As noted in Section 3.3 rotational relaxation need not be considered for this problem since it occurs at heights greater than 100 km. The source function $J(\nu, \tau)$ may be written,

$$J(\nu, \tau) = \alpha(\tau)E(\nu, T) + \beta(\tau)J^*(\nu, \tau) \quad (3.3.1)$$

where $J^*(\nu, \tau)$ is the source function for noncoherent scattering with vibrational relaxation. From the above discussion, it is evident that

$$\begin{aligned}
 \alpha(\tau) &\rightarrow 1 \text{ as } p \rightarrow \infty \\
 \alpha(\tau) &\rightarrow 0 \text{ as } p \rightarrow 0 \\
 \beta(\tau) &\rightarrow 0 \text{ as } p \rightarrow \infty \\
 \beta(\tau) &\rightarrow 1 \text{ as } p \rightarrow 0
 \end{aligned}
 \tag{3.3.2}$$

Curtis and Goody (1956) have derived an expression for the source function for the situation described above. They give

$$J(\nu, \tau) = \frac{\theta}{\theta + \lambda} E(\nu, T) + \frac{\lambda E(\nu, T)}{\theta + \lambda} X \tag{3.3.3}$$

where

$$X = \frac{\iint \rho k_\nu I(\nu, \tau, \mu) d\nu d\omega}{\iint \rho k_\nu E(\nu, T) d\nu d\omega}$$

the integrations being over all frequencies of the band and over all solid angle. The source function given by Eq. (3.3.3) obviously satisfies the relations Eq. (3.3.2).

Now consider the function X . This may be written

$$X = \frac{\int_{\nu_1}^{\nu_2} \int_0^{2\pi} \int_0^\pi k_\nu I(\nu, \tau, \mu) \sin \theta d\theta d\phi d\nu}{\int_{\nu_1}^{\nu_2} \int_0^{2\pi} \int_0^\pi k_\nu E(\nu, T) \sin \theta d\theta d\phi d\nu} \tag{3.3.5}$$

where the band extends from ν' to ν'' .

Since $\mu = \cos \theta$ and k_ν and $E(\nu, T)$ are independent of angle θ , then

$$X = \frac{2\pi \int_{\nu'}^{\nu''} \int_{-1}^{+1} k_\nu I(\nu, \tau, \mu) d\mu d\nu}{4\pi \int_{\nu'}^{\nu''} k_\nu E(\nu, T) d\nu} \quad (3.3.5)$$

$$= \frac{\int_{\nu'}^{\nu''} \int_{-1}^{+1} k_\nu I(\nu, \tau, \mu) d\mu d\nu}{2 \int_{\nu'}^{\nu''} k_\nu E(\nu, T) d\nu}$$

Now consider the denominator of Eq. (3.3.5). The black-body specific intensity is a slowly varying function of ν , and to an excellent approximation is constant over a few wave numbers. If it is assumed constant over a band then

$$\int_{\nu'}^{\nu''} k_\nu E(\nu, T) d\nu \approx E(\nu_0, T) \int_{\nu'}^{\nu''} k_\nu d\nu = E(\nu_0, T) S \quad (3.3.6)$$

where ν_0 is the band center and S the integrated band intensity.

A better approximation is obtained by considering the following.

At the heights where vibrational relaxation becomes of importance

(above about 65 km) pressures are so low that the line profile is given

by the Doppler formula. The Doppler half-width at 250°K for a wave

number of 600 cm^{-1} is $5.122 \times 10^{-4} \text{ cm}^{-1}$. Now the spacing between the rotational lines of the P- and R-branches of the 15-micron fundamental is approximately 1.5 cm^{-1} and the rotational line spacing for the Q-branch starts at $1.0 \times 10^{-2} \text{ cm}^{-1}$ for the lowest wave numbers and increases to around 0.2 cm^{-1} for the weakest lines at the higher wave numbers. Thus the band may be considered as composed of nonoverlapping lines, even the lines making up the Q-branch. Therefore

$$\int_{\nu'}^{\nu''} k_{\nu} E(\nu, T) d\nu \approx \sum_{i=1}^n [E(\nu_i, T) \int_{\nu'}^{\nu''} k_{\nu_i} d\nu_i] = \sum_{i=1}^n E(\nu_i, T) S_i \quad (3.3.7)$$

where n is the number of lines and the integration over ν_i means that the integral is evaluated only considering the i th line by itself.

Hence Eq. (3.3.3) may now be written

$$J(\nu, \tau) = \frac{\Theta}{\Theta + \lambda} E(\nu, T) + \frac{\lambda E(\nu, T)}{\Theta + \lambda} \frac{\int_{-1}^{+1} \int_{\nu'}^{\nu''} k_{\nu} I(\nu, \tau, +\mu) d\nu d\mu}{2 \sum_{i=1}^n S_i E(\nu_i, T)} \quad (3.3.8)$$

$$= \alpha(\tau) E(\nu, T) + \beta(\tau) \int_{-1}^{+1} \int_{\nu'}^{\nu''} k_{\nu} I(\nu, \tau, \mu) d\nu d\mu$$

where

$$\alpha(\tau) = \frac{\Theta}{\Theta + \lambda} \text{ and } \beta(\tau) = \frac{\lambda E(\nu, T)}{2(\Theta + \lambda) \sum_{i=1}^n S_i E(\nu_i, T)}$$

Note that $\alpha(\tau)$ and $\beta(\tau)$ satisfy the relations Eq. (3.3.2). To determine $J(v, \tau)$ requires a knowledge of $I(v, \tau, \mu)$, which is rather inconvenient since a knowledge of $J(v, \tau)$ is required before $I(v, \tau, \mu)$ can be evaluated. The standard procedure is to derive the appropriate Milne integral equation (cf., Busbridge, 1960) for $J(v, \tau)$. Equation (3.3.8) is rewritten

$$\begin{aligned}
 J(v, \tau) = & \alpha(\tau)E(v, T) + \beta(\tau) \int_0^{+1} \int_{v'}^{v''} k_v I(v, \tau, +\mu) dv d\mu \\
 & + \beta(\tau) \int_0^{+1} \int_{v'}^{v''} k_v I(v, \tau, -\mu) dv d\mu
 \end{aligned}
 \tag{3.3.9}$$

Equations (3.1.2a) and (3.1.2b) are then substituted into Eq. (3.3.9), giving

$$\begin{aligned}
 J(v, \tau) = & \alpha(\tau)E(v, T) + \beta(\tau) \int_{v'}^{v''} k_v \int_0^{+1} [I(v, \tau_0, +\mu)e^{-(\tau_0 - \tau)/\mu} + I(v, 0, -\mu)e^{-\tau/\mu}] d\mu dv \\
 & + \beta(\tau) \int_{\tau}^{\tau_0} \int_{v'}^{v''} k_v J(v, t) \int_0^{+1} \frac{e^{-(t - \tau)/\mu}}{\mu} d\mu dv dt \\
 & + \beta(\tau) \int_0^{\tau} \int_{v'}^{v''} k_v J(v, t) \int_0^{+1} \frac{e^{-(\tau - t)/\mu}}{\mu} d\mu dv dt
 \end{aligned}$$

Thus

$$\begin{aligned}
J(\nu, \tau) = & \alpha(\tau)E(\nu, T) + \beta(\tau) \int_{\nu'}^{\nu''} k_{\nu} \int_0^{+1} I(\nu, \tau_0, +\mu) e^{-(\tau_0 - \tau)/\mu} d\mu d\nu \\
& + \beta(\tau) \int_0^{\tau_0} \int_{\nu'}^{\nu''} k_{\nu} J(\nu, t) Ei_1(|t - \tau|) d\nu dt
\end{aligned}
\tag{3.3.10}$$

where Ei_1 is the first exponential integral (cf., Section 3.1), and it has been assumed that there is no incident radiation on the top of the atmosphere.

Equation (3.3.10) is the Milne integral equation for the problem. However, this is more complicated than the ones usually obtained in that the right-hand side contains double integrals. An analytic solution is difficult to obtain even when only one integral appears on the right-hand side of the Milne equation, and then only for a limited number of cases. However, several numerical methods have been developed to deal with integral equations and a numerical method will be discussed in Section 4.2. Once $J(\nu, \tau)$ has been determined, the specific intensities may be evaluated and the fluxes are then readily determined.

It is interesting to note from Eq. (3.3.10) that $J(\nu, \tau)$ must be a slowly varying function of frequency since only in the first term in the right-hand side is there any dependence on frequency, and since $E(\nu, T)$ is a slowly varying function of frequency for small frequency intervals. This simplifies matters somewhat since over a band $J(\nu, \tau)$ can be assumed to be approximately constant.

Curtis and Goody (1956) were able to derive a relation between the source function $J(\nu, \tau)$ and the heating rate ($^{\circ}\text{K day}^{-1}$) viz.,

$$\frac{dT}{dt} = \frac{1.99}{\lambda} (\bar{J} - \bar{E}) \quad (3.3.11)$$

where the bars denote average values of $J(\nu, \tau)$ and $E(\nu, T)$ over the band. Once $\bar{J}(\tau)$ has been determined, the evaluation of the heating rate is straight forward.

It is interesting to note that if $\bar{J}(\tau) = \bar{E}(T)$ for an atmospheric layer then there will be no heating (or cooling) of that layer due to radiative transfer. This is an interesting point and worth examining further. The atmosphere is certainly not in thermodynamic equilibrium, i.e., the state of the atmosphere as a whole is not derivable from the basic laws of thermodynamics. Thus Kirchhoff's law, $E(\nu, T) = \epsilon_{\nu}/k_{\nu}$, is not applicable to this system as a whole. The concept of local thermodynamic equilibrium provides a way round this difficulty. This is based on the assumption that the complete system may be divided into small regions, in each of these regions Kirchhoff's law may be applied. Consequently each of these small regions is in thermodynamic equilibrium, and the source function is given by the black-body specific intensity. Thus there will be no heating (or cooling) of this region due to radiative transfer. At levels in the atmosphere above 65 km, where vibrational relaxation becomes important, local thermodynamic equilibrium can no longer be assumed even for small regions

and the source function is not equal to the black-body specific intensity. At levels below 65 km the source function and black-body specific intensities are not exactly equal but to a first approximation may be assumed equal with very little error, this is evident from examining Eq. (3.3.3).

If it were possible to accurately evaluate $J(\nu, \tau)$ for the complete range of atmospheric pressures then Eq. (3.3.11) would provide a convenient method of obtaining the heating rate due to radiative transfer. Unfortunately determining $J(\nu, \tau)$ involves an accurate knowledge of the relaxation time for the gas, a quantity which, as has been pointed out in Section 3.2, is not accurately known.

3.4 THE EVALUATION OF THE ABSORPTION COEFFICIENT FOR VARIOUS ATMOSPHERIC PRESSURES

3.4.1 Preliminary Remarks

The absorption coefficient k_ν depends on pressure. For example, at high pressures collisional broadening is the most important process and the absorption profile for a spectral line is given by the Lorentz formula. At much lower pressures Doppler broadening of the spectral line is the important process and the absorption profile is given by the Doppler formula. It is important to consider how the shape and width of a spectral line varies with pressure.

The shapes and widths of spectral lines have been under intensive investigation for some years, both theoretically and experimentally.

Most of the effort has been concentrated on the study of spectral lines associated with atomic transitions. There are probably two main reasons for this. The first one is that atomic lines are simpler to examine experimentally. They are more isolated than their molecular counterparts and thus can be examined without the wings of other lines modifying the true shape as happens with lines associated with molecular transitions. Second, theoretical computations involving atoms are inherently simpler than the corresponding ones for molecules.

The meteorologist is interested in the heating and cooling of the atmosphere due to infrared radiative transfer. Therefore, the widths and shapes of lines associated with the three molecules CO_2 , O_3 , and H_2O need to be thoroughly investigated. The vibration-rotation bands of these molecules which are of importance to atmospheric heating and cooling are sufficiently far in the infrared to be associated with the electronic ground state of the molecule. Thus electronic transitions do not have to be considered.

The line half-width for the individual lines of a particular vibration-rotation band is a very important parameter which needs to be known as accurately as possible. This is not necessarily a constant. The line half-width associated with collisional broadening appears to depend on whether the collisions are between like or unlike molecules. The CO_2 molecule provides a good example. For self-broadened CO_2 the line half-width associated with the 15-micron band

is around 0.1 cm^{-1} at 1 atm, whereas for nitrogen broadened CO_2 the line half-width is around 0.064 cm^{-1} at 1 atm. Also, there is a dependence of the line half-width on the rotational quantum number of the lines making up the vibration-rotation band, depending on the polarity of the molecule.

Two references which deal with spectral line shapes and have proved useful are Breene (1955) and Benedict et al. (1956). The first reference is an extensive review of the literature dealing with spectral line shapes while the second deals specifically with the widths and shapes of infrared lines.

3.4.2 Absorption Associated with Collisional Broadening

For sometime it has been known that the width of a spectral line depends on the pressure. One of the earliest theories to give the line profile and thus the absorption coefficient for a pressure broadened line was developed by Lorentz. It is relatively easy to see why collisions should broaden spectral lines, although as would be expected a theoretical treatment is rather involved. An atom or molecule emits radiation when it drops from a higher energy level to a lower one and absorbs radiation if the reverse process takes place. If another particle passes close to the emitting or absorbing atom or molecule, it will perturb the energy levels and consequently the energy associated with the emission or absorption will be spread out over a greater frequency interval. Obviously, the rate of perturbing collisions will

depend on the pressure and consequently the higher the pressure the broader the line and vice versa. Some shift in the position of the line center and asymmetries of the line profile might be expected due to the perturbing influence of the collisions. These points will be taken up below.

The line half-width would be expected to be dependent on the intermolecular forces. In the case of polar molecules the line half-width associated with collisional broadening varies with the rotational quantum number of the radiating molecule. Also, the half-width may vary with the nature of the colliding particles, specifically it could be different for self-broadening and foreign gas broadening. Both of these effects have been found for CO_2 . Madden (1961) investigated self-broadened CO_2 and found a variation of the line half-width with rotational quantum number for part of the 15-micron CO_2 vibration-rotation band. The half-width varied from 0.126 cm^{-1} for $J = 4$ to 0.06 cm^{-1} for $J = 56$ (temperature 300°K , pressure 1 atm), for the P-branch of the 15-micron fundamental. Kaplan and Eggers (1956) obtained a half-width of 0.064 cm^{-1} (temperature 298°K , pressure 1 atm) for CO_2 broadened by nitrogen, again for the 15-micron fundamental. The half-width measured by Kaplan and Eggers would seem to be the one most applicable for atmospheric investigations.

The absorption coefficient for the classical Lorentz line shape is given by,

$$k_\nu = \frac{S\alpha_L}{\pi} \frac{1}{(\nu - \nu_0)^2 + \alpha_L^2} \quad (3.4.1)$$

where α_L is the line half-width due to collisional broadening, S is the integrated line intensity and ν_0 the frequency of the center of the line. It is easy to show that

$$\int_0^\infty k_\nu d\nu = \int_{-\infty}^\infty k_\nu d\nu = S$$

The theoretical evaluation of α_L is difficult, so experimental values are used. Since the Lorentz line shape is associated with collisional broadening, then α_L should be proportional to the number of collisions. From the kinetic theory of gases the number of collisions is proportional to $p\sqrt{T}$ whence

$$\alpha_L = \alpha_L^0 \frac{p}{p_0} \sqrt{\frac{T_0}{T}} \quad (3.4.2)$$

where α_L^0 is the half-width at some standard pressure p_0 and temperature T_0 .

As mentioned above, collisions may have three main effects on the line shape, viz.,

- (1) the center of the line may be displaced toward lower frequencies by an amount proportional to the total pressure;
- (2) the line may become asymmetrical; and

- (3) the line may be broadened, the broadening being proportional to the total pressure.

Lindholm (1945) developed a theory for the pressure broadening of a spectral line due to atomic collisions which takes into account the above three effects. He considers that the frequency perturbation is associated with a van der Waal's type force, viz.,

$$\Delta\nu = -b/R^6$$

where R is the distance between the radiating and perturbing atoms and b is a constant. Kleman and Lindholm (1945) have verified the Lindholm line shape for argon broadened sodium. However, there is some doubt if this line shape may be applied to infrared molecular lines. For close collisions only R^{-8} and other higher order terms need be considered. Also as Benedict et al. (1956) note, it would appear that vibration-rotation spectra will not show much asymmetry since the polarizabilities of the upper and lower states of the molecule are the same. Also they did not observe any asymmetries in their examinations of infrared spectra. However, there does appear to be an exponential die-away in the wings of a self-broadened CO₂ line. This exponential die-away would have to be considered if infrared flux computations were being made for a pure CO₂ atmosphere, but it is doubtful if it need be considered for computations involving CO₂ in the earth's atmosphere, since no experimental evidence has been forthcoming regarding an exponential die-away for foreign gas broadened CO₂. At the

moment several groups are looking for such a die-away for foreign gas broadened CO_2 using very long path lengths (Benedict, 1962).

Plass and Warner (1952), and Curtis and Goody (1954) have investigated the effects on infrared transfer in the atmosphere of assuming a line shape very close to Lindholm's. The latter authors conclude that due to the other inaccuracies involved it would not be useful to consider a non-Lorentzian line shape in infrared flux computations in the atmosphere. Plass (1954) noted that it was probably unrealistic to consider a line shape based on Lindholm's theory since, as noted above, infrared lines most likely do not follow such a shape.

In conclusion, it appears that at the present time the Lorentz line shape is satisfactory for evaluating the absorption coefficient for collisional broadening.

3.4.3 Absorption Associated with Doppler Broadening

If the gas pressure is low enough so that the collisional frequency is small, then line broadening due to the Doppler effect becomes significant. In this case the Doppler effect is associated with the thermal motion of the molecules. Needless to say, close to the earth's surface the collisional frequency is very high and collisional broadening completely swamps any Doppler broadening. For CO_2 in the earth's atmosphere Doppler broadening becomes important around 30 km (about 10 mb). The line half-width and the line shape associated with Doppler broadening are easily derived from the kinetic theory of gases

(cf., Aller, 1953). The absorption coefficient for a Doppler broadened line is given by

$$k_{\nu} = \frac{S}{\alpha \sqrt{\pi}} \exp \left[-\left(\frac{\nu - \nu_0}{\alpha} \right)^2 \right] \quad (3.4.3)$$

where α is the Doppler half-width given by

$$\alpha = \frac{\nu_0}{c} \left(\frac{2KT}{m} \right)^{1/2} \quad (3.4.4)$$

where m is the mass of the molecule. It is convenient to use half the Doppler width at half-maximum, α_D . From Eq. (3.4.3) it is easy to show that

$$\alpha_D = \alpha (\ln 2)^{1/2} \quad (3.4.5)$$

Also, it is easy to show that

$$\int_0^{\infty} k_{\nu} d\nu = \int_{-\infty}^{\infty} k_{\nu} d\nu = S$$

From Eq. (3.4.5) and (3.4.4)

$$\alpha_D = \frac{\nu_0}{c} \left(\frac{2(\ln 2)KT}{m} \right)^{1/2} \approx 3.58 \times 10^{-7} \left(\frac{T}{M} \right)^{1/2} \nu_0 \quad (3.4.6)$$

where M is the molecular weight.

Equation (3.4.1) may now be written

$$k_\nu = \frac{S(\ln 2)^{1/2}}{\alpha_D \sqrt{\pi}} \exp \left[- \frac{(\nu - \nu_0)^2 \ln 2}{\alpha_D^2} \right] \quad (3.4.7)$$

It is evident from Eqs. (3.4.3) or (3.4.7) that the curve k_ν vs. ν follows a normal distribution.

Table III gives values for α_D for different frequencies in the 15-micron region for CO_2 and for different temperatures.

TABLE III
 α_D IN cm^{-1} FOR VARIOUS TEMPERATURES AND FREQUENCIES

Temperature (°K)	ν_0 (cm^{-1})			
	500	600	700	800
300	4.675 (-4)	5.610 (-4)	6.545 (-4)	7.480 (-4)
250	4.268 (-4)	5.122 (-4)	5.975 (-4)	6.829 (-4)
200	3.817 (-4)	4.581 (-4)	5.344 (-4)	6.107 (-4)

It is interesting to note that α_D varies considerably with frequency but not as much with temperature. Since the spectral region of interest extends from 500 to 800 cm^{-1} , it is thus necessary to take this variation with frequency into account.

3.4.4 Absorption Associated with Natural Broadening

Natural broadening is caused by radiation damping and is due to the finite lifetime of the excited states of the atoms or molecules.

The line half-width is given by

$$\alpha_N \approx \frac{\pi c}{t} \quad (3.4.8)$$

where t is the lifetime of the excited state. t is approximately 10^{-4} sec for the infrared region being considered. Thus $\alpha_N \approx 2.65 \times 10^{-8}$ cm^{-1} . The absorption coefficient is given by

$$k_\nu \propto \frac{1}{1 + \left(\frac{\nu - \nu_0}{\alpha_N} \right)^2} \quad (3.4.9)$$

(cf., Aller, 1953; Mitchell and Zemansky, 1934).

3.4.5 Comparison of Line Half-Widths

It is instructive to compare the half-widths associated with collisional, Doppler and natural broadening. Table IV lists the half-widths for comparison.

TABLE IV
HALF-WIDTHS FOR COLLISIONAL, DOPPLER,
AND NATURAL BROADENING

α_L	=	6.4	$\times 10^{-2} \text{ cm}^{-1}$	($T = 300^\circ\text{K}$, 1 atm pressure)*
α_D	=	5.610	$\times 10^{-4} \text{ cm}^{-1}$	($\nu_0 = 600 \text{ cm}^{-1}$, $T = 300^\circ\text{K}$)**
α_N	=	2.65	$\times 10^{-8} \text{ cm}^{-1}$	***

*Kaplan and Eggers (1956) value.

**Taken from Table III.

***Using Eq. (3.4.8). This is probably the least accurate of the three.

It is evident that α_L and α_D become nearly equal at a pressure of about 10 mb (approximately 30 km) and thus above 30 km Doppler broadening should be considered. Only at pressures near 10^{-3} mb (approximately 90 km) does α_L become of the order of α_N , but at this pressure α_D is much greater than either.

3.4.6 Absorption Taking into Account Collisional, Doppler, and Natural Broadening

It is possible to obtain an expression for the absorption coefficient taking into account collisional, Doppler, and natural broadening. The appropriate equation is generally written (Mitchell and Zemansky, 1934),

$$k_\nu = \frac{k_0 a}{\pi} \int_{-\infty}^{\infty} \frac{e^{-x^2}}{a^2 + (\omega - x)^2} dx \quad (3.4.10a)$$

$$= \frac{k_0}{\sqrt{\pi}} \int_0^{\infty} \exp \left[-ax - \frac{x^4}{4} \right] \cos \omega x \, dx \quad (3.4.10b)$$

where

$$k_0 = \frac{S}{\alpha_D} \left(\frac{\ln 2}{\pi} \right)^{1/2}$$

$$a = \frac{\alpha_L + \alpha_N}{\alpha_D} (\ln 2)^{1/2}$$

and

$$\omega = \frac{\nu - \nu_0}{\alpha_D} (\ln 2)^{1/2}$$

Equation (3.4.10a) may be written in the form

$$\frac{k_v}{k_0} = \frac{a}{\pi} \int_{-\infty}^{\infty} \frac{e^{-x^2}}{a^2 + (\omega - x)^2} dx \quad (3.4.11)$$

The right-hand side of this equation is the real part of the error function for complex argument, viz.,

$$w(z) = \frac{i}{\pi} \int_{-\infty}^{\infty} \frac{e^{-x^2}}{z - x} dx \quad (3.4.12)$$

where $z = \omega + i a$ and $w(z) = u(\omega, z) + i v(\omega, a)$. Tabulations of this function over a fairly wide range of ω are given by Faddeeva and Terentev (1961) with appropriate interpolation coefficients.

A number of series have been developed to approximate the value of Eq. (3.4.10). Unfortunately no one series approximates Eq. (3.4.10) over the range of values of ω and a , which is of interest in the atmosphere. A review of the various series which may be used to approximate Eq. (3.4.10) is given by Penner (1959). Two useful series expansions have been developed by Plass and Fivel (1953), and Harris (1948). The Plass-Fivel approximation is useful for small values of a ; i.e., $\alpha_D > \alpha_L + \alpha_N$. It may be written

$$k_v = k_0 [(\cos 2\omega a + \sin 2\omega a) \exp(a^2 - \omega^2) + \frac{1}{\sqrt{\pi}} \sum_{n=1}^{\infty} \sum_{m=0}^M \frac{(2m+n)! \sin\left(\frac{1}{2} n\pi\right) a^n}{2^{2n} n! m! \omega^{2m+n+1}}$$

$$\begin{aligned}
&= \frac{S}{\alpha_D} \left(\frac{\ln 2}{\pi} \right)^{1/2} [(\cos 2\omega a + \sin 2\omega a) \exp(a^2 - \omega^2)] \\
&\quad (3.4.13) \\
&+ \frac{S(\alpha_I + \alpha_N)}{\pi(\nu - \nu_0)^2} \left[1 + \left(\frac{3}{2} - a^2 \right) \frac{1}{\omega^2} + \left(\frac{15}{4} - 5a^2 + a^4 \right) \frac{1}{\omega^4} + \dots \right]
\end{aligned}$$

As will be discussed later this approximation is useful for pressures lower than 0.05 mb. The Harris approximation is useful for values of a up to 0.3 and ω in the range of 0 to 8.0. It may be written

$$\frac{k_V}{k_0} = H_0(\omega) + a H_1(\omega) + a^2 H_2(\omega) + a^3 H_3(\omega) + a^4 H_4(\omega) + \dots$$

$$H_0(\omega) = e^{-\omega^2}$$

$$H_1(\omega) = \frac{-2}{\sqrt{\pi}} [1 - 2\omega F(\omega)]$$

$$H_2(\omega) = (1 - 2\omega^2) e^{-\omega^2}$$

$$H_3(\omega) = \frac{-2}{\sqrt{\pi}} \left[\frac{2}{3} (1 - \omega^2) - 2\omega \left(1 - \frac{2}{3} \omega^2 \right) F(\omega) \right]$$

$$H_4(\omega) = \left(\frac{1}{2} - 2\omega^2 + \frac{2}{3} \omega^4 \right) e^{-\omega^2}$$

$$F(\omega) = e^{-\omega^2} \int_0^\omega e^{t^2} dt = \int_0^\omega e^{-(\omega^2 - t^2)} dt$$

It turns out that this approximation is useful for pressures lower than 2.5 mb and up to about 0.005 cm^{-1} from the line center.

3.4.7 Practical Determination of the Absorption Coefficient for Various Atmospheric Pressures

The above discussion on the absorption coefficients due to the various physical broadening processes enables a decision to be made on what absorption coefficient to use at various atmospheric pressures. It is evident that for pressures greater than 20 mb the Lorentz formula is adequate. The problem remains of handling the absorption at pressures lower than 20 mb.

From the results presented in Table V several conclusions can be drawn. At 20 mb the effect of Doppler broadening is beginning to be noticeable. Even at as low a pressure as 0.1 mb the Plass-Fivel approximation is not very satisfactory unless $\Delta\nu > 0.002 \text{ cm}^{-1}$, but as the pressure is decreased it becomes more useful toward the line center. The wings of the line, $\Delta\nu > 0.003 \text{ cm}^{-1}$, can be approximated reasonably well using the Lorentz formula. The Harris formula may be used up to pressures of about 3 mb with reasonable accuracy. However, one difficulty with the Harris formula is the evaluation of the integral $F(\omega)$. This integral may be expressed in terms of a series involving the incomplete Γ function. It may more easily be evaluated by dividing the interval 0 to ω logarithmically and applying a seven point Legendre-Gauss quadrature in each of these subintervals.

The pressure region from 3 to 20 mb poses some difficulty. No satisfactory approximation appears to be available. The method chosen was to abstract a small table from the larger Faddeeva-Terentev tables

TABLE V

COMPARISON OF ABSORPTION COEFFICIENTS EVALUATED USING VARIOUS FORMULAE AT PRESSURES LOWER THAN 50 MB
(The line intensity was chosen as $1.0 \text{ cm}^{-2} \text{ atm}^{-1}$, and the frequency was 600 cm^{-1} , temperature 250°K)

$\Delta \nu \text{ (cm}^{-1}\text{)}$	$k_\nu \text{ (D)}^{(1)}$	30 mb		20 mb		10 mb	
		$k_\nu \text{ (L)}^{(2)}$	$k_\nu \text{ (FT)}^{(3)}$	$k_\nu \text{ (L)}$	$k_\nu \text{ (FT)}$	$k_\nu \text{ (L)}$	$k_\nu \text{ (FT)}$
0.0001	8.191 (2)	1.653 (2)	1.569 (2)	2.472 (2)	2.223 (2)	4.855 (2)	3.668 (2)
0.0002	7.667 (2)	1.640 (2)	1.559 (2)	2.428 (2)	2.198 (2)	4.531 (2)	3.578 (2)
0.0004	5.886 (2)	1.589 (2)	1.520 (2)	2.266 (2)	2.100 (2)	3.577 (2)	3.247 (2)
0.0006	3.789 (2)	1.510 (2)	1.459 (2)	2.039 (2)	1.952 (2)	2.647 (2)	2.782 (2)
0.0008	2.045 (2)	1.413 (2)	1.381 (2)	1.788 (2)	1.772 (2)	1.941 (2)	2.274 (2)
0.001	9.255 (1)	1.304 (2)	1.290 (2)	1.544 (2)	1.577 (2)	1.445 (2)	1.798 (2)
0.0014	1.117 (1)	1.082 (2)	1.093 (2)	1.132 (2)	1.202 (2)	8.597 (1)	1.081 (2)
0.002	1.250 (-1)	7.951 (1)	8.120 (1)	7.226 (1)	7.767 (1)	4.620 (1)	5.389 (1)
0.003	2.063 (-6)	4.817 (1)	4.880 (1)	3.830 (1)	4.037 (1)	2.165 (1)	2.331 (1)
0.004	4.158 (-13)	3.105 (1)		2.310 (1)		1.242 (1)	
0.005	1.024 (-21)	2.131 (1)		1.530 (1)		8.017 (0)	
0.01	0.000	5.894 (0)		4.009 (0)		2.029 (0)	
0.02	0.000	1.514 (0)		1.014 (0)		5.088 (-1)	
0.03	0.000	6.763 (-1)		4.519 (-1)		2.263 (-1)	
0.04	0.000	3.811 (-1)		2.544 (-1)		1.273 (-1)	
0.05	0.000	2.441 (-1)		1.629 (-1)		8.147 (-2)	
0.10	0.000	6.109 (-2)		4.074 (-2)		2.037 (-2)	

(1) $k_\nu \text{ (D)}$ is evaluated using the Doppler formula.

(2) $k_\nu \text{ (L)}$ is evaluated using the Lorentz formula.

(3) $k_\nu \text{ (FT)}$ is evaluated using the Faddeeva-Trautman tables.

TABLE V (Continued)

$\Delta\nu$ (cm^{-1})	2 mb			1 mb			
	k_V (L)	k_V (FT)	k_V (HAR) ⁽¹⁾	k_V (L)	k_V (FT)	k_V (HAR)	k_V (PF) ⁽²⁾
0.0001	1.544 (3)	6.665 (2)	6.721 (2)	1.445 (3)	7.259 (2)	7.398 (2)	1.571 (7)
0.0002	7.226 (2)	6.327 (2)	6.372 (2)	4.620 (2)	6.861 (2)	6.972 (2)	2.532 (5)
0.0004	2.310 (2)	5.148 (2)	5.159 (2)	1.242 (2)	5.482 (2)	5.507 (2)	5.124 (3)
0.0006	1.083 (2)	3.678 (2)	3.659 (2)	5.595 (1)	3.787 (2)	3.738 (2)	9.380 (2)
0.0008	6.207 (1)	2.340 (2)	2.309 (2)	3.163 (1)	2.280 (2)	2.204 (2)	3.722 (2)
0.001	4.009 (1)	1.360 (2)	1.335 (2)	2.029 (1)	1.217 (2)	1.154 (2)	1.654 (2)
0.0014	2.062 (1)	4.236 (1)	4.189 (1)	1.037 (1)	2.844 (1)	2.732 (1)	3.080 (1)
0.002	1.014 (1)	1.264 (1)	1.281 (1)	5.088 (0)	6.110 (0)	6.524 (0)	6.375 (0)
0.003	4.519 (0)	4.877 (0)	4.913 (0)	2.263 (0)	2.375 (0)	2.461 (0)	2.456 (0)
0.004	2.544 (0)		2.661 (0)	1.273 (0)		1.332 (0)	1.332 (0)
0.005	1.629 (0)		1.676 (0)	8.147 (-1)		8.383 (-1)	8.383 (-1)
0.01	4.074 (-1)		4.128 (-1)	2.037 (-1)		2.053 (-1)	2.052 (-1)
0.02	1.019 (-1)			5.093 (-12)			5.104 (-2)
0.03	4.527 (-2)			2.264 (-2)			2.266 (-2)
0.04	2.547 (-2)			1.273 (-2)			1.274 (-2)
0.05	1.630 (-2)			8.149 (-3)			8.154 (-3)
0.10	4.074 (-3)			2.037 (-3)			2.038 (-3)

(1) k_V (HAR) is evaluated using the Harris formula.

(2) k_V (PF) is evaluated using the Plass-Fivel formula.

TABLE V (Continued)

$\Delta \nu$ (cm^{-1})	0.1 mb				0.01 mb			
	k_ν (L)	k_ν (FT)	k_ν (HAR)	k_ν (PF)	k_ν (L)	k_ν (FT)	k_ν (HAR)	k_ν (PF)
0.0001	2.029 (2)	8.203 (2)	8.105 (2)	1.596 (6)	2.037 (1)	8.282 (2)	8.182 (2)	1.663 (5)
0.0002	5.088 (1)	7.670 (2)	7.592 (2)	2.640 (4)	5.093 (0)	7.739 (2)	7.659 (2)	3.426 (3)
0.0004	1.273 (1)	5.867 (2)	5.847 (2)	1.049 (3)	1.273 (0)	5.903 (2)	5.882 (2)	6.363 (2)
0.0006	5.658 (0)	3.757 (2)	3.786 (2)	4.357 (2)	5.659 (-1)	3.759 (2)	3.789 (2)	3.848 (2)
0.0008	3.183 (0)	2.019 (2)	2.064 (2)	2.217 (2)	3.183 (-1)	2.001 (2)	2.047 (2)	2.063 (2)
0.001	2.037 (0)	9.118 (1)	9.509 (1)	1.002 (2)	2.037 (-1)	8.883 (1)	9.282 (1)	9.334 (1)
0.0014	1.039 (0)	1.183 (1)	1.286 (1)	1.322 (1)	1.039 (-1)	1.030 (1)	1.135 (1)	1.139 (1)
0.002	5.093 (-1)	7.410 (-1)	7.702 (-1)	7.551 (-1)	5.093 (-2)	4.645 (-1)	1.919 (-1)	1.904 (-1)
0.003	2.264 (-1)		2.472 (-1)	2.467 (-1)	2.264 (-2)		2.564 (-2)	2.558 (-2)
0.004	1.273 (-1)		1.337 (-1)	1.337 (-1)	1.273 (-2)		1.387 (-2)	1.386 (-2)
0.005	8.149 (-2)		8.416 (-2)	8.416 (-2)	8.149 (-3)		8.728 (-3)	8.728 (-3)
0.01	2.037 (-2)		2.057 (-2)	2.060 (-2)	2.037 (-3)		2.133 (-3)	2.136 (-3)
0.02	5.093 (-3)			5.123 (-3)	5.093 (-4)			5.313 (-4)
0.03	2.264 (-3)			2.275 (-3)	2.264 (-4)			2.359 (-4)
0.04	1.273 (-3)			1.279 (-3)	1.273 (-4)			1.327 (-4)
0.05	8.149 (-4)			8.185 (-4)	8.149 (-5)			8.489 (-5)
0.10	2.037 (-4)			2.046 (-4)	2.037 (-5)			2.122 (-5)

TABLE V (Concluded)

$\Delta\nu$ (cm ⁻¹)	0.001 mb			
	k_ν (L)	k_ν (FT)	k_ν (HAR)	k_ν (PF)
0.0001	2.037 (0)	8.289 (2)	8.189 (2)	2.329 (4)
0.0002	5.093 (-1)	7.746 (2)	7.666 (2)	1.128 (3)
0.0004	1.273 (-1)	5.907 (2)	5.886 (2)	5.951 (2)
0.0006	5.659 (-2)	3.760 (2)	3.789 (2)	3.797 (2)
0.0008	3.183 (-2)	2.000 (2)	2.045 (2)	2.048 (2)
0.001	2.037 (-2)	8.859 (1)	9.259 (1)	9.266 (1)
0.0014	1.039 (-2)	1.015 (1)	1.120 (1)	1.120 (1)
0.002	5.093 (-3)	1.068 (-1)	1.341 (-1)	1.339 (-1)
0.003	2.264 (-3)		3.483 (-3)	3.476 (-3)
0.004	1.273 (-3)		1.883 (-3)	1.883 (-3)
0.005	8.149 (-4)		1.185 (-3)	1.185 (-3)
0.01	2.037 (-4)		2.896 (-4)	2.901 (-4)
0.02	5.093 (-5)			7.214 (-5)
0.03	2.264 (-5)			3.204 (-5)
0.04	1.273 (-5)			1.801 (-5)
0.05	8.149 (-6)			1.153 (-5)
0.10	2.037 (-6)			2.881 (-6)

and use an interpolation procedure. This subsidiary table extends from $a = 0.2$ (.1)-2.6 and from $\omega = 0.00$ (0.02)-0.1 (.1)-5.0. It was found that linear interpolation gave fairly good accuracy but quadratic interpolation gave somewhat improved results and was thus used.

From the above considerations, the scheme shown in Table VI was devised to evaluate the absorption coefficient for various atmospheric pressures.

TABLE VI
EVALUATION OF ABSORPTION COEFFICIENT FOR VARIOUS
ATMOSPHERIC PRESSURES
(All pressures in mb)

$1000 \leq P < 20$	Lorentz formula.
$20 < P \leq 2$	Interpolation from Faddeeva-Terentev tables to $\Delta\nu = 0.003 \text{ cm}^{-1}$ with Lorentz formula for wings.
$2 < P \leq 0.05$	Harris approximation to $\Delta\nu = 0.003 \text{ cm}^{-1}$ then Lorentz formula for wings.
$P < 0.05$	Doppler formula for center of line, up to $\Delta\nu = 0.0014 \text{ cm}^{-1}$, Plass-Fivel approximation from 0.0014 cm^{-1} to 0.003 cm^{-1} with Lorentz for wings. (The Plass-Fivel approximation is used rather than Harris's since it does not involve an integral and thus is simpler to evaluate.)

It is interesting to note that the integral occurring in Eq.

(3.4.10) may be written in the form

$$\frac{k_v}{k_0} = \frac{a}{\pi} \int_{-\infty}^{\infty} e^{-x^2} f(x) dx \quad (3.4.15)$$

where

$$f(x) = \frac{1}{a^2 + (\omega - x)^2}$$

Now Eq. (3.4.15) is in the form suitable for applying Hermite-Gauss quadrature (cf., Kopal, 1961) since the weighting function is e^{-x^2} . This very tempting method was tried with no great success. It is satisfactory for pressures greater than about 20 mb but as the pressure is reduced the peak in the curve $e^{-x^2} f(x)$ vs. x becomes very sharp for small values of ω (proportional to Δv), i.e., close to the line center. This means that the expansion of $f(x)$ in terms of the Hermite polynomials is unsatisfactory for values of x near ω . Even using a seventeen point quadrature formula gave no noticeable improvement (cf., Rosser, 1950). However, the peak rapidly diminishes in intensity as the wings are approached and the Hermite-Gauss quadrature formula gives accurate results, but in this region the Lorentz formula is adequate, anyway.

3.5 MODELS FOR MOLECULAR BAND ABSORPTION

3.5.1 Preliminary Remarks

The transmissivity at a given frequency was defined in Section 3.1 by

$$\begin{aligned} \gamma_\nu(t, \tau) &= e^{-(t-\tau)/\mu} \\ &= \exp \left[- \int_{z_t}^{z_\tau} N k_\nu dz \right] \end{aligned} \tag{3.5.1}$$

It is necessary to know the value of Eq. (3.5.1) for all frequencies of the band so that Eq. (3.1.4a) and (3.1.4b) may be integrated over frequency to give the fluxes. Unfortunately due to the large number of rotational lines in a vibration-rotation band this would require a fantastic number of computations even for a fast digital computer. Thus attempts have been made to devise a "model" for the positions and intensities of the rotational lines so that the transmissivity could be evaluated analytically. Elsasser (1942) was one of the first investigators to try this. He assumed that the rotational lines are equally spaced with equal intensities and half-widths. Using this rather simple model it is not too difficult to obtain an expression for the transmissivity. Unfortunately, no important molecular band exhibits the regularity this model requires. Although the 15-micron CO_2 fundamental comes closest. However, if the other weaker but still

important CO_2 bands in this region are included, then the Elsasser model becomes most unsatisfactory.

The next advance was by Matossi et al. (1946, 1949), who derived analytic expressions for the total absorption over a band assuming unequally spaced lines of unequal intensity. Unfortunately, their expressions only apply for moderately strong absorption and they are rather involved. However, their work is important since it contains the germ of the idea which is at the basis of the statistical spectral model.

The statistical model (Goody, 1952) assumes a random disposition for the rotational lines in a band with the line intensities being specified by a probability function. This model was derived with the water vapor and ozone infrared bands in mind, these bands exhibiting considerable randomness in their rotational line positions. It suffers from the disadvantage of assuming an infinite interval.

The next step was to combine the two models discussed above to give the random Elsasser model (Plass, 1958). Here the band is represented by a number of Elsasser bands randomly distributed in the interval with different line intensities and spacing in each Elsasser band. This is an obvious improvement on the two previous models.

The latest model has been introduced by Wyatt et al. (1962). It is called the "quasirandom model." In this model the interval is divided into a number of smaller intervals in which the rotational

lines are assumed to be randomly placed. The lines in each of the smaller intervals are grouped by intensities. These groups can be made fine enough to simulate the real intensity distribution reasonably accurately. They were also able to derive an analytic expression for the transmissivity of a finite interval as well as one for the contributions from the wings of lines outside this interval. In both cases the Lorentz line shape was assumed. This model is the most realistic of the various models so far introduced and is discussed in considerable detail in the next section.

3.5.2 The Quasirandom Model

In the quasirandom model, as noted above, the frequency interval is divided into a number of smaller intervals δ_τ . For convenience it is assumed that these subintervals are all of equal size. (This is not necessary for the theory, but in practice they would be so chosen.) Each subinterval contains n_τ lines with their line centers at frequencies ν_i ($i = 1, 2, \dots, n_\tau$). Thus the transmissivity at frequency ν due to these lines is

$$\gamma_\tau(\nu) = \frac{1}{\delta^{n_\tau}} \prod_{i=1}^{n_\tau} \int_{\delta_\tau} \exp[-k(\nu, \nu_i)u] d\nu_i \quad (3.5.2)$$

where $k(\nu, \nu_i)$ is the absorption coefficient and u is the amount of absorbing gas per unit area (optical mass). The rotational lines are assumed to occur at random within each subintervals. As pointed out

by Wyatt et al. (1962), the transmissivity calculated using Eq. (3.5.2) applies at any particular frequency. However, since Eq. (3.5.2) corresponds to the average of all permutations of the positions of the spectral lines in δ_τ , then the transmissivity may be assumed to be representative of the transmissivity of the whole interval δ_τ , i.e., it may be called the "average transmissivity" for δ_τ . A difficulty arises in evaluating Eq. (3.5.2) due to the large number of lines in a particular band. Wyatt et al., suggest dividing the lines in each δ_τ into subgroups by intensity decades. The average intensities of the lines in each decade are used in the calculations of the transmissivities. Thus

$$\gamma_\tau(\nu) = \prod_{i=1}^m \left\{ \left[\frac{1}{\delta_\tau} \int \exp[-k_i(\nu, \nu_i)u] d\nu_i \right]^{n_i} \right\} \quad (3.5.3)$$

where m is the number of intensity decades and $n_\tau = \sum_{i=1}^m n_i$ is the total number of lines in δ_τ . Now the transmissivity at ν will naturally be influenced by the wings of lines outside. The wing transmissivities γ_i are calculated assuming a random distribution for the spectral lines in the intervals δ_i . Thus the total transmissivity at ν is the product of all the transmissivities since a random distribution is being considered, i.e.,

$$\gamma(\nu) = \prod_{j=1}^{\infty} \gamma_j(\nu) \quad (3.5.4)$$

where $\gamma_j(\nu)$ is the transmissivity at ν due to the n_j lines in the interval δ_j .

Wyatt et al. (1962), have given analytic expressions for the transmissivities due to the direct and wing contributions for the Lorentz line shape. Assuming a Lorentz line shape then,

$$\gamma_\tau(\nu) = \frac{1}{\delta} \int_{\delta_\tau} \exp - \frac{S_\tau \alpha_L}{\pi} \frac{u}{(\nu - \nu_\tau)^2 + \alpha_L^2} d\nu_\tau \quad (3.5.5)$$

Now let

$$\begin{aligned} \xi_\tau &= \frac{S_\tau u}{\pi \alpha_L} \\ \rho &= 2\alpha_L/\delta \\ \eta &= 2y/\delta \\ \epsilon &= 2z/\delta \\ y &= \nu_\tau - \nu_0 - 1/2 \delta \\ z &= \nu - \nu_0 - 1/2 \delta \end{aligned} \quad (3.5.6)$$

where the frequency interval is $[\nu_0, \nu_0 + \delta]$. Thus Eq. (3.5.5) may now be written

$$\gamma_\tau(\nu) = \frac{1}{2} \int_{-1}^{+1} \exp \left[- \frac{\rho^2 \xi_\tau}{(\epsilon - \eta)^2 + \rho^2} \right] d\eta \quad (3.5.7)$$

If the assumption is made that the interval δ_τ is large compared to the half-widths of the lines, i.e. $(\epsilon-\eta)^2 \gg \rho^2$, then Eq. (3.5.7) may be easily integrated to give the transmissivity contribution due to the wings, i.e.,

$$\begin{aligned} \gamma_\tau(\nu) = & \frac{1}{2} \left\{ (\epsilon+1) \exp\left(-\frac{A}{(\epsilon+1)^2}\right) - (\epsilon-1) \exp\left(-\frac{A}{(\epsilon-1)^2}\right) \right\} \\ & - \frac{1}{2} \pi^{1/2} A^{1/2} \left[\operatorname{erf}\left(\frac{A^{1/2}}{\epsilon-1}\right) - \operatorname{erf}\left(\frac{A^{1/2}}{\epsilon+1}\right) \right] \end{aligned} \quad (3.5.8)$$

where $A = \rho^2 \xi_\tau$. For the direct contribution to $\gamma_\tau(\nu)$, if the frequency is taken at the center of the interval then

$$\gamma_\tau(\nu) = \Omega(\xi_\tau, \rho) \quad (3.5.9)$$

where

$$\begin{aligned} \Omega(\xi, \rho) = & \exp\left[-\frac{\xi \rho^2}{(1+\rho)}\right] \\ & - \frac{1}{2} \rho \xi \exp\left(-\frac{1}{2} \xi\right) \left[I_0\left(\frac{1}{2} \xi\right) + I_1\left(\frac{1}{2} \xi\right) \right] (\pi - \psi) \\ & + 2\rho \exp\left(-\frac{1}{2} \xi\right) \sum_{n=1}^{\infty} I_n\left(\frac{1}{2} \xi\right) \sin n\psi \\ & + \rho \xi \exp\left(-\frac{1}{2} \xi\right) \sum_{n=1}^{\infty} \left[I_n\left(\frac{1}{2} \xi\right) + I_{n+1}\left(\frac{1}{2} \xi\right) \right] \frac{\sin n\psi}{n} \end{aligned} \quad (3.5.10)$$

$\psi = 2 \tan^{-1} \rho$ and I_n denotes the Bessel function of imaginary argument

and order n .

A similar procedure to the above may be developed for the Doppler line shape. The transmissivity for this line shape is given by

$$\gamma_{\tau}(\nu) = \frac{1}{\delta} \int_{\delta_{\tau}} \exp \left[- \frac{S_{\tau} u (\ln 2)^{1/2}}{\alpha_D \pi^{1/2}} \exp \left(- \frac{(\nu - \nu_{\tau})^2 \ln 2}{\alpha_D^2} \right) \right] d\nu_{\tau} \quad (3.5.11)$$

Now let

$$\xi_{\tau} = \frac{S_{\tau} u}{\alpha_D} \left(\frac{\ln 2}{\pi} \right)^{1/2}$$

$$y = \nu_{\tau} - \nu_0 - \frac{1}{2} \delta$$

$$\eta = 2y/\delta$$

$$\rho = \frac{2\alpha_D (\ln 2)^{1/2}}{\delta}$$

where the frequency interval is $[\nu_0, \nu_0 + \delta]$, and Eq. (3.5.11) becomes

$$\gamma_{\tau}(\nu) = \frac{1}{2} \int_{-1}^{+1} \exp \left[- \xi_{\tau} \exp \left(- \frac{\eta^2}{\rho^2} \right) \right] d\eta \quad (3.5.13)$$

Unfortunately no analytic value for this integral appears to be available. As noted in Section 3.4 the absorption coefficient evaluated using the Doppler line shape falls off very rapidly with the distance from the line center, the wings being given by the Lorentz formula. Thus if the transmissivity due to the wings needs to be evaluated Eq.

(3.5.8) would be satisfactory. The analytic expression for the transmissivity using the Lorentz line shape, Eq. (3.5.9), is a rather involved expression involving infinite sums of Bessel functions of imaginary argument. Also Eq. (3.5.13) appears to have no analytic solution. For the line profile involving collisional, Doppler, and natural broadening, viz., Eq. (3.4.1) the expression becomes even more involved,

$$\gamma_{\tau}(\nu) = \frac{1}{\delta} \int_{\delta_{\tau}} \exp \left[-\frac{k_0 a u}{\pi} \int_{-\infty}^{\infty} \frac{e^{-x^2}}{a^2 + (\omega - x)^2} dx \right] d\nu_{\tau} \quad (3.5.14)$$

In view of the complexity of these three expressions for the transmissivity, it was decided to devise a numerical method for evaluating them. Equations (3.5.7) and (3.5.13) may be evaluated numerically using Legendre-Gauss quadrature. Unfortunately, due to the nature of the integrands in both Eqs. (3.5.7) and (3.5.13), it is necessary to divide the interval into subintervals and then to apply the quadrature formula in each subinterval. Seven subintervals were chosen and spaced as follows,

$$0.0, 0.001, 0.005, 0.01, 0.05, 0.1, 0.5, 1.0 \quad (3.5.7)$$

The seven-point quadrature formula applied to Eq. (3.5.7) using the above subintervals gave exactly the same values as given by Wyatt et al. (1962), who used Eq. (3.5.10).

Unfortunately, no tabulations for Eq. (3.5.13) have been located. However, since the difference between the 7-, 15-, and 32-point quadrature formulae is so small as to be of probably no practical significance for this work, the 7-point formula should prove satisfactory. In the case of Eq. (3.5.13) ρ is constant (relating to Doppler broadening) once δ has been set, unlike the ρ in Eq. (3.5.7) (relating to Lorentz broadening) which varies with pressure. Equation (3.5.14) may be evaluated using the numerical technique outlined above, except that the absorption coefficient cannot be evaluated as easily as in Eqs. (3.5.7) and (3.5.13). The techniques discussed in Eqs. (3.4.6) and (3.4.7) would have to be used.

One disadvantage of the quasirandom model is that it underestimates the transmissivity of the Q-branches. There are two reasons for this. The lines of a Q-branch are grouped close together and are neither uniformly nor randomly distributed over the averaging interval. This will cause the transmissivity to be underestimated (or the absorptivity to be overestimated). Also the lines of a Q-branch are fairly evenly spaced. Thus the contributions due to the wings of the lines will cause the transmissivity to be underestimated. This will be pressure dependent decreasing in importance at low pressures.

3.6 APPROXIMATIONS USED IN SOLVING THE RADIATIVE TRANSFER EQUATION

3.6.1 The Curtis-Godson Approximation

In the denser parts of the atmosphere where collisional broaden-

ing is the most important broadening mechanism then the Lorentz formula gives the appropriate line shape. The absorption coefficient associated with this line shape is

$$k_\nu = \frac{S\alpha_L}{\pi} \frac{1}{(\nu - \nu_0)^2 + \alpha_L^2} \quad (3.6.1)$$

where α_L is the line half-width due to collisional broadening, S is the integrated line intensity and ν_0 the frequency of the line center. Collisional broadening has been discussed at some length in Section 3.4.2. As noted in that section α_L depends on both the pressure and temperature, viz.,

$$\alpha_L = \alpha_L^0 \frac{p}{p_0} \sqrt{\frac{T_0}{T}} \quad (3.6.2)$$

It is evident that for an atmospheric layer where pressure and temperature vary over the layer the absorption coefficient cannot be evaluated using Eq. (3.6.1). In practice sufficiently thin layers must be considered over which pressure and temperature remain approximately constant. However, Curtis (1952), and Godson (1953) proposed an approximate method for dealing with thicker layers. If the gas considered has a constant mixing ratio, e.g., carbon dioxide, then the absorption coefficient may be evaluated for the layer using Eq. (3.6.1) with a mean pressure \bar{p} used in Eq. (3.6.2) to derive a mean line half-width $\bar{\alpha}_L$.

This approximation becomes exact for the so-called "thick-layer" and

"thin-layer" cases.

The thin-and thick-layer approximations are relatively simple to derive. The mean absorption for a single line over some interval $\Delta\nu$ may be written.

$$\bar{A} = \frac{1}{\Delta\nu} \int_{-\infty}^{\infty} \left\{ 1 - \exp \left[- \int_{u_1}^{u_2} k_\nu du \right] \right\} d\nu \quad (3.6.3)$$

where u is the amount of absorbing gas per unit area. Substituting for k_ν from Eq. (3.6.1) gives

$$\bar{A} = \frac{1}{\Delta\nu} \int_{-\infty}^{\infty} \left\{ 1 - \exp \left[- \frac{1}{\pi} \int_{u_1}^{u_2} \frac{S\alpha_L du}{(\nu - \nu_0)^2 + \alpha_L^2} \right] \right\} d\nu \quad (3.6.4)$$

Expanding the exponential term in the integrand of Eq. (3.6.3) gives

$$\bar{A} = \frac{1}{\Delta\nu} \int_{-\infty}^{\infty} \left\{ \int_{u_1}^{u_2} k_\nu du - \frac{1}{2!} \left(\int_{u_1}^{u_2} k_\nu du \right)^2 + \dots \right\} d\nu$$

If the absorption is small, as in the thin-layer case,

$$\begin{aligned} \bar{A} &\approx \frac{1}{\Delta\nu} \int_{-\infty}^{\infty} \int_{u_1}^{u_2} k_\nu du d\nu \\ &= \frac{1}{\Delta\nu} \int_{u_1}^{u_2} \int_{-\infty}^{\infty} k_\nu d\nu du = \frac{1}{\Delta\nu} \int_{u_1}^{u_2} S du \end{aligned} \quad (3.6.5)$$

where S is the line intensity. S is generally given in $\text{cm}^{-1} (\text{atm cm})^{-1}$ for a particular temperature. If an isothermal layer is considered then Eq. (3.6.5) becomes

$$\bar{A} \approx \frac{1}{\Delta\nu} S(u_2 - u_1) \quad (3.6.6)$$

For a sufficiently thick layer of absorbing gas complete absorption will occur near the line center and thus increasing the thickness of the layer will only increase the absorption in the wings of the line. In this case then $(\nu - \nu_0)^2 > \alpha_L^2$ since only wings are being considered and thus α_L^2 can be neglected in the denominator of Eq. (3.6.1). Using Eq. (3.6.4) the average absorption for the thick-layer case can now be written,

$$\bar{A} = \int_{-\infty}^{\infty} \left\{ 1 - \exp \left[- \frac{1}{\pi} \int_{u_1}^{u_2} \frac{S \alpha_L du}{(\nu - \nu_0)^2} \right] \right\} d\nu \quad (3.6.7)$$

Letting $(\nu - \nu_0) = z$, Eq. (3.6.5) becomes

$$\bar{A} \approx \frac{1}{\Delta\nu} \int_{-\infty}^{\infty} \left\{ 1 - \exp \left(- \frac{c}{z^2} \right) \right\} dz \quad (3.6.8)$$

where

$$c = \frac{1}{\pi} \int_{u_1}^{u_2} S \alpha_L du$$

Writing \bar{A} in the form

$$\bar{A} \approx \frac{1}{\Delta\nu} \left\{ \int_{-\infty}^0 (1 - e^{-c/z^2}) dz + \int_0^{\infty} (1 - e^{-c/z^2}) dz \right\}$$

putting $z = 1/y$, and integrating by parts, it is easy to show that

$$\begin{aligned} \bar{A} &\approx \frac{1}{\Delta\nu} 2 \sqrt{c} \Gamma\left(\frac{1}{2}\right) = \frac{2\sqrt{c\pi}}{\Delta\nu} \\ &= \frac{2}{\Delta\nu} \left(\int_{u_1}^{u_2} S\alpha_L du \right)^{1/2} \end{aligned} \quad (3.6.9)$$

For a homogeneous layer Eq. (3.6.9) reduces to

$$\bar{A} \approx \frac{2}{\Delta\nu} (S(u_2-u_1)\alpha_L)^{1/2} \quad (3.6.10)$$

This approximation for \bar{A} is sometimes called the "opaque line center approximation." The Curtis-Godson approximation hinges on choosing a mean α_L , say $\bar{\alpha}_L$, in Eq. (3.6.10) such that the \bar{A} 's evaluated from Eqs. (3.6.9) and (3.6.10) are equal. It is also desirable to have the Curtis-Godson approximation valid for the thin-layer case. Then

$$S(u_2-u_1)\bar{\alpha}_L = \int_{u_1}^{u_2} S\alpha_L du \quad (3.6.11)$$

consequently

$$\begin{aligned}
 \bar{\alpha}_L &= \frac{\int_{u_1}^{u_2} S \alpha_L du}{S(u_2 - u_1)} \\
 &= \frac{\int_{u_1}^{u_2} S \alpha_L du}{\int_{u_1}^{u_2} S du}
 \end{aligned}
 \tag{3.6.12}$$

using Eqs. (3.6.5) and (3.6.6). If a fairly thin layer is chosen then it may be assumed to be isothermal. Now

$$\alpha_L = \alpha_L^0 \frac{p}{p_0} \sqrt{\frac{T_0}{T}}$$

where α_L^0 is the line half-width at some standard pressure p_0 and standard temperature T_0 . Therefore Eq. (3.6.12) becomes

$$\bar{p} = \frac{\int_{u_1}^{u_2} p du}{\int_{u_1}^{u_2} du} = \frac{\int_{u_1}^{u_2} p du}{(u_2 - u_1)}
 \tag{3.6.13}$$

since the layer (u_2, u_1) is isothermal. If a constant mixing ratio is assumed, as is true for carbon dioxide in the earth's atmosphere, then $u = rp$ where r is a constant. Hence Eq. (3.6.13) now becomes

$$\bar{p} = \frac{p_1 + p_2}{2}
 \tag{3.6.14}$$

Equations (3.6.13) and (3.6.14) are true in the limiting cases of thin

layers and thick layers, but are only approximate between these two cases.

The accuracy of the Curtis-Godson approximation has been checked by Godson (1953, 1955) and Kaplan (1959) for transmissivity and flux calculations and by Walshaw and Rodgers (1962) for heating-rate calculations. It has been found reasonably satisfactory for transmissivities and Walshaw and Rodgers state that it is satisfactory for heating-rate calculations involving carbon dioxide.

In this study the Curtis-Godson approximation is used, since the Walshaw and Rodgers check seem satisfactory. It will be used in the form given by Eq. (3.6.14), care being taken that the temperature variations over the layer considered are kept reasonably small.

3.6.2 Approximate Methods for Performing the Angular Integration in the Flux Equation

As discussed in Section 3.1 the determination of the upward and downward fluxes requires an integration over frequency, angle, and optical thickness. For example,

$$\begin{aligned}
 F_+(\tau) &= 2\pi \int_{\nu} E(\nu, T_g) \int_0^{+1} \gamma_{\nu}(\tau_g, \tau) \mu \, d\mu \, d\nu \\
 &- 2\pi \int_{\nu} \int_{\tau}^{\tau_g} E(\nu, T_t) \int_0^{+1} \frac{\partial \gamma_{\nu}(t, \tau)}{\partial t} \mu \, d\mu \, dt \, d\nu
 \end{aligned}
 \tag{3.6.15}$$

Using a model for an absorption band, such as the quasirandom model

(cf., 3.5.2), makes the integration over frequency relatively simple. This is because the transmissivity obtained from such a model is an average transmissivity for a finite frequency interval. It would be convenient if the angular integration occurring in Eq. (3.6.15) could be disposed of, once and for all. The astrophysicists in their work perform the angular integration using Gaussian quadrature.

Consider only the parts of Eq. (3.6.15) involving angular integration, viz.,

$$2 \int_0^{+1} e^{-t/\mu} \mu \, d\mu$$

where t has been written for $(\tau_g - \tau)$ or $(t - \tau)$ as the case may be. By introducing $y = 2\mu - 1$,

$$2 \int_0^{+1} e^{-t/\mu} \mu \, d\mu = \int_{-1}^{+1} e^{-t/(1/2(y+1))} \frac{y+1}{2} dy \quad (3.6.16)$$

Legendre-Gauss quadrature may now be applied to Eq. (3.6.16) to give

$$\begin{aligned} \int_{-1}^{+1} e^{-t/(1/2(y+1))} \frac{y+1}{2} dy &\approx \sum_{i=1}^n H_i e^{-t/(1/2(y_i+1))} \frac{y_i+1}{2} \\ &= \sum_{i=1}^n H_i e^{-t/z_i} z_i \end{aligned} \quad (3.6.17)$$

where H_i are the appropriate weights and $z_i = (y_i+1)/2$ with y_i the Gaussian abscissae.

It would be more convenient if an average value for $1/\mu$, say ζ , could be determined such that

$$2 \int_0^{+1} e^{-(t-\tau)/\mu} \mu \, d\mu = \gamma_v(t, \tau) \zeta \quad (3.6.18)$$

where

$$\gamma_v(t, \tau) \zeta = e^{-(t-\tau)\zeta}$$

Now

$$\int_0^{+1} e^{-(t-\tau)/\mu} \mu \, d\mu = \text{Ei}_3(t-\tau)$$

where Ei_3 is the third exponential integral (cf., 3.1). Roberts (1930) noting the similarity between 2Ei_3 and an exponential suggested using $\zeta = 3/2$. Elsasser (1942) evaluating transmissivities using his band model found that $\zeta = 5/3$ (or 1.66) appeared to give the best results. The value $\zeta = 5/3$ is the value generally quoted in the literature.

If ζ is determined from the transcendental equation

$$2\text{Ei}_3(t) = e^{-t\zeta}$$

then ζ ranges from 1 to 2 for t varying from zero to infinity. It is

possible using least squares to determine a suitable ζ , i.e., one which minimizes

$$\int_0^{\infty} (2Ei_3(t) - e^{-t\zeta})^2 dt$$

or makes

$$\frac{\partial}{\partial \zeta} \int_0^{\infty} (2Ei_3(t) - e^{-t\zeta})^2 dt = 0 \quad (3.6.19)$$

After some manipulation Eq. (3.6.19) reduces to

$$24(1+\zeta)\ln(1+\zeta) + 3\zeta^3 - 13\zeta^2 - 24\zeta = 0 \quad (3.6.20)$$

The value of ζ obtained by solving Eq. (3.6.20) is 1.543. However, it is dangerous to use this value of ζ as the effective value in Eq. (3.6.18) since, if a molecular band model is used, a mean transmissivity for a finite interval is used for $\gamma_\nu(t, \tau)$. This mean transmissivity has already involved an integration of $e^{-(t-\tau)/\mu}$ over frequency, viz.,

$$\gamma_\nu(t, \tau) = \frac{1}{\delta} \int_{\delta} e^{-(t-\tau)/\mu} d\nu$$

It would be desirable to compare these approximations experimentally. The method using Gaussian quadrature should be the most accurate. Thus in Section 4.1.2, a quantity proportional to the flux emitted by a slab to space is evaluated for various pressures and optical masses using 4- and 2-point Gaussian quadrature as well as for $\zeta = 1.54$ and 1.66.

4. EVALUATION OF THE COOLING RATES IN THE STRATOSPHERE AND MESOSPHERE DUE TO CARBON DIOXIDE

4.1 TRANSMISSIVITY DETERMINATION USING THE QUASIRANDOM MODEL

4.1.1 Transmissivity Determination and Comparison with Experimental Measurements

The quasirandom model was discussed in some detail in Section 3.5.2. This section deals with the practical evaluation of the transmissivities and the comparison with laboratory measurements.

The interval, over which the average transmissivity was evaluated, was chosen as 5 cm^{-1} . This gave 70 intervals covering the region of interest, 505 to 855 cm^{-1} . This choice of interval gives a reasonable resolution without involving excessive ~~com~~puting time.

The line intensities and positions were computed using the procedure described in Appendix B. These results were punched on cards which were then used as the data for a program which,

- (1) scanned across the spectrum of lines, dividing it into 5 cm^{-1} intervals;
- (2) grouped the lines in each interval into 5 intensity subgroups; and
- (3) evaluated the mean intensity and counted the number of lines in each subgroup.

This procedure was carried out for the six temperatures for which the line intensities were evaluated, and again, only shifting the measure-

ment grid by 2.5 cm^{-1} (staggered grid). These results were also punched on cards to provide an input for the transmissivity program.

The transmissivities were calculated using the procedures outlined in Section 3.5.2. Since computations were available for only six temperatures, viz., 175, 200, 225, 250, 275, and 300°K , it was necessary to place the temperature at which the transmissivity was to be evaluated into one of six groups defined by, 162.5 to 187.5, 187.5 to 212.5, 212.5 to 237.5, 237.5 to 262.5, 262.5 to 287.5, and 287.5 to 312.5. The line profile used in the transmissivity calculations were chosen according to the procedure given in Section 3.4.7.

Wyatt et al. (1962) used the Benedict modification of the Lorentz line shape in the great majority of their calculations (cf., 3.4.2). Some of the transmissivities were calculated using this modification for the wings. It gives an exponential die-away for the wings and only applies at distances exceeding 2.5 cm^{-1} from the line center.

Most of the experimental results give absorptivities rather than transmissivities, and usually the total absorption for the band. The transmissivities calculated above are average transmissivities over a 5-cm^{-1} interval. Thus it is easy to calculate the integrated transmissivity or absorptivity for the band to compare with other calculations and experimental measurements.

The experimental measurements made at Ohio State University and recently published by Burch et al. (1962a,b) are compared with the

theoretical calculations. Yamamoto and Sasamori (1958) have also carried out calculations of the integrated absorptivity for the 15-micron carbon dioxide bands using a fairly detailed calculation scheme which would be rather difficult to adapt for machine computation.

Figure 2 displays the results of the calculation and the measurements of Burch et al. (1962b). Burch et al. (1962b) used a wide slit in their measurements since they were interested in obtaining the integrated absorptivity for the whole band and for fairly large sections of the band. The calculations are presented in the form of a histogram since the calculated transmissivities are average values for an interval, in this case 5 cm^{-1} . Use of the quasirandom model apparently underestimates the transmissivities for the Q-branches. At low pressures the model appears to underestimate the transmissivity for the whole band as shown in Figure 2(c). However, at pressures as low as this, the experimental error becomes greatest. Table VII presents values for $\int A_\nu d\nu$ calculated using the quasirandom model and taken from the experimental results of Burch et al. (1962b). A_ν is the absorptivity. The integration extends from 545 to 855 cm^{-1} .

Wyatt et al. (1962) have suggested computing the transmissivities using the staggered and unstaggered grids, then taking a running mean of both sets of values. This should give improved accuracy only if the transmissivity for a small interval were desired but should have very little effect on $\int A_\nu d\nu$. This was verified by calculation.

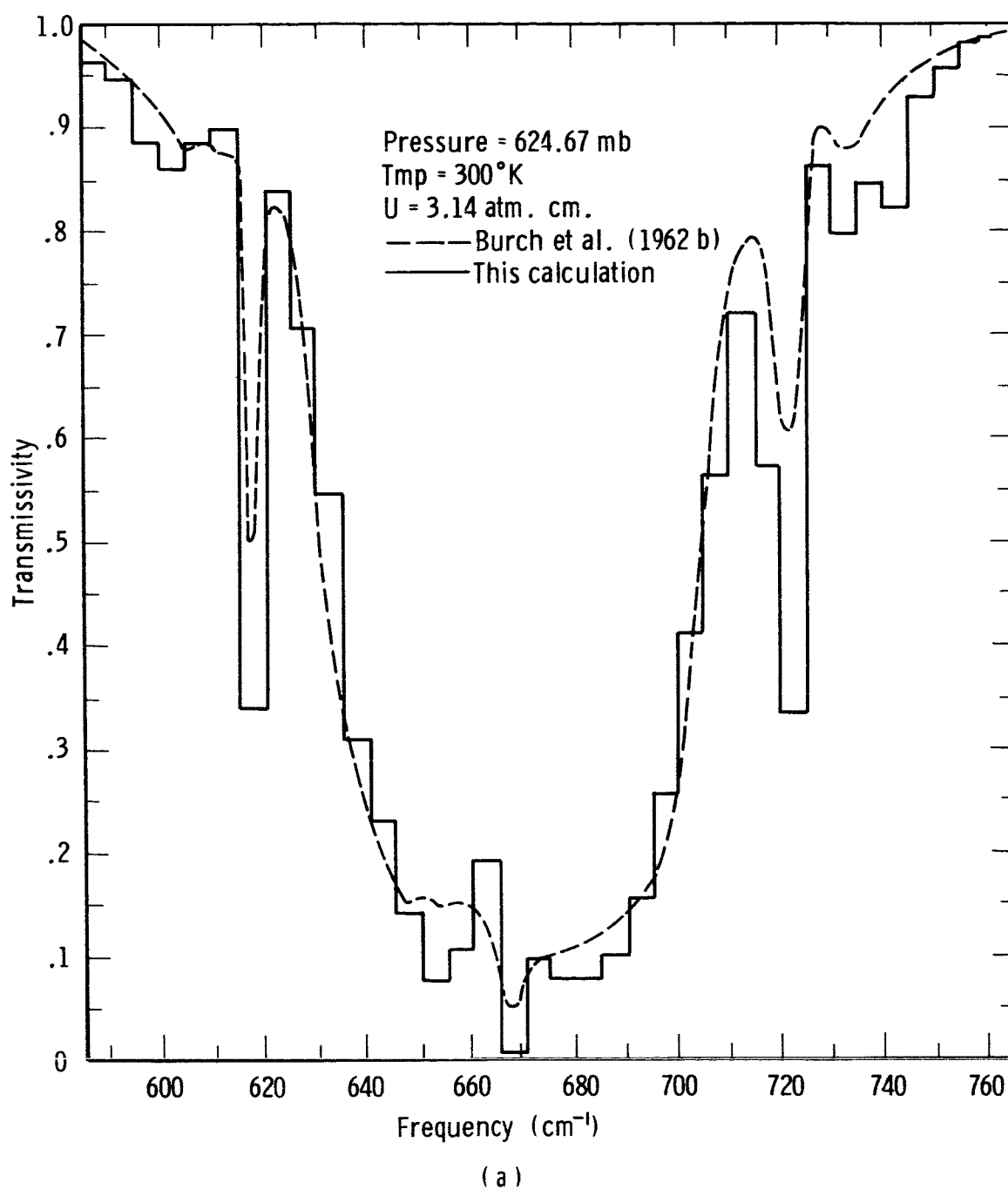


Figure 2. Calculated and experimental transmissivities vs. frequency for different pressures and optical masses.

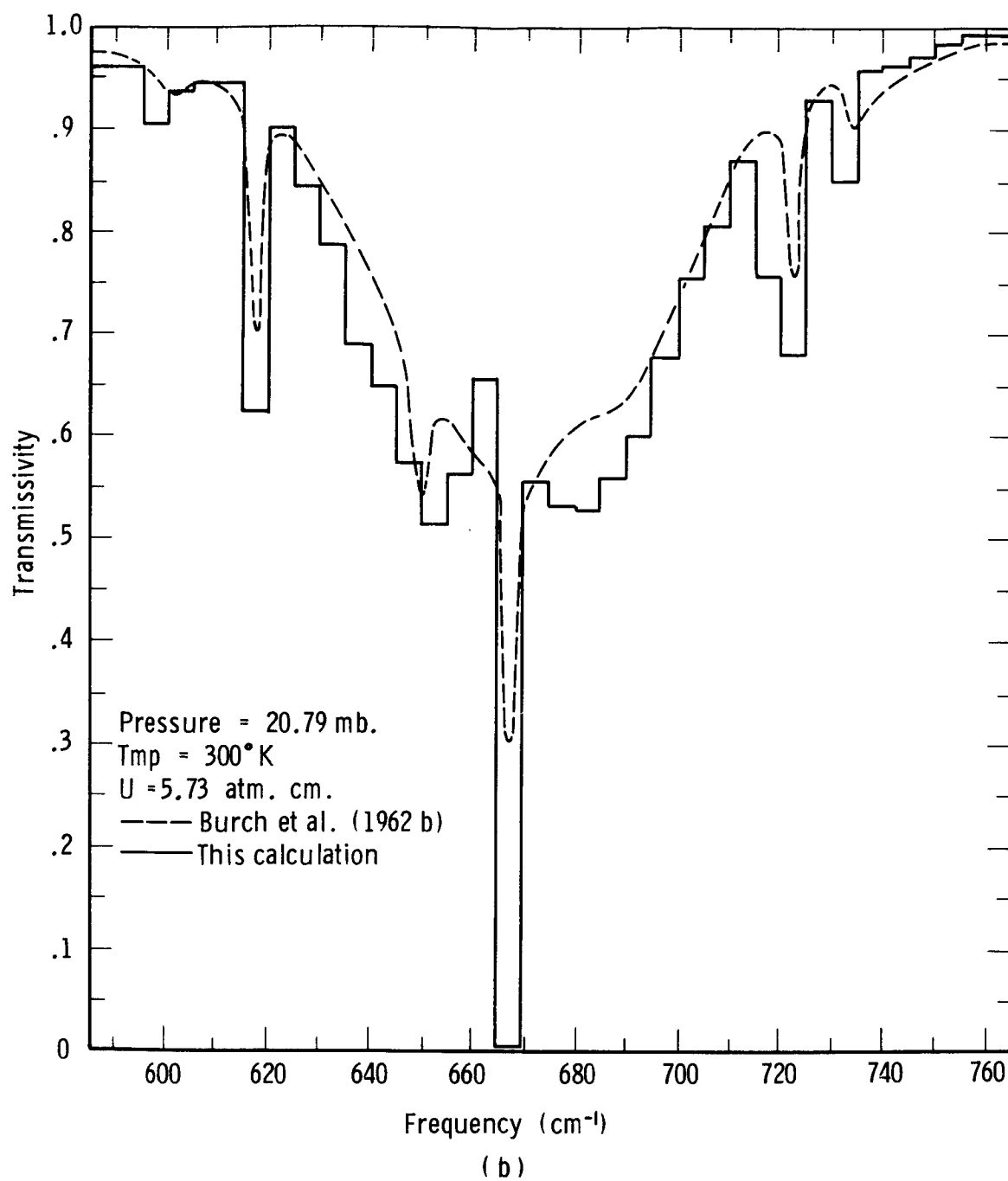


Figure 2 (Continued)

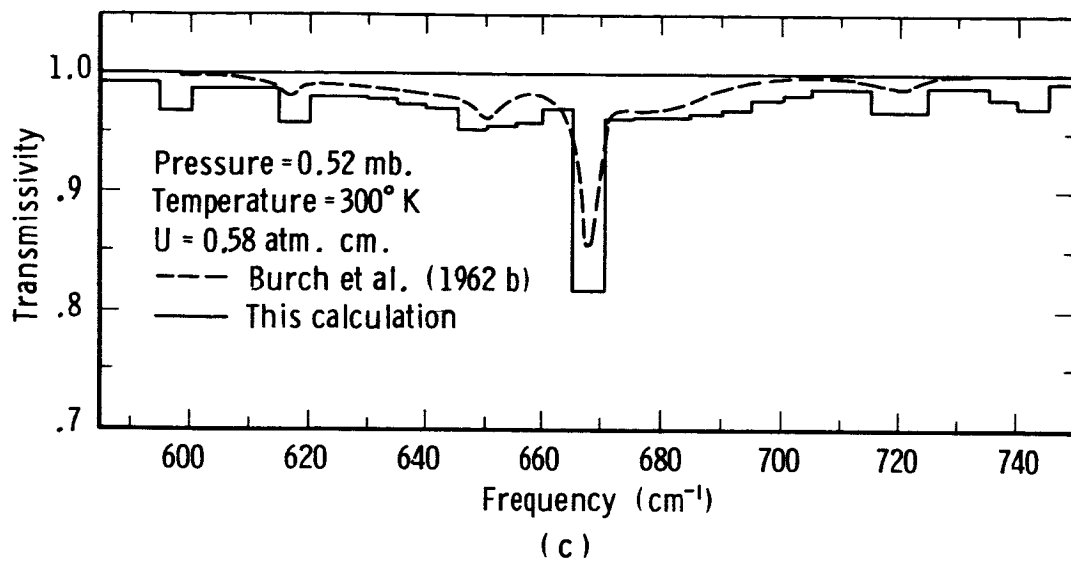


Figure 2 (Concluded)

TABLE VII

COMPARISON BETWEEN VALUES OF $\int A_\nu d\nu$ CALCULATED USING THE QUASIRANDOM MODEL, AND EXPERIMENTALLY MEASURED BY BURCH ET AL. (1962b)

Pressure (mb)	Temperature (°C)	Optical Mass (atm cm)	$\int A_\nu d\nu$ (cm ⁻¹)	
			Experimental	Theoretical
0.520	26.5	0.58	3.37	5.80
1.386	27	1.53	8.86	10.07
5.025	27	5.56	21.7	26.71
8.377	27	9.20	32.6	39.34
20.793	27	5.73	34.6	43.29
40.254	27	5.73	43.8	53.95
84.772	27	5.73	54.7	67.33
207.93	27	5.73	69.5	83.62
405.20	27	5.73	81.9	93.98
1022.3	27	5.73	95.3	103.86

Figure 3 displays $\int A_\nu d\nu$ vs. the optical mass (in atm cm) for pressures of 1 atm and 0.2 atm. In this figure the results of this calculation, the calculation of Yamamoto and Sasamori (1958) and the experimental measurements of Burch et al. (1962b) are presented. It is evident that Yamamoto and Sasamori's calculations agree best with the experimental results. Also the results given by Wyatt et al. (1962) agree more closely with the experimental results than this calculation does. In both these calculations the strength of the second strongest band (cf., Appendix B) is taken as 16.6 cm⁻¹ (atm cm)⁻¹ while Madden (1961) gives 30 cm⁻¹ (atm cm)⁻¹ for this band. Madden's value was used in the present calculations.

The Benedict modification of the Lorentz formula for the wings

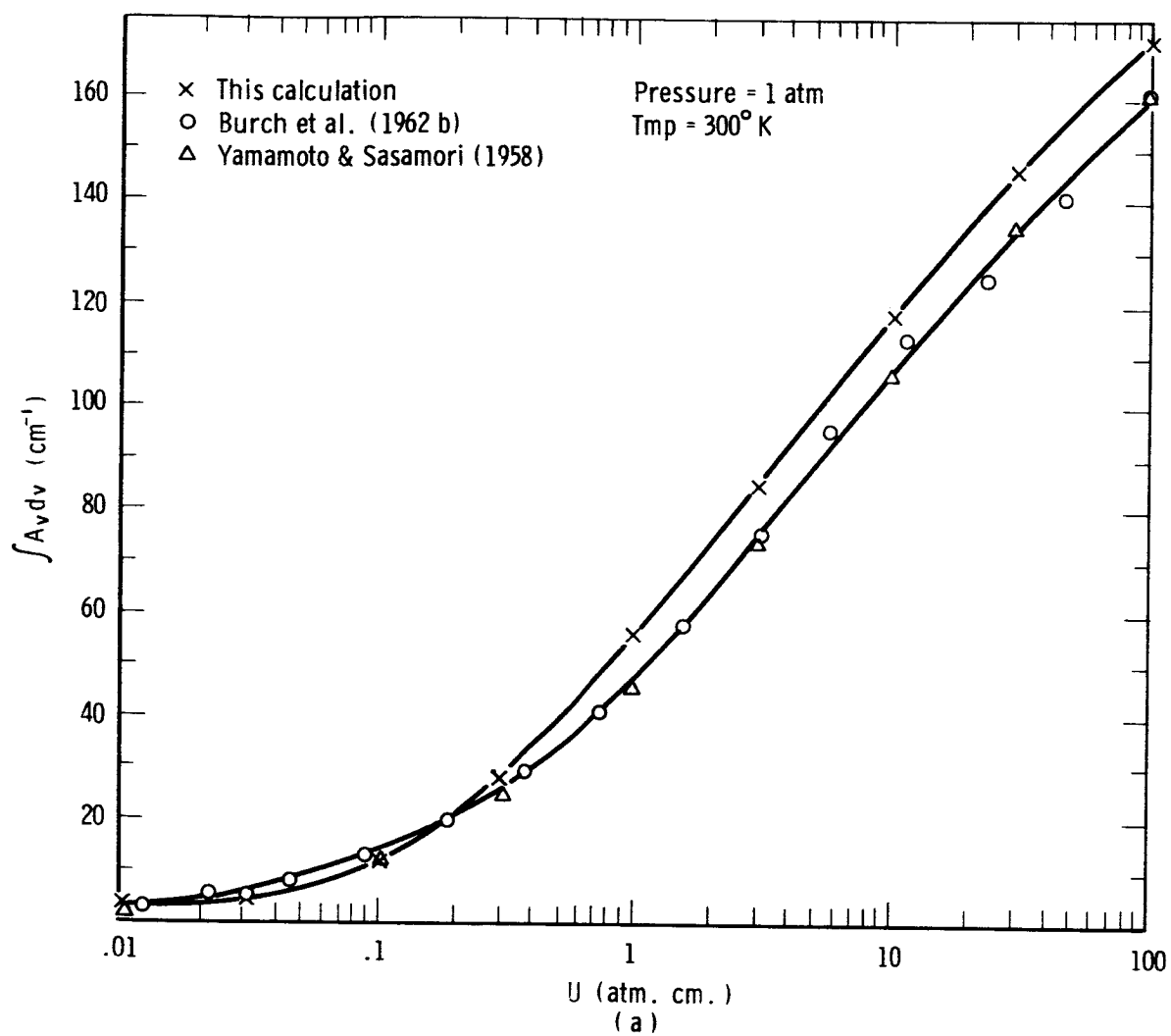


Figure 3. $\int A_v dv$ vs. optical mass for pressures of 1 and 0.2 atm.

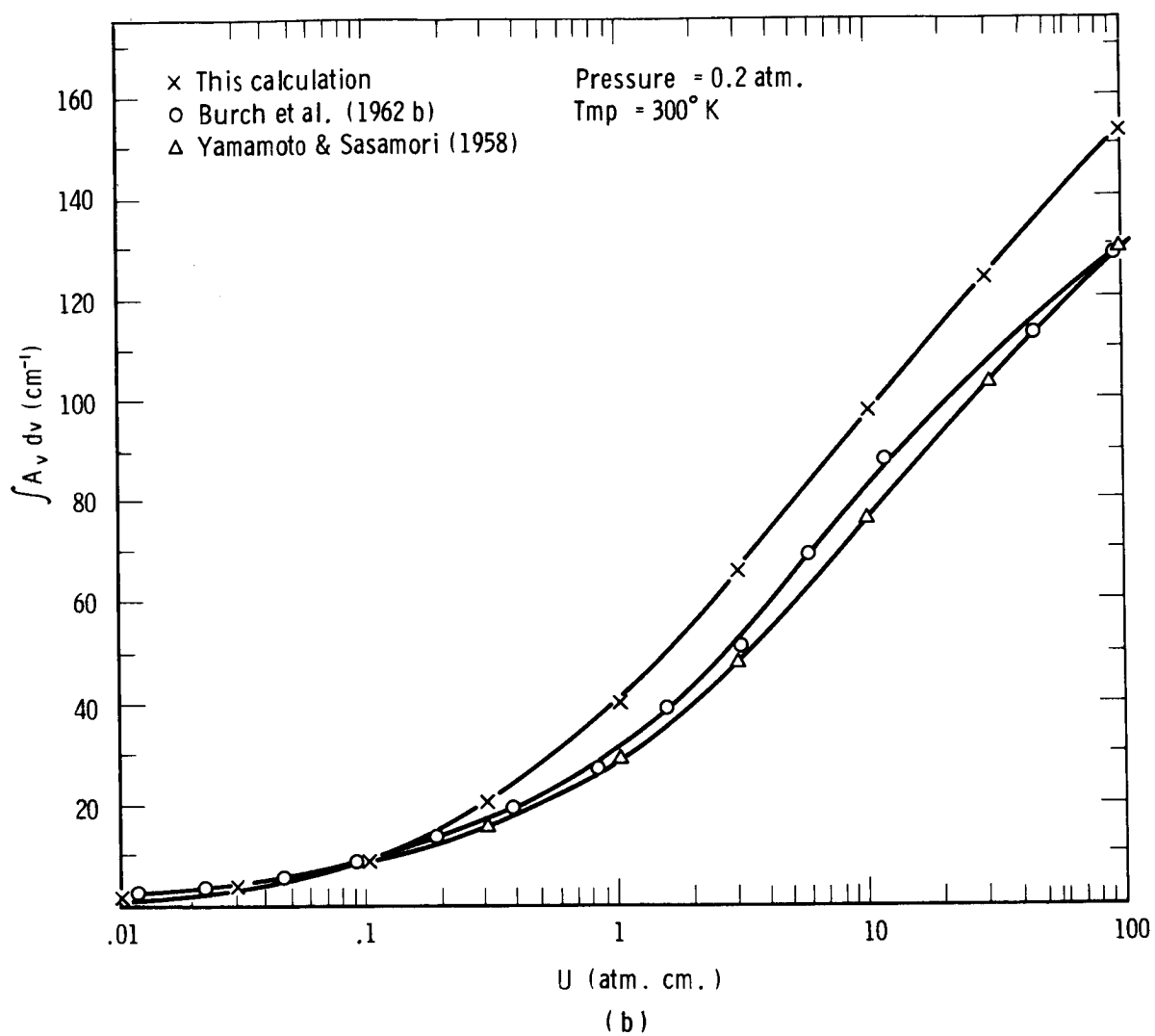


Figure 3 (Concluded)

will increase the transmissivity slightly or decrease the absorptivity a little. On testing this modification of the Lorentz formula, it was found that it only reduced the integrated absorptivity $\int A_\nu d\nu$ by between 1 and 2 percent. This is inconsequential.

It is disappointing that the calculated transmissivities are not closer to the experimental values. It would be possible, but not very satisfying, to apply an empirical correction to the transmissivities calculated for the Q-branches. If the frequency interval over which the average transmissivity is determined using the quasirandom model (in this case 5 cm^{-1}) were reduced to, say, 1 cm^{-1} , then a corresponding increase in accuracy should be evident. Unfortunately, this would increase the computing time considerably. Since this study is essentially a pilot investigation, it was felt that this could be investigated later and the transmissivities calculated using the 5 cm^{-1} intervals accepted, realizing their limitations.

4.1.2 Test of Approximate Methods for Performing the Angular Integration in the Flux Equation

The theoretical bases for the various approximate methods for performing the angular integration in the flux equation were discussed in Section 3.6.2.

The equation for the upward directed flux may be written (cf., Section 3.1)

$$\begin{aligned}
F_+(\tau) &= 2\pi \int_{\nu} E(\nu, T_g) \int_0^{+1} \gamma_{\nu}(\tau_g, \tau) \mu \, d\mu \, d\nu \\
&+ 2\pi \int_{\nu} \int_{\tau_g}^{\tau} E(\nu, T_t) \int_0^{+1} \frac{\partial \gamma_{\nu}(t, \tau)}{\partial t} \mu \, d\mu \, dt \, d\nu
\end{aligned}$$

If only a slab (τ_1, τ_2) is considered, then the upward directed flux at τ_1 due to the slab (τ_1, τ_2) where $\tau_1 < \tau_2$ is given by,

$$F_+^*(\tau_1) = 2\pi \int_{\nu} \int_{\tau_2}^{\tau_1} E(\nu, T_t) \int_0^{+1} \frac{\partial \gamma_{\nu}(t, \tau_1)}{\partial t} \mu \, d\mu \, dt \, d\nu$$

If it is assumed that a mean value of E can be used for the slab (τ_1, τ_2) and also that E does not vary much with frequency then

$$\begin{aligned}
F_+(\tau_1) &= 2\pi \bar{E} \int_{\nu} \int_{\tau_2}^{\tau_1} \int_0^{+1} \frac{\partial \gamma_{\nu}(t, \tau_1)}{\partial t} \mu \, d\mu \, dt \, d\nu \\
&= 2\pi \bar{E} \int_{\nu} \int_0^{+1} (\gamma_{\nu}(\tau_1, \tau_1) - \gamma_{\nu}(\tau_2, \tau_1)) \mu \, d\mu \, d\nu \\
&\quad (4.1.1) \\
&= \pi \bar{E} \int_{\nu} \left[1 - 2 \int_0^{+1} \gamma_{\nu}(\tau_2, \tau_1) \mu \, d\mu \right] d\nu \\
&= \pi \bar{E} \int_{\nu} \left[1 - 2 \int_0^{+1} e^{-(\tau_2 - \tau_1)/\mu} \mu \, d\mu \right] d\nu
\end{aligned}$$

Now let

$$I^* = \int_v \left[1 - 2 \int_0^{+1} e^{-(\tau_2 - \tau_1)/\mu} \mu d\mu \right] dv \quad (4.1.2)$$

I^* is proportional to the flux emitted by the slab to space. The angular integration in Eq. (4.1.2) was performed using 4- and 2-point Gaussian quadrature as well as for $\xi = 1.543$ and 1.66. The frequency integration was from 577.5 to 757.5 cm^{-1} , since the transmissivities from 507.5 to 577.5 cm^{-1} and from 757.5 to 852.5 cm^{-1} were unity in all the cases considered. Table VIII lists the values of I^* obtained using Eq. (4.1.2).

TABLE VIII

VALUES OF I^* OBTAINED USING VARIOUS APPROXIMATIONS
FOR THE ANGULAR INTEGRATION

(I^* is in cm^{-1} sterad and the temperature is 175°K)

	Gaussian		$\xi = 1.543$	$\xi = 1.66$
	4-point	2-point		
P = 1013 mb U = 25.0 atm cm	101.92	102.45	100.26	101.78
P = 1013 mb U = 0.02 atm cm	4.01	4.11	3.33	3.57
P = 20 mb U = 0.6 atm cm	11.22	11.33	10.54	10.93

It is evident from Table VIII that there is very little difference

between the 2- and 4-point Gaussian. $\zeta = 1.66$ gives results closer to the 2- and 4-point Gaussian values than $\zeta = 1.543$, thus confirming Elsasser's (1942) assertions. In this study the 2-point Gaussian quadrature formula is used to obtain acceptable accuracy with minimum computing.

4.1.3 Test of the Validity of Using the Lorentz Line Shape at Pressures Lower than 20 mb

Plass and Fivel (1953) discussed the possibility of using the Lorentz line shape up to heights of 50 km (approximately 0.8 mb). They were able to show that for very strong lines the radiative transfer would be the same as calculated using the Lorentz line shape up to 50 km. The reason is that for a strong line only the transfer in the wings is important. As shown in Eqs. (3.4.6) and (3.4.7) the wings are described by the Lorentz shape for all pressures. Also for weak lines they found the Lorentz line shape was satisfactory up to 50 km. This is because the total emission of a weak line determines the radiation loss. However, for lines of intermediate strength they note that Doppler effects must be considered. Lines of intermediate strength are very important for radiative transfer. It was decided to test the possibility of using the Lorentz line shape at pressures lower than 20 mb (approximately 26.5 km).

Now, as shown in Eq. (4.1.2) the quantity I^* is proportional to the upward flux from the slab (τ_1, τ_2) . This is a convenient quantity

to use in the test of the approximation. Table IX shows the result of the calculation. I^* was determined using 2-point Gaussian quadrature for the angular integration.

TABLE IX
COMPARISON BETWEEN I^* EVALUATED USING THE LORENTZ LINE SHAPE
AND THE LORENTZ BROADENED DOPPLER LINE SHAPE (THE MIXED LINE
SHAPE) AT PRESSURES BELOW 20 MB

Pressure (mb)	Height (km)	Temperature (°K)	Optical Mass (cm^{-2})atm cm	I^* (cm^{-1} sterad)	
				Lorentz	Mixed
20	26.6	275	0.6	18.72	20.78
10	31.2	250	1.5	19.96	21.80
5	36.	250	0.75	10.84	12.70
2.5	41.	250	0.375	5.68	7.67
1.25	46.4	250	0.188	2.92	5.08
0.625	52.	250	0.0938	1.48	3.88
0.313	57.5	250	0.0469	0.60	3.30

The transmissivities for the mixed line shape were evaluated using the procedure outlined in Section 3.4.7.

It is easy to see from Table IX that using the Lorentz line profile introduces considerable error when applied to a whole band at pressures lower than 20 mb. In this study, for pressures lower than 20 mb, the mixed line shape is used according to the procedure of Section 3.4.7. Actually, as seen in Section 3.4.6, Doppler effects begin to be felt as low as 30 mb, but the error involved in neglecting them from 30 to 20 mb is reasonably small.

4.2 EVALUATION OF THE SOURCE FUNCTION FOR VIBRATIONALLY RELAXING CARBON DIOXIDE

In section 3.3 the radiative transfer equation for a vibrationally relaxing gas was discussed and an integral equation was derived for the source function, viz.,

$$\begin{aligned}
 J(\nu, \tau) = & \alpha(\tau)E(\nu, T) + \beta(\tau) \int_{\nu'}^{\nu''} k_{\nu} \int_0^{+1} I(\nu, \tau_0, +\mu) e^{-(\tau_0 - \tau)/\mu} d\mu d\nu \\
 & + \beta(\tau) \int_0^{\tau_0} \int_{\nu'}^{\nu''} k_{\nu} J(\nu, t) \text{Ei}_1(|t - \tau|) d\nu dt
 \end{aligned}
 \tag{4.2.1}$$

As noted in Section 3.3, $J(\nu, \tau)$ is a slowly varying function with frequency and it may be assumed to be approximately constant for the band. Also, as is evident from Eq. (4.2.1) $J(\nu, \tau)$ is isotropic. Using these two facts Eq. (4.2.1) may now be written.

$$\begin{aligned}
 \bar{J}(\tau) = & \alpha(\tau)\bar{E}(T) + \beta(\tau) \int_{\nu'}^{\nu''} k_{\nu} \int_0^{+1} I(\nu, \tau_0, +\mu) e^{-(\tau_0 - \tau)/\mu} d\mu d\nu \\
 & + \beta(\tau) \int_0^{\tau_0} \bar{J}(t) \int_{\nu'}^{\nu''} k_{\nu} \text{Ei}_1(|t - \tau|) d\nu dt
 \end{aligned}
 \tag{4.2.2}$$

where $\bar{J}(\tau)$ and $\bar{E}(T)$ are average values of $J(\nu, \tau)$ and $E(\nu, \tau)$ for the band.

Now k_{ν} is given by the Doppler formula at the heights where vibrational relaxation must be considered. The wings of the lines are

given by the Lorentz formula, but due to the low pressures the wing effects can be neglected to a reasonably good approximation. Thus,

$$k_\nu = \frac{S}{\alpha_D} \left(\frac{\ln 2}{\pi} \right)^{1/2} \exp \left[- \frac{(\nu - \nu_0)^2}{\alpha_D^2} \ln 2 \right] \quad (4.2.3)$$

which is the equation appropriate for a normal distribution. It is well known that as the standard deviation of a normal distribution tends to zero, then the normal distribution may be represented by a Dirac delta function, $\delta(x)$, which has the very useful properties,

$$\int_{-\infty}^{\infty} \delta(x) dx = 1$$

$$\int_{-\infty}^{\infty} \delta(x - x_0) f(x) dx = f(x_0)$$

The Doppler line half-width is quite small, around $5.6 \times 10^{-4} \text{ cm}^{-1}$ and

$$\frac{1}{S} \int_{-\infty}^{\infty} k_\nu d\nu = 1$$

Therefore we may write to a good approximation,

$$k_\nu = S \delta(\nu - \nu_0)$$

In other words, at very low pressures the individual rotational lines of the band, including even the Q-branch, may be considered as separate

and nonoverlapping.

Equation (4.2.2) may now be written

$$\begin{aligned} \bar{J}(\tau) = & \alpha(\tau)\bar{E}(T) + \beta(\tau) \sum_{j=1}^m S_j \int_{-\infty}^{\infty} \delta(\nu - \nu_j) \int_0^{+1} I(\nu, \tau_0, +\mu) e^{-(\tau_0 - \tau)/\mu} d\mu d\nu \\ & + \beta(\tau) \int_0^{\tau_0} \bar{J}(t) \sum_{j=1}^m S_j \int_{-\infty}^{\infty} \delta(\nu - \nu_j) \text{Ei}_1(|t - \tau|) d\nu dt \end{aligned} \quad (4.2.4)$$

$$= \alpha(\tau)\bar{E}(T) + \beta(\tau) \sum_{j=1}^m S_j \left[\int_0^{+1} I(\nu, \tau_0, +\mu) e^{-(\tau_0 - \tau)/\mu} d\mu \right]_{\nu = \nu_j}$$

$$+ \beta(\tau) \int_0^{\tau_0} \bar{J}(t) \sum_{j=1}^m S_j \left[\text{Ei}_1(|t - \tau|) \right]_{\nu = \nu_j} dt$$

$I(\nu_j, \tau_0, +\mu)$ can be evaluated rather easily using Eq. (3.1.2a). It has to be only evaluated for the frequencies of the line centers and for the 15-micron fundamental.* The level corresponding to τ_0 was taken as around 65 km. A program was written to perform this calculation. Account was taken of the wing effects due to neighbouring lines at the higher pressures. To perform the angular integration in Eq.

*It was noted in Section 3.2 that at levels where vibrational relaxation must be considered the optical mass of CO_2 has become so small that only the 15-micron band will have much influence on the radiative transfer.

(4.2.4), 4-point Gaussian quadrature was used. Thus $I(\nu_j, \tau_0, +\mu)$ has to be evaluated for four angles. Not unexpectedly, it turned out that for the strong lines, $I(\nu_j, \tau_0, +\mu)$ was given by the black-body specific intensity.

Now Eq. (4.2.4) can be written,

$$\bar{J}(\tau) = g(\tau) + \beta(\tau) \int_0^{\tau_0} K(t, \tau) \bar{J}(t) dt \quad (4.2.5)$$

This is a Fredholm integral equation of the second kind, which is inherently simpler to solve than if it were of the first or third kind. The simplest method of solution is to use a quadrature method for evaluating the integral term. Thus,

$$\bar{J}(t_k) = g(t_k) - \beta(t_k) \sum_{i=1}^n \int_{t_{i-1}}^{t_i} \bar{J}(t_k) \sum_{j=1}^m S_j \text{Ei}_1(|t^j - t_k^j|) dt \quad (4.2.6)$$

where t_n refers to the top of the atmosphere and t_0 to the level τ_0 .

If $\bar{J}(t_k)$ is assumed constant over the intervals (t_i, t_{i-1}) , then

$$\begin{aligned} & \sum_{i=1}^n \int_{t_{i-1}}^{t_i} \bar{J}(t_i) \sum_{j=1}^m S_j \text{Ei}_1(|t^j - t_k^j|) dt \\ &= \sum_{i=1}^n \bar{J}(t_i) \sum_{j=1}^m S_j \int_{t_{i-1}}^{t_i^j} \text{Ei}_1(|t^j - t_k^j|) dt^j \end{aligned} \quad (4.2.7)$$

It is easy to show by integration by parts that

$$\int_a^b \text{Ei}_1(x) dx = (b \text{Ei}_1(b) - a \text{Ei}_1(a)) - (e^{-b} - e^{-a})$$

Thus Eq. (4.2.7) now becomes

$$\begin{aligned} & \sum_{i=1}^n \bar{J}(t_i) \sum_{j=1}^m S_j \left[(t_i^j - t_k^j) \text{Ei}_1(|t_i^j - t_k^j|) \right. \\ & - (t_{i-1}^j - t_k^j) \text{Ei}_1(|t_{i-1}^j - t_k^j|) - \exp(-|t_i^j - t_k^j|) \\ & \left. + \exp(-|t_{i-1}^j - t_k^j|) \right] = - \sum_{i=1}^n b_{ki} \bar{J}(t_i) \end{aligned} \quad (4.2.8)$$

Equation (4.2.6) may now be written

$$\bar{J}(t_k) = g(t_k) + \beta(t_k) \sum_{i=1}^n b_{ki} \bar{J}(t_i) \quad (4.2.9)$$

It is convenient to take t_k as the optical thickness $(t_k + t_{k-1})/2$. Now

Eq. (4.2.9) may be expressed as

$$\sum_{i=1}^n \left[\left(b_{ki} - \frac{\delta_{ki}}{\beta(t_k)} \right) \bar{J}(t_i) \right] = - \frac{g(t_k)}{\beta(t_k)} \quad (4.2.10)$$

This is a set of n simultaneous equations in the n unknowns $J(t_i)$.

These equations may be written

$$\vec{A}\vec{x} = \vec{c} \quad (4.2.11)$$

where A is the matrix $[a_{ki}]$ with $a_{ki} = b_{ki} - \delta_{ki}/\beta(t_k)$. \vec{x} is the vector $[\bar{J}(t_i)]$ and \vec{c} is the vector $[-g(t_k)/\beta(t_k)]$.

It turns out that the matrix A has a rather special form. A is a diagonally dominant matrix. It thus has a unique inverse and consequently Eq. (4.2.11) has a unique solution.

It was noted in Section 3.2 that the vibrational relaxation time for CO_2 -air mixtures probably lies between 10^{-5} and 10^{-6} sec at 1 atm. The source function J was evaluated for the region 65 to 100 km using relaxation times of 10^{-5} and 10^{-6} sec at 1 atm. The U.S. Standard Atmosphere (1962) was used for this region. The relaxation times were assumed to be independent of temperature for the range of values encountered in the atmosphere. The region from 65 to 100 km was divided into 17 layers each approximately 2 km thick. Equation (4.2.11) therefore consisted of 17 simultaneous linear equations in 17 unknowns. They were solved on a digital computer using a Gauss-Jordan elimination technique.

A convenient way to represent the results is to plot \bar{J}/\bar{E} vs. pressure. \bar{J} is the source function calculated using the procedure outlined above and \bar{E} the mean black-body specific intensity for the

layer. Figure 4 displays the results of this calculation as well as those obtained by Curtis and Goody (1956). In their calculation, Curtis and Goody used line strengths and temperatures which were different from those used in this study. They also used an essentially different method. Nevertheless there is fair agreement between the Curtis and Goody curve and the one obtained using a relaxation time of 10^{-6} sec. The results obtained with a relaxation time of 10^{-5} sec are similar to those of Curtis and Goody but displaced to higher pressures. Both the relaxation time and the radiative lifetime of the CO_2 molecule need to be known as accurately as possible so that the source function may be accurately computed.

The results obtained in this study indicate that vibrational relaxation must be taken into account in radiative transfer calculations somewhere between 60 and 75 km.

The source function was also evaluated for a warm mesosphere such as is observed over Fort Churchill during winter. The temperature profile for this case is shown in Figure 5. A relaxation time of 10^{-5} sec was used. For this situation the ratio \bar{J}/\bar{E} is very little different from that evaluated for the standard atmosphere except for pressures below 2 dynes cm^{-2} .

Table X presents a comparison between \bar{J}/\bar{E} and $\theta/(\theta + \lambda)$ for selected levels.

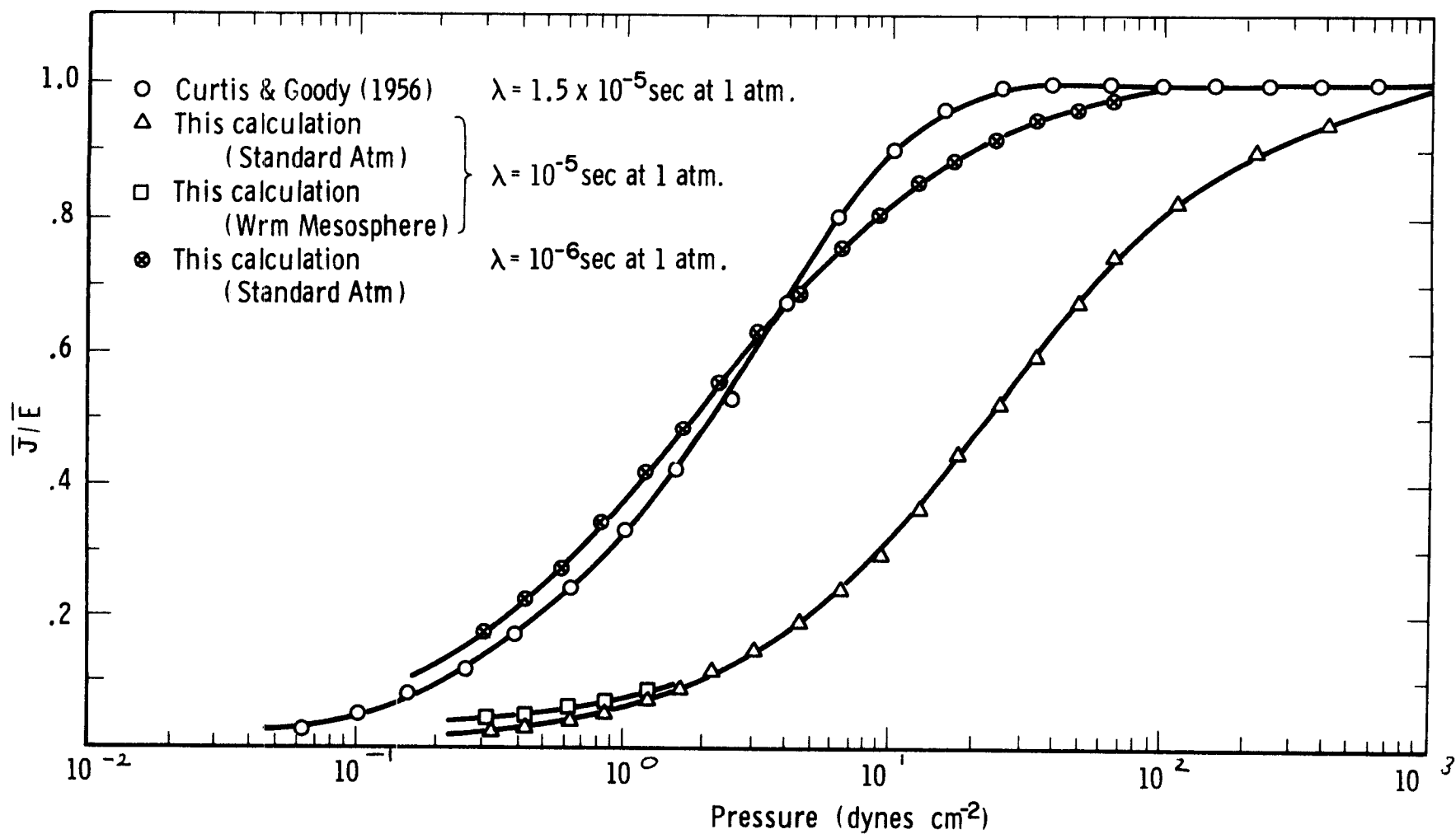


Figure 4. \bar{J}/\bar{E} vs. pressure.

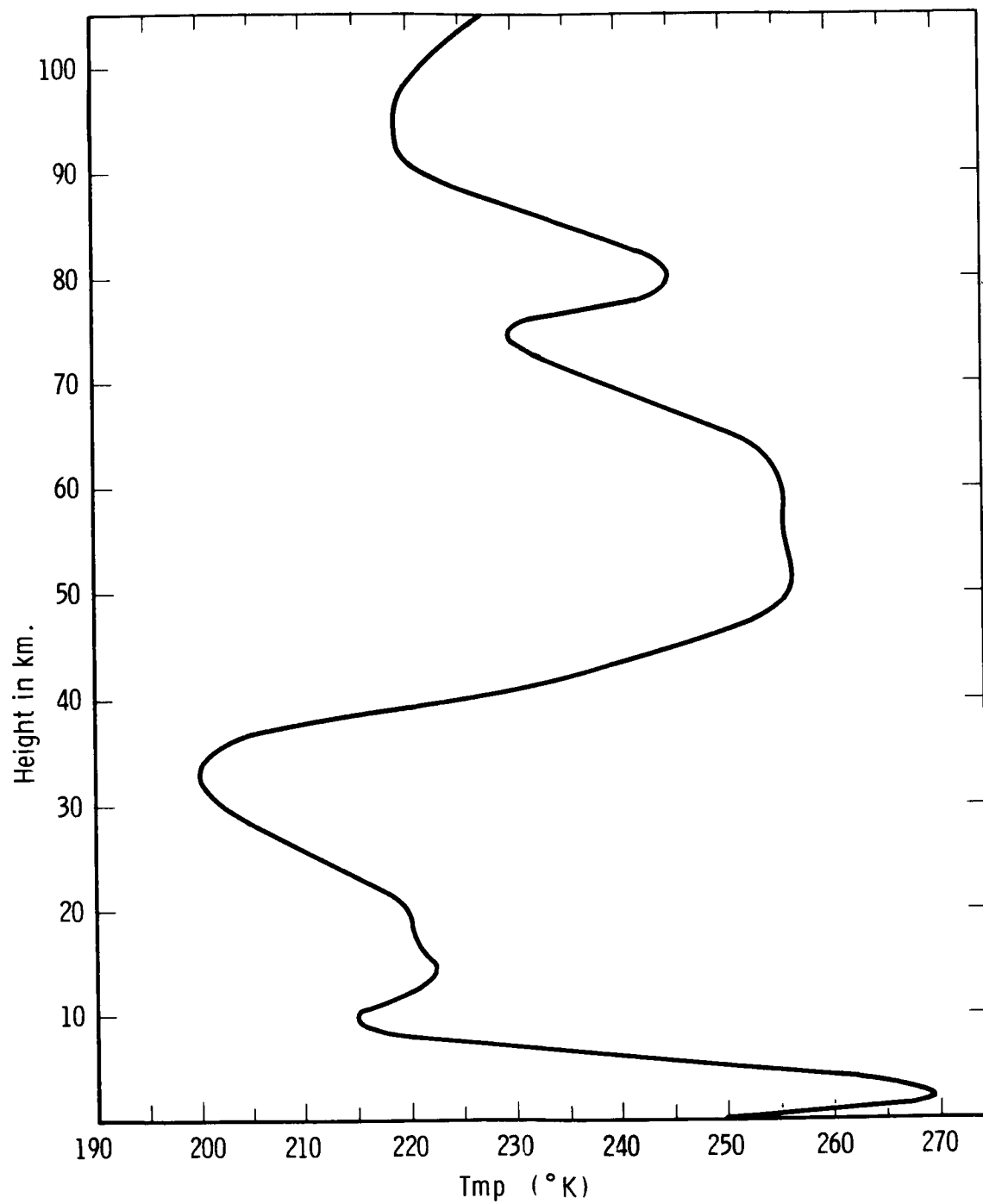


Figure 5. Temperature profile for warm mesosphere case, from Stroud et al. (1960).

TABLE X

COMPARISON BETWEEN \bar{J}/\bar{E} AND $\theta/(\theta+\lambda)$ FOR THE
U. S. STANDARD ATMOSPHERE (1962)

(\bar{P} and \bar{T} are the average pressures and temperatures for 2-km layers)

P(dynes cm ⁻²)	T(°K)	$\lambda(1 \text{ atm}) = 10^{-5} \text{ sec}$		$\lambda(1 \text{ atm}) = 10^{-6} \text{ sec}$	
		\bar{J}/\bar{E}	$\theta/(\theta+\lambda)$	\bar{J}/\bar{E}	$\theta/(\theta+\lambda)$
6.857 (1)	224	.74	.74	.97	.97
3.498 (1)	208	.59	.59	.94	.94
1.785 (1)	192	.44	.42	.88	.88
9.103	181	.29	.27	.80	.80
4.645	181	.19	.16	.68	.66
2.370	181	.12	.088	.55	.50
1.210	183	.077	.047	.41	.34
6.172 (-1)	197	.045	.024	.27	.20
3.149 (-1)	209	.027	.013	.17	.11

The first term on the right-hand side of Eq. (4.2.2) is $\alpha(\tau)\bar{E}(T)$ where

$$\alpha(\tau) = \theta/(\theta+\lambda)$$

The results presented in Table X clearly show that this is the dominant term in Eq. (4.2.2) with the remaining terms becoming of significance at lower pressures. It is instructive to examine the approximations which have been used in deriving the above results.

The matrix A in Eq. (4.2.11) is very strongly diagonally dominant. The diagonal term for the first few rows is, in fact, about three orders of magnitude greater than the next largest element in the same row. The nondiagonal elements are the b_{ki} defined in Eq. (4.2.8). Tracing back to Eq. (4.2.1), the b_{ki} are formed to be associated with

$$\int_0^{\tau_0} \int_{\nu'}^{\nu''} k_{\nu} J(\nu, t) \text{Ei}_1(|t-\tau|) d\nu dt$$

$$\approx \int_0^{\tau_0} \bar{J}(t) \int_{\nu'}^{\nu''} k_{\nu} \text{Ei}_1(|t-\tau|) d\nu dt$$

The integration over frequency was performed by assuming that k_{ν} could be represented by the Dirac delta function.

A rough calculation showed that the integral was overestimated for strong lines, approximately correct for intermediate strength lines (10^{-1} - 10^{-2} cm^{-1} ($\text{atm cm})^{-1}$) and slightly underestimated for weak lines. However it would take a considerable error in the b_{ki} to influence the large diagonal terms. A similar statement applies to the b_{ii} in the diagonal elements. The diagonal dominance of A is the most important facet of the problem.

The remaining term to be considered is $-g(t_k)/\beta(t_k)$. Now

$$\frac{g(t_k)}{\beta(t_k)} \approx \frac{\alpha(\tau)E(\nu, T)}{\beta(\tau)} + \int_{\nu'}^{\nu''} k_{\nu} \int_0^{+1} I(\nu, \tau_0, +\mu) e^{-(\tau_0-\tau)/\mu} d\mu d\nu$$

(4.2.12)

The first term on the right-hand side of Eq. (4.2.12) can be accurately evaluated. It is of the order of the diagonal elements of A, about 10^4 at 65 km decreasing in value with increasing height. The delta function approximation was used to evaluate the second term. Again

a rough calculation shows that the integral is overestimated for strong lines, approximately correct for intermediate strength lines and slightly underestimated for weak lines. The errors would be most important at lower pressures; at higher pressures the first term is larger than the second term by about an order of magnitude.

It is difficult to arrive at an accurate estimate for the errors introduced by the above method for determining the source function. The above discussion serves to point in what direction the errors lie. The difficulty in comparing these results with those of Curtis and Goody (1956) is that they use a somewhat different method. Essentially they compute the cooling rates and then use these values to determine the source function.

To sum up, it appears from the results presented here that vibrational relaxation becomes of importance between 60 and 75 km. The lack of accurate values for the relaxation time and, to a lesser extent, the radiative lifetime for CO₂-air mixtures makes it difficult to accurately compute the source function.

4.3 FLUX DETERMINATION

The equations needed for the flux determination were discussed in Section 3.1. They are

$$F_+(\tau) = 2\pi \int_v J(v, \tau_g) \int_0^{+1} \gamma_v(\tau_g, \tau) \mu \, d\mu \, dv$$

(4.3.1a)

$$- 2\pi \int_v \int_{\tau_g}^{\tau} J(v, t) \int_0^{+1} \frac{\partial \gamma_v(t, \tau)}{\partial t} \mu \, d\mu \, dt \, dv$$

$$F_-(\tau) = - 2\pi \int_v \int_0^{\tau} J(v, t) \int_0^{+1} \frac{\partial \gamma_v(\tau, t)}{\partial t} \mu \, d\mu \, dt \, dv$$

(4.3.1b)

It is convenient to change from the optical thickness t , to the optical mass v . Equation (4.3.1) may now be written as

$$F_+(u_j) = 2\pi \int_v E(v, u_0) \int_0^{+1} \gamma_v(u_0, u_j) \mu \, d\mu \, dv$$

(4.3.2a)

$$- 2\pi \int_v \int_{u_j}^{u_0} J(v, v) \int_0^{+1} \frac{\partial \gamma_v(v, u_j)}{\partial v} \mu \, d\mu \, dv \, dv$$

$$F_-(u_j) = -2\pi \int_v \int_{u_n}^{u_j} J(v, v) \int_0^{+1} \frac{\partial \gamma_v(u_j, v)}{\partial v} \mu \, d\mu \, dv \, dv$$

(4.3.2b)

where u_0 corresponds to τ_g and u_n to τ_0 . Remembering that the transmissivities are average values over finite intervals then Eq. (4.3.2) may be readily evaluated by dividing the atmosphere into layers. The

angular integration may be performed using Gaussian quadrature. Then Eq. (4.3.2) becomes,

$$F_+(u_j) = \pi \sum_{\ell=1}^2 H_{\ell} \left[\left(\sum_{k=1}^m J(v_k, u_0) \gamma_{v_k}(u_0, u_j) \delta_k \right) \eta_{\ell} \right. \\ \left. + \left(\sum_{k=1}^m \sum_{i=0}^{j-1} J(v_k, u_{i+1}) (\gamma_{v_k}(u_{i+1}, u_j) - \gamma_{v_k}(u_i, u_j)) \delta_k \right) \eta_{\ell} \right] \eta_{\ell} \quad (4.3.3a)$$

$$F_-(u_j) = \pi \sum_{\ell=1}^2 H_{\ell} \left[\sum_{k=1}^m \sum_{i=j}^{n-1} J(v_k, u_{i+1}) (\gamma_{v_k}(u_j, u_{i+1}) \right. \\ \left. - \gamma_{v_k}(u_j, u_i)) \eta_{\ell} \delta_k \right] \eta_{\ell} \quad (4.3.3b)$$

where H_{ℓ} and η_{ℓ} are the Gaussian weights and abscissae, respectively. The optical masses and transmissivities are readily determined once the atmospheric model has been chosen. The carbon dioxide concentration was taken as 0.033% by volume (Glueckauf, 1951). Unfortunately there is some variation in the carbon dioxide concentration in the troposphere, but stratospheric and mesospheric concentrations probably remain more constant than tropospheric concentrations.

The division of the atmosphere into layers poses some problems. It would be desirable to make the layers as thin as possible so that they would be more homogeneous. This introduces two difficulties.

First, the computing time for the transmissivities becomes excessive, and second, transmissivities for thick layers are required for the evaluation of the fluxes using Eq. (4.3.3). This is because the multiplication together of the transmissivities for the thin layers can introduce round-off error.

The atmosphere was divided into 24 layers. Fairly thick layers, 8 in all, were chosen up to 10 mb. The remaining 16 slabs were obtained by dividing the previous pressure by 2. This gives layers about 3 to 4 km thick.

The upward and downward directed fluxes were computed for the U.S. Standard Atmosphere (1962). The source functions above 60 km were obtained using the method discussed in Section 4.2. The fluxes were evaluated for the frequency interval 507.5 to 852.5 cm^{-1} . Figure 6 displays the results of this calculation. These results agree reasonably well in shape with those given by Plass (1956b). It should be noted that the curves show very little change in slope at pressures lower than about .3 mb (around 55 km). This point will be taken up in the next section.

4.4 COOLING RATE CALCULATIONS

The cooling (or heating) rate may be expressed in terms of the flux divergence

$$\frac{dT}{dt} = \frac{1}{c_p \rho} \frac{dF(\tau)}{dz} \quad (4.4.1)$$

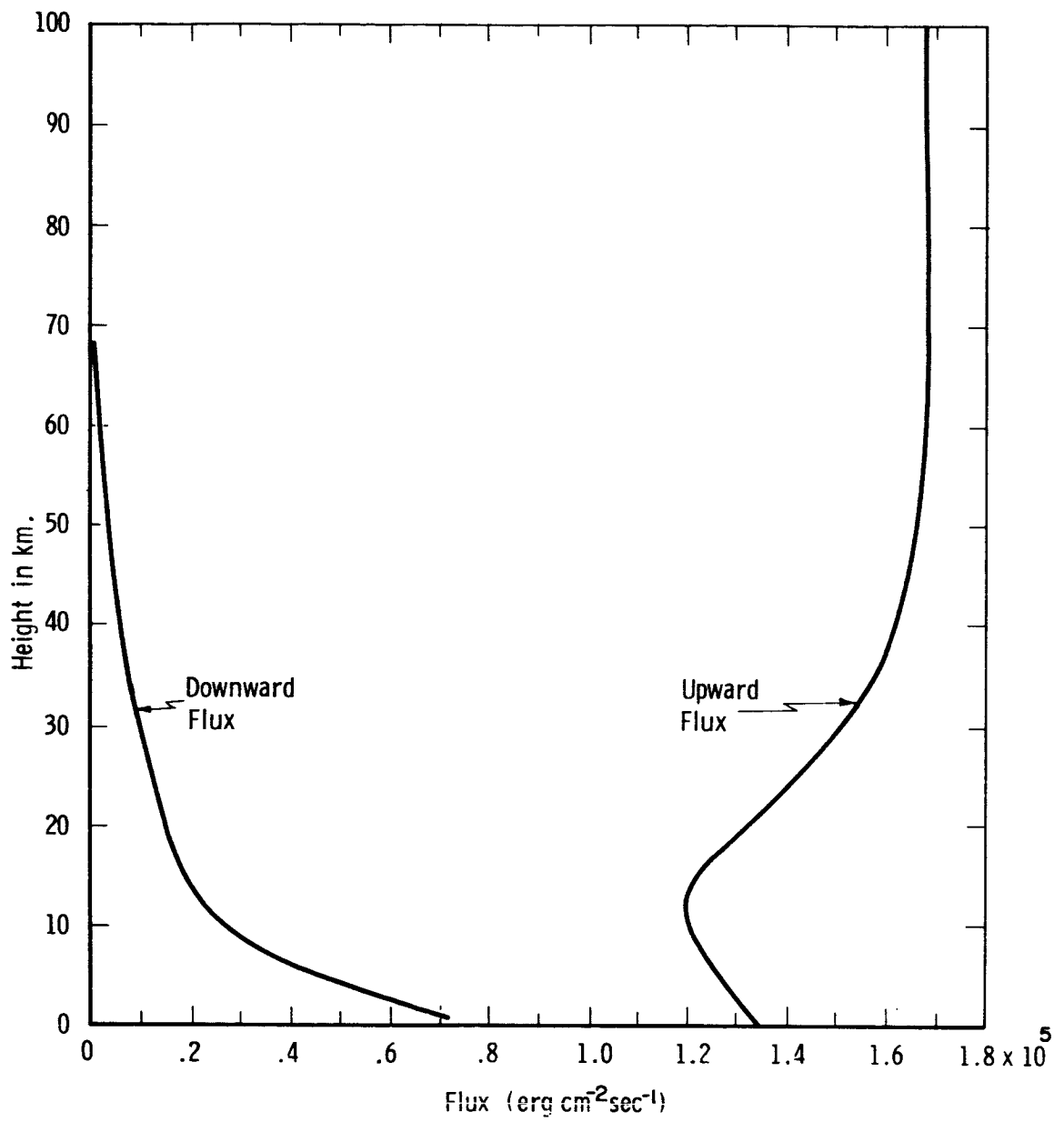


Figure 6. Upward and downward fluxes for U. S. Standard Atmosphere (1962).

$F(\tau)$ is the net flux at level τ . Using the hydrostatic relation

Eq. (4.4.1) becomes

$$\frac{dT}{dt} = \frac{g}{c_p} \frac{dF(\tau)}{dp} \quad (4.4.2)$$

It is important to note that the evaluation of the cooling rate involves a differentiation. This will be a numerical differentiation. Unfortunately numerical differentiation can introduce appreciable error (cf., Hildebrand, 1956). Integration is a smoothing process but differentiation acts in the other direction accentuating any irregularities present in the data.

It is useful to estimate what change in flux will give a reasonable cooling rate for a given pressure change. Table XI lists some values obtained using the fluxes obtained in Section 4.3.

TABLE XI

ΔF AND F COMPUTED AT SEVERAL REPRESENTATIVE LEVELS (U. S. STANDARD ATMOSPHERE (1962)) FOR A COOLING RATE OF 1°K DAY^{-1}

z (km)	p (dynes cm^{-2})		Δp	F (ergs $\text{cm}^{-2} \text{ sec}^{-1}$)	ΔF for $\Delta T = 1^\circ\text{K Day}^{-1}$
4	.6	(6)	.2 (6)	.775240 (5)	.338 (5)
20	.5	(5)	.25 (5)	.120235 (6)	.299 (4)
35	.5	(4)	.25 (4)	.152267 (6)	.299 (3)
50	.625	(3)	.313 (3)	.163332 (6)	.374 (2)
65	.781	(2)	.391 (2)	.167626 (6)	.465 (1)
81	.489	(1)	.245 (1)	.168312 (6)	.292
96	.306	(0)	.153	.167751 (6)	.182 (-1)

The Δp 's correspond to 3 to 4 km thick layers. An examination of this table shows that the flux must be known as accurately as possible. The ratio $\Delta F/F$ is about 1.7×10^{-5} for a $10 \text{ K}^\circ\text{day}^{-1}$ cooling rate at 81 km, and about 2.8×10^{-4} for the same cooling rate at 65 km. These results imply considerable accuracy in the flux-evaluations.

At higher pressures, due to the greater value of Δp for a given layer, $\Delta F/F$ becomes larger. For example at 35 km a $\Delta F/F$ of 9.8×10^{-3} corresponds to a cooling rate of 5°K day^{-1} for the 3 to 4 km thick layer.

Table XII presents the cooling rates computed using the fluxes determined in Section 4.3.

TABLE XII

COOLING RATES UP TO 30 KM FOR THE U. S. STANDARD ATMOSPHERE (1962)
OVER THE FREQUENCY RANGES 507.5 TO 857.5 cm^{-1} AND 630 TO 715 cm^{-1}

z (km)	p (dynes cm^{-2})	ΔT ($^\circ\text{K Day}^{-1}$)	
		(507.5-857.5 cm^{-1})	(630-715 cm^{-1})
1.89	.8 (6)		
		0.48	0.015
4.07	.6 (6)		
		0.44	0.39
6.96	.4 (6)		
		0.40	0.08
11.45	.2 (6)		
		0.91	0.36
15.73	.1 (6)		
		2.04	1.24
20.02	.5 (5)		
		4.26	3.15
24.35	.25 (5)		
		5.54	4.6
30.31	.1 (5)		

The cooling rates are given for the whole spectral region under investigation, 507.5 to 857.5 cm^{-1} and also for the region encompassing the 15-micron fundamental, 630-715 cm^{-1} .

Above 30 km the cooling rates become unrealistically large, for example $\Delta T(507.5-857.5 \text{ cm}^{-1})$ equals $60^\circ\text{K day}^{-1}$ around 50 km. At levels above 30 km the 15-micron fundamental will be the most important contributor to the infrared radiative transfer. By considering this band alone some of the "noise" introduced by the much weaker bands will be eliminated. Large cooling rates are still obtained with a maximum of $36^\circ\text{K day}^{-1}$ at 55 km. This value is probably much too large. The cooling rate drops off rapidly above 60 km becoming almost zero around 70 km. Above 70 km a heating is indicated. This is probably spurious due to the influence of low pressures on the cooling rate calculations.

Plass (1956b) gives cooling rates up to 70 km. His maximum cooling rate is about 6°K day^{-1} around 45 km. The values obtained in this study and those of Plass agree reasonably well up to about 30 km. Above 30 km the differences become more marked, Plass's maximum being about 1/5 that obtained for the 15-micron fundamental in this calculation.

It is instructive to examine Plass's work in more detail. He evaluated the fluxes using essentially the same method as used in Section 4.3. Plass took laboratory measurements for the transmissivities instead of calculated values as used in this study. An important dif-

ference between the two procedures is that Plass used the Lorentz line shape to 50 km. The mixed line shape was used above 25 km in this calculation. In Section 4.1.3 it was noted that using the Lorentz line shape above 30 km can introduce considerable error in flux calculations, the fluxes being underestimated. Plass estimated the error in the upward and downward fluxes to be around 3% with the error for the cooling rates about 30% at 50 km becoming uncertain above 60 km. This error for the cooling rate might be somewhat optimistic due to the influence of Δp on cooling rate calculations at low pressures. A .25% error in the net flux at 50 km could correspond to a cooling rate of $10^\circ\text{K day}^{-1}$. (cf., Table XI)

The transmissivity determinations are the main source of error in this calculation. The quasirandom model underestimates the transmissivity and unfortunately the flux calculations involve multiplying the transmissivities together to obtain transmissivities for thicker layers. Values for the transmissivities were only carried to 4 significant figures since the approximations used for the absorption coefficient at pressures lower than 20 mb do not justify greater accuracy. Much more accurate transmissivities are needed if fluxes accurate enough for cooling rate calculations are to be obtained. The logical solution is not to use a spectral band model but to integrate directly across the band to obtain the fluxes.

If very thick layers are used the pressure change is large and the error can be reduced. For example, the cooling rate was 8.4°K

day⁻¹ for the region 25 to 85 km calculated for the 15-micron fundamental.

As noted in Section 3.3 Curtis and Goody (1956) give an expression for the cooling rate in terms of the source function, viz.,

$$\frac{dT}{dt} = \frac{1.99}{\lambda} (\bar{J} - \bar{E})$$

To use this expression it is necessary to know \bar{J} as accurately as possible, particularly at the higher pressures. Table XIII presents the cooling rates obtained using this method above 80 km.

TABLE XIII
COOLING RATES ABOVE 80 KM FOR U. S. STANDARD ATMOSPHERE (1962)

z (km)	p (dynes cm ⁻²)	$\Delta T(^{\circ}\text{K Day}^{-1})$	
		$\lambda(1 \text{ atm}) = 10^{-5} \text{ sec}$	$\lambda(1 \text{ atm}) = 10^{-6} \text{ sec}$
80.5	9.103	22.8	64.8
82.5	6.503	17.6	58.7
84.5	4.645	13.4	47.9
86.5	3.318	9.5	45.0
88.0	2.370	7.2	37.9
90.0	1.693	5.4	30.2
91.5	1.210	4.2	26.8
93.5	8.640 (-1)	3.8	26.8
95.5	6.172 (-1)	3.2	24.4
97.5	4.409 (-1)	2.6	21.2
99.5	3.149 (-1)	2.2	18.3

The cooling rates below 80 km are very large and probably unrealistic.

Also the cooling rates corresponding to $\lambda(1 \text{ atm}) = 10^{-6} \text{ sec}$ are much

larger than those for $\lambda(1 \text{ atm}) = 10^{-5} \text{ sec}$. The cooling rates are sensitive to the accuracy of \bar{J} . If \bar{J} is 10% too low then the corrected cooling rate at 80 km would be around $36^\circ\text{K day}^{-1}$ and a 20% error would reduce the cooling rate to $12^\circ\text{K day}^{-1}$, both for $\lambda(1 \text{ atm}) = 10^{-6} \text{ sec}$. In calculations of the type used to derive the source function \bar{J} , it is probable that errors of this size could easily arise.

It is difficult to decide on reasonable cooling rates for the atmosphere in the vicinity of the mesopause. The mesopeak at 50 km is situated at a temperature maximum. The temperature increases rapidly above the mesopause as the thermosphere is entered. Energy probably flows from these regions of higher temperature to the region of minimum temperature at the mesopause. Chamberlain (1962) investigated the nature of the mesopause but only considered conduction of energy from the thermosphere. His main conclusion was that 80 km should be the level of the mesopause. He obtained cooling rates roughly comparable to those obtained by Curtis and Goody (1956). Unfortunately, energy may be transported by other means than conduction. Convection might be an important energy transporter from levels below the mesopause. In this case larger cooling rates might be in order.

To sum up, it is evident that very accurate calculations are needed if reliable cooling rates are to be computed. It is possible that some of the errors might cancel giving a false impression of accuracy. Reasonable values for fluxes are not too difficult to obtain

but the accuracy required for the computation of flux divergences is much more difficult to achieve. Vibrational relaxation becomes of importance between 60 and 75 km but the source function \bar{J} must be evaluated very accurately if cooling rates are to be determined with as little error as possible near the mesopause.

4.5 DISCUSSION OF THE PROBLEM OF COOLING RATE DETERMINATION

In Section 4.4 it is demonstrated that the problem of calculating cooling rates in the stratosphere and mesosphere is difficult. As noted in the Introduction (Section 1) a knowledge of cooling rates is very important if dynamical investigations of the stratosphere and mesosphere are to progress beyond the most elementary stages. In this section the cooling rate problem is examined rather generally.

If flux divergences could be measured in the atmosphere then an important advance would be made. Unfortunately this is a very difficult problem. An experiment designed to measure flux divergences would measure the upward and downward fluxes very accurately at two atmospheric levels. The flux divergences would then be calculated in the manner used in this study. As shown in Section 4.4 the net fluxes would have to be known very accurately if reliable flux divergences and cooling rates were to be obtained. The lower the pressure the greater the accuracy needed in the flux measurements. Kondrat'yev (1963) gives a complete discussion of the problem. His main conclusion is that only for very thick layers at lower pressures would it be pos-

sible to experimentally determine reasonably accurate flux divergences. This is in agreement with the conclusions of Section 4.4 regarding theoretical calculations based on essentially a similar procedure.

The other method of calculating the cooling rate is based on an accurate knowledge of the source function J . It is probably only useful for the upper mesosphere. It was shown in Section 4.4 that an accurate knowledge of J must be known if precise cooling rates are to be determined. To calculate the source function accurate values for the vibrational relaxation time and radiative lifetime are required. Unfortunately both these quantities are not known very precisely at the moment. It will probably be some years before really good experimental measurements are available. Equation (3.3.10) is the basic equation for determining the source function. It is feasible to carry out the integrations over frequency by integrating numerically across the band. This is a task of great magnitude. This method of determining cooling rates might be inherently more accurate if good relaxation times and radiative lifetimes were known. It is interesting to note that if cooling rates for the upper mesosphere could be accurately measured then it would be possible to arrive at better values for the vibrational relaxation time for carbon dioxide.

5. CONCLUSIONS

The foregoing study was initiated with the object of determining the possibility of accurately calculating mesospheric cooling rates. In the course of the investigation a number of more general problems associated with atmospheric infrared radiative transfer had to be examined. It turned out that inherent inaccuracies in the methods employed limit the accuracy of the calculated cooling rates. Nevertheless the study has served to focus attention on aspects of the infrared transfer problem which require further study both experimental and theoretical.

The main results are:

- (1) A table of the rotational line positions and intensities for 2080 carbon dioxide lines in the 12- to 18-micron spectral region.
- (2) The angular integration in the flux equations can be performed quite accurately using 2-point Gaussian quadrature. The use of an effective optical mass gives reasonable accuracy if $\sec \theta$ is chosen as 1.66, in agreement with Elsasser's (1942) result.
- (3) The use of the quasirandom model in cooling rate calculations is not satisfactory. The main reason is that at low pressures the model underestimates the transmissivities where they are needed as accurately as possible.

It also underestimates the transmissivities for the Q-branches. This model is reasonably satisfactory if only estimates for fluxes and transmissivities are desired. An extension to the model was developed enabling it to be applied when Doppler broadening must be considered.

- (4) Using the Lorentz line shape at pressures lower than 20 mb can introduce appreciable error in calculations involving the whole band, for example, flux calculations. Plass and Fivel's (1953) conclusions that the Lorentz line shape can be used up to 50 km for strong and weak lines are valid. The importance of intermediate strength lines in calculations involving an entire band cannot be neglected.
- (5) The source function for vibrationally relaxing carbon dioxide was determined above 60 km for vibrational relaxation times of 10^{-5} and 10^{-6} sec at 1 atm. The value of the source function and the level at which relaxation becomes of significance were greatly influenced by the choice of vibrational relaxation time. The results obtained in this study indicate that local thermodynamic equilibrium starts to break down between 60 and 75 km.

- (6) Cooling rates in the stratosphere and particularly the mesosphere are difficult to obtain. This is due to the high accuracy required in the flux calculations and in the source function when vibrational relaxation is considered. Values up to 30 km appear reasonable but increase to unrealistically large values above this height. A cooling rate of $8.4^{\circ}\text{K day}^{-1}$ was determined for the very thick layer 25 to 85 km. Above 80 km cooling rates evaluated using Eq. (3.3.11) and a relaxation time of 10^{-5} sec appear reasonable. However, it is difficult to decide on reasonable cooling rates in the vicinity of the mesopause due to the complicated processes involved in energy transport in that region.

6. SUGGESTIONS FOR FURTHER RESEARCH

The preceding investigation indicates that it would be desirable to evaluate fluxes by integrating directly across the band rather than use spectral band models. Unfortunately this is a time consuming task and would take considerable time even using present day digital computers. The use of spectral band models can introduce appreciable error. Consequently it is probably fruitless to attempt the development of more complicated models. The more complicated the model, the greater the computer time needed in using it to evaluate transmissivities. The quasirandom model consumed a considerable amount of computer time.

A more accurate value for the vibrational relaxation time of CO₂-air mixtures is urgently needed. This is a very elusive quantity to arrive at either experimentally or theoretically. A precise knowledge of the quantity is necessary if worthwhile values for source functions and cooling rates are to be obtained for the upper mesosphere.

Experimental measurements of the flux divergence at mesospheric levels would be extremely useful. Unfortunately, as noted previously, this is an exceedingly difficult task and some years will probably elapse before such results are obtained.

One important aspect of the infrared radiative transfer problem should not be overlooked. More accurate laboratory measurements of

carbon dioxide band strengths in the 15-micron region are required. High-resolution studies of the bands at low pressures would show the influence of foreign gases on the line shape. Most of the laboratory measurements to date have been made using either pure carbon dioxide or carbon dioxide-air mixtures with large percentages of carbon dioxide. Ideally, measurements should be made over long path lengths with very low carbon dioxide concentrations.

APPENDIX A

PHYSICAL DETAILS OF THE CARBON DIOXIDE MOLECULE

The carbon dioxide molecule is a linear triatomic molecule. This linear structure of the carbon dioxide molecule makes it easier to deal with theoretically than, for example, water vapor and ozone, both of which have triangular structures (cf., Herzberg, 1945). Since the activity of a molecule in the infrared depends on change of its electric moment, the manner in which it vibrates is very important. Figure 7 shows the possible modes of vibration for a linear molecule such as carbon dioxide.

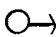

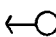






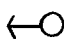
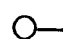
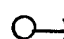
<u>Change in electric moment</u>	<u>O</u>	<u>C</u>	<u>O</u>	<u>Mode</u>
none				ν_1
\perp	  in	  out	  in	ν_2
\parallel				ν_3

Figure 7. Possible vibrations for the carbon dioxide molecule and changes in electric moment.

In mode ν_1 the carbon atom does not move and thus the electric moment is zero and does not change with the vibration of the oxygen atoms. Thus there are no pure rotation lines for carbon dioxide as

in the case of water or no vibration-rotation band at the frequency ν_1 . The vibration ν_2 is the degenerate representation of two equal frequencies and the band corresponding to the fundamental of ν_2 is centered about 15-microns (667.3 cm^{-1}). The ν_2 mode is sometimes called the bending mode. The ν_2 band has a strong Q-branch which indicates that the change in electric moment is perpendicular to the axis of symmetry. The fundamental associated with the ν_3 mode is around 4.3 microns (2349.3 cm^{-1}), the ν_3 mode is sometimes called the valence mode. The Q-branch associated with this mode is weak indicating that the change in electric moment is parallel to the axis of symmetry. The fundamental vibration ν_1 may be studied using the Raman effect. It is found that the intense Raman line at 1340 cm^{-1} is really two lines at 1285.5 cm^{-1} and 1388.3 cm^{-1} . This puzzling effect is due to $2\nu_2$ being very close in frequency to ν_1 , and a Fermi resonance thus takes place. The Fermi resonance effect occurs if two vibrational levels belonging to different vibrations (or combinations of vibrations) have nearly the same energy, then a "resonance" occurs which leads to a perturbation of the energy levels. The Fermi resonance causes many combination bands of carbon dioxide to be displaced from their normal positions.

As shown in Herzberg (1945) the total vibrational energy is given by:

$$E(\nu_1, \nu_2, \nu_3, \dots) = h \nu_1(\nu_1 + 1/2) + h \nu_2(\nu_2 + 1/2) + h \nu_3(\nu_3 + 1/2) + \dots$$

or the term values by

$$G(v_1, v_2, v_3, \dots) = \omega_1 \left(v_1 + \frac{1}{2} \right) + \omega_2 \left(v_2 + \frac{1}{2} \right) + \omega_3 \left(v_3 + \frac{1}{2} \right) + \dots$$

where

$$G(v_1, v_2, v_3, \dots) = E(v_1, v_2, v_3, \dots)/hc$$

The v_i 's are the vibrational quantum numbers and ω_i 's are the classical vibrational frequencies. If the molecule is doubly degenerate, as is the carbon dioxide molecule, then two of the ω 's would be the same. Stull et al. (1962) give a formula for the unperturbed energy levels of carbon dioxide to third order, viz.,

$$\begin{aligned} G(v_1, v_2, v_3; l) = & \sum_{i=1}^3 \omega_i \left(v_i + \frac{1}{2} d_i \right) + \sum_{i=1}^3 \sum_{j \geq 1} x_{ij} \left(v_i + \frac{1}{2} d_i \right) \left(v_j + \frac{1}{2} d_j \right) \\ & + \sum_{j=1}^3 \sum_{i \geq j} \sum_{k \geq j} y_{ijk} \left(v_i + \frac{1}{2} d_i \right) \left(v_j + \frac{1}{2} d_j \right) \left(v_k + \frac{1}{2} d_k \right) + \dots + g_{22} l^2 \end{aligned}$$

where d_i is the degeneracy index associated with the v_i mode (for carbon dioxide, $d_1 = d_3 = 1$, $d_2 = 2$). The vibrational constants ω_i , x_{ij} , y_{ijk} , g_{22} , may be expressed in terms of the potential constants of the molecule but are usually determined experimentally. l is a quantum number associated with the degeneracy of one mode. It is the angular momentum (in units of $h/2\pi$) of the molecule about the symmetry

axis of the degenerate vibration (for carbon dioxide the ν_2 mode is degenerate) and has the values

$$\pm\nu_2, \pm(\nu_2-2), \pm(\nu_2-4), \dots, \pm 1 \text{ or } 0$$

Generally the positive and negative levels coincide but under the influence of rotation the levels split, this is l -type coupling.

The vibrational transitions in the infrared are dipole transitions with the following selection rules applicable (Herzberg, 1945).

$$\Delta l = 0 \quad \nu_2 - \text{even}, \quad \nu_3 - \text{odd}$$

$$\Delta l = \pm 1 \quad \nu_2 - \text{odd}, \quad \nu_3 - \text{even}$$

These apply for symmetric molecules such as carbon dioxide.

Figure 7 lists the vibration bands of importance in the 15-micron region of the spectrum. Levels for which all the vibrational quantum numbers ν_i are zero except one are called fundamental levels and naturally the ground state has all the quantum numbers zero. Thus a transition involving a fundamental level and the ground state is called a fundamental frequency and in absorption due to the greater population of the ground state, a fundamental frequency is the strongest. In Figure 7 only one fundamental frequency is evident, band 1, and it is also the strongest. When only one ν_i is different from zero but greater than one, then the level is called an overtone level; and when two or more of the ν_i 's are greater than zero, then the level is called

a combination level. Transitions which end at levels higher than the ground in absorption are called difference frequencies or difference combinations. Thus in Figure 7 all the bands except for band 1 are difference combinations.

Now if a vibration band of a molecule, such as carbon dioxide, is examined using a high-resolution spectrometer it is found to consist of a large number of individual lines. This fine structure is a consequence of the rotation of the molecule. The rotational energy of a linear molecule is given by (Herzberg, 1945),

$$F_v(J) = B_v J(J+1) \quad (A.2)$$

where J is the rotational quantum number and

$$B_v = B_e - \sum_i \alpha_i \left(v_i + \frac{d_i}{2} \right) \quad (A.3)$$

where d_i is the degree of degeneracy of the vibration, α_i are constants for each molecule and B_e is the rotational constant. In the case of carbon dioxide i has a maximum value of 3. The rotational quantum number J corresponds to the total angular momentum and, in general, takes on the values,

$$l, \quad l + 1, \quad l + 2, \dots$$

For a molecule such as carbon dioxide ($C^{12}O_2^{16}$ is only being considered) the rotational levels are alternating symmetrical and antisymmetrical

and consequently

$$J = 0, 2, 4, \dots \quad \text{when } l = 0$$

This is because the ratio of the statistical weights of the antisymmetric and symmetric states is $s/(s+1)$ where s is the quantum number for the nuclear spin. For O^{16} s is zero and consequently the statistical weight for the antisymmetric rotational levels is zero. For l greater than zero, each rotational level is doubly degenerate and thus alternate levels are present.

Combining the effects of vibration and rotation gives the total energy of a level as

$$T = G(v_1, v_2, v_3; l) + F_v(J) \quad (A.4)$$

The frequency of a line in a vibration-rotation band is then given by

$$\nu = \nu_0 + F_v(J') - F_v(J'') \quad (A.5)$$

where ν_0 is the frequency of the band center, J' is the rotational quantum number for the upper vibrational state and J'' that for the lower.

As is to be expected certain selection rules must be obeyed, viz.,

$$(1) \quad l = 0 \text{ in both upper and lower states (|| bands)}$$

$$\Delta J = \pm 1, \text{ only P- and R-branches, no Q-branch } (\Delta J = +1$$

corresponds to a R-branch, $\Delta J = -1$ corresponds

to a P-branch and $\Delta J = 0$ corresponds to a Q-

branch)

(2) $\Delta l = \pm 1$ (1 bands)

$\Delta J = \pm 1$, P-, Q-, and R-branches are present with the Q-

$\Delta J = 0$ branch stronger than either the P- or R-branches.

(3) $\Delta l = 0$, but $l \neq 0$ (|| bands)

$\Delta J = \pm 1$, P-, Q-, and R-branches are present with the Q-

$\Delta J = 0$ branch weak

Table XV lists the quantum numbers for the upper and lower states of the carbon dioxide bands in the 15-micron region. For all the bands $\Delta l = \pm 1$, hence the bands all have strong Q-branches.

APPENDIX E

CALCULATION OF THE LINE POSITIONS AND INTENSITIES FOR THE CARBON DIOXIDE BANDS IN THE 15-MICRON REGION OF THE SPECTRUM

The positions of the rotational lines of the various vibration bands in the 15-micron region may be determined using Eq. (A.5) with the following rotational constants (Stull, et al. 1961).

B_e	α_1	α_2	α_3
0.3925	0.00058	-0.00045	0.00307

The intensity of an individual rotation line (if a rigid-rotator model is assumed) is given by

$$S_{J''} = \frac{S_{v''} g_{J''} (A_{J''})^2 (1 - e^{-hc\nu/kT}) e^{-hcF_v(J'')/kT}}{Q_J v_0 (1 - e^{-hc\nu_0/kT}) g} \quad (B.1)$$

where $S_{v''}$ is the total band intensity, Q_J the rotational partition function for a rigid rotator given by

$$Q_J = \sum_{J''} (2J'' + 1) e^{-hcF_v(J'')/kT}$$

which may be approximated by (Herzberg, 1945),

$$Q_J = \frac{kT}{hcB_e} + \frac{1}{3} + \frac{1}{15} \frac{hcB_e}{kT} + \frac{4}{315} \left(\frac{hcB_e}{kT} \right)^2 + \frac{1}{315} \left(\frac{hcB_e}{kT} \right)^3 + \dots \quad (B.2)$$

$g_{J',l'}$ is a weighting function given by

$$g_{J',l'} = (2J'+1) \text{ for } l' = 0$$

$$g_{J',l'} = 2(2J'+1) \text{ for } l' \neq 0$$

and $g = 1$ for l'' or $l' = 0$, $g = 2$ when neither l'' or $l' = 0$. The values of $(A_{J'',l'',J',l'})^{J',l'}$ are tabulated by Penner (1959) using Dennison's (1931) values.

Equation (B.1) may now be written

$$S_{J''} = \frac{S_{v''}^{v'} F(J'') v (1 - e^{-hc\nu/kT}) e^{-hcF_v(J'')/kT}}{Q_J v_0 (1 - e^{-hc\nu_0/kT})} \quad (\text{B.3})$$

where

$$F(J'') = g_{J',l'} (A_{J'',l'',J',l'})^{J',l'} / g$$

Only certain values of $F(J'')$ are required, these are given in Table XIV.

An interaction which slightly modifies Eq. (B.1) is the Coriolis vibration-rotation interaction. Madden (1961) notes that a consideration of the Coriolis interaction leads to Eq. (B.1) being multiplied by $(1-\zeta m)^2$ where m is the ordinal number of the line and ζ is a parameter depending on the strength of the Coriolis interaction and the vibrational transition. Using experimental data, Madden has obtained a value for

TABLE XIV

VALUES FOR $F(J'')$

$F(J'') =$	$\left[\begin{array}{l} (J'' + 2)/2 \\ (2J'' + 1)/2 \\ (J'' - 1)/2 \end{array} \right.$	$\Delta J = +1$
$l'' = 0$		$\Delta J = 0$
$\Delta l = +1$		$\Delta J = -1$
$F(J'') =$	$\left[\begin{array}{l} J''/2 \\ (2J'' + 1)/2 \\ (J'' + 1)/2 \end{array} \right.$	$\Delta J = +1$
$l' = 0$		$\Delta J = 0$
$\Delta l = -1$		$\Delta J = -1$
$F(J'') =$	$\left[\begin{array}{l} \frac{(J'' + 2 \pm 1'')(J'' + 1 \pm 1'')}{4(J'' + 1)} \\ \frac{(2J'' + 1)(J'' + 1 \pm 1'')(J'' \mp 1'')}{4J''(J'' + 1)} \\ \frac{(J'' - 1 \mp 1'')(J'' \mp 1'')}{4J''} \end{array} \right.$	$\Delta J = +1$
$l', l'' = 0$		$\Delta J = 0$
$\Delta l = \pm 1$		$\Delta J = -1$

$\zeta = +0.0035$ for the (020:0) - (010:1) band of CO_2 and Benedict has predicted $\zeta = +0.0016$ for the 15-micron fundamental which has not yet been experimentally verified. In this work the Coriolis effect has been neglected.

The band strength $S_{v',l}^{v'}$ is given by

$$S_{v',l}^{v'} = \sum_J S_J$$

It has been shown (cf., Madden, 1961) that

$$S_{v'',v'}^{v'} = \frac{8\pi^3 N_0 \nu_0 [1 - e^{-hc\nu_0/kT}] |R_{v'',v'}^{v'}|^2 g e^{-hcG(v'',l'')/kT}}{3hc Q_v} \quad (\text{B.4})$$

where Q_v is the vibrational partition function, N_0 is the molecular density at 300°K and 1 atm, $R_{v'',v'}^{v'}$ is the vibrational transition moment and g is the weight factor given above. Q_v may be represented by (Herzberg, 1945),

$$Q_v = \prod_i (1 - e^{-hc\nu_i^0/kT})^{-d_i}$$

where ν_i^0 are the frequencies of the fundamentals and d_i are the degrees of degeneracy of the vibration ν_i^0 .

When Eq. (B.3) is used to calculate the intensity of a rotational line a difficulty becomes apparent. The band strength $S_{v'',v'}^{v'}$ varies with temperature and is generally given for just one temperature. This difficulty may be circumvented using a scheme given by Stull et al. (1961). Equation (B.3) may be written

$$S_{J'',J'} = \frac{C(v'',l'')^{(v',l')} F(J') \nu (1 - e^{-hc\nu/kT}) e^{-hcF_v(J'')/kT}}{\nu_0 (1 - e^{-hc\nu_0/kT})} \quad (\text{B.5})$$

where

$$C_{(v'',l'')}^{(v',l')} = S_{v'',v'}^{v'} / Q_J \quad (\text{B.6})$$

Using Eqs. (B.6) and (B.4) $C_{(v'',l'')}^{(v',l')}$ for any vibrational transition and temperature may be related to $C_{(v'',l'')}^{(v',l')*}$ for another vibrational transition and temperature. Therefore

$$C_{(v'',l'')}^{(v',l')}(T) = I_R C_{(v'',l'')}^{(v',l')*}(T_0) \frac{N_0(T)Q(T_0)}{N_0(T_0)Q(T)} \exp \left[\frac{hc}{k} \left\{ \frac{G(v'',l'')^*}{T_0} - \frac{G(v'',l'')}{T} \right\} \right] \frac{g_{v_0}(1-e^{-hc\nu_0/kT})}{g_{v_0}^*(1-e^{-hc\nu_0^*/kT_0})} \quad (B.7)$$

where Q is the total partition function

$$Q = Q_V Q_J$$

and

$$I_R = |R_{(v'',l'')}^{(v',l')}|^2 / |R_{(v'',l'')}^{(v',l')*}|^2$$

The * refers to some standard state. The value of the normalization constant $C_{(v'',l'')}^{(v',l')*}$ has been determined by Stull et al. (1961). They give

$$C_{(000:0)}^{(010:1)}(300^\circ K) = 0.69$$

It is reasonable to assume $N_0(T) = N_0(T_0)$. Values of I_R are given by Stull et al. (1961) based on data of Yamamoto and Sasamori (1958).

Madden (1961) has given some newer data for $S_{v''}^{v'}$, and R the vibrational transition moment for some of the transitions considered by Yamamoto

and Sasamori. If $T = T_0$ then from Eqs. (B.4) and (B.7)

$$I_R = \frac{\nu_0^* g^* S_{v'',v'''}^{\nu'} \exp \left[-\frac{hc}{kT} \left\{ G(v'',l'')^* - G(v'',l''') \right\} \right]}{\nu_0 g S_{v'',v'''}^{\nu'*}} \quad (B.8)$$

If the * refers to the 15-micron fundamental then I_R may easily be evaluated. Table XV gives value for I_R computed by Stull et al. (1961)

TABLE XV
VIBRATIONAL QUANTUM NUMBERS, BAND CENTERS, BAND INTENSITIES,
AND I_R FACTORS FOR 14 BANDS IN THE 15-MICRON REGION FOR A
TEMPERATURE OF 300°K

Band Code	Level		Band Center	Band Intensity (cm ⁻² atm ⁻¹)		I_R	
	Lower	Upper		Yamamoto and Sasamori	Madden	Stull <u>et al.</u>	Corrected
1	000:0	010:1	667.40	212	194*	1.000	1.000
2	010:1	020:0	618.03	4.7	4.27	0.539	0.583
3	010:1	100:0	720.83	6.2		0.711	0.726
4	010:1	020:2	667.76	16.6	30	0.906	1.896
5	020:0	030:1	647.02	1.13	1.0	2.524	2.532
6	020:0	110:1	791.48	0.022		0.048	0.0455
7	020:2	030:1	597.29	0.157	0.14	0.218	0.244
8	020:2	110:1	741.75	0.14		0.194	0.196
9	020:2	030:3	668.3	0.85		1.177	1.322
10	100:0	030:1	544.26	0.0044	0.0040	0.016	0.0252
11	030:3	040:2	581.2	0.0042		0.150	0.185
12	030:3	120:2	756.75	0.0059		0.209	0.200
13	030:1	120:2	828.18	0.00049		0.024	0.0108
14	030:1	120:0	740.5	0.014		0.695	0.690

*Burch et al. (1962a) give 330 ± 90 cm⁻² atm⁻¹ (300°K) for the intensity of band 1. Since their result is greater than most of the previous measurements, Madden's value is used.

as well as values computed using Madden's data where available and otherwise Yamamoto and Sasamori's (1958) data. Table XV displays the band intensities, vibrational quantum numbers for the upper and lower levels and a band code.

Using the above procedures a program was written to compute the rotational line positions and intensities for bands 1 to 14. The intensities were computed for six temperatures from 175 (25) - 300°K. Lines of intensities less than $10^{-6} \text{ cm}^{-2} \text{ atm}^{-1}$ at 300°K were neglected. The results are shown in Table XVI in order of increasing wave number. The band code consists of five digits. The first two refer to the coded bands in Table XV. The third digit indicates a P-, Q-, or R-branch; 0, 1 and 2 refer to P-, Q-, and R-branches, respectively. The last two digits indicate the rotational quantum number for the line. For example,

11244 means band 11, R-branch, $J = 44$

20 1 means band 2, P-branch, $J = 1$

Table XVII lists some of the line positions and intensities calculated using the above procedures and also from data published by Madden (1961). The agreement between observed and calculated values is satisfactory. This provides a check on the calculations.

TABLE XVI

ROTATIONAL LINE POSITIONS AND INTENSITIES FOR THE 14 BANDS GIVEN IN
TABLE XV FOR SIX TEMPERATURES FROM 175° TO 300°K

(Frequencies are given in cm^{-1} and the intensities in $\text{cm}^{-1} (\text{atm cm})^{-1}$)

BAND CODE	WAVE NUMBER	INTENSITY					
		T=300K	T=275K	T=250K	T=225K	T=200K	T=175K
10056	506.46	.1119E-05	.4032E-06	.1158E-06	.2462E-07	.3456E-08	.2683E-09
10054	507.60	.1639E-05	.6132E-06	.1844E-06	.4141E-07	.6230E-08	.5287E-09
10052	508.76	.2362E-05	.9163E-06	.2878E-06	.6818E-07	.1096E-07	.1014E-08
10050	509.93	.3348E-05	.1345E-05	.4405E-06	.1099E-06	.1884E-07	.1892E-08
10048	511.12	.4667E-05	.1939E-05	.6612E-06	.1733E-06	.3161E-07	.3437E-08
10046	512.32	.6397E-05	.2745E-05	.9730E-06	.2673E-06	.5174E-07	.6072E-08
10044	513.54	.8621E-05	.3815E-05	.1404E-05	.4036E-06	.8267E-07	.1044E-07
10042	514.78	.1142E-04	.5206E-05	.1984E-05	.5959E-06	.1289E-06	.1744E-07
10040	516.03	.1487E-04	.6973E-05	.2749E-05	.8604E-06	.1960E-06	.2835E-07
10038	517.29	.1902E-04	.9163E-05	.3731E-05	.1215E-05	.2906E-06	.4479E-07
10036	518.57	.2391E-04	.1181E-04	.4959E-05	.1676E-05	.4201E-06	.6876E-07
10034	519.87	.2950E-04	.1493E-04	.6453E-05	.2259E-05	.5920E-06	.1026E-06
10032	521.18	.3573E-04	.1850E-04	.8216E-05	.2974E-05	.8126E-06	.1486E-06
10030	522.51	.4246E-04	.2246E-04	.1023E-04	.3822E-05	.1086E-05	.2088E-06
10028	523.85	.4946E-04	.2669E-04	.1246E-04	.4792E-05	.1413E-05	.2848E-06
10026	525.21	.5646E-04	.3104E-04	.1482E-04	.5857E-05	.1787E-05	.3765E-06
10024	526.58	.6308E-04	.3528E-04	.1719E-04	.6972E-05	.2196E-05	.4819E-06
10022	527.97	.6890E-04	.3916E-04	.1945E-04	.8075E-05	.2618E-05	.5967E-06
10020	529.37	.7347E-04	.4237E-04	.2142E-04	.9083E-05	.3025E-05	.7137E-06
10018	530.79	.7633E-04	.4460E-04	.2291E-04	.9905E-05	.3380E-05	.8226E-06
10016	532.23	.7704E-04	.4555E-04	.2373E-04	.1044E-04	.3641E-05	.9114E-06
10014	533.68	.7524E-04	.4496E-04	.2372E-04	.1060E-04	.3767E-05	.9667E-06
10012	535.14	.7068E-04	.4262E-04	.2273E-04	.1029E-04	.3721E-05	.9757E-06
10010	536.62	.6324E-04	.3843E-04	.2069E-04	.9475E-05	.3475E-05	.9280E-06
100 8	538.12	.5300E-04	.3241E-04	.1758E-04	.8129E-05	.3017E-05	.8179E-06
100 6	539.63	.4018E-04	.2470E-04	.1348E-04	.6278E-05	.2351E-05	.6452E-06
100 4	541.16	.2521E-04	.1555E-04	.8524E-05	.3992E-05	.1505E-05	.4167E-06
11052	541.58	.1069E-05	.3158E-06	.7153E-07	.1137E-07	.1112E-08	.5422E-10
11051	542.32	.1280E-05	.3848E-06	.8903E-07	.1453E-07	.1467E-08	.7463E-10
100 2	542.70	.8656E-05	.5352E-05	.2942E-05	.1382E-05	.5235E-06	.1457E-06
11050	543.05	.1526E-05	.4667E-06	.1103E-06	.1846E-07	.1925E-08	.1020E-09
11049	543.80	.1811E-05	.5637E-06	.1359E-06	.2334E-07	.2511E-08	.1385E-09
101 2	544.27	.2171E-04	.1342E-04	.7379E-05	.3467E-05	.1313E-05	.3654E-06
101 4	544.30	.1904E-04	.1174E-04	.6436E-05	.3013E-05	.1136E-05	.3144E-06
101 6	544.34	.1759E-04	.1081E-04	.5899E-05	.2747E-05	.1028E-05	.2821E-06
101 8	544.40	.1632E-04	.9974E-05	.5409E-05	.2500E-05	.9273E-06	.2513E-06
10110	544.47	.1502E-04	.9122E-05	.4908E-05	.2247E-05	.8237E-06	.2199E-06
11048	544.54	.2142E-05	.6777E-06	.1668E-06	.2934E-07	.3255E-08	.1868E-09
10112	544.56	.1367E-04	.8239E-05	.4392E-05	.1987E-05	.7182E-06	.1882E-06
10114	544.67	.1229E-04	.7338E-05	.3868E-05	.1727E-05	.6137E-06	.1574E-06
10116	544.78	.1090E-04	.6438E-05	.3351E-05	.1473E-05	.5135E-06	.1284E-06
10118	544.92	.9528E-05	.5563E-05	.2855E-05	.1233E-05	.4205E-06	.1023E-06
102 0	545.04	.1740E-04	.1089E-04	.5993E-05	.2820E-05	.1070E-05	.2985E-06
10120	545.07	.8213E-05	.4732E-05	.2390E-05	.1012E-05	.3369E-06	.7941E-07
10122	545.24	.6978E-05	.3962E-05	.1966E-05	.8152E-06	.2641E-06	.6013E-07

TABLE XVI (Continued)

BAND CODE	WAVE NUMBER	INTENSITY					
		T=300K	T=275K	T=250K	T=225K	T=200K	T=175K
11047	545.28	.2522E-05	.8112E-06	.2036E-06	.3669E-07	.4194E-08	.2503E-09
10124	545.42	.5843E-05	.3265E-05	.1589E-05	.6437E-06	.2025E-06	.4440E-07
10126	545.61	.4821E-05	.2647E-05	.1262E-05	.4983E-06	.1518E-06	.3196E-07
10128	545.83	.3920E-05	.2112E-05	.9847E-06	.3783E-06	.1114E-06	.2243E-07
7068	546.02	.1152E-05	.3273E-06	.7071E-07	.1061E-07	.9655E-09	.4294E-10
11046	546.02	.2957E-05	.9667E-06	.2473E-06	.4563E-07	.5373E-08	.3330E-09
10130	546.05	.3140E-05	.1659E-05	.7547E-06	.2815E-06	.7988E-07	.1534E-07
10132	546.30	.2479E-05	.1281E-05	.5683E-06	.2054E-06	.5603E-07	.1023E-07
10134	546.56	.1928E-05	.9742E-06	.4203E-06	.1469E-06	.3843E-07	.6650E-08
102 2	546.63	.3492E-04	.2159E-04	.1186E-04	.5574E-05	.2110E-05	.5873E-06
7067	546.75	.1470E-05	.4271E-06	.9490E-07	.1474E-07	.1399E-08	.6573E-10
11045	546.77	.3454E-05	.1147E-05	.2990E-06	.5645E-07	.6841E-08	.4400E-09
10136	546.83	.1477E-05	.7287E-06	.3054E-06	.1030E-06	.2578E-07	.4213E-08
10138	547.12	.1115E-05	.5362E-06	.2179E-06	.7082E-07	.1691E-07	.2602E-08
7066	547.47	.1867E-05	.5551E-06	.1268E-06	.2036E-07	.2015E-08	.9993E-10
11044	547.51	.4017E-05	.1354E-05	.3597E-06	.6946E-07	.8657E-08	.5774E-09
7065	548.20	.2362E-05	.7183E-06	.1685E-06	.2798E-07	.2886E-08	.1509E-09
102 4	548.22	.5121E-04	.3158E-04	.1730E-04	.8100E-05	.3053E-05	.8448E-06
11043	548.26	.4652E-05	.1592E-05	.4305E-06	.8500E-07	.1089E-07	.7525E-09
7064	548.93	.2976E-05	.9255E-06	.2230E-06	.3824E-07	.4109E-08	.2264E-09
11042	549.01	.5365E-05	.1863E-05	.5128E-06	.1034E-06	.1362E-07	.9741E-09
7063	549.65	.3736E-05	.1187E-05	.2937E-06	.5201E-07	.5816E-08	.3375E-09
11041	549.76	.6161E-05	.2171E-05	.6078E-06	.1252E-06	.1692E-07	.1252E-08
102 6	549.84	.6576E-04	.4039E-04	.2203E-04	.1025E-04	.3839E-05	.1053E-05
7062	550.38	.4670E-05	.1517E-05	.3849E-06	.7035E-07	.6185E-08	.4996E-09
11040	550.50	.7046E-05	.2518E-05	.7168E-06	.1507E-06	.2090E-07	.1599E-08
7061	551.11	.5815E-05	.1929E-05	.5022E-06	.9467E-07	.1145E-07	.7346E-09
11039	551.25	.8024E-05	.2906E-05	.8412E-06	.1805E-06	.2566E-07	.2027E-08
102 8	551.46	.7798E-04	.4765E-04	.2583E-04	.1193E-04	.4425E-05	.1199E-05
7060	551.84	.7212E-05	.2442E-05	.6520E-06	.1267E-06	.1592E-07	.1073E-08
11038	552.00	.9098E-05	.3340E-05	.9822E-06	.2149E-06	.3130E-07	.2552E-08
7059	552.57	.8909E-05	.3079E-05	.8424E-06	.1687E-06	.2201E-07	.1557E-08
11037	552.76	.1027E-04	.3820E-05	.1141E-05	.2544E-06	.3796E-07	.3190E-08
10210	553.11	.8746E-04	.5309E-04	.2855E-04	.1307E-04	.4787E-05	.1277E-05
7058	553.30	.1096E-04	.3865E-05	.1083E-05	.2235E-06	.3026E-07	.2244E-08
11036	553.51	.1155E-04	.4349E-05	.1319E-05	.2996E-06	.4574E-07	.3961E-08
7057	554.04	.1343E-04	.4831E-05	.1387E-05	.2945E-06	.4134E-07	.3213E-08
11035	554.26	.1292E-04	.4928E-05	.1517E-05	.3508E-06	.5478E-07	.4883E-08
7056	554.77	.1639E-04	.6011E-05	.1766E-05	.3859E-06	.5615E-07	.4569E-08
10212	554.77	.9395E-04	.5658E-04	.3014E-04	.1363E-04	.4924E-05	.1290E-05
11034	555.02	.1440E-04	.5558E-05	.1735E-05	.4084E-06	.6520E-07	.5978E-08
7055	555.50	.1992E-04	.7448E-05	.2239E-05	.5032E-06	.7581E-07	.6453E-08
11033	555.77	.1598E-04	.6238E-05	.1975E-05	.4728E-06	.7710E-07	.7266E-08
2083	556.09	.1129E-05	.2907E-06	.5587E-07	.7267E-08	.5528E-09	.1954E-10
7054	556.24	.2412E-04	.9186E-05	.2824E-05	.6525E-06	.1018E-06	.9054E-08

TABLE XVI (Continued)

BAND CODE	WAVE NUMBER	INTENSITY					
		T=300K	T=275K	T=250K	T=225K	T=200K	T=175K
10214	556.44	.9739E-04	.5811E-04	.3062E-04	.1366E-04	.4851E-05	.1243E-05
11032	556.53	.1765E-04	.6969E-05	.2236E-05	.5443E-06	.9061E-07	.8769E-08
7053	556.98	.2907E-04	.1128E-04	.3546E-05	.8416E-06	.1358E-06	.1262E-07
11031	557.29	.1941E-04	.7748E-05	.2519E-05	.6230E-06	.1058E-06	.1051E-07
2081	557.51	.2054E-05	.5595E-06	.1150E-06	.1625E-07	.1371E-08	.5534E-10
7052	557.71	.3491E-04	.1379E-04	.4430E-05	.1080E-05	.1801E-06	.1746E-07
11030	558.04	.2125E-04	.8572E-05	.2822E-05	.7090E-06	.1228E-06	.1250E-07
10216	558.13	.9791E-04	.5780E-04	.3007E-04	.1321E-04	.4599E-05	.1150E-05
7051	558.45	.4174E-04	.1679E-04	.5509E-05	.1378E-05	.2374E-06	.2401E-07
11029	558.80	.2316E-04	.9437E-05	.3146E-05	.8022E-06	.1415E-06	.1476E-07
2079	558.93	.3679E-05	.1059E-05	.2325E-06	.3560E-07	.3321E-08	.1526E-09
7050	559.19	.4971E-04	.2034E-04	.6816E-05	.1749E-05	.3111E-06	.3278E-07
11028	559.56	.2512E-04	.1034E-04	.3487E-05	.9023E-06	.1621E-06	.1731E-07
10218	559.83	.9576E-04	.5586E-04	.2864E-04	.1236E-04	.4212E-05	.1023E-05
7049	559.93	.5896E-04	.2454E-04	.8394E-05	.2209E-05	.4053E-06	.4446E-07
11027	560.32	.2713E-04	.1127E-04	.3845E-05	.1009E-05	.1845E-06	.2015E-07
2077	560.36	.6487E-05	.1969E-05	.4612E-06	.7640E-07	.7862E-08	.4099E-09
7048	560.67	.6964E-04	.2948E-04	.1028E-04	.2774E-05	.5249E-06	.5989E-07
11026	561.08	.2915E-04	.1222E-04	.4217E-05	.1122E-05	.2086E-06	.2328E-07
7047	561.41	.8192E-04	.3525E-04	.1254E-04	.3464E-05	.6756E-06	.8013E-07
10220	561.55	.9135E-04	.5258E-04	.2653E-04	.1123E-04	.3733E-05	.8792E-06
2075	561.79	.1126E-04	.3602E-05	.8980E-06	.1606E-06	.1818E-07	.1072E-08
11025	561.85	.3118E-04	.1319E-04	.4599E-05	.1239E-05	.2343E-06	.2670E-07
7046	562.16	.9595E-04	.4195E-04	.1522E-04	.4304E-05	.8643E-06	.1065E-06
11024	562.61	.3319E-04	.1416E-04	.4986E-05	.1361E-05	.2613E-06	.3039E-07
7045	562.90	.1119E-03	.4971E-04	.1838E-04	.5318E-05	.1099E-05	.1405E-06
2073	563.23	.1924E-04	.6475E-05	.1716E-05	.3306E-06	.4109E-07	.2732E-08
10222	563.29	.8514E-04	.4829E-04	.2394E-04	.9916E-05	.3209E-05	.7300E-06
11023	563.37	.3516E-04	.1512E-04	.5380E-05	.1486E-05	.2896E-06	.3433E-07
7044	563.64	.1300E-03	.5864E-04	.2208E-04	.6535E-05	.1389E-05	.1841E-06
11022	564.14	.3706E-04	.1607E-04	.5769E-05	.1611E-05	.3187E-06	.3849E-07
7043	564.39	.1504E-03	.6885E-04	.2640E-04	.7987E-05	.1745E-05	.2397E-06
2071	564.66	.3236E-04	.1144E-04	.3218E-05	.6666E-06	.9073E-07	.6778E-08
11021	564.91	.3887E-04	.1698E-04	.6151E-05	.1737E-05	.3483E-06	.4282E-07
10224	565.04	.7763E-04	.4333E-04	.2107E-04	.8523E-05	.2678E-05	.5867E-06
7042	565.13	.1732E-03	.8048E-04	.3140E-04	.9708E-05	.2179E-05	.3098E-06
11020	565.67	.4055E-04	.1784E-04	.6520E-05	.1861E-05	.3780E-06	.4726E-07
7041	565.88	.1987E-03	.9364E-04	.3717E-04	.1173E-04	.2705E-05	.3977E-06
2069	566.10	.5357E-04	.1988E-04	.5921E-05	.1316E-05	.1957E-06	.1637E-07
11019	566.44	.4209E-04	.1864E-04	.6869E-05	.1980E-05	.4073E-06	.5175E-07
7040	566.63	.2269E-03	.1084E-03	.4377E-04	.1411E-04	.3336E-05	.5070E-06
10226	566.81	.6932E-04	.3802E-04	.1810E-04	.7139E-05	.2173E-05	.4568E-06
11018	567.21	.4345E-04	.1937E-04	.7194E-05	.2093E-05	.4358E-06	.5622E-07
7039	567.38	.2580E-03	.1250E-03	.5129E-04	.1686E-04	.4089E-05	.6418E-06
2067	567.55	.8730E-04	.3394E-04	.1069E-04	.2546E-05	.4123E-06	.3852E-07

TABLE XVI (Continued)

BAND CODE	WAVE NUMBER	INTENSITY					
		T=300K	T=275K	T=250K	T=225K	T=200K	T=175K
11017	567.98	.4462E-04	.2001E-04	.7487E-05	.2198E-05	.4628E-06	.6058E-07
7038	568.13	.2922E-03	.1434E-03	.5980E-04	.2005E-04	.4981E-05	.8068E-06
10228	568.59	.6067E-04	.3265E-04	.1520E-04	.5831E-05	.1715E-05	.3449E-06
11016	568.75	.4556E-04	.2055E-04	.7742E-05	.2293E-05	.4879E-06	.6474E-07
7037	568.88	.3294E-03	.1638E-03	.6937E-04	.2370E-04	.6031E-05	.1007E-05
2065	569.00	.1400E-03	.5695E-04	.1895E-04	.4821E-05	.8486E-06	.8824E-07
11015	569.52	.4626E-04	.2098E-04	.7955E-05	.2375E-05	.5104E-06	.6861E-07
7036	569.63	.3697E-03	.1862E-03	.8005E-04	.2786E-04	.7255E-05	.1248E-05
11014	570.29	.4669E-04	.2129E-04	.8120E-05	.2442E-05	.5298E-06	.7208E-07
7035	570.38	.4131E-03	.2106E-03	.9190E-04	.3257E-04	.8674E-05	.1536E-05
10230	570.39	.5207E-04	.2747E-04	.1248E-04	.4648E-05	.1317E-05	.2527E-06
2063	570.45	.2210E-03	.9393E-04	.3294E-04	.8942E-05	.1706E-05	.1968E-06
11013	571.07	.4684E-04	.2146E-04	.8233E-05	.2493E-05	.5457E-06	.7508E-07
7034	571.14	.4596E-03	.2371E-03	.1050E-03	.3785E-04	.1030E-04	.1877E-05
11012	571.84	.4671E-04	.2149E-04	.8288E-05	.2527E-05	.5575E-06	.7751E-07
7033	571.89	.5090E-03	.2657E-03	.1192E-03	.4374E-04	.1216E-04	.2277E-05
2061	571.90	.3432E-03	.1522E-03	.5620E-04	.1624E-04	.3350E-05	.4273E-06
10232	572.20	.4386E-04	.2264E-04	.1002E-04	.3618E-05	.9857E-06	.1797E-06
11011	572.62	.4627E-04	.2138E-04	.8286E-05	.2541E-05	.5648E-06	.7929E-07
7032	572.65	.5612E-03	.2963E-03	.1348E-03	.5026E-04	.1427E-04	.2743E-05
2059	573.36	.5246E-03	.2425E-03	.9406E-04	.2887E-04	.6425E-05	.9034E-06
11010	573.39	.4555E-04	.2112E-04	.8223E-05	.2536E-05	.5675E-06	.8038E-07
7031	573.40	.6159E-03	.3287E-03	.1515E-03	.5741E-04	.1663E-04	.3280E-05
10234	574.03	.3627E-04	.1830E-04	.7883E-05	.2751E-05	.7186E-06	.1242E-06
7030	574.16	.6728E-03	.3629E-03	.1694E-03	.6520E-04	.1925E-04	.3894E-05
110 9	574.17	.4454E-04	.2072E-04	.8100E-05	.2510E-05	.5654E-06	.8072E-07
2057	574.83	.7889E-03	.3795E-03	.1544E-03	.5026E-04	.1203E-04	.1859E-05
7029	574.92	.7316E-03	.3987E-03	.1884E-03	.7360E-04	.2215E-04	.4589E-05
110 8	574.95	.4326E-04	.2019E-04	.7921E-05	.2466E-05	.5585E-06	.8031E-07
7028	575.68	.7918E-03	.4357E-03	.2083E-03	.8259E-04	.2531E-04	.5367E-05
110 7	575.72	.4176E-04	.1954E-04	.7691E-05	.2404E-05	.5471E-06	.7919E-07
10236	575.87	.2945E-04	.1450E-04	.6068E-05	.2044E-05	.5107E-06	.8335E-07
2055	576.29	.1167E-02	.5836E-03	.2487E-03	.8565E-04	.2201E-04	.3723E-05
7027	576.44	.8528E-03	.4738E-03	.2292E-03	.9213E-04	.2873E-04	.6231E-05
110 6	576.50	.4008E-04	.1880E-04	.7421E-05	.2327E-05	.5320E-06	.7744E-07
7026	577.20	.9141E-03	.5125E-03	.2506E-03	.1021E-03	.3239E-04	.7180E-05
110 5	577.28	.3832E-04	.1801E-04	.7127E-05	.2242E-05	.5144E-06	.7523E-07
10238	577.73	.2350E-04	.1128E-04	.4576E-05	.1484E-05	.3539E-06	.5438E-07
2053	577.76	.1699E-02	.8816E-03	.3928E-03	.1429E-03	.3930E-04	.7258E-05
7025	577.96	.9750E-03	.5515E-03	.2726E-03	.1125E-03	.3627E-04	.8211E-05
110 4	578.07	.3667E-04	.1726E-04	.6845E-05	.2158E-05	.4968E-06	.7295E-07
7024	578.72	.1035E-02	.5903E-03	.2947E-03	.1232E-03	.4034E-04	.9317E-05
110 3	578.85	.3551E-04	.1674E-04	.6648E-05	.2100E-05	.4846E-06	.7139E-07
2051	579.24	.2433E-02	.1308E-02	.6086E-03	.2333E-03	.6853E-04	.1377E-04
7023	579.48	.1092E-02	.6284E-03	.3169E-03	.1340E-03	.4455E-04	.1049E-04

TABLE XVI (Continued)

BAND CCCE	WAVE NUMBER	INTENSITY					
		T=300K	T=275K	T=250K	T=225K	T=200K	T=175K
10240	579.61	.1842E-04	.8606E-05	.3381E-05	.1054E-05	.2392E-06	.3449E-07
7022	580.25	.1147E-02	.6652E-03	.3386E-03	.1449E-03	.4885E-04	.1172E-04
2049	580.71	.3426E-02	.1907E-02	.9245E-03	.3727E-03	.1166E-03	.2542E-04
7021	581.01	.1199E-02	.7002E-03	.3596E-03	.1556E-03	.5319E-04	.1299E-04
111 3	581.21	.1249E-04	.5886E-05	.2337E-05	.7384E-06	.1704E-06	.2509E-07
111 4	581.21	.2214E-04	.1042E-04	.4132E-05	.1303E-05	.2998E-06	.4402E-07
111 5	581.21	.3035E-04	.1426E-04	.5643E-05	.1775E-05	.4071E-06	.5953E-07
111 6	581.22	.3758E-04	.1762E-04	.6954E-05	.2180E-05	.4983E-06	.7252E-07
111 7	581.23	.4399E-04	.2058E-04	.8098E-05	.2530E-05	.5757E-06	.8331E-07
111 8	581.23	.4967E-04	.2317E-04	.9088E-05	.2828E-05	.6403E-06	.9206E-07
111 9	581.24	.5464E-04	.2541E-04	.9930E-05	.3076E-05	.6926E-06	.9885E-07
11110	581.25	.5891E-04	.2731E-04	.1063E-04	.3276E-05	.7328E-06	.1038E-06
11111	581.26	.6250E-04	.2886E-04	.1118E-04	.3427E-05	.7616E-06	.1069E-06
11112	581.27	.6541E-04	.3008E-04	.1160E-04	.3533E-05	.7792E-06	.1083E-06
11113	581.28	.6766E-04	.3098E-04	.1188E-04	.3596E-05	.7865E-06	.1082E-06
11114	581.29	.6925E-04	.3155E-04	.1203E-04	.3616E-05	.7841E-06	.1066E-06
11115	581.31	.7022E-04	.3183E-04	.1206E-04	.3599E-05	.7729E-06	.1038E-06
11116	581.32	.7060E-04	.3183E-04	.1198E-04	.3546E-05	.7540E-06	.9989E-07
11117	581.34	.7041E-04	.3156E-04	.1180E-04	.3462E-05	.7283E-06	.9528E-07
11118	581.35	.6971E-04	.3105E-04	.1152E-04	.3351E-05	.6970E-06	.8987E-07
11119	581.37	.6853E-04	.3033E-04	.1117E-04	.3216E-05	.6611E-06	.8394E-07
11120	581.39	.6692E-04	.2941E-04	.1074E-04	.3063E-05	.6217E-06	.7768E-07
11121	581.41	.6494E-04	.2834E-04	.1026E-04	.2895E-05	.5799E-06	.7124E-07
11122	581.43	.6263E-04	.2713E-04	.9732E-05	.2716E-05	.5366E-06	.6476E-07
11123	581.45	.6005E-04	.2580E-04	.9171E-05	.2530E-05	.4927E-06	.5837E-07
11124	581.47	.5725E-04	.2440E-04	.8586E-05	.2340E-05	.4490E-06	.5217E-07
11125	581.49	.5428E-04	.2294E-04	.7989E-05	.2150E-05	.4061E-06	.4624E-07
10242	581.50	.1420E-04	.6446E-05	.2448E-05	.7320E-06	.1577E-06	.2128E-07
11126	581.52	.5118E-04	.2144E-04	.7387E-05	.1963E-05	.3647E-06	.4066E-07
11127	581.54	.4801E-04	.1992E-04	.6790E-05	.1780E-05	.3251E-06	.3547E-07
11128	581.57	.4481E-04	.1842E-04	.6205E-05	.1603E-05	.2878E-06	.3070E-07
11129	581.59	.4160E-04	.1693E-04	.5637E-05	.1436E-05	.2531E-06	.2637E-07
11130	581.62	.3844E-04	.1548E-04	.5092E-05	.1277E-05	.2210E-06	.2247E-07
11131	581.65	.3534E-04	.1409E-04	.4573E-05	.1130E-05	.1916E-06	.1901E-07
11132	581.68	.3234E-04	.1275E-04	.4085E-05	.9930E-06	.1651E-06	.1596E-07
11133	581.70	.2945E-04	.1148E-04	.3629E-05	.8676E-06	.1413E-06	.1330E-07
11134	581.74	.2670E-04	.1028E-04	.3206E-05	.7536E-06	.1201E-06	.1100E-07
11135	581.77	.2409E-04	.9169E-05	.2818E-05	.6507E-06	.1015E-06	.9035E-08
7020	581.78	.1246E-02	.7328E-03	.3796E-03	.1660E-03	.5748E-04	.1427E-04
11136	581.80	.2163E-04	.8134E-05	.2463E-05	.5586E-06	.8517E-07	.7366E-08
11137	581.83	.1934E-04	.7181E-05	.2141E-05	.4768E-06	.7103E-07	.5962E-08
11138	581.87	.1721E-04	.6309E-05	.1852E-05	.4046E-06	.5885E-07	.4791E-08
11139	581.90	.1525E-04	.5516E-05	.1594E-05	.3414E-06	.4846E-07	.3822E-08
11140	581.94	.1346E-04	.4800E-05	.1364E-05	.2864E-06	.3965E-07	.3028E-08
11141	581.97	.1182E-04	.4157E-05	.1162E-05	.2389E-06	.3224E-07	.2382E-08

TABLE XVI (Continued)

BAND CODE	WAVE NUMBER	INTENSITY					
		T=300K	T=275K	T=250K	T=225K	T=200K	T=175K
11142	582.01	.1034E-04	.3584E-05	.9844E-06	.1982E-06	.2605E-07	.1861E-08
11143	582.05	.9000E-05	.3075E-05	.8299E-06	.1635E-06	.2092E-07	.1443E-08
11144	582.09	.7803E-05	.2626E-05	.6961E-06	.1342E-06	.1669E-07	.1112E-08
11145	582.13	.6736E-05	.2232E-05	.5809E-06	.1095E-06	.1324E-07	.8502E-09
11146	582.17	.5791E-05	.1889E-05	.4823E-06	.8882E-07	.1044E-07	.6458E-09
2047	582.19	.4746E-02	.2730E-02	.1377E-02	.5828E-03	.1938E-03	.4566E-04
11147	582.22	.4957E-05	.1591E-05	.3985E-06	.7168E-07	.8178E-08	.4872E-09
11148	582.26	.4225E-05	.1334E-05	.3276E-06	.5753E-07	.6369E-08	.3650E-09
11149	582.30	.3587E-05	.1114E-05	.2680E-06	.4592E-07	.4930E-08	.2715E-09
11150	582.35	.3032E-05	.9255E-06	.2182E-06	.3645E-07	.3793E-08	.2007E-09
11151	582.39	.2552E-05	.7656E-06	.1768E-06	.2878E-07	.2900E-08	.1473E-09
11152	582.44	.2139E-05	.6305E-06	.1425E-06	.2260E-07	.2205E-08	.1073E-09
11153	582.49	.1786E-05	.5169E-06	.1143E-06	.1766E-07	.1666E-08	.7770E-10
11154	582.54	.1485E-05	.4219E-06	.9124E-07	.1372E-07	.1251E-08	.5587E-10
7019	582.55	.1287E-02	.7624E-03	.3982E-03	.1758E-03	.6167E-04	.1556E-04
11155	582.59	.1230E-05	.3428E-06	.7248E-07	.1060E-07	.9340E-09	.3990E-10
11156	582.64	.1014E-05	.2773E-06	.5730E-07	.8148E-08	.6931E-09	.2830E-10
7018	583.31	.1322E-02	.7883E-03	.4149E-03	.1850E-03	.6565E-04	.1682E-04
10244	583.40	.1075E-04	.4740E-05	.1737E-05	.4973E-06	.1015E-06	.1276E-07
2045	583.68	.6463E-02	.3838E-02	.2011E-02	.8915E-03	.3142E-03	.7978E-04
7017	584.08	.1350E-02	.8100E-03	.4295E-03	.1932E-03	.6934E-04	.1803E-04
112 3	584.35	.1795E-05	.8461E-06	.3359E-06	.1061E-06	.2448E-07	.3605E-08
7016	584.85	.1371E-02	.8269E-03	.4415E-03	.2003E-03	.7266E-04	.1915E-04
112 4	585.14	.4251E-05	.2001E-05	.7930E-06	.2500E-06	.5752E-07	.8443E-08
2043	585.17	.8654E-02	.5297E-02	.2878E-02	.1334E-02	.4970E-03	.1356E-03
10246	585.33	.8011E-05	.3423E-05	.1208E-05	.3306E-06	.6372E-07	.7450E-08
7015	585.62	.1382E-02	.8385E-03	.4506E-03	.2061E-03	.7550E-04	.2016E-04
112 5	585.93	.6465E-05	.3272E-05	.1294E-05	.4069E-06	.9332E-07	.1364E-07
7014	586.40	.1385E-02	.8443E-03	.4565E-03	.2103E-03	.7779E-04	.2102E-04
2041	586.66	.1139E-01	.7176E-02	.4037E-02	.1952E-02	.7671E-03	.2241E-03
112 6	586.72	.9743E-05	.4567E-05	.1802E-05	.5648E-06	.1291E-06	.1878E-07
7013	587.17	.1378E-02	.8439E-03	.4589E-03	.2129E-03	.7944E-04	.2171E-04
10248	587.26	.5869E-05	.2427E-05	.8241E-06	.2150E-06	.3905E-07	.4230E-08
112 7	587.51	.1247E-04	.5834E-05	.2295E-05	.7168E-06	.1631E-06	.2359E-07
7012	587.94	.1360E-02	.8370E-03	.4576E-03	.2137E-03	.8037E-04	.2219E-04
2039	588.15	.1473E-01	.9541E-02	.5548E-02	.2794E-02	.1155E-02	.3600E-03
112 8	588.31	.1509E-04	.7036E-05	.2759E-05	.8582E-06	.1942E-06	.2792E-07
5078	588.57	.1134E-05	.2554E-06	.4180E-07	.4470E-08	.2663E-09	.6880E-11
7011	588.71	.1333E-02	.8234E-03	.4523E-03	.2125E-03	.8053E-04	.2245E-04
112 9	589.10	.1753E-04	.8150E-05	.3183E-05	.9858E-06	.2218E-06	.3165E-07
10250	589.21	.4228E-05	.1691E-05	.5512E-06	.1369E-06	.2337E-07	.2337E-08
7010	589.49	.1295E-02	.8030E-03	.4431E-03	.2093E-03	.7986E-04	.2246E-04
2037	589.65	.1872E-01	.1245E-01	.7469E-02	.3909E-02	.1695E-02	.5623E-03
11210	589.89	.1976E-04	.9156E-05	.3562E-05	.1097E-05	.2454E-06	.3473E-07
5076	590.00	.1984E-05	.4711E-06	.8216E-07	.9496E-08	.6234E-09	.1825E-10

TABLE XVI (Continued)

			INTENSITY					
BAND	CCCE	WAVE NUMBER	T=300K	T=275K	T=250K	T=225K	T=200K	T=175K
7117		597.43	.2397E-02	.1437E-02	.7613E-03	.3422E-03	.1228E-03	.3190E-04
7118		597.44	.2370E-02	.1412E-02	.7425E-03	.3308E-03	.1173E-03	.3005E-04
7119		597.46	.2327E-02	.1377E-02	.7188E-03	.3172E-03	.1112E-03	.2804E-04
7120		597.48	.2271E-02	.1335E-02	.6908E-03	.3018E-03	.1045E-03	.2592E-04
7121		597.50	.2201E-02	.1285E-02	.6593E-03	.2850E-03	.9736E-04	.2376E-04
7122		597.52	.2122E-02	.1229E-02	.6250E-03	.2672E-03	.9003E-04	.2158E-04
7123		597.54	.2033E-02	.1168E-02	.5887E-03	.2488E-03	.8262E-04	.1944E-04
7124		597.56	.1937E-02	.1104E-02	.5509E-03	.2301E-03	.7525E-04	.1737E-04
7125		597.58	.1836E-02	.1038E-02	.5124E-03	.2113E-03	.6804E-04	.1539E-04
7126		597.61	.1731E-02	.9695E-03	.4736E-03	.1928E-03	.6108E-04	.1353E-04
7127		597.63	.1623E-02	.9008E-03	.4352E-03	.1748E-03	.5444E-04	.1180E-04
7128		597.66	.1514E-02	.8325E-03	.3976E-03	.1574E-03	.4819E-04	.1021E-04
7129		597.68	.1406E-02	.7652E-03	.3611E-03	.1409E-03	.4236E-04	.8770E-05
7130		597.71	.1299E-02	.6996E-03	.3262E-03	.1254E-03	.3699E-04	.7474E-05
7131		597.74	.1194E-02	.6364E-03	.2929E-03	.1109E-03	.3208E-04	.6322E-05
7132		597.77	.1092E-02	.5759E-03	.2616E-03	.9746E-04	.2763E-04	.5307E-05
7133		597.79	.9947E-03	.5186E-03	.2324E-03	.8515E-04	.2365E-04	.4423E-05
1094		597.80	.1497E-05	.3689E-06	.6730E-07	.8219E-08	.5782E-09	.1850E-10
7134		597.83	.9016E-03	.4646E-03	.2053E-03	.7396E-04	.2011E-04	.3659E-05
7135		597.86	.8134E-03	.4142E-03	.1804E-03	.6386E-04	.1699E-04	.3005E-05
11220		597.89	.2787E-04	.1224E-04	.4466E-05	.1272E-05	.2581E-06	.3223E-07
7136		597.89	.7306E-03	.3674E-03	.1577E-03	.5482E-04	.1426E-04	.2450E-05
7137		597.92	.6532E-03	.3244E-03	.1371E-03	.4679E-04	.1189E-04	.1983E-05
7138		597.96	.5814E-03	.2850E-03	.1186E-03	.3971E-04	.9853E-05	.1594E-05
7139		597.99	.5152E-03	.2492E-03	.1021E-03	.3351E-04	.8113E-05	.1272E-05
7140		598.03	.4545E-03	.2168E-03	.8739E-04	.2812E-04	.6639E-05	.1008E-05
7141		598.06	.3992E-03	.1878E-03	.7443E-04	.2346E-04	.5399E-05	.7929E-06
7142		598.10	.3491E-03	.1619E-03	.6307E-04	.1947E-04	.4363E-05	.6195E-06
7143		598.14	.3040E-03	.1389E-03	.5318E-04	.1606E-04	.3504E-05	.4806E-06
7144		598.18	.2636E-03	.1187E-03	.4461E-04	.1318E-04	.2797E-05	.3702E-06
7145		598.22	.2276E-03	.1009E-03	.3723E-04	.1075E-04	.2219E-05	.2833E-06
7146		598.26	.1957E-03	.8540E-04	.3092E-04	.8728E-05	.1750E-05	.2152E-06
7147		598.31	.1675E-03	.7194E-04	.2555E-04	.7044E-05	.1371E-05	.1624E-06
7148		598.35	.1428E-03	.6033E-04	.2101E-04	.5655E-05	.1068E-05	.1217E-06
7149		598.39	.1212E-03	.5037E-04	.1719E-04	.4515E-05	.8270E-06	.9057E-07
7150		598.44	.1025E-03	.4186E-04	.1400E-04	.3585E-05	.6364E-06	.6695E-07
7151		598.48	.8630E-04	.3463E-04	.1134E-04	.2831E-05	.4868E-06	.4915E-07
7152		598.53	.7236E-04	.2853E-04	.9144E-05	.2224E-05	.3701E-06	.3583E-07
7153		598.58	.6042E-04	.2339E-04	.7337E-05	.1738E-05	.2797E-06	.2595E-07
7154		598.63	.5024E-04	.1910E-04	.5858E-05	.1350E-05	.2102E-06	.1867E-07
5064		598.66	.4084E-04	.1294E-04	.3193E-05	.5637E-06	.6287E-07	.3638E-08
7155		598.68	.4161E-04	.1552E-04	.4655E-05	.1044E-05	.1569E-06	.1333E-07
11221		598.70	.2736E-04	.1193E-04	.4314E-05	.1216E-05	.2435E-06	.2989E-07
2025		598.72	.5327E-01	.4028E-01	.2821E-01	.1783E-01	.9797E-02	.4403E-02
7156		598.73	.3432E-04	.1256E-04	.3681E-05	.8025E-06	.1165E-06	.9462E-08

TABLE XVI (Continued)

BAND CODE	WAVE NUMBER	INTENSITY					
		T=300K	T=275K	T=250K	T=225K	T=200K	T=175K
7157	598.78	.2819E-04	.1012E-04	.2897E-05	.6138E-06	.8597E-07	.6669E-08
7158	598.83	.2306E-04	.8114E-03	.2269E-05	.4669E-06	.6307E-07	.4669E-08
7159	598.88	.1879E-04	.6479E-05	.1768E-05	.3533E-06	.4599E-07	.3246E-08
7160	598.94	.1525E-04	.5151E-05	.1372E-05	.2659E-06	.3334E-07	.2242E-08
7161	598.99	.1233E-04	.4078E-05	.1059E-05	.1991E-06	.2403E-07	.1538E-08
7162	599.05	.9922E-05	.3214E-05	.8136E-06	.1483E-06	.1721E-07	.1048E-08
7163	599.10	.7955E-05	.2522E-05	.6221E-06	.1099E-06	.1226E-07	.7097E-09
7164	599.16	.6353E-05	.1970E-05	.4734E-06	.8098E-07	.8679E-08	.4772E-09
7165	599.20	.2962E-05	.7782E-06	.1532E-06	.2055E-07	.1625E-08	.6042E-10
7165	599.22	.5053E-05	.1533E-05	.3586E-06	.5937E-07	.6109E-08	.3187E-09
7166	599.28	.4003E-05	.1187E-05	.2703E-06	.4330E-07	.4275E-08	.2115E-09
7167	599.34	.3159E-05	.9154E-06	.2028E-06	.3141E-07	.2974E-08	.1394E-09
7168	599.40	.2482E-05	.7029E-06	.1514E-06	.2267E-07	.2057E-08	.9125E-10
7169	599.46	.1934E-05	.5374E-06	.1126E-06	.1627E-07	.1414E-08	.5935E-10
11222	599.50	.2666E-04	.1154E-04	.4136E-05	.1153E-05	.2277E-06	.2745E-07
7170	599.53	.1515E-05	.4091E-06	.8326E-07	.1162E-07	.9665E-09	.3834E-10
7171	599.59	.1177E-05	.3101E-06	.6130E-07	.8258E-08	.6568E-09	.2461E-10
72 2	599.65	.8115E-04	.5119E-04	.2884E-04	.1398E-04	.5507E-05	.1615E-05
5062	600.11	.6394E-04	.2116E-04	.5498E-05	.1035E-05	.1249E-06	.8009E-08
2023	600.25	.5909E-01	.4543E-01	.3246E-01	.2103E-01	.1191E-01	.5568E-02
11223	600.31	.2582E-04	.1108E-04	.3935E-05	.1085E-05	.2110E-06	.2498E-07
72 3	600.44	.1808E-03	.1139E-03	.6411E-04	.3102E-04	.1220E-04	.3568E-05
1090	600.60	.5772E-05	.1614E-05	.3425E-06	.5033E-07	.4462E-08	.1922E-09
11224	601.12	.2484E-04	.1058E-04	.3718E-05	.1012E-05	.1940E-06	.2253E-07
72 4	601.22	.2854E-03	.1796E-03	.1009E-03	.4872E-04	.1911E-04	.5572E-05
5060	601.57	.9850E-04	.3400E-04	.9289E-05	.1859E-05	.2425E-06	.1716E-07
2021	601.77	.6408E-01	.5003E-01	.3641E-01	.2412E-01	.1405E-01	.6811E-02
11225	601.92	.2375E-04	.1003E-04	.3489E-05	.9381E-06	.1770E-06	.2014E-07
1088	602.01	.1108E-04	.3291E-05	.7516E-06	.1208E-06	.1197E-07	.5957E-09
72 5	602.01	.3896E-03	.2447E-03	.1372E-03	.6609E-04	.2584E-04	.7503E-05
11226	602.73	.2258E-04	.9446E-05	.3252E-05	.8630E-06	.1602E-06	.1785E-07
72 6	602.80	.4905E-03	.3075E-03	.1719E-03	.8257E-04	.3216E-04	.9293E-05
4087	602.99	.1132E-05	.2587E-06	.4311E-07	.4714E-08	.2888E-09	.7738E-11
5058	603.03	.1493E-03	.5366E-04	.1540E-04	.3270E-05	.4596E-06	.3580E-07
2019	603.30	.6783E-01	.5370E-01	.3974E-01	.2687E-01	.1606E-01	.8046E-02
1086	603.42	.2092E-04	.6600E-05	.1619E-05	.2839E-06	.3141E-07	.1798E-08
11227	603.54	.2134E-04	.8845E-05	.3011E-05	.7884E-06	.1439E-06	.1568E-07
72 7	603.59	.5862E-03	.3666E-03	.2044E-03	.9780E-04	.3793E-04	.1090E-04
4086	603.70	.1553E-05	.3656E-06	.6314E-07	.7211E-08	.4665E-09	.1341E-10
11228	604.36	.2006E-04	.8234E-05	.2771E-05	.7153E-06	.1283E-06	.1367E-07
72 8	604.39	.6752E-03	.4210E-03	.2340E-03	.1115E-03	.4303E-04	.1228E-04
5056	604.50	.2226E-03	.8323E-04	.2503E-04	.5632E-05	.8506E-06	.7269E-07
1084	604.83	.3892E-04	.1301E-04	.3423E-05	.6539E-06	.8049E-07	.5287E-08
2017	604.84	.6995E-01	.5608E-01	.4213E-01	.2902E-01	.1775E-01	.9160E-02
4034	605.11	.2889E-05	.7211E-06	.1335E-06	.1661E-07	.1196E-08	.3944E-10

TABLE XVI (Continued)

BAND CODE	WAVE NUMBER	INTENSITY					
		T=300K	T=275K	T=250K	T=225K	T=200K	T=175K
11229	605.17	.1875E-04	.7621E-05	.2534E-05	.6447E-06	.1135E-06	.1182E-07
72 9	605.18	.7564E-03	.4702E-03	.2603E-03	.1235E-03	.4739E-04	.1343E-04
4085	605.41	.2122E-05	.5146E-06	.9204E-07	.1097E-07	.7492E-09	.2307E-10
4083	605.82	.3917E-05	.1006E-05	.1928E-06	.2502E-07	.1899E-08	.6699E-10
5054	605.97	.3266E-03	.1268E-03	.3991E-04	.9494E-05	.1537E-05	.1436E-06
7210	605.97	.8291E-03	.5137E-03	.2832E-03	.1337E-03	.5097E-04	.1433E-04
11230	605.98	.1743E-04	.7014E-05	.2304E-05	.5773E-06	.9975E-07	.1013E-07
1082	606.24	.7126E-04	.2522E-04	.7104E-05	.1475E-05	.2016E-06	.1514E-07
2015	606.38	.7007E-01	.5681E-01	.4326E-01	.3029E-01	.1891E-01	.1002E-01
4082	606.53	.5291E-05	.1398E-05	.2772E-06	.3749E-07	.2997E-08	.1130E-09
7211	606.77	.8926E-03	.5509E-03	.3024E-03	.1419E-03	.5374E-04	.1497E-04
11231	606.79	.1613E-04	.6419E-05	.2082E-05	.5136E-06	.8703E-07	.8624E-08
4081	607.24	.7118E-05	.1934E-05	.3966E-06	.5589E-07	.4703E-08	.1895E-09
5052	607.44	.4713E-03	.1898E-03	.6242E-04	.1566E-04	.2712E-05	.2762E-06
7212	607.56	.9466E-03	.5818E-03	.3177E-03	.1482E-03	.5571E-04	.1537E-04
11232	607.61	.1484E-04	.5844E-05	.1870E-05	.4540E-06	.7540E-07	.7281E-08
1080	607.66	.1285E-03	.4807E-04	.1447E-04	.3260E-05	.4932E-06	.4224E-07
2013	607.92	.6792E-01	.5561E-01	.4284E-01	.3044E-01	.1935E-01	.1050E-01
4080	607.95	.9539E-05	.2664E-05	.5648E-06	.8289E-07	.7337E-08	.3155E-09
7213	608.36	.9907E-03	.6062E-03	.3293E-03	.1526E-03	.5689E-04	.1553E-04
11233	608.42	.1359E-04	.5291E-05	.1670E-05	.3989E-06	.6488E-07	.6101E-08
4079	608.66	.1273E-04	.3655E-05	.8006E-06	.1223E-06	.1138E-07	.5219E-09
5050	608.92	.6690E-03	.2790E-03	.9571E-04	.2529E-04	.4670E-05	.5168E-06
1078	609.09	.2280E-03	.9006E-04	.2893E-04	.7058E-05	.1179E-05	.1148E-06
7214	609.16	.1025E-02	.6242E-03	.3371E-03	.1552E-03	.5732E-04	.1548E-04
11234	609.24	.1239E-04	.4766E-05	.1484E-05	.3482E-06	.5545E-07	.5073E-08
4078	609.38	.1693E-04	.4993E-05	.1130E-05	.1795E-06	.1755E-07	.8577E-09
2011	609.46	.6332E-01	.5228E-01	.4069E-01	.2927E-01	.1890E-01	.1046E-01
7215	609.96	.1050E-02	.6358E-03	.3413E-03	.1559E-03	.5706E-04	.1522E-04
11235	610.06	.1123E-04	.4270E-05	.1310E-05	.3022E-06	.4707E-07	.4186E-08
4077	610.09	.2242E-04	.6790E-05	.1586E-05	.2621E-06	.2691E-07	.1400E-08
5048	610.40	.9338E-03	.4029E-03	.1439E-03	.3996E-04	.7850E-05	.9409E-06
1076	610.51	.3984E-03	.1659E-03	.5678E-04	.1497E-04	.2755E-05	.3037E-06
7216	610.76	.1065E-02	.6414E-03	.3420E-03	.1550E-03	.5615E-04	.1478E-04
4076	610.81	.2958E-04	.9196E-05	.2217E-05	.3807E-06	.4101E-07	.2271E-08
11236	610.88	.1014E-04	.3807E-05	.1151E-05	.2607E-06	.3969E-07	.3429E-08
20 9	611.01	.5622E-01	.4675E-01	.3670E-01	.2668E-01	.1745E-01	.9824E-02
4075	611.52	.3887E-04	.1240E-04	.3084E-05	.5501E-06	.6215E-07	.3658E-08
7217	611.56	.1071E-02	.6413E-03	.3395E-03	.1525E-03	.5468E-04	.1420E-04
11237	611.69	.9107E-05	.3376E-05	.1005E-05	.2235E-06	.3325E-07	.2788E-08
5046	611.89	.1282E-02	.5712E-03	.2121E-03	.6177E-04	.1288E-04	.1666E-05
1074	611.94	.6852E-03	.3004E-03	.1094E-03	.3109E-04	.6289E-05	.7827E-06
9075	611.99	.1060E-05	.2524E-06	.4419E-07	.5135E-08	.3395E-09	.1003E-10
4074	612.24	.5087E-04	.1665E-04	.4270E-05	.7908E-06	.9364E-07	.5854E-08
7218	612.36	.1068E-02	.6357E-03	.3341E-03	.1488E-03	.5273E-04	.1350E-04

TABLE XVI (Continued)

BAND CODE	WAVE NUMBER	INTENSITY					
		T=300K	T=275K	T=250K	T=225K	T=200K	T=175K
11238	612.52	.8143E-05	.2980E-05	.8735E-06	.1905E-06	.2768E-07	.2250E-08
20 7	612.57	.4675E-01	.3910E-01	.3091E-01	.2266E-01	.1498E-01	.8547E-02
9074	612.71	.1387E-05	.3389E-06	.6119E-07	.7382E-08	.5115E-09	.1606E-10
4073	612.96	.6632E-04	.2226E-04	.5885E-05	.1131E-05	.1403E-06	.9306E-08
7219	613.16	.1057E-02	.6253E-03	.3261E-03	.1438E-03	.5036E-04	.1269E-04
11239	613.34	.7247E-05	.2617E-05	.7548E-06	.1614E-06	.2288E-07	.1803E-08
5044	613.37	.1729E-02	.7950E-03	.3064E-03	.9340E-04	.2061E-04	.2870E-05
1072	613.38	.1160E-02	.5346E-03	.2067E-03	.6324E-04	.1402E-04	.1964E-05
9073	613.43	.1808E-05	.4530E-06	.8432E-07	.1056E-07	.7662E-09	.2553E-10
4072	613.67	.8611E-04	.2964E-04	.8071E-05	.1609E-05	.2089E-06	.1470E-07
7220	613.96	.1039E-02	.6105E-03	.3157E-03	.1378E-03	.4767E-04	.1182E-04
20 5	614.12	.3517E-01	.2954E-01	.2347E-01	.1732E-01	.1154E-01	.6656E-02
9072	614.15	.2347E-05	.6031E-06	.1157E-06	.1502E-07	.1141E-08	.4032E-10
11240	614.16	.6420E-05	.2287E-05	.6489E-06	.1360E-06	.1880E-07	.1434E-08
4071	614.39	.1114E-03	.3928E-04	.1102E-04	.2277E-05	.3092E-06	.2305E-07
7221	614.77	.1015E-02	.5918E-03	.3034E-03	.1311E-03	.4474E-04	.1091E-04
1070	614.82	.1933E-02	.9354E-03	.3835E-03	.1260E-03	.3056E-04	.4801E-05
5042	614.86	.2293E-02	.1086E-02	.4338E-03	.1381E-03	.3219E-04	.4807E-05
9071	614.87	.3035E-05	.7993E-06	.1579E-06	.2126E-07	.1689E-08	.6326E-10
11241	614.98	.5662E-05	.1988E-05	.5548E-06	.1139E-06	.1535E-07	.1133E-08
4070	615.11	.1435E-03	.5185E-04	.1497E-04	.3206E-05	.4551E-06	.3593E-07
7222	615.57	.9845E-03	.5698E-03	.2895E-03	.1237E-03	.4164E-04	.9974E-05
9070	615.59	.3910E-05	.1055E-05	.2145E-06	.2992E-07	.2487E-08	.9859E-10
20 3	615.68	.2189E-01	.1844E-01	.1471E-01	.1090E-01	.7307E-02	.4243E-02
11242	615.80	.4972E-05	.1721E-05	.4719E-06	.9488E-07	.1245E-07	.8881E-09
4069	615.83	.1841E-03	.6813E-04	.2025E-04	.4490E-05	.6659E-06	.5562E-07
1068	616.26	.3171E-02	.1609E-02	.6981E-03	.2459E-03	.6504E-04	.1143E-04
9069	616.31	.5016E-05	.1386E-05	.2901E-06	.4191E-07	.3638E-08	.1526E-09
5040	616.36	.2989E-02	.1456E-02	.6018E-03	.1997E-03	.4903E-04	.7828E-05
7223	616.38	.9492E-03	.5450E-03	.2743E-03	.1158E-03	.3844E-04	.9039E-05
4068	616.56	.2353E-03	.8915E-04	.2725E-04	.6255E-05	.9687E-06	.8552E-07
11243	616.63	.4346E-05	.1482E-05	.3994E-06	.7857E-07	.1003E-07	.6914E-09
9068	617.03	.6409E-05	.1813E-05	.3904E-06	.5838E-07	.5293E-08	.2347E-09
7224	617.18	.9097E-03	.5180E-03	.2582E-03	.1077E-03	.3520E-04	.8120E-05
20 1	617.25	.7457E-02	.6293E-02	.5029E-02	.3736E-02	.2512E-02	.1464E-02
4067	617.28	.2995E-03	.1161E-03	.3650E-04	.8669E-05	.1401E-05	.1306E-06
11244	617.45	.3782E-05	.1271E-05	.3362E-06	.6470E-07	.8037E-08	.5344E-09
1066	617.70	.5119E-02	.2719E-02	.1247E-02	.4699E-03	.1352E-03	.2648E-04
9067	617.76	.8157E-05	.2362E-05	.5229E-06	.8091E-07	.7654E-08	.3585E-09
5038	617.86	.3828E-02	.1916E-02	.8177E-03	.2823E-03	.7282E-04	.1239E-04
7225	617.99	.8667E-03	.4893E-03	.2414E-03	.9945E-04	.3200E-04	.7233E-05
4066	618.00	.3797E-03	.1506E-03	.4866E-04	.1195E-04	.2014E-05	.1982E-06
21 2	618.03	.3706E-01	.3125E-01	.2495E-01	.1852E-01	.1243E-01	.7238E-02
21 4	618.04	.6498E-01	.5467E-01	.4352E-01	.3219E-01	.2152E-01	.1245E-01
21 6	618.05	.9006E-01	.7549E-01	.5982E-01	.4400E-01	.2921E-01	.1676E-01

TABLE XVI (Continued)

		INTENSITY					
BAND CODE	WAVE NUMBER	T=300K	T=275K	T=250K	T=225K	T=200K	T=175K
21 8	618.06	.1113E 00	.9283E-01	.7312E-01	.5338E-01	.3511E-01	.1990E-01
2110	618.08	.1280E 00	.1061E 00	.8291E-01	.5995E-01	.3897E-01	.2175E-01
2112	618.10	.1398E 00	.1149E 00	.8899E-01	.6361E-01	.4075E-01	.2233E-01
2114	618.12	.1466E 00	.1194E 00	.9140E-01	.6446E-01	.4060E-01	.2177E-01
2116	618.15	.1484E 00	.1196E 00	.9045E-01	.6280E-01	.3880E-01	.2029E-01
2118	618.18	.1459E 00	.1162E 00	.8661E-01	.5909E-01	.3572E-01	.1816E-01
2120	618.22	.1397E 00	.1098E 00	.8051E-01	.5387E-01	.3177E-01	.1565E-01
2122	618.26	.1305E 00	.1010E 00	.7280E-01	.4767E-01	.2737E-01	.1303E-01
11245	618.28	.3277E-05	.1084E-05	.2816E-06	.5297E-07	.6397E-08	.4102E-09
2124	618.30	.1191E 00	.9073E-01	.6414E-01	.4102E-01	.2287E-01	.1048E-01
2126	618.35	.1063E 00	.7964E-01	.5513E-01	.3437E-01	.1856E-01	.8163E-02
2128	618.40	.9304E-01	.6837E-01	.4628E-01	.2807E-01	.1464E-01	.6161E-02
2130	618.45	.7978E-01	.5746E-01	.3796E-01	.2235E-01	.1124E-01	.4510E-02
9066	618.48	.1034E-04	.3063E-05	.6970E-06	.1115E-06	.1100E-07	.5440E-09
2132	618.51	.6710E-01	.4730E-01	.3045E-01	.1738E-01	.8398E-02	.3203E-02
2134	618.57	.5539E-01	.3816E-01	.2390E-01	.1319E-01	.6112E-02	.2209E-02
2136	618.63	.4489E-01	.3018E-01	.1836E-01	.9778E-02	.4335E-02	.1480E-02
2138	618.70	.3573E-01	.2342E-01	.1382E-01	.7085E-02	.2997E-02	.9630E-03
4065	618.73	.4795E-03	.1946E-03	.6457E-04	.1639E-04	.2879E-05	.2987E-06
2140	618.77	.2794E-01	.1782E-01	.1018E-01	.5018E-02	.2020E-02	.6091E-03
7226	618.80	.8212E-03	.4595E-03	.2242E-03	.9120E-04	.2887E-04	.6390E-05
2142	618.84	.2147E-01	.1331E-01	.7349E-02	.3475E-02	.1328E-02	.3746E-03
2144	618.92	.1621E-01	.9760E-02	.5200E-02	.2354E-02	.8519E-03	.2240E-03
2146	619.00	.1204E-01	.7025E-02	.3606E-02	.1559E-02	.5332E-03	.1303E-03
2148	619.09	.8789E-02	.4965E-02	.2451E-02	.1011E-02	.3256E-03	.7372E-04
11246	619.11	.2827E-05	.9206E-06	.2346E-06	.4313E-07	.5060E-08	.3127E-09
1064	619.15	.8133E-02	.4518E-02	.2186E-02	.8793E-03	.2746E-03	.5975E-04
2150	619.18	.6310E-02	.3446E-02	.1634E-02	.6411E-03	.1941E-03	.4058E-04
9065	619.21	.1305E-04	.3956E-05	.9247E-06	.1529E-06	.1573E-07	.8199E-09
2152	619.27	.4456E-02	.2349E-02	.1068E-02	.3980E-03	.1130E-03	.2174E-04
5036	619.36	.4815E-02	.2472E-02	.1088E-02	.3900E-03	.1054E-03	.1905E-04
2154	619.37	.3095E-02	.1573E-02	.6844E-03	.2418E-03	.6418E-04	.1133E-04
4064	619.45	.6030E-03	.2502E-03	.8527E-04	.2236E-04	.4090E-05	.4473E-06
2156	619.47	.2115E-02	.1035E-02	.4302E-03	.1438E-03	.3560E-04	.5748E-05
2158	619.57	.1422E-02	.6692E-03	.2653E-03	.8370E-04	.1929E-04	.2839E-05
22 1	619.60	.7490E-02	.6320E-02	.5050E-02	.3751E-02	.2522E-02	.1470E-02
7227	619.61	.7738E-03	.4290E-03	.2070E-03	.8307E-04	.2585E-04	.5599E-05
2160	619.68	.9407E-03	.4251E-03	.1605E-03	.4770E-04	.1020E-04	.1364E-05
2162	619.79	.6124E-03	.2653E-03	.9525E-04	.2662E-04	.5272E-05	.6385E-06
2164	619.90	.3923E-03	.1627E-03	.5546E-04	.1454E-04	.2660E-05	.2909E-06
11247	619.94	.2428E-05	.7781E-06	.1945E-06	.3492E-07	.3978E-08	.2366E-09
9064	619.94	.1641E-04	.5085E-05	.1221E-05	.2086E-06	.1223E-07	.1228E-08
2166	620.02	.2473E-03	.9811E-04	.3169E-04	.7782E-05	.1311E-05	.1290E-06
2168	620.14	.1534E-03	.5813E-04	.1777E-04	.4077E-05	.6314E-06	.5573E-07
4063	620.18	.7554E-03	.3203E-03	.1121E-03	.3034E-04	.5777E-05	.6651E-06

TABLE XVI (Continued)

BAND CODE	WAVE NUMBER	INTENSITY					
		T=300K	T=275K	T=250K	T=225K	T=200K	T=175K
2170	620.27	.9371E-04	.3385E-04	.9774E-05	.2092E-05	.2970E-06	.2344E-07
2172	620.40	.5633E-04	.1938E-04	.5276E-05	.1051E-05	.1365E-06	.9600E-08
7228	620.42	.7253E-03	.3982E-03	.1900E-03	.7516E-04	.2298E-04	.4866E-05
2174	620.53	.3333E-04	.1091E-04	.2796E-05	.5176E-06	.6126E-07	.3829E-08
1062	620.60	.1272E-01	.7376E-02	.3758E-02	.1611E-02	.5448E-03	.1313E-03
2176	620.66	.1941E-04	.6033E-05	.1454E-05	.2495E-06	.2687E-07	.1487E-08
9063	620.66	.2056E-04	.6509E-05	.1604E-05	.2831E-06	.3155E-07	.1825E-08
11248	620.77	.2077E-05	.6546E-06	.1604E-06	.2812E-07	.3108E-08	.1778E-09
2178	620.80	.1113E-04	.3281E-05	.7419E-06	.1178E-06	.1152E-07	.5626E-09
5034	620.87	.5946E-02	.3127E-02	.1417E-02	.5264E-03	.1488E-03	.2847E-04
4062	620.91	.9425E-03	.4083E-03	.1466E-03	.4096E-04	.8112E-05	.9825E-06
2180	620.95	.6284E-05	.1754E-05	.3716E-06	.5451E-07	.4822E-08	.2073E-09
2182	621.09	.3492E-05	.9220E-06	.1827E-06	.2470E-07	.1973E-08	.7437E-10
22 3	621.17	.2212E-01	.1863E-01	.1485E-01	.1101E-01	.7375E-02	.4282E-02
7229	621.23	.6762E-03	.3676E-03	.1733E-03	.6757E-04	.2029E-04	.4197E-05
2184	621.24	.1910E-05	.4765E-06	.8818E-07	.1096E-07	.7888E-09	.2599E-10
9062	621.39	.2564E-04	.8295E-05	.2098E-05	.3829E-06	.4430E-07	.2696E-08
2186	621.40	.1029E-05	.2421E-06	.4177E-07	.4767E-08	.3082E-09	.8849E-11
11249	621.59	.1769E-05	.5482E-06	.1317E-06	.2252E-07	.2413E-08	.1327E-09
4061	621.63	.1171E-02	.5182E-03	.1908E-03	.5500E-04	.1132E-04	.1442E-05
7230	622.04	.6273E-03	.3375E-03	.1572E-03	.6036E-04	.1779E-04	.3591E-05
1060	622.06	.1957E-01	.1183E-01	.6341E-02	.2891E-02	.1056E-02	.2808E-03
9061	622.12	.3185E-04	.1053E-04	.2730E-05	.5129E-06	.6182E-07	.3955E-08
4060	622.36	.1449E-02	.6548E-03	.2472E-03	.7346E-04	.1571E-04	.2101E-05
5032	622.38	.7206E-02	.3878E-02	.1806E-02	.6937E-03	.2045E-03	.4129E-04
11250	622.43	.1500E-05	.4570E-06	.1075E-06	.1793E-07	.1862E-08	.9839E-10
22 5	622.75	.3574E-01	.3001E-01	.2384E-01	.1758E-01	.1171E-01	.6752E-02
9060	622.85	.3940E-04	.1330E-04	.3536E-05	.6849E-06	.8577E-07	.5764E-08
7231	622.85	.5790E-03	.3083E-03	.1417E-03	.5358E-04	.1549E-04	.3049E-05
4059	623.09	.1786E-02	.8237E-03	.3187E-03	.9760E-04	.2167E-04	.3041E-05
11251	623.26	.1267E-05	.3792E-06	.8738E-07	.1420E-07	.1429E-08	.7242E-10
1058	623.52	.2962E-01	.1866E-01	.1050E-01	.5078E-02	.1997E-02	.5846E-03
9059	623.58	.4855E-04	.1672E-04	.4558E-05	.9096E-06	.1183E-06	.8342E-08
7232	623.67	.5318E-03	.2800E-03	.1271E-03	.4727E-04	.1339E-04	.2569E-05
4058	623.82	.2193E-02	.1032E-02	.4089E-03	.1290E-03	.2972E-04	.4373E-05
5030	623.89	.8567E-02	.4711E-02	.2251E-02	.8924E-03	.2736E-03	.5813E-04
11252	624.09	.1065E-05	.3133E-06	.7065E-07	.1119E-07	.1089E-08	.5294E-10
9058	624.31	.5957E-04	.2093E-04	.5846E-05	.1202E-05	.1622E-06	.1199E-07
22 7	624.33	.4779E-01	.3995E-01	.3156E-01	.2313E-01	.1528E-01	.8717E-02
7233	624.48	.4861E-03	.2531E-03	.1133E-03	.4145E-04	.1150E-04	.2149E-05
4057	624.56	.2681E-02	.1286E-02	.5222E-03	.1695E-03	.4051E-04	.6245E-05
1056	624.98	.4413E-01	.2890E-01	.1704E-01	.8733E-02	.3691E-02	.1185E-02
9057	625.05	.7280E-04	.2609E-04	.7462E-05	.1579E-05	.2210E-06	.1712E-07
4056	625.29	.3264E-02	.1597E-02	.6635E-03	.2217E-03	.5488E-04	.8859E-05
7234	625.30	.4421E-03	.2275E-03	.1004E-03	.3613E-04	.9812E-05	.1784E-05

TABLE XVI (Continued)

BAND CODE	WAVE NUMBER	INTENSITY					
		T=300K	T=275K	T=250K	T=225K	T=200K	T=175K
5028	625.41	.9986E-02	.5602E-02	.2743E-02	.1120E-02	.3562E-03	.7937E-04
9056	625.78	.8859E-04	.3238E-04	.9478E-05	.2064E-05	.2993E-06	.2428E-07
22 9	625.91	.5782E-01	.4805E-01	.3769E-01	.2738E-01	.1790E-01	.1007E-01
4055	626.02	.3957E-02	.1974E-02	.8390E-03	.2883E-03	.7392E-04	.1248E-04
7235	626.12	.4003E-03	.2035E-03	.8856E-04	.3130E-04	.8316E-05	.1470E-05
1054	626.45	.6467E-01	.4399E-01	.2714E-01	.1470E-01	.6659E-02	.2337E-02
9055	626.51	.1074E-03	.4000E-04	.1198E-04	.2683E-05	.4030E-06	.3421E-07
4054	626.76	.4778E-02	.2428E-02	.1056E-02	.3729E-03	.9896E-04	.1747E-04
5026	626.93	.1140E-01	.6518E-02	.3264E-02	.1370E-02	.4510E-03	.1050E-03
7236	626.93	.3607E-03	.1812E-03	.7766E-04	.2696E-04	.7002E-05	.1202E-05
9054	627.25	.1296E-03	.4919E-04	.1507E-04	.3469E-05	.5393E-06	.4785E-07
4053	627.49	.5746E-02	.2974E-02	.1322E-02	.4797E-03	.1317E-03	.2427E-04
2211	627.50	.6550E-01	.5403E-01	.4202E-01	.3021E-01	.1949E-01	.1078E-01
7237	627.75	.3235E-03	.1604E-03	.6774E-04	.2308E-04	.5858E-05	.9761E-06
1052	627.92	.9322E-01	.6577E-01	.4239E-01	.2422E-01	.1173E-01	.4487E-02
9053	627.99	.1558E-03	.6022E-04	.1886E-04	.4461E-05	.7173E-06	.6648E-07
4052	628.23	.6881E-02	.3627E-02	.1647E-02	.6139E-03	.1742E-03	.3351E-04
5024	628.45	.1274E-01	.7413E-02	.3790E-02	.1631E-02	.5546E-03	.1346E-03
7238	628.57	.2889E-03	.1414E-03	.5878E-04	.1965E-04	.4869E-05	.7868E-06
9052	628.72	.1864E-03	.7339E-04	.2349E-04	.5706E-05	.9484E-06	.9173E-07
4051	628.97	.8207E-02	.4403E-02	.2043E-02	.7812E-03	.2290E-03	.4594E-04
2213	629.09	.7067E-01	.5781E-01	.4449E-01	.3158E-01	.2006E-01	.1087E-01
1050	629.39	.1322E 00	.9658E-01	.6493E-01	.3906E-01	.2017E-01	.8382E-02
7239	629.39	.2568E-03	.1240E-03	.5073E-04	.1663E-04	.4021E-05	.6297E-06
9051	629.46	.2222E-03	.8904E-04	.2911E-04	.7258E-05	.1246E-05	.1257E-06
4050	629.71	.9746E-02	.5320E-02	.2521E-02	.9889E-03	.2993E-03	.6254E-04
5022	629.98	.1393E-01	.8230E-02	.4289E-02	.1890E-02	.6618E-03	.1668E-03
9050	630.20	.2637E-03	.1075E-03	.3590E-04	.9182E-05	.1628E-05	.1711E-06
7240	630.21	.2272E-03	.1082E-03	.4355E-04	.1399E-04	.3300E-05	.5003E-06
4049	630.44	.1153E-01	.6400E-02	.3095E-02	.1245E-02	.3887E-03	.8457E-04
2215	630.68	.7334E-01	.5939E-01	.4517E-01	.3160E-01	.1971E-01	.1044E-01
1048	630.87	.1843E 00	.1393E 00	.9751E-01	.6163E-01	.3386E-01	.1523E-01
9049	630.94	.3116E-03	.1293E-03	.4405E-04	.1155E-04	.2113E-05	.2312E-06
7241	631.03	.2001E-03	.9402E-04	.3720E-04	.1171E-04	.2691E-05	.3947E-06
4048	631.18	.1357E-01	.7663E-02	.3781E-02	.1559E-02	.5018E-03	.1136E-03
5020	631.51	.1485E-01	.8907E-02	.4724E-02	.2128E-02	.7651E-03	.1996E-03
9048	631.68	.3667E-03	.1547E-03	.5378E-04	.1445E-04	.2726E-05	.3103E-06
7242	631.86	.1755E-03	.8128E-04	.3161E-04	.9741E-05	.2181E-05	.3092E-06
4047	631.92	.1591E-01	.9134E-02	.4596E-02	.1941E-02	.6439E-03	.1515E-03
2217	632.28	.7365E-01	.5897E-01	.4424E-01	.3044E-01	.1860E-01	.9589E-02
1046	632.35	.2527E 00	.1973E 00	.1436E 00	.9516E-01	.5548E-01	.2694E-01
9047	632.42	.4297E-03	.1842E-03	.6533E-04	.1798E-04	.3496E-05	.4135E-06
4046	632.67	.1858E-01	.1084E-01	.5559E-02	.2403E-02	.8211E-03	.2006E-03
7243	632.68	.1533E-03	.6994E-04	.2672E-04	.8059E-05	.1756E-05	.2405E-06
5018	633.04	.1543E-01	.9378E-02	.5054E-02	.2321E-02	.8552E-03	.2302E-03

TABLE XVI (Continued)

BAND CODE	WAVE NUMBER	INTENSITY					
		T=300K	T=275K	T=250K	T=225K	T=200K	T=175K
9046	633.17	.5013E-03	.2184E-03	.7896E-04	.2225E-04	.4455E-05	.5473E-06
4045	633.41	.2160E-01	.1280E-01	.6690E-02	.2959E-02	.1041E-02	.2638E-03
7244	633.50	.1333E-03	.5990E-04	.2247E-04	.6630E-05	.1405E-05	.1858E-06
1044	633.83	.3407E 00	.2743E 00	.2072E 00	.1437E 00	.8870E-01	.4633E-01
2219	633.88	.7184E-01	.5679E-01	.4197E-01	.2834E-01	.1692E-01	.8467E-02
9045	633.91	.5823E-03	.2577E-03	.9494E-04	.2738E-04	.5642E-05	.7193E-06
4044	634.15	.2501E-01	.1504E-01	.8010E-02	.3624E-02	.1311E-02	.3445E-03
7245	634.33	.1154E-03	.5106E-04	.1881E-04	.5424E-05	.1118E-05	.1425E-06
5016	634.58	.1557E-01	.9579E-02	.5237E-02	.2447E-02	.9217E-03	.2552E-03
9044	634.65	.6735E-03	.3027E-03	.1136E-03	.3350E-04	.7100E-05	.9386E-06
4043	634.90	.2883E-01	.1760E-01	.9542E-02	.4413E-02	.1641E-02	.4468E-03
7246	635.16	.9944E-04	.4332E-04	.1566E-04	.4413E-05	.8834E-06	.1085E-06
1042	635.32	.4515E 00	.3744E 00	.2930E 00	.2123E 00	.1383E 00	.7750E-01
9043	635.40	.7755E-03	.3538E-03	.1352E-03	.4076E-04	.8880E-05	.1216E-05
2221	635.49	.6827E-01	.5321E-01	.3867E-01	.2558E-01	.1488E-01	.7205E-02
4042	635.64	.3308E-01	.2050E-01	.1131E-01	.5343E-02	.2041E-02	.5753E-03
7247	635.98	.8535E-04	.3659E-04	.1297E-04	.3570E-05	.6940E-06	.8208E-07
5014	636.13	.1521E-01	.9453E-02	.5234E-02	.2484E-02	.9539E-03	.2708E-03
9042	636.14	.8890E-03	.4116E-03	.1600E-03	.4931E-04	.1104E-04	.1565E-05
4041	636.39	.3779E-01	.2376E-01	.1333E-01	.6434E-02	.2523E-02	.7356E-03
1040	636.81	.5880E 00	.5016E 00	.4061E 00	.3066E 00	.2105E 00	.1260E 00
7248	636.81	.7294E-04	.3076E-04	.1069E-04	.2873E-05	.5418E-06	.6165E-07
9041	636.89	.1015E-02	.4765E-03	.1885E-03	.5931E-04	.1363E-04	.1999E-05
2223	637.10	.6332E-01	.4861E-01	.3467E-01	.2242E-01	.1268E-01	.5922E-02
4040	637.14	.4299E-01	.2740E-01	.1564E-01	.7703E-02	.3099E-02	.9338E-03
7249	637.64	.6207E-04	.2574E-04	.8769E-05	.2299E-05	.4205E-06	.4599E-07
9040	637.64	.1153E-02	.5490E-03	.2208E-03	.7093E-04	.1672E-04	.2535E-05
5012	637.67	.1428E-01	.8960E-02	.5016E-02	.2413E-02	.9423E-03	.2734E-03
4039	637.88	.4867E-01	.3145E-01	.1825E-01	.9169E-02	.3782E-02	.1177E-02
1038	638.31	.7523E 00	.6592E 00	.5512E 00	.4330E 00	.3122E 00	.1992E 00
9039	638.39	.1304E-02	.6294E-03	.2573E-03	.8433E-04	.2038E-04	.3191E-05
7250	638.47	.5260E-04	.2144E-04	.7157E-05	.1830E-05	.3243E-06	.3407E-07
4038	638.63	.5487E-01	.3593E-01	.2118E-01	.1085E-01	.4587E-02	.1473E-02
2225	638.71	.5742E-01	.4334E-01	.3030E-01	.1912E-01	.1049E-01	.4707E-02
9038	639.14	.1467E-02	.7180E-03	.2983E-03	.9968E-04	.2469E-04	.3989E-05
5010	639.22	.1278E-01	.8078E-02	.4565E-02	.2221E-02	.8800E-03	.2600E-03
7251	639.30	.4439E-04	.1778E-04	.5812E-05	.1448E-05	.2486E-06	.2507E-07
4037	639.38	.6157E-01	.4084E-01	.2445E-01	.1277E-01	.5527E-02	.1830E-02
1036	639.81	.9455E 00	.8499E 00	.7328E 00	.5976E 00	.4516E 00	.3060E 00
9037	639.89	.1644E-02	.8150E-03	.3439E-03	.1171E-03	.2971E-04	.4949E-05
4036	640.13	.6876E-01	.4619E-01	.2808E-01	.1494E-01	.6617E-02	.2257E-02
7252	640.13	.3731E-04	.1468E-04	.4696E-05	.1140E-05	.1894E-06	.1832E-07
2227	640.32	.5097E-01	.3778E-01	.2584E-01	.1588E-01	.8424E-02	.3623E-02
9036	640.64	.1834E-02	.9204E-03	.3943E-03	.1368E-03	.3552E-04	.6095E-05
50 8	640.77	.1071E-01	.6811E-02	.3878E-02	.1905E-02	.7638E-03	.2292E-03

TABLE XVI (Continued)

BAND CODE	WAVE NUMBER	INTENSITY					
		T=300K	T=275K	T=250K	T=225K	T=200K	T=175K
4035	640.89	.7645E-01	.5199E-01	.3207E-01	.1737E-01	.7870E-02	.2763E-02
7253	640.97	.3122E-04	.1207E-04	.3776E-05	.8928E-06	.1435E-06	.1329E-07
1034	641.31	.1167E 01	.1074E 01	.9536E 00	.8058E 00	.6365E 00	.4567E 00
9035	641.39	.2035E-02	.1034E-02	.4497E-03	.1588E-03	.4218E-04	.7451E-05
4034	641.64	.8459E-01	.5821E-01	.3643E-01	.2008E-01	.9298E-02	.3358E-02
7254	641.80	.2602E-04	.9871E-05	.3022E-05	.6953E-06	.1080E-06	.9581E-08
2229	641.94	.4432E-01	.3222E-01	.2152E-01	.1285E-01	.6580E-02	.2703E-02
9034	642.15	.2248E-02	.1156E-02	.5099E-03	.1833E-03	.4975E-04	.9040E-05
50 6	642.33	.8113E-02	.5188E-02	.2972E-02	.1471E-02	.5953E-03	.1808E-03
4033	642.39	.9315E-01	.6485E-01	.4115E-01	.2307E-01	.1091E-01	.4050E-02
7255	642.63	.2160E-04	.8040E-05	.2407E-05	.5386E-06	.8084E-07	.6859E-08
1032	642.81	.1413E 01	.1331E 01	.1214E 01	.1061E 01	.8739E 00	.6617E 00
9033	642.90	.2471E-02	.1285E-02	.5750E-03	.2102E-03	.5829E-04	.1088E-04
4032	643.15	.1021E 00	.7187E-01	.4622E-01	.2635E-01	.1272E-01	.4849E-02
7256	643.47	.1785E-04	.6520E-05	.1907E-05	.4150E-06	.6014E-07	.4877E-08
2231	643.57	.3778E-01	.2690E-01	.1753E-01	.1015E-01	.5001E-02	.1956E-02
9032	643.66	.2702E-02	.1422E-02	.6446E-03	.2396E-03	.6782E-04	.1301E-04
50 4	643.89	.5088E-02	.3265E-02	.1879E-02	.9350E-03	.3810E-03	.1167E-03
4031	643.90	.1113E 00	.7923E-01	.5163E-01	.2990E-01	.1473E-01	.5761E-02
7257	644.30	.1470E-04	.5263E-05	.1504E-05	.3180E-06	.4447E-07	.3444E-08
1030	644.32	.1679E 01	.1616E 01	.1513E 01	.1364E 01	.1168E 01	.9306E 00
9031	644.41	.2941E-02	.1564E-02	.7184E-03	.2714E-03	.7836E-04	.1542E-04
4030	644.66	.1208E 00	.8688E-01	.5733E-01	.3373E-01	.1694E-01	.6792E-02
7258	645.14	.1205E-04	.4230E-05	.1180E-05	.2424E-06	.3269E-07	.2416E-08
9030	645.17	.3183E-02	.1711E-02	.7960E-03	.3054E-03	.8991E-04	.1814E-04
2233	645.19	.3160E-01	.2200E-01	.1396E-01	.7824E-02	.3701E-02	.1373E-02
4029	645.41	.1304E 00	.9475E-01	.6330E-01	.3780E-01	.1934E-01	.7945E-02
50 2	645.45	.1746E-02	.1123E-02	.6482E-03	.3236E-03	.1324E-03	.4081E-04
1028	645.84	.1956E 01	.1921E 01	.1841E 01	.1710E 01	.1520E 01	.1269E 01
9029	645.93	.3427E-02	.1861E-02	.8766E-03	.3414E-03	.1024E-03	.2117E-04
7259	645.98	.9838E-05	.3385E-05	.9218E-06	.1838E-06	.2388E-07	.1683E-08
4028	646.17	.1400E 00	.1028E 00	.6947E-01	.4209E-01	.2193E-01	.9221E-02
9028	646.69	.3671E-02	.2013E-02	.9594E-03	.3791E-03	.1158E-03	.2450E-04
2235	646.82	.2594E-01	.1763E-01	.1088E-01	.5889E-02	.2668E-02	.9365E-03
7260	646.82	.8000E-05	.2697E-05	.7165E-06	.1386E-06	.1735E-07	.1165E-08
4027	646.93	.1495E 00	.1108E 00	.7578E-01	.4655E-01	.2469E-01	.1062E-01
51 2	647.02	.4377E-02	.2816E-02	.1625E-02	.8112E-03	.3320E-03	.1023E-03
51 4	647.03	.3837E-02	.2462E-02	.1417E-02	.7049E-03	.2872E-03	.8799E-04
51 6	647.04	.3545E-02	.2267E-02	.1298E-02	.6424E-03	.2599E-03	.7893E-04
51 8	647.05	.3286E-02	.2090E-02	.1190E-02	.5844E-03	.2342E-03	.7028E-04
5110	647.07	.3024E-02	.1911E-02	.1079E-02	.5251E-03	.2080E-03	.6144E-04
5112	647.09	.2751E-02	.1725E-02	.9653E-03	.4642E-03	.1812E-03	.5256E-04
5114	647.11	.2472E-02	.1535E-02	.8497E-03	.4031E-03	.1547E-03	.4391E-04
5116	647.14	.2190E-02	.1346E-02	.7356E-03	.3436E-03	.1294E-03	.3580E-04
5118	647.17	.1914E-02	.1162E-02	.6261E-03	.2873E-03	.1058E-03	.2847E-04

TABLE XVI (Continued)

		INTENSITY					
BAND CODE	WAVE NUMBER	T=300K	T=275K	T=250K	T=225K	T=200K	T=175K
5120	647.21	.1648E-02	.9879E-03	.5236E-03	.2357E-03	.8470E-04	.2209E-04
5122	647.25	.1399E-02	.8263E-03	.4303E-03	.1895E-03	.6631E-04	.1670E-04
5124	647.29	.1170E-02	.6802E-03	.3475E-03	.1495E-03	.5078E-04	.1231E-04
5126	647.34	.9647E-03	.5510E-03	.2756E-03	.1156E-03	.3803E-04	.8850E-05
1026	647.35	.2232E 01	.2233E 01	.2190E 01	.2090E 01	.1923E 01	.1678E 01
5128	647.39	.7835E-03	.4391E-03	.2148E-03	.8761E-04	.2785E-04	.6200E-05
5130	647.44	.6269E-03	.3443E-03	.1644E-03	.6510E-04	.1994E-04	.4234E-05
9027	647.45	.3909E-02	.2165E-02	.1043E-02	.4181E-03	.1300E-03	.2813E-04
5132	647.50	.4942E-03	.2657E-03	.1236E-03	.4742E-04	.1396E-04	.2818E-05
5134	647.56	.3838E-03	.2016E-03	.9127E-04	.3386E-04	.9561E-05	.1828E-05
5136	647.62	.2937E-03	.1506E-03	.6620E-04	.2370E-04	.6401E-05	.1156E-05
7261	647.66	.6479E-05	.2139E-05	.5542E-06	.1040E-06	.1253E-07	.8007E-09
4026	647.69	.1589E 00	.1188E 00	.8214E-01	.5115E-01	.2759E-01	.1212E-01
5138	647.69	.2214E-03	.1106E-03	.4716E-04	.1626E-04	.4190E-05	.7122E-06
5140	647.76	.1644E-03	.7996E-04	.3300E-04	.1094E-04	.2682E-05	.4278E-06
52 0	647.80	.3546E-02	.2283E-02	.1319E-02	.6597E-03	.2704E-03	.8352E-04
5142	647.83	.1202E-03	.5686E-04	.2268E-04	.7211E-05	.1678E-05	.2504E-06
5144	647.91	.8666E-04	.3978E-04	.1531E-04	.4659E-05	.1027E-05	.1428E-06
5146	647.99	.6152E-04	.2737E-04	.1015E-04	.2951E-05	.6145E-06	.7941E-07
5148	648.08	.4303E-04	.1853E-04	.6609E-05	.1832E-05	.3594E-06	.4303E-07
5150	648.17	.2964E-04	.1234E-04	.4226E-05	.1115E-05	.2056E-06	.2272E-07
9026	648.21	.4140E-02	.2313E-02	.1127E-02	.4580E-03	.1448E-03	.3202E-04
5152	648.26	.2012E-04	.8087E-05	.2655E-05	.6651E-06	.1149E-06	.1169E-07
5154	648.36	.1345E-04	.5213E-05	.1638E-05	.3888E-06	.6285E-07	.5865E-08
4025	648.45	.1678E 00	.1266E 00	.8848E-01	.5582E-01	.3060E-01	.1373E-01
2237	648.46	.2090E-01	.1386E-01	.8296E-02	.4331E-02	.1874E-02	.6203E-03
5156	648.46	.8859E-05	.3305E-05	.9921E-06	.2228E-06	.3359E-07	.2867E-08
7262	648.50	.5226E-05	.1689E-05	.4266E-06	.7761E-07	.8990E-08	.5467E-09
5158	648.56	.5748E-05	.2062E-05	.5904E-06	.1252E-06	.1756E-07	.1366E-08
5160	648.67	.3674E-05	.1265E-05	.3450E-06	.6891E-07	.8971E-08	.6340E-09
5162	648.78	.2313E-05	.7638E-06	.1980E-06	.3718E-07	.4482E-08	.2868E-09
3083	648.82	.1684E-05	.4317E-06	.8259E-07	.1070E-07	.8105E-09	.2855E-10
1024	648.87	.2493E 01	.2538E 01	.2541E 01	.2488E 01	.2363E 01	.2149E 01
5164	648.89	.1435E-05	.4536E-06	.1116E-06	.1967E-07	.2189E-08	.1265E-09
9025	648.97	.4358E-02	.2457E-02	.1210E-02	.4980E-03	.1601E-03	.3614E-04
4024	649.21	.1763E 00	.1341E 00	.9469E-01	.6048E-01	.3368E-01	.1542E-01
7263	649.34	.4199E-05	.1328E-05	.3269E-06	.5761E-07	.6414E-08	.3707E-09
52 2	649.38	.7033E-02	.4523E-02	.2610E-02	.1303E-02	.5332E-03	.1642E-03
9024	649.73	.4559E-02	.2592E-02	.1290E-02	.5376E-03	.1755E-03	.4044E-04
4023	649.98	.1640E 00	.1412E 00	.1006E 00	.6507E-01	.3678E-01	.1717E-01
2239	650.09	.1655E-01	.1069E-01	.6197E-02	.3112E-02	.1283E-02	.3992E-03
7264	650.18	.3360E-05	.1039E-05	.2492E-06	.4253E-07	.4550E-08	.2498E-09
1022	650.40	.2723E 01	.2816E 01	.2874E 01	.2881E 01	.2817E 01	.2661E 01
9023	650.49	.4740E-02	.2717E-02	.1366E-02	.5759E-03	.1908E-03	.4483E-04
3081	650.72	.3065E-05	.8312E-06	.1701E-06	.2343E-07	.2010E-08	.8088E-10

TABLE XVI (Continued)

BAND CODE	WAVE NUMBER	INTENSITY					
		T=300K	T=275K	T=250K	T=225K	T=200K	T=175K
4022	650.74	.1909E 00	.1476E 00	.1062E 00	.6948E-01	.3984E-01	.1894E-01
52 4	650.95	.1030E-01	.6611E-02	.3803E-02	.1892E-02	.7707E-03	.2361E-03
7265	651.03	.2677E-05	.8101E-06	.1891E-06	.3124E-07	.3208E-08	.1671E-09
9022	651.26	.4895E-02	.2828E-02	.1435E-02	.6121E-03	.2058E-03	.4924E-04
4021	651.50	.1968E 00	.1533E 00	.1113E 00	.7362E-01	.4280E-01	.2071E-01
2241	651.74	.1287E-01	.8084E-02	.4534E-02	.2187E-02	.8570E-03	.2498E-03
7266	651.87	.2125E-05	.6287E-06	.1428E-06	.2283E-07	.2249E-08	.1111E-09
1020	651.93	.2902E 01	.3047E 01	.3164E 01	.3240E 01	.3255E 01	.3182E 01
9021	652.02	.5020E-02	.2922E-02	.1496E-02	.6453E-03	.2199E-03	.5357E-04
4020	652.27	.2016E 00	.1581E 00	.1158E 00	.7738E-01	.4558E-01	.2244E-01
52 6	652.53	.1322E-01	.8448E-02	.4838E-02	.2393E-02	.9682E-03	.2940E-03
3079	652.61	.5491E-05	.1573E-05	.3439E-06	.5244E-07	.4872E-08	.2231E-09
7267	652.72	.1680E-05	.4857E-06	.1074E-06	.1659E-07	.1567E-08	.7334E-10
9020	652.79	.5111E-02	.2996E-02	.1547E-02	.6744E-03	.2329E-03	.5769E-04
4019	653.03	.2049E 00	.1619E 00	.1195E 00	.8066E-01	.4811E-01	.2406E-01
2243	653.38	.9836E-02	.6002E-02	.3251E-02	.1502E-02	.5582E-03	.1519E-03
1018	653.46	.3014E 01	.3206E 01	.3383E 01	.3533E 01	.3636E 01	.3668E 01
9019	653.56	.5162E-02	.3047E-02	.1586E-02	.6984E-03	.2442E-03	.6149E-04
7268	653.56	.1323E-05	.3737E-06	.8032E-07	.1200E-07	.1086E-08	.4810E-10
4018	653.80	.2068E 00	.1644E 00	.1223E 00	.8334E-01	.5031E-01	.2555E-01
52 8	654.12	.1566E-01	.9957E-02	.5667E-02	.2782E-02	.1115E-02	.3344E-03
9018	654.32	.5171E-02	.3072E-02	.1612E-02	.7164E-03	.2535E-03	.6481E-04
7269	654.41	.1038E-05	.2862E-06	.5980E-07	.8627E-08	.7479E-09	.3134E-10
3077	654.50	.9685E-05	.2927E-05	.6824E-06	.1126E-06	.1154E-07	.5995E-09
4017	654.57	.2070E 00	.1656E 00	.1241E 00	.8532E-01	.5208E-01	.2683E-01
1016	654.99	.3041E 01	.3273E 01	.3504E 01	.3723E 01	.3916E 01	.4063E 01
2245	655.03	.7389E-02	.4374E-02	.2284E-02	.1009E-02	.3547E-03	.8986E-04
9017	655.09	.5133E-02	.3069E-02	.1622E-02	.7273E-03	.2603E-03	.6751E-04
4016	655.34	.2054E 00	.1652E 00	.1247E 00	.8647E-01	.5335E-01	.2787E-01
5210	655.70	.1754E-01	.1108E-01	.6258E-02	.3043E-02	.1205E-02	.3559E-03
9016	655.86	.5046E-02	.3034E-02	.1615E-02	.7303E-03	.2641E-03	.6945E-04
4015	656.11	.2019E 00	.1633E 00	.1241E 00	.8672E-01	.5404E-01	.2859E-01
3075	656.38	.1681E-04	.5354E-05	.1329E-05	.2366E-06	.2669E-07	.1569E-08
1014	656.53	.2968E 01	.3229E 01	.3500E 01	.3777E 01	.4051E 01	.4309E 01
9015	656.63	.4906E-02	.2966E-02	.1589E-02	.7244E-03	.2646E-03	.7048E-04
2247	656.68	.5458E-02	.3129E-02	.1573E-02	.6635E-03	.2199E-03	.5170E-04
4014	656.88	.1964E 00	.1597E 00	.1221E 00	.8596E-01	.5407E-01	.2896E-01
5212	657.29	.1882E-01	.1180E-01	.6598E-02	.3172E-02	.1238E-02	.3589E-03
9014	657.41	.4712E-02	.2863E-02	.1543E-02	.7089E-03	.2614E-03	.7047E-04
4013	657.65	.1889E 00	.1543E 00	.1186E 00	.8413E-01	.5338E-01	.2891E-01
1012	658.07	.2787E 01	.3060E 01	.3353E 01	.3667E 01	.4000E 01	.4348E 01
9013	658.18	.4463E-02	.2725E-02	.1477E-02	.6833E-03	.2542E-03	.6930E-04
3073	658.25	.2874E-04	.9628E-05	.2540E-05	.4873E-06	.6033E-07	.3997E-08
2249	658.33	.3964E-02	.2198E-02	.1062E-02	.4267E-03	.1331E-03	.2893E-04
4012	658.42	.1793E 00	.1471E 00	.1137E 00	.8116E-01	.5192E-01	.2841E-01

TABLE XVI (Continued)

BAND CODE	WAVE NUMBER	INTENSITY					
		T=300K	T=275K	T=250K	T=225K	T=200K	T=175K
5214	658.89	.1949E-01	.1210E-01	.6694E-02	.3174E-02	.1218E-02	.3455E-03
9012	658.95	.4160E-02	.2551E-02	.1390E-02	.6472E-03	.2428E-03	.6688E-04
4011	659.19	.1676E 00	.1381E 00	.1073E 00	.7702E-01	.4964E-01	.2743E-01
1010	659.62	.2492E 01	.2758E 01	.3051E 01	.3375E 01	.3734E 01	.4134E 01
9011	659.72	.3803E-02	.2342E-02	.1282E-02	.6007E-03	.2270E-03	.6314E-04
4010	659.97	.1540E 00	.1273E 00	.9933E-01	.7171E-01	.4653E-01	.2594E-01
2251	659.99	.2831E-02	.1517E-02	.7029E-03	.2685E-03	.7862E-04	.1576E-04
3071	660.11	.4834E-04	.1702E-04	.4764E-05	.9827E-06	.1332E-06	.9919E-08
5215	660.49	.1957E-01	.1202E-01	.6564E-02	.3064E-02	.1153E-02	.3191E-03
9010	660.50	.3396E-02	.2099E-02	.1154E-02	.5437E-03	.2069E-03	.5806E-04
40 9	660.74	.1383E 00	.1148E 00	.8992E-01	.6523E-01	.4260E-01	.2394E-01
10 8	661.17	.2087E 01	.2324E 01	.2591E 01	.2894E 01	.3240E 01	.3642E 01
90 9	661.28	.2942E-02	.1825E-02	.1008E-02	.4770E-03	.1826E-03	.5166E-04
40 8	661.52	.1209E 00	.1006E 00	.7911E-01	.5765E-01	.3786E-01	.2143E-01
2253	661.66	.1989E-02	.1028E-02	.4563E-03	.1653E-03	.4533E-04	.8348E-05
3069	661.96	.8005E-04	.2957E-04	.8768E-05	.1941E-05	.2874E-06	.2397E-07
90 8	662.05	.2449E-02	.1523E-02	.8445E-03	.4015E-03	.1546E-03	.4405E-04
5218	662.09	.1911E-01	.1160E-01	.6245E-02	.2864E-02	.1054E-02	.2836E-03
40 7	662.30	.1018E 00	.8499E-01	.6704E-01	.4905E-01	.3237E-01	.1844E-01
10 6	662.72	.1582E 01	.1770E 01	.1985E 01	.2234E 01	.2524E 01	.2872E 01
90 7	662.83	.1925E-02	.1201E-02	.6679E-03	.3188E-03	.1234E-03	.3538E-04
40 6	663.07	.8142E-01	.6811E-01	.5388E-01	.3956E-01	.2622E-01	.1502E-01
2255	663.32	.1374E-02	.6844E-03	.2905E-03	.9966E-04	.2552E-04	.4305E-05
90 6	663.61	.1386E-02	.8663E-03	.4831E-03	.2314E-03	.8995E-04	.2594E-04
5220	663.69	.1820E-01	.1090E-01	.5776E-02	.2598E-02	.9331E-03	.2432E-03
3067	663.80	.1304E-03	.5049E-04	.1584E-04	.3754E-05	.6057E-06	.5640E-07
40 5	663.85	.6004E-01	.5033E-01	.3991E-01	.2939E-01	.1955E-01	.1126E-01
10 4	664.28	.9916E 00	.1114E 01	.1255E 01	.1420E 01	.1615E 01	.1854E 01
90 5	664.39	.8515E-03	.5334E-03	.2982E-03	.1433E-03	.5589E-04	.1620E-04
40 4	664.63	.3829E-01	.3215E-01	.2554E-01	.1886E-01	.1258E-01	.7274E-02
2257	664.99	.9344E-03	.4476E-03	.1814E-03	.5880E-04	.1403E-04	.2160E-05
90 4	665.17	.3620E-03	.2272E-03	.1273E-03	.6129E-04	.2398E-04	.6978E-05
5222	665.30	.1694E-01	.9997E-02	.5203E-02	.2290E-02	.8007E-03	.2016E-03
40 3	665.41	.1730E-01	.1454E-01	.1157E-01	.8561E-02	.5728E-02	.3321E-02
3065	665.64	.2092E-03	.8473E-04	.2807E-04	.7111E-05	.1247E-05	.1292E-06
10 2	665.84	.3402E 00	.3831E 00	.4328E 00	.4913E 00	.5615E 00	.6480E 00
2259	666.67	.6250E-03	.2877E-03	.1111E-03	.3397E-04	.7531E-05	.1055E-05
5224	666.91	.1542E-01	.8955E-02	.4571E-02	.1965E-02	.6671E-03	.1617E-03
11 2	667.40	.8528E 00	.9601E 00	.1085E 01	.1231E 01	.1407E 01	.1624E 01
11 4	667.41	.7477E 00	.8397E 00	.9460E 00	.1070E 01	.1217E 01	.1397E 01
11 6	667.42	.6909E 00	.7730E 00	.8669E 00	.9753E 00	.1102E 01	.1254E 01
11 8	667.43	.6405E 00	.7130E 00	.7947E 00	.8874E 00	.9934E 00	.1116E 01
1110	667.45	.5894E 00	.6519E 00	.7210E 00	.7974E 00	.8821E 00	.9764E 00
3063	667.47	.3303E-03	.1398E-03	.4880E-04	.1319E-04	.2507E-05	.2882E-06
1112	667.47	.5364E 00	.5887E 00	.6449E 00	.7051E 00	.7689E 00	.8355E 00

TABLE XVI (Continued)

BAND CODE	WAVE NUMBER	INTENSITY					
		T=300K	T=275K	T=250K	T=225K	T=200K	T=175K
1114	667.49	.4820E 00	.5241E 00	.5679E 00	.6125E 00	.6567E 00	.6983E 00
1116	667.52	.4272E 00	.4597E 00	.4918E 00	.5223E 00	.5492E 00	.5696E 00
1118	667.55	.3734E 00	.3970E 00	.4187E 00	.4370E 00	.4495E 00	.4533E 00
1120	667.59	.3217E 00	.3375E 00	.3503E 00	.3585E 00	.3600E 00	.3518E 00
1122	667.63	.2732E 00	.2824E 00	.2880E 00	.2885E 00	.2820E 00	.2662E 00
1124	667.67	.2286E 00	.2326E 00	.2327E 00	.2277E 00	.2161E 00	.1964E 00
1126	667.72	.1885E 00	.1885E 00	.1847E 00	.1761E 00	.1619E 00	.1412E 00
41 2	667.76	.8782E-01	.7390E-01	.5888E-01	.4362E-01	.2923E-01	.1699E-01
1128	667.77	.1532E 00	.1503E 00	.1440E 00	.1336E 00	.1186E 00	.9904E-01
41 3	667.77	.1520E 00	.1277E 00	.1017E 00	.7519E-01	.5030E-01	.2916E-01
41 4	667.77	.2079E 00	.1745E 00	.1386E 00	.1023E 00	.6829E-01	.3947E-01
41 5	667.77	.2586E 00	.2167E 00	.1718E 00	.1265E 00	.8415E-01	.4844E-01
41 6	667.78	.3049E 00	.2550E 00	.2017E 00	.1480E 00	.9811E-01	.5620E-01
41 7	667.79	.3469E 00	.2895E 00	.2283E 00	.1670E 00	.1102E 00	.6276E-01
41 8	667.79	.3847E 00	.3201E 00	.2516E 00	.1833E 00	.1204E 00	.6812E-01
41 9	667.80	.4180E 00	.3468E 00	.2716E 00	.1970E 00	.1286E 00	.7226E-01
4110	667.81	.4469E 00	.3694E 00	.2881E 00	.2079E 00	.1349E 00	.7519E-01
4111	667.82	.4711E 00	.3880E 00	.3012E 00	.2162E 00	.1393E 00	.7696E-01
1130	667.82	.1226E 00	.1179E 00	.1103E 00	.9934E-01	.8503E-01	.6769E-01
4112	667.83	.4906E 00	.4024E 00	.3109E 00	.2218E 00	.1419E 00	.7762E-01
4113	667.84	.5056E 00	.4128E 00	.3173E 00	.2249E 00	.1426E 00	.7724E-01
4114	667.85	.5160E 00	.4193E 00	.3204E 00	.2255E 00	.1418E 00	.7592E-01
4115	667.87	.5220E 00	.4220E 00	.3205E 00	.2239E 00	.1395E 00	.7377E-01
1132	667.88	.9672E-01	.9103E-01	.8296E-01	.7241E-01	.5959E-01	.4509E-01
4116	667.88	.5238E 00	.4212E 00	.3178E 00	.2202E 00	.1358E 00	.7092E-01
4117	667.90	.5216E 00	.4170E 00	.3124E 00	.2147E 00	.1310E 00	.6747E-01
4118	667.91	.5157E 00	.4098E 00	.3048E 00	.2075E 00	.1252E 00	.6357E-01
4119	667.93	.5065E 00	.3998E 00	.2950E 00	.1990E 00	.1186E 00	.5932E-01
1134	667.94	.7516E-01	.6914E-01	.6130E-01	.5175E-01	.4084E-01	.2928E-01
4120	667.95	.4942E 00	.3875E 00	.2836E 00	.1894E 00	.1115E 00	.5486E-01
4121	667.97	.4797E 00	.3730E 00	.2707E 00	.1789E 00	.1039E 00	.5028E-01
4122	667.99	.4619E 00	.3569E 00	.2566E 00	.1677E 00	.9613E-01	.4569E-01
1136	668.00	.5754E-01	.5167E-01	.4450E-01	.3625E-01	.2737E-01	.1853E-01
4123	668.01	.4426E 00	.3393E 00	.2417E 00	.1562E 00	.8823E-01	.4116E-01
4124	668.03	.4218E 00	.3207E 00	.2262E 00	.1444E 00	.8038E-01	.3678E-01
4125	668.05	.3998E 00	.3014E 00	.2104E 00	.1327E 00	.7269E-01	.3260E-01
1138	668.07	.4340E-01	.3799E-01	.3173E-01	.2489E-01	.1793E-01	.1143E-01
4126	668.08	.3769E 00	.2816E 00	.1946E 00	.1211E 00	.6526E-01	.2866E-01
4127	668.10	.3535E 00	.2617E 00	.1788E 00	.1098E 00	.5818E-01	.2500E-01
4128	668.13	.3299E 00	.2419E 00	.1634E 00	.9890E-01	.5151E-01	.2164E-01
1140	668.14	.3225E-01	.2748E-01	.2222E-01	.1676E-01	.1149E-01	.6874E-02
4129	668.15	.3063E 00	.2224E 00	.1484E 00	.8855E-01	.4528E-01	.1859E-01
4130	668.18	.2829E 00	.2033E 00	.1341E 00	.7879E-01	.3955E-01	.1584E-01
12 0	668.18	.6909E 00	.7786E 00	.8807E 00	.1001E 01	.1146E 01	.1326E 01
4131	668.21	.2601E 00	.1850E 00	.1204E 00	.6968E-01	.3430E-01	.1341E-01

TABLE XVI (Continued)

BAND CODE	WAVE NUMBER	INTENSITY					
		T=300K	T=275K	T=250K	T=225K	T=200K	T=175K
1142	668.21	.2361E-01	.1955E-01	.1528E-01	.1106E-01	.7198E-02	.4029E-02
4132	668.24	.2380E 00	.1674E 00	.1076E 00	.6126E-01	.2956E-01	.1126E-01
4133	668.26	.2168E 00	.1508E 00	.9558E-01	.5353E-01	.2530E-01	.9384E-02
1144	668.29	.1703E-01	.1369E-01	.1032E-01	.7153E-02	.4409E-02	.2301E-02
4134	668.30	.1965E 00	.1351E 00	.8445E-01	.4651E-01	.2152E-01	.7765E-02
91 3	668.31	.2586E-02	.1625E-02	.9117E-03	.4399E-03	.1726E-03	.5037E-04
91 4	668.31	.4586E-02	.2877E-02	.1612E-02	.7761E-03	.3037E-03	.8835E-04
91 5	668.31	.6286E-02	.3937E-02	.2201E-02	.1057E-02	.4124E-03	.1195E-03
91 6	668.32	.7782E-02	.4864E-02	.2713E-02	.1299E-02	.5048E-03	.1456E-03
4135	668.33	.1773E 00	.1205E 00	.7423E-01	.4016E-01	.1818E-01	.6378E-02
91 8	668.33	.1029E-01	.6397E-02	.3545E-02	.1685E-02	.6487E-03	.1848E-03
91 7	668.33	.9111E-02	.5681E-02	.3159E-02	.1508E-02	.5833E-03	.1672E-03
91 9	668.34	.1132E-01	.7016E-02	.3874E-02	.1833E-02	.7017E-03	.1985E-03
2261	668.34	.4113E-03	.1816E-03	.6676E-04	.1921E-04	.3948E-05	.5019E-06
9110	668.35	.1220E-01	.7539E-02	.4146E-02	.1952E-02	.7426E-03	.2083E-03
4136	668.36	.1593E 00	.1069E 00	.6490E-01	.3449E-01	.1526E-01	.5202E-02
9111	668.36	.1295E-01	.7969E-02	.4362E-02	.2043E-02	.7717E-03	.2146E-03
1146	668.37	.1210E-01	.9429E-02	.6852E-02	.4535E-02	.2641E-02	.1281E-02
9112	668.37	.1355E-01	.8306E-02	.4525E-02	.2106E-02	.7897E-03	.2175E-03
9113	668.38	.1402E-01	.8554E-02	.4635E-02	.2143E-02	.7971E-03	.2172E-03
4137	668.39	.1424E 00	.9438E-01	.5644E-01	.2944E-01	.1273E-01	.4212E-02
9114	668.39	.1435E-01	.8714E-02	.4695E-02	.2156E-02	.7947E-03	.2142E-03
9115	668.41	.1455E-01	.8792E-02	.4707E-02	.2145E-02	.7835E-03	.2086E-03
9116	668.42	.1463E-01	.8791E-02	.4676E-02	.2114E-02	.7644E-03	.2009E-03
4138	668.43	.1268E 00	.8293E-01	.4883E-01	.2499E-01	.1055E-01	.3386E-02
9117	668.44	.1459E-01	.8718E-02	.4605E-02	.2064E-02	.7384E-03	.1914E-03
9118	668.45	.1444E-01	.8578E-02	.4498E-02	.1998E-02	.7067E-03	.1806E-03
1148	668.46	.8468E-02	.6389E-02	.4466E-02	.2819E-02	.1547E-02	.6951E-03
4139	668.46	.1124E 00	.7253E-01	.4203E-01	.2109E-01	.8692E-02	.2703E-02
9119	668.47	.1420E-01	.8379E-02	.4359E-02	.1918E-02	.6704E-03	.1687E-03
9120	668.49	.1387E-01	.8127E-02	.4194E-02	.1827E-02	.6306E-03	.1561E-03
4140	668.50	.9916E-01	.6313E-01	.3598E-01	.1770E-01	.7114E-02	.2142E-02
9121	668.51	.1346E-01	.7830E-02	.4006E-02	.1727E-02	.5883E-03	.1432E-03
5226	668.53	.1375E-01	.7844E-02	.3921E-02	.1643E-02	.5402E-03	.1256E-03
9122	668.53	.1298E-01	.7496E-02	.3801E-02	.1620E-02	.5444E-03	.1302E-03
4141	668.53	.8712E-01	.5469E-01	.3065E-01	.1477E-01	.5787E-02	.1686E-02
1150	668.55	.5839E-02	.4259E-02	.2859E-02	.1717E-02	.8858E-03	.3676E-03
9123	668.55	.1245E-01	.7132E-02	.3582E-02	.1509E-02	.4999E-03	.1174E-03
4142	668.57	.7620E-01	.4716E-01	.2598E-01	.1226E-01	.4678E-02	.1317E-02
9124	668.57	.1187E-01	.6744E-02	.3354E-02	.1397E-02	.4556E-03	.1049E-03
9125	668.59	.1125E-01	.6340E-02	.3121E-02	.1283E-02	.4122E-03	.9303E-04
4143	668.61	.6637E-01	.4047E-01	.2191E-01	.1012E-01	.3758E-02	.1022E-02
9126	668.62	.1061E-01	.5927E-02	.2886E-02	.1171E-02	.3702E-03	.8182E-04
1152	668.64	.3966E-02	.2793E-02	.1797E-02	.1025E-02	.4960E-03	.1895E-03
9127	668.64	.9958E-02	.5509E-02	.2653E-02	.1062E-02	.3301E-03	.7139E-04

TABLE XVI (Continued)

BAND CODE	WAVE NUMBER	INTENSITY					
		T=300K	T=275K	T=250K	T=225K	T=200K	T=175K
4144	668.65	.5756E-01	.3458E-01	.1838E-01	.8305E-02	.3001E-02	.7879E-03
9128	668.67	.9294E-02	.5093E-02	.2425E-02	.9574E-03	.2923E-03	.6180E-04
4145	668.69	.4970E-01	.2940E-01	.1535E-01	.6779E-02	.2381E-02	.6030E-03
9129	668.69	.8631E-02	.4683E-02	.2203E-02	.8574E-03	.2570E-03	.5309E-04
9130	668.72	.7975E-02	.4283E-02	.1990E-02	.7630E-03	.2245E-03	.4526E-04
4146	668.73	.4274E-01	.2489E-01	.1275E-01	.5503E-02	.1878E-02	.4583E-03
1154	668.74	.2654E-02	.1802E-02	.1110E-02	.6003E-03	.2715E-03	.9518E-04
9131	668.75	.7333E-02	.3897E-02	.1788E-02	.6749E-03	.1947E-03	.3829E-04
4147	668.78	.3660E-01	.2097E-01	.1054E-01	.4443E-02	.1472E-02	.3459E-03
9132	668.78	.6711E-02	.3527E-02	.1597E-02	.5933E-03	.1678E-03	.3215E-04
9133	668.80	.6113E-02	.3177E-02	.1419E-02	.5185E-03	.1436E-03	.2680E-04
4148	668.82	.3121E-01	.1759E-01	.8666E-02	.3567E-02	.1147E-02	.2593E-03
1156	668.84	.1750E-02	.1144E-02	.6733E-03	.3444E-03	.1453E-03	.4660E-04
9134	668.84	.5541E-02	.2846E-02	.1254E-02	.4504E-03	.1221E-03	.2218E-04
4149	668.86	.2650E-01	.1469E-01	.7093E-02	.2849E-02	.8884E-03	.1931E-03
9135	668.87	.5000E-02	.2538E-02	.1102E-02	.3890E-03	.1032E-03	.1822E-04
9136	668.90	.4492E-02	.2252E-02	.9638E-03	.3340E-03	.8663E-04	.1485E-04
4150	668.91	.2241E-01	.1221E-01	.5777E-02	.2263E-02	.6839E-03	.1428E-03
9137	668.93	.4016E-02	.1988E-02	.8381E-03	.2851E-03	.7226E-04	.1203E-04
1158	668.94	.1136E-02	.7144E-03	.4011E-03	.1937E-03	.7608E-04	.2224E-04
4151	668.95	.1887E-01	.1011E-01	.4681E-02	.1787E-02	.5233E-03	.1048E-03
9138	668.97	.3575E-02	.1747E-02	.7251E-03	.2420E-03	.9589E-04	.9667E-05
9139	669.00	.3169E-02	.1528E-02	.6240E-03	.2042E-03	.4932E-04	.7715E-05
4152	669.00	.1582E-01	.8325E-02	.3776E-02	.1404E-02	.3980E-03	.7647E-04
9140	669.04	.2796E-02	.1330E-02	.5343E-03	.1714E-03	.4036E-04	.6113E-05
4153	669.05	.1321E-01	.6828E-02	.3030E-02	.1098E-02	.3009E-03	.5540E-04
1160	669.05	.7271E-03	.4389E-03	.2347E-03	.1068E-03	.3893E-04	.1034E-04
9141	669.07	.2456E-02	.1152E-02	.4551E-03	.1430E-03	.3283E-04	.4810E-05
4154	669.10	.1099E-01	.5576E-02	.2420E-02	.8533E-03	.2261E-03	.3986E-04
9142	669.11	.2148E-02	.9932E-03	.3857E-03	.1187E-03	.2653E-04	.3759E-05
9143	669.15	.1871E-02	.8524E-03	.3252E-03	.9794E-04	.2131E-04	.2916E-05
4155	669.15	.9105E-02	.4533E-02	.1924E-02	.6598E-03	.1689E-03	.2849E-04
1162	669.16	.4583E-03	.2653E-03	.1349E-03	.5772E-04	.1948E-04	.4688E-05
9144	669.19	.1622E-02	.7281E-03	.2728E-03	.8037E-04	.1701E-04	.2247E-05
4156	669.20	.7511E-02	.3669E-02	.1521E-02	.5075E-03	.1254E-03	.2022E-04
9145	669.23	.1401E-02	.6191E-03	.2277E-03	.6559E-04	.1350E-04	.1719E-05
4157	669.25	.6171E-02	.2956E-02	.1198E-02	.3882E-03	.9261E-04	.1426E-04
1164	669.27	.2845E-03	.1577E-03	.7614E-04	.3057E-04	.9532E-05	.2071E-05
9146	669.27	.1204E-02	.5240E-03	.1891E-03	.5323E-04	.1064E-04	.1306E-05
3061	669.29	.5130E-03	.2265E-03	.8326E-04	.2395E-04	.4923E-05	.6259E-06
4158	669.30	.5050E-02	.2371E-02	.9383E-03	.2954E-03	.6796E-04	.9987E-05
9147	669.32	.1031E-02	.4414E-03	.1563E-03	.4297E-04	.8342E-05	.9857E-06
42 1	669.33	.1597E 00	.1345E 00	.1072E 00	.7950E-01	.5335E-01	.3105E-01
4159	669.35	.4116E-02	.1894E-02	.7315E-03	.2236E-03	.4958E-04	.6948E-05
9148	669.36	.8792E-03	.3702E-03	.1285E-03	.3449E-04	.6498E-05	.7387E-06

TABLE XVI (Continued)

BAND CODE	WAVE NUMBER	INTENSITY					
		T=300K	T=275K	T=250K	T=225K	T=200K	T=175K
1166	669.39	.1740E-03	.9225E-04	.4221E-04	.1587E-04	.4560E-05	.8916E-06
9149	669.40	.7464E-03	.3091E-03	.1052E-03	.2754E-04	.5031E-05	.5498E-06
4160	669.41	.3341E-02	.1506E-02	.5676E-03	.1684E-03	.3595E-04	.4801E-05
9150	669.45	.6311E-03	.2569E-03	.8564E-04	.2187E-04	.3872E-05	.4064E-06
4161	669.46	.2701E-02	.1193E-02	.4383E-03	.1261E-03	.2592E-04	.3295E-05
9151	669.49	.5313E-03	.2126E-03	.6939E-04	.1727E-04	.2962E-05	.2984E-06
1168	669.51	.1049E-03	.5309E-04	.2298E-04	.8079E-05	.2133E-05	.3741E-06
4162	669.52	.2175E-02	.9402E-03	.3369E-03	.9396E-04	.1858E-04	.2247E-05
9152	669.54	.4455E-03	.1751E-03	.5595E-04	.1357E-04	.2252E-05	.2176E-06
4163	669.57	.1744E-02	.7380E-03	.2577E-03	.6964E-04	.1323E-04	.1521E-05
9153	669.59	.3720E-03	.1436E-03	.4489E-04	.1060E-04	.1702E-05	.1576E-06
4164	669.63	.1393E-02	.5767E-03	.1962E-03	.5134E-04	.9374E-05	.1024E-05
9154	669.64	.3094E-03	.1172E-03	.3585E-04	.8239E-05	.1279E-05	.1133E-06
1170	669.64	.6225E-04	.3005E-04	.1229E-04	.4030E-05	.9754E-06	.1530E-06
9155	669.69	.2562E-03	.9527E-04	.2849E-04	.6369E-05	.9551E-06	.8097E-07
4165	669.69	.1108E-02	.4488E-03	.1486E-03	.3765E-04	.6601E-05	.6840E-06
9156	669.74	.2113E-03	.7709E-04	.2253E-04	.4897E-05	.7091E-06	.5746E-07
4166	669.75	.8783E-03	.3477E-03	.1121E-03	.2747E-04	.4621E-05	.4540E-06
12 2	669.75	.1370E 01	.1542E 01	.1742E 01	.1977E 01	.2260E 01	.2608E 01
1172	669.77	.3640E-04	.1674E-04	.6456E-05	.1971E-05	.4362E-06	.6099E-07
9157	669.79	.1736E-03	.6211E-04	.1773E-04	.3745E-05	.5233E-06	.4050E-07
4167	669.81	.6932E-03	.2682E-03	.8412E-04	.1994E-04	.3216E-05	.2994E-06
9158	669.84	.1420E-03	.4981E-04	.1389E-04	.2849E-05	.3839E-06	.2835E-07
4168	669.87	.5450E-03	.2060E-03	.6283E-04	.1439E-04	.2225E-05	.1961E-06
9159	669.89	.1157E-03	.3978E-04	.1082E-04	.2156E-05	.2799E-06	.1972E-07
1174	669.90	.2097E-04	.9170E-05	.3331E-05	.9446E-06	.1907E-06	.2369E-07
4169	669.93	.4267E-03	.1576E-03	.4671E-04	.1034E-04	.1530E-05	.1276E-06
9160	669.95	.9391E-04	.3163E-04	.8395E-05	.1623E-05	.2029E-06	.1362E-07
9161	670.00	.7591E-04	.2503E-04	.6481E-05	.1215E-05	.1462E-06	.9343E-08
4170	670.00	.3328E-03	.1200E-03	.3457E-04	.7386E-05	.1046E-05	.8248E-07
2263	670.02	.2664E-03	.1127E-03	.3935E-04	.1063E-04	.2021E-05	.2324E-06
1176	670.03	.1190E-04	.4943E-05	.1688E-05	.4438E-06	.8152E-07	.8970E-08
9162	670.06	.6111E-04	.1973E-04	.4980E-05	.9051E-06	.1048E-06	.6368E-08
4171	670.06	.2585E-03	.9098E-04	.2546E-04	.5249E-05	.7115E-06	.5296E-07
9163	670.11	.4899E-04	.1548E-04	.3808E-05	.6706E-06	.7462E-07	.4311E-08
42 2	670.11	.1763E 00	.1484E 00	.1182E 00	.8756E-01	.5868E-01	.3410E-01
4172	670.13	.2001E-03	.6869E-04	.1866E-04	.3712E-05	.4809E-06	.3378E-07
5228	670.15	.1201E-01	.6725E-02	.3286E-02	.1339E-02	.4254E-03	.9466E-04
9164	670.17	.3913E-04	.1210E-04	.2898E-05	.4942E-06	.5283E-07	.2899E-08
1178	670.17	.6653E-05	.2621E-05	.8399E-06	.2044E-06	.3407E-07	.3310E-08
4173	670.19	.1542E-03	.5163E-04	.1362E-04	.2611E-05	.3231E-06	.2140E-07
9165	670.23	.3112E-04	.9409E-05	.2195E-05	.3623E-06	.3719E-07	.1936E-08
4174	670.26	.1184E-03	.3865E-04	.9888E-05	.1827E-05	.2159E-06	.1347E-07
9166	670.29	.2465E-04	.7288E-05	.1655E-05	.2643E-06	.2602E-07	.1285E-08
1180	670.32	.3664E-05	.1367E-05	.4105E-06	.9226E-07	.1392E-07	.1190E-08

TABLE XVI (Continued)

BAND CODE	WAVE NUMBER	INTENSITY					
		T=300K	T=275K	T=250K	T=225K	T=200K	T=175K
4175	670.32	.9052E-04	.2881E-04	.7147E-05	.1272E-05	.1434E-06	.8424E-08
9167	670.35	.1945E-04	.5620E-05	.1241E-05	.1917E-06	.1810E-07	.8467E-09
4176	670.39	.6895E-04	.2138E-04	.5141E-05	.8808E-06	.9469E-07	.5233E-08
9168	670.41	.1529E-04	.4316E-05	.9270E-06	.1384E-06	.1252E-07	.5543E-09
1182	670.46	.1988E-05	.7016E-06	.1971E-06	.4082E-07	.5564E-08	.4172E-09
4177	670.46	.5231E-04	.1580E-04	.3682E-05	.6069E-06	.6217E-07	.3229E-08
9169	670.47	.1197E-04	.3300E-05	.6890E-06	.9933E-07	.8607E-08	.3605E-09
4178	670.53	.3953E-04	.1163E-04	.2624E-05	.4159E-06	.4058E-07	.1979E-08
9170	670.54	.9332E-05	.2512E-05	.5097E-06	.7094E-07	.5884E-08	.2329E-09
4179	670.60	.2976E-04	.8520E-05	.1861E-05	.2836E-06	.2633E-07	.1205E-08
9171	670.60	.7248E-05	.1904E-05	.3752E-06	.5041E-07	.3998E-08	.1495E-09
1184	670.61	.1062E-05	.3542E-06	.9292E-07	.1770E-07	.2174E-08	.1425E-09
92 2	670.66	.7503E-02	.4718E-02	.2650E-02	.1281E-02	.5033E-03	.1472E-03
9172	670.67	.5606E-05	.1437E-05	.2750E-06	.3563E-07	.2701E-08	.9529E-10
4180	670.68	.2232E-04	.6217E-05	.1314E-05	.1924E-06	.1699E-07	.7293E-09
9173	670.73	.4320E-05	.1080E-05	.2005E-06	.2505E-07	.1814E-08	.6035E-10
4181	670.75	.1667E-04	.4517E-05	.9237E-06	.1298E-06	.1090E-07	.4383E-09
9174	670.80	.3315E-05	.8082E-06	.1456E-06	.1752E-07	.1212E-08	.3796E-10
4182	670.82	.1240E-04	.3267E-05	.6462E-06	.8718E-07	.6952E-08	.2617E-09
9175	670.86	.2534E-05	.6022E-06	.1052E-06	.1219E-07	.8044E-09	.2373E-10
42 3	670.90	.1964E 00	.1651E 00	.1314E 00	.9715E-01	.6499E-01	.3768E-01
4183	670.90	.9191E-05	.2354E-05	.4500E-06	.5823E-07	.4409E-08	.1552E-09
9176	670.93	.1930E-05	.4468E-06	.7564E-07	.8440E-08	.5309E-09	.1473E-10
4184	670.97	.6785E-05	.1689E-05	.3119E-06	.3870E-07	.2780E-08	.9146E-10
9177	671.00	.1464E-05	.3300E-06	.5414E-07	.5813E-08	.3484E-09	.9085E-11
4185	671.05	.4989E-05	.1206E-05	.2151E-06	.2558E-07	.1742E-08	.5354E-10
9178	671.07	.1106E-05	.2428E-06	.3857E-07	.3982E-08	.2273E-09	.5566E-11
3059	671.10	.7841E-03	.3609E-03	.1393E-03	.4259E-04	.9443E-05	.1323E-05
4186	671.13	.3655E-05	.8580E-06	.1477E-06	.1683E-07	.1086E-08	.3114E-10
4187	671.21	.2667E-05	.6077E-06	.1010E-06	.1101E-07	.6728E-09	.1799E-10
4188	671.28	.1938E-05	.4286E-06	.6869E-07	.7167E-08	.4145E-09	.1033E-10
12 4	671.32	.2007E 01	.2254E 01	.2539E 01	.2871E 01	.3266E 01	.3748E 01
4189	671.36	.1403E-05	.3010E-06	.4652E-07	.4642E-08	.2539E-09	.5887E-11
92 3	671.45	.7800E-02	.4900E-02	.2749E-02	.1326E-02	.5202E-03	.1518E-03
4190	671.45	.1012E-05	.2105E-06	.3135E-07	.2991E-08	.1546E-09	.3335E-11
42 4	671.69	.2170E 00	.1821E 00	.1447E 00	.1068E 00	.7125E-01	.4117E-01
2265	671.71	.1698E-03	.6873E-04	.2276E-04	.5766E-05	.1011E-05	.1047E-06
5230	671.77	.1029E-01	.5646E-02	.2693E-02	.1065E-02	.3261E-03	.6920E-04
92 4	672.23	.8207E-02	.5148E-02	.2883E-02	.1388E-02	.5432E-03	.1580E-03
42 5	672.48	.2369E 00	.1985E 00	.1574E 00	.1159E 00	.7706E-01	.4435E-01
12 6	672.90	.2575E 01	.2880E 01	.3229E 01	.3632E 01	.4104E 01	.4667E 01
3057	672.90	.1179E-02	.5648E-03	.2288E-03	.7415E-04	.1769E-04	.2723E-05
92 5	673.02	.8641E-02	.5411E-02	.3024E-02	.1452E-02	.5665E-03	.1641E-03
42 6	673.27	.2556E 00	.2138E 00	.1690E 00	.1241E 00	.8220E-01	.4708E-01
2267	673.40	.1065E-03	.4119E-04	.1292E-04	.3061E-05	.4937E-06	.4596E-07

TABLE XVI (Continued)

BAND CODE	WAVE NUMBER	INTENSITY					
		T=300K	T=275K	T=250K	T=225K	T=200K	T=175K
5232	673.40	.8650E-02	.4645E-02	.2159E-02	.8276E-03	.2435E-03	.4910E-04
92 6	673.81	.9063E-02	.5664E-02	.3158E-02	.1512E-02	.5875E-03	.1694E-03
42 7	674.06	.2727E 00	.2275E 00	.1794E 00	.1312E 00	.8654E-01	.4929E-01
12 8	674.48	.3050E 01	.3395E 01	.3783E 01	.4223E 01	.4726E 01	.5310E 01
92 7	674.60	.9453E-02	.5893E-02	.3276E-02	.1563E-02	.6047E-03	.1734E-03
3055	674.70	.1745E-02	.8685E-03	.3685E-03	.1264E-03	.3235E-04	.5455E-05
42 8	674.85	.2879E 00	.2395E 00	.1882E 00	.1371E 00	.8998E-01	.5092E-01
5234	675.03	.7138E-02	.3746E-02	.1694E-02	.6278E-03	.1771E-03	.3384E-04
2249	675.09	.6573E-04	.2426E-04	.7193E-05	.1591E-05	.2355E-06	.1964E-07
92 8	675.40	.9798E-02	.6091E-02	.3375E-02	.1604E-02	.6173E-03	.1758E-03
42 9	675.64	.3010E 00	.2496E 00	.1954E 00	.1417E 00	.9249E-01	.5196E-01
1210	676.06	.3418E 01	.3779E 01	.4178E 01	.4619E 01	.5108E 01	.5653E 01
92 9	676.19	.1009E-01	.6252E-02	.3451E-02	.1633E-02	.6248E-03	.1767E-03
4210	676.43	.3119E 00	.2577E 00	.2009E 00	.1450E 00	.9404E-01	.5240E-01
3053	676.48	.2540E-02	.1312E-02	.5820E-03	.2108E-03	.5777E-04	.1063E-04
5236	676.66	.5785E-02	.2963E-02	.1301E-02	.4654E-03	.1256E-03	.2265E-04
2271	676.78	.3994E-04	.1405E-04	.3930E-05	.8103E-06	.1098E-06	.8171E-08
9210	676.98	.1032E-01	.6373E-02	.3503E-02	.1649E-02	.6271E-03	.1759E-03
4211	677.23	.3204E 00	.2638E 00	.2048E 00	.1469E 00	.9464E-01	.5227E-01
1212	677.65	.3667E 01	.4023E 01	.4406E 01	.4815E 01	.5249E 01	.5702E 01
9211	677.78	.1048E-01	.6451E-02	.3530E-02	.1653E-02	.6241E-03	.1735E-03
4212	678.02	.3267E 00	.2679E 00	.2069E 00	.1475E 00	.9432E-01	.5160E-01
3051	678.26	.3636E-02	.1947E-02	.9017E-03	.3442E-03	.1007E-03	.2018E-04
5238	678.30	.4605E-02	.2299E-02	.9789E-03	.3372E-03	.8679E-04	.1474E-04
2273	678.48	.2388E-04	.7996E-05	.2108E-05	.4040E-06	.5000E-07	.3311E-08
9212	678.57	.1059E-01	.6487E-02	.3533E-02	.1644E-02	.6161E-03	.1696E-03
4213	678.82	.3306E 00	.2699E 00	.2073E 00	.1469E 00	.9314E-01	.5042E-01
1214	679.24	.3797E 01	.4127E 01	.4470E 01	.4820E 01	.5166E 01	.5491E 01
9213	679.37	.1062E-01	.6481E-02	.3510E-02	.1622E-02	.6032E-03	.1644E-03
4214	679.62	.3322E 00	.2699E 00	.2061E 00	.1450E 00	.9116E-01	.4879E-01
5240	679.94	.3603E-02	.1750E-02	.7215E-03	.2388E-03	.5851E-04	.9323E-05
3049	680.03	.5121E-02	.2838E-02	.1370E-02	.5499E-03	.1714E-03	.3725E-04
9214	680.17	.1060E-01	.6433E-02	.3464E-02	.1590E-02	.5860E-03	.1579E-03
2275	680.18	.1406E-04	.4473E-05	.1109E-05	.1973E-06	.2224E-07	.1306E-08
4215	680.41	.3316E 00	.2680E 00	.2034E 00	.1421E 00	.8846E-01	.4678E-01
1216	680.84	.3813E 01	.4100E 01	.4385E 01	.4655E 01	.4893E 01	.5072E 01
9215	680.97	.1051E-01	.6347E-02	.3397E-02	.1547E-02	.5649E-03	.1503E-03
4216	681.21	.3289E 00	.2644E 00	.1994E 00	.1381E 00	.8513E-01	.4444E-01
5242	681.59	.2770E-02	.1308E-02	.5210E-03	.1654E-03	.3847E-04	.5734E-05
9216	681.77	.1036E-01	.6224E-02	.3309E-02	.1495E-02	.5404E-03	.1420E-03
3047	681.80	.7092E-02	.4062E-02	.2040E-02	.8598E-03	.2848E-03	.6690E-04
2277	681.89	.8148E-05	.2460E-05	.5729E-06	.9440E-07	.9668E-08	.5020E-09
4217	682.01	.3243E 00	.2591E 00	.1940E 00	.1333E 00	.8128E-01	.4185E-01
1218	682.43	.3725E 01	.3958E 01	.4172E 01	.4352E 01	.4475E 01	.4511E 01
9217	682.57	.1016E-01	.6067E-02	.3203E-02	.1435E-02	.5131E-03	.1330E-03

TABLE XVI (Continued)

BAND CODE	WAVE NUMBER	INTENSITY					
		T=300K	T=275K	T=250K	T=225K	T=200K	T=175K
4218	682.81	.3178E 00	.2523E 00	.1876E 00	.1277E 00	.7699E-01	.3907E-01
5244	683.23	.2093E-02	.9595E-03	.3688E-03	.1121E-03	.2468E-04	.3429E-05
9218	683.37	.9907E-02	.5880E-02	.3081E-02	.1368E-02	.4837E-03	.1235E-03
3045	683.55	.9658E-02	.5710E-02	.2979E-02	.1315E-02	.4617E-03	.1169E-03
2279	683.60	.4648E-05	.1330E-05	.2904E-06	.4423E-07	.4106E-08	.1879E-09
4219	683.61	.3096E 00	.2443E 00	.1801E 00	.1214E 00	.7237E-01	.3617E-01
8068	683.74	.1203E-05	.3395E-06	.7288E-07	.1087E-07	.9834E-09	.4353E-10
1220	684.04	.3549E 01	.3721E 01	.3860E 01	.3948E 01	.3962E 01	.3870E 01
9219	684.17	.9610E-02	.5666E-02	.2946E-02	.1296E-02	.4527E-03	.1139E-03
4220	684.41	.3000E 00	.2350E 00	.1719E 00	.1147E 00	.6753E-01	.3321E-01
8067	684.66	.1534E-05	.4431E-06	.9781E-07	.1510E-07	.1425E-08	.6662E-10
5246	684.89	.1555E-02	.6911E-03	.2559E-03	.7431E-04	.1545E-04	.1995E-05
9220	684.97	.9273E-02	.5430E-02	.2800E-02	.1219E-02	.4206E-03	.1041E-03
4221	685.22	.2890E 00	.2249E 00	.1631E 00	.1077E 00	.6255E-01	.3024E-01
3043	685.29	.1293E-01	.7880E-02	.4263E-02	.1968E-02	.7304E-03	.1986E-03
2281	685.31	.2610E-05	.7069E-06	.1445E-06	.2030E-07	.1704E-08	.6848E-10
8066	685.58	.1949E-05	.5758E-06	.1306E-06	.2085E-07	.2053E-08	.1013E-09
1222	685.64	.3304E 01	.3413E 01	.3478E 01	.3482E 01	.3401E 01	.3209E 01
9221	685.78	.8903E-02	.5176E-02	.2646E-02	.1140E-02	.3881E-03	.9446E-04
4222	686.02	.2770E 00	.2139E 00	.1537E 00	.1004E 00	.5752E-01	.2732E-01
8065	686.50	.2465E-05	.7450E-06	.1737E-06	.2865E-07	.2939E-08	.1530E-09
5248	686.54	.1137E-02	.4888E-03	.1741E-03	.4819E-04	.9443E-05	.1129E-05
9222	686.58	.8504E-02	.4907E-02	.2486E-02	.1059E-02	.3557E-03	.8504E-04
4223	686.83	.2642E 00	.2024E 00	.1441E 00	.9302E-01	.5252E-01	.2449E-01
2283	687.03	.1443E-05	.3694E-06	.7057E-07	.9128E-08	.6907E-09	.2431E-10
3041	687.03	.1701E-01	.1067E-01	.5979E-02	.2880E-02	.1127E-02	.3283E-03
1224	687.25	.3008E 01	.3058E 01	.3057E 01	.2989E 01	.2835E 01	.2576E 01
9223	687.39	.8083E-02	.4627E-02	.2322E-02	.9781E-03	.3237E-03	.7598E-04
8064	687.42	.3107E-05	.9598E-06	.2298E-06	.3917E-07	.4185E-08	.2295E-09
4224	687.63	.2506E 00	.1904E 00	.1342E 00	.8562E-01	.4762E-01	.2178E-01
9224	688.19	.7645E-02	.4341E-02	.2157E-02	.8976E-03	.2927E-03	.6737E-04
5250	688.20	.8168E-03	.3396E-03	.1161E-03	.3059E-04	.5632E-05	.6219E-06
8063	688.33	.3899E-05	.1231E-05	.3026E-06	.5326E-07	.5923E-08	.3420E-09
4225	688.44	.2365E 00	.1782E 00	.1243E 00	.7832E-01	.4288E-01	.1922E-01
3039	688.76	.2200E-01	.1419E-01	.8216E-02	.4121E-02	.1697E-02	.5274E-03
14061	688.85	.1147E-05	.2912E-06	.5506E-07	.7033E-08	.5240E-09	.1808E-10
1226	688.86	.2682E 01	.2680E 01	.2623E 01	.2500E 01	.2297E 01	.2003E 01
9225	689.00	.7197E-02	.4051E-02	.1993E-02	.8188E-03	.2628E-03	.5929E-04
8062	689.24	.4874E-05	.1572E-05	.3966E-06	.7204E-07	.8334E-08	.5063E-09
4226	689.25	.2222E 00	.1659E 00	.1145E 00	.7121E-01	.3836E-01	.1684E-01
9226	689.81	.6742E-02	.3762E-02	.1831E-02	.7425E-03	.2345E-03	.5179E-04
5252	689.86	.5774E-03	.2317E-03	.7594E-04	.1900E-04	.3279E-05	.3332E-06
4227	690.05	.2077E 00	.1536E 00	.1049E 00	.6434E-01	.3408E-01	.1464E-01
8061	690.15	.6068E-05	.2000E-05	.5173E-06	.9693E-07	.1166E-07	.7445E-09
1228	690.48	.2344E 01	.2298E 01	.2200E 01	.2040E 01	.1810E 01	.1510E 01

TABLE XVI (Continued)

BAND CODE	WAVE NUMBER	INTENSITY					
		T=300K	T=275K	T=250K	T=225K	T=200K	T=175K
3037	690.48	.2795E-01	.1851E-01	.1106E-01	.5764E-02	.2491E-02	.8236E-03
9227	690.62	.6287E-02	.3475E-02	.1673E-02	.6693E-03	.2078E-03	.4491E-04
14059	690.66	.1755E-05	.4643E-06	.9226E-07	.1252E-07	.1007E-08	.3829E-10
4228	690.86	.1932E 00	.1416E 00	.9554E-01	.5779E-01	.3007E-01	.1263E-01
8060	691.06	.7525E-05	.2532E-05	.6716E-06	.1297E-06	.1621E-07	.1087E-08
9228	691.43	.5836E-02	.3195E-02	.1520E-02	.5997E-03	.1829E-03	.3866E-04
5254	691.53	.4015E-03	.1553E-03	.4872E-04	.1155E-04	.1864E-05	.1738E-06
4229	691.67	.1789E 00	.1298E 00	.8655E-01	.5159E-01	.2637E-01	.1082E-01
8059	691.97	.9293E-05	.3192E-05	.8677E-06	.1727E-06	.2242E-07	.1578E-08
1230	692.10	.2009E 01	.1930E 01	.1804E 01	.1623E 01	.1389E 01	.1105E 01
3035	692.19	.3488E-01	.2367E-01	.1458E-01	.7880E-02	.3564E-02	.1250E-02
9229	692.24	.5392E-02	.2923E-02	.1374E-02	.5343E-03	.1600E-03	.3304E-04
14057	692.47	.2642E-05	.7273E-06	.1516E-06	.2183E-07	.1888E-08	.7892E-10
4230	692.48	.1649E 00	.1184E 00	.7798E-01	.4579E-01	.2297E-01	.9197E-02
8058	692.87	.1143E-04	.4006E-05	.1116E-05	.2288E-06	.3080E-07	.2274E-08
9230	693.05	.4959E-02	.2661E-02	.1235E-02	.4732E-03	.1391E-03	.2803E-04
5256	693.20	.2747E-03	.1023E-03	.3065E-04	.6874E-05	.1035E-05	.8821E-07
4231	693.30	.1512E 00	.1074E 00	.6988E-01	.4040E-01	.1987E-01	.7763E-02
1232	693.72	.1690E 01	.1589E 01	.1447E 01	.1262E 01	.1037E 01	.7846E 00
8057	693.77	.1401E-04	.5006E-05	.1428E-05	.3014E-06	.4208E-07	.3255E-08
9231	693.86	.4540E-02	.2410E-02	.1105E-02	.4167E-03	.1201E-03	.2361E-04
3033	693.90	.4274E-01	.2970E-01	.1881E-01	.1052E-01	.4970E-02	.1842E-02
4232	694.11	.1381E 00	.9705E-01	.6230E-01	.3544E-01	.1709E-01	.6505E-02
14055	694.27	.3913E-05	.1120E-05	.2445E-06	.3724E-07	.3458E-08	.1583E-09
8056	694.67	.1709E-04	.6229E-05	.1818E-05	.3950E-06	.5715E-07	.4629E-08
9232	694.68	.4139E-02	.2173E-02	.9833E-03	.3649E-03	.1031E-03	.1975E-04
5258	694.87	.1849E-03	.6620E-04	.1892E-04	.4005E-05	.5610E-06	.4358E-07
4233	694.92	.1256E 00	.8724E-01	.5524E-01	.3091E-01	.1460E-01	.5411E-02
1234	695.35	.1395E 01	.1282E 01	.1136E 01	.9578E 00	.7553E 00	.5412E 00
9233	695.49	.3756E-02	.1950E-02	.8704E-03	.3177E-03	.8793E-04	.1640E-04
8055	695.57	.2077E-04	.7716E-05	.2305E-05	.5149E-06	.7716E-07	.6537E-08
3031	695.59	.5139E-01	.3651E-01	.2374E-01	.1373E-01	.6752E-02	.2637E-02
4234	695.74	.1136E 00	.7803E-01	.4873E-01	.2681E-01	.1239E-01	.4470E-02
14053	696.06	.5700E-05	.1693E-05	.3866E-06	.6220E-07	.6184E-08	.3092E-09
9234	696.31	.3393E-02	.1741E-02	.7665E-03	.2750E-03	.7452E-04	.1352E-04
8054	696.46	.2514E-04	.9516E-05	.2907E-05	.6676E-06	.1036E-06	.9171E-08
4235	696.55	.1024E 00	.6947E-01	.4276E-01	.2312E-01	.1045E-01	.3666E-02
5260	696.55	.1224E-03	.4209E-04	.1146E-04	.2284E-05	.2970E-06	.2096E-07
1236	696.98	.1131E 01	.1015E 01	.8730E 00	.7105E 00	.5359E 00	.3627E 00
9235	697.13	.3052E-02	.1548E-02	.6715E-03	.2368E-03	.6276E-04	.1107E-04
3029	697.28	.6062E-01	.4397E-01	.2932E-01	.1747E-01	.8929E-02	.3663E-02
8053	697.36	.3030E-04	.1168E-04	.3650E-05	.1382E-06	.1382E-06	.1278E-07
4236	697.37	.9183E-01	.6155E-01	.3733E-01	.1982E-01	.8764E-02	.2985E-02
14051	697.84	.8168E-05	.2514E-05	.5995E-06	.1017E-06	.1079E-07	.5874E-09
9236	697.94	.2734E-02	.1369E-02	.5854E-03	.2027E-03	.5252E-04	.9000E-05

TABLE XVI (Continued)

BAND CCDE	WAVE NUMBER	INTENSITY					
		T=300K	T=275K	T=250K	T=225K	T=200K	T=175K
4737	698.19	.8202E-01	.5428E-01	.3243E-01	.1690E-01	.7301E-02	.2414E-02
5262	698.23	.7980E-04	.2630E-04	.6806E-05	.1276E-05	.1536E-06	.9815E-08
8052	698.25	.3638E-04	.1428E-04	.4559E-05	.1105E-05	.1832E-06	.1769E-07
1238	698.61	.9011E 00	.7878E 00	.6572E 00	.5152E 00	.3708E 00	.2362E 00
9237	698.76	.2438E-02	.1206E-02	.5077E-03	.1725E-03	.4369E-04	.7266E-05
3C27	698.96	.7011E-01	.5185E-01	.3538E-01	.2170E-01	.1149E-01	.4934E-02
4238	699.00	.7293E-01	.4765E-01	.2802E-01	.1433E-01	.6045E-02	.1938E-02
8051	699.14	.4350E-04	.1738E-04	.5669E-05	.1410E-05	.2415E-06	.2431E-07
9238	699.58	.2165E-02	.1057E-02	.4381E-03	.1461E-03	.3612E-04	.5826E-05
14C49	699.61	.1151E-04	.3668E-05	.9115E-06	.1626E-06	.1840E-07	.1086E-08
4239	699.82	.6457E-01	.4163E-01	.2409E-01	.1208E-01	.4973E-02	.1545E-02
5264	699.91	.5118E-04	.1615E-04	.3967E-05	.6978E-06	.7755E-07	.4474E-08
8050	700.02	.5179E-04	.2106E-04	.7013E-05	.1789E-05	.3165E-06	.3320E-07
1240	700.25	.7053E 00	.6002E 00	.4847E 00	.3652E 00	.2502E 00	.1496E 00
9239	700.40	.1914E-02	.9221E-03	.3762E-03	.1230E-03	.2967E-04	.4638E-05
3025	700.63	.7943E-01	.5981E-01	.4171E-01	.2627E-01	.1438E-01	.6443E-02
4240	700.64	.5693E-01	.3620E-01	.2061E-01	.1013E-01	.4067E-02	.1224E-02
8049	700.91	.6142E-04	.2541E-04	.8635E-05	.2259E-05	.4123E-06	.4502E-07
9240	701.22	.1686E-02	.8008E-03	.3214E-03	.1030E-03	.2423E-04	.3667E-05
14C47	701.38	.1595E-04	.5255E-05	.1359E-05	.2545E-06	.3060E-07	.1953E-08
4241	701.46	.4997E-01	.3133E-01	.1754E-01	.8446E-02	.3305E-02	.9621E-03
5266	701.60	.3230E-04	.9748E-05	.2269E-05	.3737E-06	.3825E-07	.1986E-08
8048	701.79	.7253E-04	.3051E-04	.1058E-04	.2836E-05	.5338E-06	.6064E-07
1242	701.89	.5426E 00	.4488E 00	.3503E 00	.2532E 00	.1647E 00	.9210E-01
9241	702.04	.1478E-02	.6923E-03	.2732E-03	.8577E-04	.1967E-04	.2880E-05
4242	702.29	.4368E-01	.2700E-01	.1486E-01	.7004E-02	.2670E-02	.7513E-03
3023	702.30	.8808E-01	.6743E-01	.4798E-01	.3096E-01	.1748E-01	.8147E-02
8047	702.67	.8530E-04	.3647E-04	.1290E-04	.3542E-05	.6870E-06	.8112E-07
9242	702.87	.1290E-02	.5958E-03	.2311E-03	.7104E-04	.1587E-04	.2246E-05
4243	703.11	.3802E-01	.2316E-01	.1252E-01	.5777E-02	.2143E-02	.5826E-03
14C45	703.14	.2174E-04	.7392E-05	.1986E-05	.3897E-06	.4966E-07	.3417E-08
5268	703.29	.2007E-04	.5782E-05	.1273E-05	.1960E-06	.1843E-07	.8583E-09
1244	703.53	.4103E 00	.3295E 00	.2482E 00	.1717E 00	.1058E 00	.5515E-01
8046	703.55	.9990E-04	.4340E-04	.1565E-04	.4399E-05	.8788E-06	.1078E-06
9243	703.69	.1122E-02	.5105E-03	.1945E-03	.5852E-04	.1272E-04	.1739E-05
4244	703.93	.3296E-01	.1977E-01	.1050E-01	.4738E-02	.1710E-02	.4487E-03
3021	703.95	.9548E-01	.7423E-01	.5380E-01	.3551E-01	.2061E-01	.9962E-02
8045	704.43	.1165E-03	.5142E-04	.1889E-04	.5435E-05	.1117E-05	.1422E-06
9244	704.51	.9714E-03	.4354E-03	.1629E-03	.4794E-04	.1014E-04	.1338E-05
4245	704.76	.2845E-01	.1681E-01	.8761E-02	.3865E-02	.1356E-02	.3432E-03
14C43	704.89	.2912E-04	.1021E-04	.2844E-05	.5836E-06	.7865E-07	.5814E-08
5270	704.99	.1227E-04	.3371E-05	.7012E-06	.1006E-06	.8677E-08	.3612E-09
1246	705.18	.3051E 00	.2375E 00	.1723E 00	.1139E 00	.6628E-01	.3213E-01
8044	705.30	.1353E-03	.6065E-04	.2269E-04	.6678E-05	.1412E-05	.1863E-06
9245	705.34	.8375E-03	.3696E-03	.1358E-03	.3907E-04	.8032E-05	.1022E-05

TABLE XVI (Continued)

BAND CODE	WAVE NUMBER	INTENSITY					
		T=300K	T=275K	T=250K	T=225K	T=200K	T=175K
4246	705.58	.2445E-01	.1422E-01	.7274E-02	.3136E-02	.1069E-02	.2607E-03
3019	705.60	.1010E 00	.7965E-01	.5870E-01	.3955E-01	.2355E-01	.1176E-01
9246	706.17	.7192E-03	.3124E-03	.1126E-03	.3166E-04	.6325E-05	.7755E-06
8043	706.18	.1565E-03	.7120E-04	.2713E-04	.8160E-05	.1774E-05	.2425E-06
4247	706.41	.2093E-01	.1198E-01	.6011E-02	.2531E-02	.8379E-03	.1967E-03
14041	706.63	.3835E-04	.1384E-04	.3992E-05	.8549E-06	.1215E-06	.9620E-08
5272	706.69	.7386E-05	.1932E-05	.3790E-06	.5063E-07	.3990E-08	.1480E-09
1248	706.83	.2231E 00	.1681E 00	.1173E 00	.7397E-01	.4055E-01	.1821E-01
9247	706.99	.6150E-03	.2629E-03	.9296E-04	.2552E-04	.4950E-05	.5845E-06
8042	707.05	.1802E-03	.8320E-04	.3227E-04	.9917E-05	.2215E-05	.3134E-06
3017	707.24	.1041E 00	.8315E-01	.6221E-01	.4269E-01	.2602E-01	.1339E-01
4248	707.24	.1784E-01	.1004E-01	.4942E-02	.2032E-02	.6526E-03	.1474E-03
9248	707.82	.5237E-03	.2202E-03	.7636E-04	.2047E-04	.3852E-05	.4375E-06
8041	707.91	.2067E-03	.9679E-04	.3818E-04	.1199E-04	.2748E-05	.4023E-06
4249	708.06	.1515E-01	.8386E-02	.4044E-02	.1622E-02	.5053E-03	.1097E-03
14039	708.36	.4962E-04	.1841E-04	.5490E-05	.1224E-05	.1831E-06	.1547E-07
5274	708.39	.4376E-05	.1089E-05	.2010E-06	.2494E-07	.1793E-08	.5907E-10
1250	708.49	.1605E 00	.1169E 00	.7834E-01	.4700E-01	.2421E-01	.1004E-01
9249	708.65	.4442E-03	.1837E-03	.6242E-04	.1632E-04	.2979E-05	.3252E-06
8040	708.78	.2360E-03	.1121E-03	.4496E-04	.1441E-04	.3389E-05	.5128E-06
3015	708.87	.1043E 00	.8420E-01	.6385E-01	.4455E-01	.2772E-01	.1465E-01
4250	708.89	.1281E-01	.6970E-02	.3293E-02	.1288E-02	.3889E-03	.8111E-04
9250	709.48	.3752E-03	.1525E-03	.5077E-04	.1295E-04	.2290E-05	.2402E-06
8039	709.65	.2683E-03	.1292E-03	.5268E-04	.1722E-04	.4153E-05	.6491E-06
4251	709.72	.1078E-01	.5768E-02	.2668E-02	.1017E-02	.2975E-03	.5955E-04
14037	710.08	.6308E-04	.2402E-04	.7395E-05	.1714E-05	.2690E-06	.2419E-07
5276	710.09	.2552E-05	.6029E-06	.1046E-06	.1204E-07	.7869E-09	.2296E-10
1252	710.15	.1135E 00	.7982E-01	.5129E-01	.2922E-01	.1412E-01	.5388E-02
9251	710.31	.3156E-03	.1261E-03	.4110E-04	.1022E-04	.1750E-05	.1761E-06
3013	710.49	.1010E 00	.8239E-01	.6322E-01	.4475E-01	.2835E-01	.1534E-01
8038	710.51	.3037E-03	.1482E-03	.6140E-04	.2047E-04	.5059E-05	.8158E-06
4252	710.55	.9044E-02	.4751E-02	.2152E-02	.7993E-03	.2262E-03	.4343E-04
9252	711.14	.2645E-03	.1038E-03	.3311E-04	.8020E-05	.1330E-05	.1283E-06
8037	711.37	.3423E-03	.1692E-03	.7121E-04	.2419E-04	.6124E-05	.1018E-05
4253	711.39	.7553E-02	.3897E-02	.1727E-02	.6247E-03	.1710E-03	.3146E-04
12054	711.41	.1097E-05	.3101E-06	.6670E-07	.9978E-08	.9058E-09	.4030E-10
5278	711.80	.1465E-05	.3282E-06	.5345E-07	.5689E-08	.3375E-09	.8689E-11
14035	711.80	.7876E-04	.3075E-04	.9754E-05	.2345E-05	.3852E-06	.3674E-07
1254	711.81	.7900E-01	.5356E-01	.3294E-01	.1779E-01	.8036E-02	.2814E-02
9253	711.98	.2207E-03	.8504E-04	.2655E-04	.6262E-05	.1004E-05	.9286E-07
3011	712.10	.9416E-01	.7743E-01	.6002E-01	.4302E-01	.2768E-01	.1528E-01
4254	712.22	.6283E-02	.3182E-02	.1379E-02	.4856E-03	.1285E-03	.2264E-04
8036	712.23	.3841E-03	.1923E-03	.8216E-04	.2843E-04	.7366E-05	.1262E-05
12053	712.31	.1324E-05	.3810E-06	.8381E-07	.1288E-07	.1210E-08	.5622E-10
9254	712.81	.1834E-03	.6938E-04	.2119E-04	.4863E-05	.7539E-06	.6675E-07

TABLE XVI (Continued)

BANC CODE	WAVE NUMBER	INTENSITY					
		T=300K	T=275K	T=250K	T=225K	T=200K	T=175K
4255	713.05	.5205E-02	.2587E-02	.1096E-02	.3755E-03	.9602E-04	.1618E-04
8035	713.08	.4291E-03	.2174E-03	.9430E-04	.3323E-04	.8805E-05	.1553E-05
3186	713.12	.1499E-05	.3513E-06	.6040E-07	.6870E-08	.4428E-09	.1269E-10
12052	713.20	.1591E-05	.4662E-06	.1048E-06	.1654E-07	.1606E-08	.7789E-10
3184	713.48	.2785E-05	.6919E-06	.1276E-06	.1581E-07	.1134E-08	.3730E-10
1256	713.48	.5409E-01	.3531E-01	.2075E-01	.1060E-01	.4467E-02	.1431E-02
14033	713.51	.9655E-04	.3860E-04	.1259E-04	.3134E-05	.5376E-06	.5421E-07
9255	713.64	.1518E-03	.5636E-04	.1683E-04	.3757E-05	.5627E-06	.4765E-07
30 9	713.71	.8357E-01	.6921E-01	.5411E-01	.3919E-01	.2555E-01	.1434E-01
3182	713.82	.5094E-05	.1340E-05	.2646E-06	.3565E-07	.2840E-08	.1068E-09
4256	713.89	.4294E-02	.2094E-02	.8671E-03	.2888E-03	.7131E-04	.1148E-04
8034	713.94	.4773E-03	.2448E-03	.1077E-03	.3862E-04	.1046E-04	.1897E-05
12051	714.09	.1904E-05	.5679E-06	.1304E-06	.2113E-07	.2119E-08	.1072E-09
3180	714.16	.9173E-05	.2551E-05	.5386E-06	.7874E-07	.6946E-08	.2978E-09
9256	714.48	.1252E-03	.4558E-04	.1330E-04	.2887E-05	.4175E-06	.3380E-07
3178	714.48	.1626E-04	.4776E-05	.1076E-05	.1703E-06	.1660E-07	.8089E-09
4257	714.72	.3529E-02	.1688E-02	.6827E-03	.2209E-03	.5264E-04	.8098E-05
8033	714.79	.5285E-03	.2742E-03	.1223E-03	.4462E-04	.1234E-04	.2301E-05
3176	714.80	.2839E-04	.8788E-05	.2110E-05	.3610E-06	.3876E-07	.2140E-08
12050	714.98	.2269E-05	.6887E-06	.1615E-06	.2684E-07	.2780E-08	.1465E-09
3174	715.11	.4877E-04	.1590E-04	.4061E-05	.7493E-06	.8843E-07	.5513E-08
1258	715.15	.3644E-01	.2287E-01	.1282E-01	.6182E-02	.2425E-02	.7080E-03
14031	715.21	.1162E-03	.4748E-04	.1591E-04	.4090E-05	.7309E-06	.7766E-07
30 7	715.30	.6946E-01	.5786E-01	.4555E-01	.3327E-01	.2192E-01	.1247E-01
9257	715.31	.1028E-03	.3670E-04	.1046E-04	.2207E-05	.3079E-06	.2381E-07
3172	715.42	.8248E-04	.2827E-04	.7669E-05	.1523E-05	.1971E-06	.1383E-07
4258	715.56	.2888E-02	.1354E-02	.5349E-03	.1682E-03	.3863E-04	.5672E-05
8032	715.64	.5825E-03	.3056E-03	.1382E-03	.5125E-04	.1447E-04	.2771E-05
3170	715.71	.1373E-03	.4942E-04	.1422E-04	.3033E-05	.4292E-06	.3379E-07
12049	715.86	.2693E-05	.8316E-06	.1990E-06	.3392E-07	.3625E-08	.1989E-09
3168	716.00	.2250E-03	.8491E-04	.2586E-04	.5914E-05	.9131E-06	.8040E-07
9258	716.15	.8404E-04	.2942E-04	.8189E-05	.1678E-05	.2258E-06	.1666E-07
3166	716.28	.3629E-03	.1434E-03	.4615E-04	.1129E-04	.1897E-05	.1863E-06
4259	716.40	.2354E-02	.1082E-02	.4171E-03	.1273E-03	.2819E-04	.3946E-05
8031	716.49	.6392E-03	.3390E-03	.1553E-03	.5853E-04	.1687E-04	.3313E-05
3164	716.55	.5759E-03	.2380E-03	.8083E-04	.2112E-04	.3852E-05	.4201E-06
12048	716.75	.3183E-05	.9996E-06	.2441E-06	.4263E-07	.4698E-08	.2682E-09
3162	716.81	.8996E-03	.3883E-03	.1389E-03	.3868E-04	.7637E-05	.9227E-06
1260	716.82	.2416E-01	.1456E-01	.7771E-02	.3531E-02	.1285E-02	.3411E-03
30 5	716.89	.5223E-01	.4369E-01	.3458E-01	.2542E-01	.1689E-01	.9711E-02
14029	716.90	.1371E-03	.5721E-04	.1965E-04	.5210E-05	.9673E-06	.1080E-06
9259	716.99	.6845E-04	.2349E-04	.6380E-05	.1269E-05	.1646E-06	.1158E-07
3160	717.06	.1383E-02	.6224E-03	.2342E-03	.6935E-04	.1479E-04	.1973E-05
4260	717.23	.1912E-02	.8605E-03	.3237E-03	.9587E-04	.2044E-04	.2727E-05
3158	717.31	.2092E-02	.9805E-03	.3873E-03	.1218E-03	.2797E-04	.4106E-05

TABLE XVI (Continued)

BAND CODE	WAVE NUMBER	INTENSITY					
		T=300K	T=275K	T=250K	T=225K	T=200K	T=175K
8030	717.33	.6981E-03	.3742E-03	.1736E-03	.6646E-04	.1952E-04	.3932E-05
3156	717.54	.3113E-02	.1518E-02	.6284E-03	.2093E-03	.5166E-04	.8320E-05
12047	717.63	.3747E-05	.1196E-05	.2979E-06	.5330E-07	.6053E-08	.3592E-09
3154	717.77	.4558E-02	.2308E-02	1.0000E-03	.3521E-03	.9318E-04	.1641E-04
9260	717.83	.5553E-04	.1867E-04	.4947E-05	.9550E-06	.1193E-06	.7995E-08
3152	717.99	.6565E-02	.3448E-02	.1561E-02	.5798E-03	.1641E-03	.3149E-04
4261	718.07	.1546E-02	.6815E-03	.2500E-03	.7182E-04	.1474E-04	.1872E-05
8029	718.18	.7589E-03	.4110E-03	.1930E-03	.7501E-04	.2245E-04	.4633E-05
3150	718.20	.9301E-02	.5060E-02	.2390E-02	.9345E-03	.2821E-03	.5882E-04
3148	718.41	.1296E-01	.7293E-02	.3587E-02	.1474E-02	.4734E-03	.1069E-03
30 3	718.47	.3249E-01	.2727E-01	.2166E-01	.1599E-01	.1068E-01	.6188E-02
1262	718.50	.1576E-01	.9105E-02	.4622E-02	.1975E-02	.6657E-03	.1600E-03
12046	718.51	.4393E-05	.1425E-05	.3618E-06	.6628E-07	.7752E-08	.4777E-09
14027	718.58	.1586E-03	.6749E-04	.2373E-04	.6474E-05	.1246E-05	.1456E-06
3146	718.60	.1776E-01	.1032E-01	.5279E-02	.2275E-02	.7754E-03	.1890E-03
9261	718.67	.4487E-04	.1477E-04	.3818E-05	.7148E-06	.8591E-07	.5483E-08
3144	718.79	.2393E-01	.1435E-01	.7616E-02	.3435E-02	.1239E-02	.3251E-03
4262	718.91	.1245E-02	.5374E-03	.1922E-03	.5353E-04	.1057E-04	.1277E-05
3142	718.97	.3170E-01	.1958E-01	.1077E-01	.5074E-02	.1933E-02	.5438E-03
8028	719.02	.8211E-03	.4491E-03	.2135E-03	.8415E-04	.2565E-04	.5418E-05
3140	719.14	.4127E-01	.2622E-01	.1492E-01	.7330E-02	.2941E-02	.8847E-03
3138	719.30	.5280E-01	.3447E-01	.2026E-01	.1035E-01	.4365E-02	.1399E-02
12045	719.39	.5129E-05	.1690E-05	.4373E-06	.8197E-07	.9868E-08	.6312E-09
3136	719.46	.6636E-01	.4445E-01	.2694E-01	.1429E-01	.6316E-02	.2150E-02
9262	719.51	.3612E-04	.1164E-04	.2933E-05	.5323E-06	.6153E-07	.3736E-08
3134	719.60	.8192E-01	.5621E-01	.3507E-01	.1928E-01	.8909E-02	.3211E-02
3132	719.74	.9927E-01	.6970E-01	.4470E-01	.2541E-01	.1224E-01	.4658E-02
4263	719.75	.9989E-03	.4219E-03	.1471E-03	.3968E-04	.7531E-05	.8649E-06
8027	719.86	.8841E-03	.4882E-03	.2347E-03	.9384E-04	.2911E-04	.6289E-05
3130	719.87	.1181E 00	.8469E-01	.5574E-01	.3270E-01	.1639E-01	.6560E-02
3128	719.99	.1377E 00	.1008E 00	.6796E-01	.4107E-01	.2136E-01	.8965E-02
30 1	720.05	.1106E-01	.9299E-02	.7401E-02	.5479E-02	.3672E-02	.2135E-02
3126	720.11	.1575E 00	.1174E 00	.8099E-01	.5031E-01	.2708E-01	.1188E-01
1264	720.18	.1012E-01	.5597E-02	.2697E-02	.1081E-02	.3367E-03	.7307E-04
3124	720.21	.1764E 00	.1338E 00	.9425E-01	.6006E-01	.3338E-01	.1526E-01
12044	720.26	.5963E-05	.1995E-05	.5259E-06	.1008E-06	.1249E-07	.8281E-09
14025	720.26	.1797E-03	.7788E-04	.2799E-04	.7841E-05	.1559E-05	.1902E-06
3122	720.31	.1933E 00	.1493E 00	.1070E 00	.6981E-01	.3995E-01	.1897E-01
9263	720.35	.2895E-04	.9133E-05	.2242E-05	.3943E-06	.4381E-07	.2528E-08
3120	720.40	.2070E 00	.1620E 00	.1183E 00	.7890E-01	.4639E-01	.2280E-01
3118	720.48	.2163E 00	.1715E 00	.1273E 00	.8657E-01	.5216E-01	.2645E-01
3116	720.55	.2200E 00	.1766E 00	.1330E 00	.9202E-01	.5667E-01	.2956E-01
4264	720.60	.7982E-03	.3298E-03	.1120E-03	.2926E-04	.5336E-05	.5820E-06
3114	720.61	.2173E 00	.1762E 00	.1344E 00	.9446E-01	.5931E-01	.3171E-01
3112	720.67	.2073E 00	.1697E 00	.1309E 00	.9323E-01	.5953E-01	.3253E-01

TABLE XVI (Continued)

BAND	CCCE	WAVE NUMBER	INTENSITY					
			T=300K	T=275K	T=250K	T=225K	T=200K	T=175K
8C26		720.70	.9474E-03	.5280E-03	.2567E-03	.1040E-03	.3282E-04	.7245E-05
3110		720.72	.1899E 00	.1567E 00	.1220E 00	.8788E-01	.5693E-01	.3169E-01
31 8		720.76	.1651E 00	.1371E 00	.1076E 00	.7825E-01	.5130E-01	.2900E-01
31 6		720.79	.1336E 00	.1115E 00	.8802E-01	.6451E-01	.4269E-01	.2443E-01
31 4		720.81	.9637E-01	.8075E-01	.6404E-01	.4719E-01	.3144E-01	.1815E-01
31 2		720.82	.5497E-01	.4617E-01	.3672E-01	.2715E-01	.1817E-01	.1055E-01
12043		721.14	.6904E-05	.2345E-05	.6294E-06	.1234E-06	.1570E-07	.1079E-08
5264		721.19	.2312E-04	.7134E-05	.1706E-05	.2905E-06	.3101E-07	.1700E-08
4265		721.44	.6353E-03	.2567E-03	.8488E-04	.2147E-04	.3758E-05	.3890E-06
8025		721.53	.1010E-02	.5680E-03	.2791E-03	.1146E-03	.3674E-04	.8284E-05
1266		721.86	.6392E-02	.3382E-02	.1545E-02	.5800E-03	.1664E-03	.3249E-04
14023		721.92	.1994E-03	.8785E-04	.3221E-04	.9248E-05	.1897E-05	.2407E-06
12042		722.01	.7960E-05	.2744E-05	.7495E-06	.1501E-06	.1963E-07	.1396E-08
9265		722.04	.1839E-04	.5549E-05	.1292E-05	.2130E-06	.2183E-07	.1135E-08
4266		722.28	.5036E-03	.1990E-03	.6403E-04	.1567E-04	.2632E-05	.2583E-06
8024		722.36	.1072E-02	.6078E-03	.3017E-03	.1254E-03	.4086E-04	.9398E-05
32 1		722.39	.1110E-01	.9332E-02	.7427E-02	.5498E-02	.3684E-02	.2142E-02
9266		722.88	.1457E-04	.4298E-05	.9740E-06	.1553E-06	.1527E-07	.7530E-09
12041		722.88	.9139E-05	.3196E-05	.8881E-06	.1817E-06	.2439E-07	.1795E-08
4267		723.13	.3977E-03	.1536E-03	.4807E-04	.1137E-04	.1832E-05	.1704E-06
8C23		723.20	.1131E-02	.6468E-03	.3242E-03	.1364E-03	.4511E-04	.1058E-04
1268		723.55	.3975E-02	.2008E-02	.8680E-03	.3046E-03	.8029E-04	.1407E-04
14021		723.58	.2162E-03	.9673E-04	.3613E-04	.1061E-04	.2238E-05	.2945E-06
9267		723.73	.1149E-04	.3314E-05	.7307E-06	.1127E-06	.1062E-07	.4962E-09
12040		723.75	.1045E-04	.3705E-05	.1047E-05	.2186E-06	.3012E-07	.2291E-08
32 3		723.94	.3277E-01	.2749E-01	.2183E-01	.1612E-01	.1077E-01	.6236E-02
4268		723.97	.3128E-03	.1180E-03	.3592E-04	.8215E-05	.1268E-05	.1116E-06
8022		724.03	.1188E-02	.6845E-03	.3464E-03	.1474E-03	.4946E-04	.1182E-04
9268		724.57	.9033E-05	.2545E-05	.5457E-06	.8130E-07	.7346E-08	.3249E-09
12039		724.61	.1189E-04	.4276E-05	.1228E-05	.2617E-06	.3696E-07	.2904E-08
4269		724.82	.2450E-03	.9029E-04	.2672E-04	.5903E-05	.8725E-06	.7267E-07
8021		724.85	.1241E-02	.7203E-03	.3678E-03	.1583E-03	.5384E-04	.1309E-04
14019		725.23	.2288E-03	.1038E-03	.3944E-04	.1182E-04	.2559E-05	.3479E-06
1270		725.24	.2434E-02	.1172E-02	.4787E-03	.1567E-03	.3786E-04	.5932E-05
9269		725.42	.7072E-05	.1946E-05	.4055E-06	.5837E-07	.5050E-08	.2113E-09
12038		725.47	.1348E-04	.4912E-05	.1434E-05	.3115E-06	.4509E-07	.3655E-08
32 5		725.49	.5292E-01	.4426E-01	.3502E-01	.2574E-01	.1710E-01	.9829E-02
4270		725.66	.1912E-03	.6879E-04	.1978E-04	.4219E-05	.5969E-06	.4699E-07
8020		725.68	.1289E-02	.7537E-03	.3881E-03	.1688E-03	.5817E-04	.1439E-04
9270		726.27	.5514E-05	.1481E-05	.3000E-06	.4169E-07	.3452E-08	.1365E-09
12037		726.33	.1522E-04	.5617E-05	.1665E-05	.3687E-06	.5466E-07	.4569E-08
8C19		726.50	.1331E-02	.7838E-03	.4070E-03	.1788E-03	.6239E-04	.1568E-04
4271		726.51	.1486E-03	.5218E-04	.1457E-04	.3000E-05	.4060E-06	.3018E-07
14017		726.88	.2359E-03	.1084E-03	.4181E-04	.1276E-04	.2828E-05	.3962E-06
1272		726.94	.1466E-02	.6728E-03	.2590E-03	.7893E-04	.1744E-04	.2436E-05

TABLE XVI (Continued)

		INTENSITY					
BAND CODE	WAVE NUMBER	T=300K	T=275K	T=250K	T=225K	T=200K	T=175K
32 7	727.02	.7073E-01	.5889E-01	.4635E-01	.3384E-01	.2229E-01	.1268E-01
9271	727.12	.4283E-05	.1123E-05	.2209E-06	.2962E-07	.2346E-08	.8759E-10
12036	727.19	.1710E-04	.6392E-05	.1924E-05	.4340E-06	.6585E-07	.5671E-08
8018	727.32	.1367E-02	.8103E-03	.4240E-03	.1880E-03	.6640E-04	.1695E-04
4272	727.36	.1150E-03	.3942E-04	.1069E-04	.2122E-05	.2745E-06	.1926E-07
9272	727.97	.3314E-05	.8477E-06	.1619E-06	.2094E-07	.1585E-08	.5584E-10
12035	728.05	.1914E-04	.7241E-05	.2212E-05	.5080E-06	.7884E-07	.6990E-08
8017	728.14	.1396E-02	.8323E-03	.4388E-03	.1963E-03	.7012E-04	.1816E-04
4273	728.21	.8872E-04	.2965E-04	.7803E-05	.1493E-05	.1846E-06	.1221E-07
14015	728.51	.2363E-03	.1098E-03	.4292E-04	.1332E-04	.3013E-05	.4336E-06
32 9	728.55	.8551E-01	.7078E-01	.5532E-01	.4005E-01	.2610E-01	.1465E-01
1274	728.63	.8698E-03	.3795E-03	.1376E-03	.3895E-04	.7851E-05	.9742E-06
9273	728.82	.2554E-05	.6371E-06	.1181E-06	.1472E-07	.1065E-08	.3537E-10
12034	728.91	.2132E-04	.8164E-05	.2530E-05	.5914E-06	.9381E-07	.8555E-08
8016	728.96	.1416E-02	.8495E-03	.4509E-03	.2035E-03	.7345E-04	.1928E-04
4274	729.06	.6815E-04	.2220E-04	.5669E-05	.1046E-05	.1234E-06	.7689E-08
9274	729.67	.1960E-05	.4768E-06	.8573E-07	.1030E-07	.7111E-09	.2225E-10
12033	729.76	.2365E-04	.9161E-05	.2879E-05	.6844E-06	.1109E-06	.1040E-07
8015	729.77	.1428E-02	.8611E-03	.4601E-03	.2093E-03	.7631E-04	.2029E-04
4275	729.91	.5214E-04	.1656E-04	.4100E-05	.7283E-06	.8198E-07	.4810E-08
3211	730.07	.9681E-01	.7955E-01	.6164E-01	.4415E-01	.2840E-01	.1567E-01
14013	730.13	.2290E-03	.1075E-03	.4251E-04	.1339E-04	.3083E-05	.4541E-06
1276	730.34	.5079E-03	.2105E-03	.7172E-04	.1883E-04	.3452E-05	.3794E-06
9275	730.52	.1499E-05	.3554E-06	.6195E-07	.7168E-08	.4721E-09	.1391E-10
8014	730.59	.1430E-02	.8668E-03	.4660E-03	.2136E-03	.7860E-04	.2115E-04
12032	730.61	.2611E-04	.1023E-04	.3259E-05	.7877E-06	.1303E-06	.1254E-07
4276	730.77	.3974E-04	.1230E-04	.2951E-05	.5046E-06	.5416E-07	.2989E-08
9278	731.37	.1142E-05	.2637E-06	.4456E-07	.4963E-08	.3117E-09	.8636E-11
8013	731.40	.1422E-02	.8661E-03	.4683E-03	.2161E-03	.8025E-04	.2184E-04
12031	731.46	.2870E-04	.1137E-04	.3669E-05	.9013E-06	.1521E-06	.1503E-07
3213	731.58	.1044E 00	.8905E-01	.6522E-01	.4614E-01	.2922E-01	.1580E-01
4277	731.62	.3017E-04	.9093E-05	.2114E-05	.3478E-06	.3558E-07	.1845E-08
14011	731.75	.2134E-03	.1010E-03	.4037E-04	.1287E-04	.3011E-05	.4526E-06
1278	732.04	.2919E-03	.1148E-03	.3670E-04	.8913E-05	.1483E-05	.1439E-06
8012	732.21	.1404E-02	.8588E-03	.4668E-03	.2168E-03	.8117E-04	.2232E-04
12030	732.31	.3141E-04	.1257E-04	.4110E-05	.1025E-05	.1765E-06	.1787E-07
4278	732.47	.2281E-04	.6695E-05	.1508E-05	.2385E-06	.2323E-07	.1132E-08
8011	733.01	.1375E-02	.8445E-03	.4613E-03	.2156E-03	.8130E-04	.2298E-04
3215	733.08	.1083E 00	.8734E-01	.6618E-01	.4614E-01	.2869E-01	.1516E-01
12029	733.15	.3422E-04	.1384E-04	.4580E-05	.1160E-05	.2034E-06	.2110E-07
4279	733.33	.1718E-04	.4909E-05	.1070E-05	.1627E-06	.1509E-07	.6897E-09
140 9	733.36	.1894E-03	.9031E-04	.3640E-04	.1173E-04	.4250E-05	.4250E-06
1280	733.75	.1652E-03	.6151E-04	.1843E-04	.4134E-05	.6229E-06	.5318E-07
8010	733.82	.1336E-02	.8233E-03	.4518E-03	.2123E-03	.8061E-04	.2259E-04
12028	733.99	.3711E-04	.1516E-04	.5076E-05	.1304E-05	.2329E-06	.2474E-07

TABLE XVI (Continued)

BAND CODE	WAVE NUMBER	INTENSITY					
		T=300K	T=275K	T=250K	T=225K	T=200K	T=175K
4280	734.18	.1289E-04	.3584E-05	.7561E-06	.1105E-06	.9740E-08	.4175E-09
3217	734.57	.1086E-04	.8665E-01	.6478E-01	.4442E-01	.2706E-01	.1392E-01
80 9	734.62	.1286E-02	.7952E-03	.4381E-03	.2069E-03	.7906E-04	.2233E-04
12027	734.83	.4005E-04	.1652E-04	.5595E-05	.1458E-05	.2650E-06	.2879E-07
140 7	734.96	.1575E-03	.7550E-04	.3064E-04	.9959E-05	.2386E-05	.3697E-06
4281	735.04	.9636E-05	.2605E-05	.5317E-06	.7459E-07	.6251E-08	.2510E-09
80 8	735.42	.1226E-02	.7604E-03	.4205E-03	.1995E-03	.7665E-04	.2181E-04
1282	735.46	.9204E-04	.3241E-04	.9085E-05	.1878E-05	.2556E-06	.1914E-07
12026	735.67	.4303E-04	.1791E-04	.6134E-05	.1620E-05	.2995E-06	.3325E-07
4282	735.90	.7174E-05	.1886E-05	.3722E-06	.5011E-07	.3989E-08	.1500E-09
3219	736.06	.1059E-04	.8340E-01	.6141E-01	.4133E-01	.2460E-01	.1228E-01
80 7	736.22	.1156E-02	.7193E-03	.3990E-03	.1900E-03	.7339E-04	.2101E-04
14164	736.22	.1283E-05	.3046E-06	.5322E-07	.6175E-08	.4081E-09	.1208E-10
14162	736.48	.2006E-05	.4975E-06	.9158E-07	.1132E-07	.8106E-09	.2657E-10
8171	736.48	.1194E-05	.3131E-06	.6156E-07	.8253E-08	.6535E-09	.2440E-10
12025	736.51	.4601E-04	.1932E-04	.6688E-05	.1790E-05	.3362E-06	.3812E-07
140 5	736.55	.1184E-03	.5702E-04	.2326E-04	.7611E-05	.1838E-05	.2878E-06
8170	736.63	.1538E-05	.4132E-06	.8364E-07	.1162E-07	.9620E-09	.3803E-10
14160	736.73	.3086E-05	.7985E-06	.1546E-06	.2033E-07	.1572E-08	.5692E-10
4283	736.76	.5320E-05	.1360E-05	.2593E-06	.3349E-07	.2531E-08	.8900E-10
8169	736.78	.1974E-05	.5429E-06	.1131E-06	.1628E-07	.1408E-08	.5888E-10
8168	736.92	.2522E-05	.7103E-06	.1522E-06	.2268E-07	.2048E-08	.9057E-10
14158	736.98	.4673E-05	.1259E-05	.2560E-06	.3574E-07	.2978E-08	.1187E-09
80 6	737.01	.1078E-02	.6725E-03	.3741E-03	.1788E-03	.6936E-04	.1997E-04
8167	737.06	.3210E-05	.9254E-06	.2039E-06	.3143E-07	.2963E-08	.1384E-09
1284	737.18	.5049E-04	.1679E-04	.4396E-05	.8359E-06	.1025E-06	.6708E-08
8166	737.20	.4070E-05	.1200E-05	.2719E-06	.4334E-07	.4260E-08	.2100E-09
14156	737.21	.6961E-05	.1951E-05	.4158E-06	.6151E-07	.5509E-08	.2409E-09
8165	737.33	.5139E-05	.1550E-05	.3608E-06	.5944E-07	.6090E-08	.3166E-09
12024	737.34	.4895E-04	.2073E-04	.7251E-05	.1965E-05	.3750E-06	.4338E-07
14154	737.44	.1020E-04	.2970E-05	.6626E-06	.1036E-06	.9949E-08	.4758E-09
8164	737.47	.6463E-05	.1993E-05	.4765E-06	.8110E-07	.8655E-08	.4742E-09
3221	737.54	.1006E-04	.7810E-01	.5654E-01	.3728E-01	.2162E-01	.1045E-01
8163	737.60	.8096E-05	.2552E-05	.6263E-06	.1101E-06	.1223E-07	.7054E-09
4284	737.62	.3530E-05	.9759E-06	.1798E-06	.2227E-07	.1597E-08	.5247E-10
14152	737.66	.1471E-04	.4442E-05	.1035E-05	.1709E-06	.1754E-07	.9147E-09
8162	737.73	.1010E-04	.3254E-05	.8193E-06	.1486E-06	.1717E-07	.1042E-08
80 5	737.81	.9939E-03	.6210E-03	.3463E-03	.1660E-03	.6464E-04	.1870E-04
8161	737.85	.1255E-04	.4130E-05	.1067E-05	.1996E-06	.2398E-07	.1530E-08
14150	737.87	.2086E-04	.6525E-05	.1587E-05	.2757E-06	.3020E-07	.1711E-08
8160	737.98	.1553E-04	.5218E-05	.1382E-05	.2667E-06	.3328E-07	.2230E-08
14148	738.08	.2909E-04	.9413E-05	.2384E-05	.4354E-06	.5075E-07	.3114E-08
8159	738.10	.1915E-04	.6566E-05	.1782E-05	.3544E-06	.4592E-07	.3230E-08
140 3	738.14	.7366E-04	.3558E-04	.1457E-04	.4788E-05	.1163E-05	.1834E-06
12023	738.17	.5183E-04	.2213E-04	.7817E-05	.2144E-05	.4154E-06	.4900E-07

TABLE XVI (Continued)

BAND CODE	WAVE NUMBER	INTENSITY					
		T=300K	T=275K	T=250K	T=225K	T=200K	T=175K
8158	738.23	.2351E-04	.8225E-05	.2287E-05	.4684E-06	.6299E-07	.4646E-08
14146	738.27	.3989E-04	.1334E-04	.3512E-05	.6727E-06	.8323E-07	.5514E-08
8157	738.34	.2874E-04	.1026E-04	.2921E-05	.6159E-06	.8589E-07	.6639E-08
8156	738.46	.3500E-04	.1274E-04	.3713E-05	.8056E-06	.1164E-06	.9421E-08
14144	738.46	.5379E-04	.1855E-04	.5071E-05	.1017E-05	.1332E-06	.9497E-08
4285	738.48	.2892E-05	.6976E-06	.1241E-06	.1473E-07	.1002E-08	.3074E-10
8155	738.58	.4244E-04	.1575E-04	.4697E-05	.1048E-05	.1569E-06	.1328E-07
80 4	738.60	.9053E-03	.5666E-03	.3167E-03	.1522E-03	.5943E-04	.1727E-04
14142	738.64	.7131E-04	.2534E-04	.7178E-05	.1503E-05	.2080E-06	.1591E-07
8154	738.69	.5126E-04	.1938E-04	.5913E-05	.1356E-05	.2101E-06	.1859E-07
8153	738.80	.6166E-04	.2374E-04	.7407E-05	.1745E-05	.2798E-06	.2586E-07
14140	738.81	.9290E-04	.3396E-04	.9954E-05	.2174E-05	.3168E-06	.2591E-07
1286	738.90	.2727E-04	.8556E-05	.2088E-05	.3645E-06	.4014E-07	.2290E-08
8152	738.91	.7387E-04	.2896E-04	.9233E-05	.2234E-05	.3702E-06	.3571E-07
14138	738.97	.1189E-03	.4467E-04	.1352E-04	.3073E-05	.4706E-06	.4102E-07
6062	738.97	.1456E-05	.4792E-06	.1238E-06	.2319E-07	.2788E-08	.1781E-09
3223	739.01	.9322E-01	.7128E-01	.5066E-01	.3266E-01	.1842E-01	.8579E-02
12022	739.01	.5462E-04	.2350E-04	.8380E-05	.2325E-05	.4570E-06	.5491E-07
8151	739.02	.8812E-04	.3517E-04	.1145E-04	.2845E-05	.4870E-06	.4899E-07
8150	739.12	.1047E-03	.4252E-04	.1414E-04	.3603E-05	.6369E-06	.6675E-07
14136	739.13	.1496E-03	.5764E-04	.1800E-04	.4246E-05	.6816E-06	.6312E-07
8149	739.23	.1239E-03	.5117E-04	.1737E-04	.4539E-05	.8278E-06	.9033E-07
14134	739.27	.1848E-03	.7295E-04	.2345E-04	.5734E-05	.9622E-06	.9436E-07
8148	739.33	.1459E-03	.6131E-04	.2124E-04	.5687E-05	.1069E-05	.1214E-06
4286	739.34	.2120E-05	.4965E-06	.8530E-07	.9695E-08	.6246E-09	.1789E-10
80 3	739.39	.8179E-03	.5126E-03	.2869E-03	.1382E-03	.5409E-04	.1576E-04
14132	739.41	.2240E-03	.9050E-04	.2991E-04	.7562E-05	.1324E-05	.1370E-06
8147	739.43	.1712E-03	.7312E-04	.2583E-04	.7086E-05	.1373E-05	.1620E-06
8146	739.52	.2001E-03	.8682E-04	.3127E-04	.8781E-05	.1753E-05	.2148E-06
14130	739.54	.2666E-03	.1100E-03	.3732E-04	.9739E-05	.1773E-05	.1931E-06
8145	739.62	.2327E-03	.1024E-03	.3765E-04	.1082E-04	.2223E-05	.2827E-06
14128	739.66	.3111E-03	.1310E-03	.4553E-04	.1224E-04	.2313E-05	.2641E-06
8144	739.71	.2696E-03	.1207E-03	.4512E-04	.1326E-04	.2803E-05	.3696E-06
140 1	739.72	.2508E-04	.1213E-04	.4979E-05	.1640E-05	.3996E-06	.6328E-07
14126	739.78	.3559E-03	.1528E-03	.5429E-04	.1500E-04	.2934E-05	.3503E-06
8143	739.80	.3110E-03	.1413E-03	.5380E-04	.1617E-04	.3512E-05	.4799E-06
12021	739.83	.5726E-04	.2483E-04	.8932E-05	.2505E-05	.4993E-06	.6107E-07
14124	739.88	.3988E-03	.1742E-03	.6320E-04	.1792E-04	.3619E-05	.4502E-06
8142	739.89	.3573E-03	.1648E-03	.6383E-04	.1960E-04	.4374E-05	.6187E-06
14122	739.98	.4372E-03	.1940E-03	.7179E-04	.2084E-04	.4334E-05	.5601E-06
8141	739.98	.4086E-03	.1912E-03	.7534E-04	.2363E-04	.5413E-05	.7920E-06
8140	740.06	.4652E-03	.2207E-03	.8848E-04	.2832E-04	.6658E-05	.1007E-05
14120	740.07	.4684E-03	.2110E-03	.7944E-04	.2356E-04	.5035E-05	.6736E-06
8139	740.14	.5274E-03	.2537E-03	.1034E-03	.3376E-04	.8138E-05	.1271E-05
14118	740.15	.4896E-03	.2235E-03	.8552E-04	.2587E-04	.5664E-05	.7820E-06

TABLE XVI (Continued)

BAND CODE	WAVE NUMBER	INTENSITY					
		T=300K	T=275K	T=250K	T=225K	T=200K	T=175K
80 2	740.18	.7453E-03	.4676E-03	.2620E-03	.1264E-03	.4957E-04	.1448E-04
4287	740.20	.1548E-05	.3519E-06	.5834E-07	.6348E-08	.3873E-09	.1034E-10
8138	740.22	.5953E-03	.2902E-03	.1201E-03	.4002E-04	.9884E-05	.1593E-05
14116	740.22	.4982E-03	.2302E-03	.8935E-04	.2750E-04	.6156E-05	.8743E-06
14114	740.28	.4921E-03	.2298E-03	.9033E-04	.2824E-04	.6446E-05	.9386E-06
8137	740.30	.6690E-03	.3304E-03	.1389E-03	.4716E-04	.1193E-04	.1982E-05
14112	740.34	.4696E-03	.2213E-03	.8798E-04	.2788E-04	.6473E-05	.9633E-06
8136	740.38	.7484E-03	.3743E-03	.1598E-03	.5526E-04	.1431E-04	.2449E-05
14110	740.39	.4302E-03	.2043E-03	.8200E-04	.2629E-04	.6192E-05	.9387E-06
141 8	740.43	.3741E-03	.1788E-03	.7234E-04	.2341E-04	.5580E-05	.8591E-06
8135	740.45	.8334E-03	.4220E-03	.1828E-03	.6438E-04	.1705E-04	.3005E-05
141 6	740.46	.3027E-03	.1455E-03	.5920E-04	.1931E-04	.4645E-05	.7238E-06
3225	740.47	.8447E-01	.6352E-01	.4425E-01	.2783E-01	.1522E-01	.6816E-02
141 4	740.48	.2184E-03	.1054E-03	.4307E-04	.1413E-04	.3422E-05	.5380E-06
141 2	740.49	.1246E-03	.6024E-04	.2470E-04	.8128E-05	.1978E-05	.3127E-06
8134	740.52	.9239E-03	.4734E-03	.2081E-03	.7457E-04	.2018E-04	.3659E-05
8133	740.59	.1019E-02	.5285E-03	.2356E-03	.8587E-04	.2374E-04	.4424E-05
1288	740.62	.1450E-04	.4286E-05	.9735E-06	.1557E-06	.1537E-07	.7618E-09
12020	740.66	.5972E-04	.2608E-04	.9464E-05	.2683E-05	.5417E-06	.6739E-07
8132	740.66	.1120E-02	.5870E-03	.2652E-03	.9830E-04	.2775E-04	.5310E-05
8131	740.73	.1224E-02	.6488E-03	.2970E-03	.1119E-03	.3221E-04	.6325E-05
6060	740.79	.2242E-05	.7698E-06	.2092E-06	.4167E-07	.5411E-08	.3816E-09
8130	740.79	.1332E-02	.7134E-03	.3308E-03	.1265E-03	.3715E-04	.7479E-05
8129	740.85	.1442E-02	.7803E-03	.3663E-03	.1422E-03	.4255E-04	.8777E-05
8128	740.91	.1553E-02	.8490E-03	.4033E-03	.1589E-03	.4841E-04	.1022E-04
8127	740.97	.1665E-02	.9189E-03	.4415E-03	.1764E-03	.5470E-04	.1181E-04
8126	741.03	.1776E-02	.9891E-03	.4805E-03	.1946E-03	.6138E-04	.1355E-04
4288	741.06	.1126E-05	.2484E-06	.3971E-07	.4135E-08	.2387E-09	.5938E-11
8125	741.08	.1884E-02	.1059E-02	.5199E-03	.2133E-03	.6838E-04	.1541E-04
8124	741.13	.1988E-02	.1127E-02	.5591E-03	.2323E-03	.7564E-04	.1739E-04
8123	741.18	.2087E-02	.1192E-02	.5975E-03	.2512E-03	.8305E-04	.1947E-04
8122	741.23	.2178E-02	.1254E-02	.6344E-03	.2699E-03	.9051E-04	.2162E-04
8121	741.27	.2260E-02	.1311E-02	.6693E-03	.2879E-03	.9788E-04	.2380E-04
8120	741.32	.2331E-02	.1362E-02	.7014E-03	.3049E-03	.1050E-03	.2597E-04
8119	741.36	.2389E-02	.1406E-02	.7298E-03	.3204E-03	.1118E-03	.2809E-04
8118	741.40	.2434E-02	.1441E-02	.7540E-03	.3342E-03	.1180E-03	.3010E-04
8117	741.43	.2462E-02	.1467E-02	.7731E-03	.3458E-03	.1235E-03	.3196E-04
8116	741.47	.2472E-02	.1482E-02	.7865E-03	.3548E-03	.1280E-03	.3360E-04
12019	741.48	.6196E-04	.2724E-04	.9967E-05	.2854E-05	.5836E-06	.7377E-07
8115	741.50	.2464E-02	.1485E-02	.7934E-03	.3608E-03	.1315E-03	.3496E-04
8114	741.53	.2436E-02	.1476E-02	.7932E-03	.3634E-03	.1337E-03	.3598E-04
8113	741.56	.2387E-02	.1453E-02	.7856E-03	.3624E-03	.1345E-03	.3661E-04
8112	741.59	.2317E-02	.1417E-02	.7699E-03	.3576E-03	.1338E-03	.3680E-04
8111	741.61	.2225E-02	.1366E-02	.7460E-03	.3485E-03	.1314E-03	.3649E-04
8110	741.64	.2111E-02	.1301E-02	.7136E-03	.3353E-03	.1273E-03	.3566E-04

TABLE XVI (Continued)

			INTENSITY					
BAND	CCCE	WAVE NUMBER	T=300K	T=275K	T=250K	T=225K	T=200K	T=175K
81	9	741.66	.1975E-02	.1221E-02	.6727E-03	.3176E-03	.1213E-03	.3427E-04
81	8	741.68	.1818E-02	.1127E-02	.6233E-03	.2956E-03	.1136E-03	.3231E-04
81	7	741.69	.1639E-02	.1020E-02	.5656E-03	.2693E-03	.1040E-03	.2977E-04
81	6	741.71	.1441E-02	.8982E-03	.4996E-03	.2388E-03	.9261E-04	.2666E-04
81	5	741.72	.1222E-02	.7634E-03	.4257E-03	.2040E-03	.7944E-04	.2298E-04
81	4	741.73	.9823E-03	.6148E-03	.3435E-03	.1651E-03	.6447E-04	.1873E-04
81	3	741.74	.7182E-03	.4501E-03	.2519E-03	.1213E-03	.4749E-04	.1384E-04
81	2	741.74	.4150E-03	.2604E-03	.1459E-03	.7036E-04	.2760E-04	.8062E-05
3227		741.92	.7492E-01	.5533E-01	.3771E-01	.2310E-01	.1222E-01	.5243E-02
142	1	742.06	.2517E-04	.1218E-04	.4996E-05	.1646E-05	.4009E-06	.6349E-07
12018		742.31	.6394E-04	.2830E-04	.1043E-04	.3016E-05	.6241E-06	.8012E-07
1290		742.35	.7591E-05	.2111E-05	.4456E-06	.6515E-07	.5750E-08	.2468E-09
6058		742.60	.3398E-05	.1215E-05	.3467E-06	.1025E-07	.7960E-09	.7960E-09
12017		743.13	.6563E-04	.2922E-04	.1085E-04	.3166E-05	.6626E-06	.8631E-07
3229		743.37	.6510E-01	.4715E-01	.3139E-01	.1868E-01	.9537E-02	.3909E-02
142	3	743.62	.7427E-04	.3587E-04	.1469E-04	.4825E-05	.1172E-05	.1848E-06
12016		743.94	.6699E-04	.3000E-04	.1122E-04	.3301E-05	.6983E-06	.9220E-07
1292		744.08	.3914E-05	.1022E-05	.2002E-06	.2671E-07	.2103E-08	.7790E-10
82	2	744.09	.8330E-04	.5225E-04	.2928E-04	.1412E-04	.5538E-05	.1618E-05
6056		744.40	.5067E-05	.1884E-05	.5636E-06	.1262E-06	.1898E-07	.1616E-08
12015		744.76	.6799E-04	.3062E-04	.1153E-04	.3418E-05	.7303E-06	.9768E-07
3231		744.80	.5546E-01	.3933E-01	.2554E-01	.1474E-01	.7244E-02	.2826E-02
82	3	744.87	.1855E-03	.1163E-03	.6507E-04	.3132E-04	.1226E-04	.3574E-05
142	5	745.17	.1199E-03	.5774E-04	.2355E-04	.7703E-05	.1860E-05	.2912E-06
12014		745.57	.6859E-04	.3105E-04	.1176E-04	.3514E-05	.7578E-06	.1026E-06
82	4	745.64	.2928E-03	.1832E-03	.1024E-03	.4918E-04	.1920E-04	.5578E-05
1294		745.82	.1987E-05	.4868E-06	.8832E-07	.1073E-07	.7513E-09	.2395E-10
6054		746.19	.7432E-05	.2870E-05	.8986E-06	.2127E-06	.3429E-07	.3193E-08
3233		746.23	.4634E-01	.3214E-01	.2032E-01	.1136E-01	.5357E-02	.1984E-02
12013		746.38	.6879E-04	.3128E-04	.1192E-04	.3586E-05	.7802E-06	.1068E-06
82	5	746.41	.3995E-03	.2495E-03	.1391E-03	.6668E-04	.2596E-04	.7510E-05
142	7	746.71	.1602E-03	.7680E-04	.3116E-04	.1012E-04	.2425E-05	.3757E-06
82	6	747.18	.5027E-03	.3134E-03	.1743E-03	.8328E-04	.3230E-04	.9299E-05
12012		747.19	.6856E-04	.3132E-04	.1200E-04	.3633E-05	.7968E-06	.1102E-06
3235		747.65	.3801E-01	.2575E-01	.1582E-01	.8543E-02	.3859E-02	.1352E-02
82	7	747.95	.6005E-03	.3734E-03	.2071E-03	.9861E-04	.3807E-04	.1090E-04
6052		747.98	.1072E-04	.4295E-05	.1405E-05	.3509E-06	.6049E-07	.6140E-08
12011		748.00	.6790E-04	.3114E-04	.1199E-04	.3652E-05	.8071E-06	.1128E-06
142	9	748.24	.1937E-03	.9229E-04	.3718E-04	.1198E-04	.2838E-05	.4337E-06
82	8	748.71	.6914E-03	.4288E-03	.2370E-03	.1124E-03	.4318E-04	.1228E-04
12010		748.81	.6680E-04	.3076E-04	.1189E-04	.3643E-05	.8106E-06	.1143E-06
3237		749.06	.3061E-01	.2022E-01	.1206E-01	.6277E-02	.2709E-02	.8947E-03
82	9	749.48	.7743E-03	.4787E-03	.2636E-03	.1244E-03	.4754E-04	.1342E-04
1209		749.61	.6529E-04	.3016E-04	.1171E-04	.3605E-05	.8073E-06	.1147E-06
6050		749.75	.1522E-04	.6313E-05	.2154E-05	.5665E-06	.1042E-06	.1149E-07

TABLE XVI (Continued)

			INTENSITY					
BAND	CCDE	WAVE NUMBER	T=300K	T=275K	T=250K	T=225K	T=200K	T=175K
14211		749.76	.2192E-03	.1037E-03	.4142E-04	.1320E-04	.3087E-05	.4639E-06
8210		750.24	.8484E-03	.5227E-03	.2867E-03	.1346E-03	.5111E-04	.1432E-04
120 8		750.41	.6340E-04	.2938E-04	.1145E-04	.3540E-05	.7972E-06	.1141E-06
3239		750.47	.2421E-01	.1558E-01	.9003E-02	.4508E-02	.1854E-02	.5755E-03
8211		751.00	.9130E-03	.5604E-03	.3059E-03	.1429E-03	.5387E-04	.1496E-04
120 7		751.21	.6116E-04	.2842E-04	.1111E-04	.3450E-05	.7807E-06	.1125E-06
14213		751.27	.2363E-03	.1108E-03	.4382E-04	.1379E-04	.3175E-05	.4675E-06
6048		751.52	.2123E-04	.9112E-05	.3238E-05	.8949E-06	.1751E-06	.2091E-07
6212		751.76	.9678E-03	.5916E-03	.3214E-03	.1492E-03	.5583E-04	.1535E-04
3241		751.86	.1881E-01	.1178E-01	.6583E-02	.3165E-02	.1237E-02	.3598E-03
120 6		752.01	.5868E-04	.2733E-04	.1071E-04	.3339E-05	.7589E-06	.1099E-06
8213		752.51	.1012E-02	.6161E-03	.3329E-03	.1536E-03	.5699E-04	.1551E-04
14215		752.78	.2450E-03	.1138E-03	.4444E-04	.1379E-04	.3116E-05	.4482E-06
120 5		752.80	.5608E-04	.2617E-04	.1029E-04	.3215E-05	.7335E-06	.1068E-06
3243		753.25	.1436E-01	.8735E-02	.4716E-02	.2173E-02	.8051E-03	.2187E-03
8214		753.26	.1047E-02	.6341E-03	.3407E-03	.1560E-03	.5740E-04	.1544E-04
6046		753.28	.2914E-04	.1292E-04	.4772E-05	.1383E-05	.2872E-06	.3703E-07
12157		753.34	.1206E-05	.3214E-06	.6444E-07	.8850E-08	.7224E-09	.2805E-10
12156		753.46	.1469E-05	.3991E-06	.8193E-07	.1158E-07	.9795E-09	.3982E-10
12155		753.58	.1782E-05	.4935E-06	.1037E-06	.1507E-07	.1320E-08	.5614E-10
120 4		753.60	.5364E-04	.2508E-04	.9875E-05	.3094E-05	.7081E-06	.1035E-06
12154		753.69	.2153E-05	.6075E-06	.1305E-06	.1950E-07	.1769E-08	.7864E-10
12153		753.80	.2590E-05	.7445E-06	.1635E-06	.2511E-07	.2356E-08	.1094E-09
12152		753.91	.3103E-05	.9083E-06	.2039E-06	.3215E-07	.3119E-08	.1511E-09
8215		754.01	.1072E-02	.6457E-03	.3448E-03	.1567E-03	.5712E-04	.1518E-04
12151		754.02	.3703E-05	.1103E-05	.2530E-06	.4095E-07	.4104E-08	.2074E-09
12150		754.12	.4400E-05	.1334E-05	.3124E-06	.5187E-07	.5367E-08	.2827E-09
12149		754.23	.5206E-05	.1606E-05	.3839E-06	.6536E-07	.6978E-08	.3827E-09
14217		754.28	.2458E-03	.1128E-03	.4348E-04	.1327E-04	.2937E-05	.4114E-06
12148		754.33	.6135E-05	.1924E-05	.4694E-06	.8190E-07	.9017E-08	.5144E-09
120 3		754.39	.5192E-04	.2430E-04	.9587E-05	.3010E-05	.6905E-06	.1012E-06
12147		754.43	.7199E-05	.2295E-05	.5710E-06	.1021E-06	.1158E-07	.6868E-09
12146		754.52	.8412E-05	.2725E-05	.6913E-06	.1265E-06	.1478E-07	.9106E-09
12145		754.62	.9787E-05	.3221E-05	.8327E-06	.1559E-06	.1876E-07	.1199E-08
3245		754.63	.1078E-01	.6360E-02	.3310E-02	.1459E-02	.5112E-03	.1292E-03
12144		754.71	.1134E-04	.3790E-05	.9980E-06	.1912E-06	.2365E-07	.1568E-08
8216		754.76	.1087E-02	.6511E-03	.3454E-03	.1557E-03	.5619E-04	.1474E-04
12143		754.80	.1308E-04	.4439E-05	.1190E-05	.2331E-06	.2965E-07	.2036E-08
12142		754.89	.1503E-04	.5175E-05	.1412E-05	.2826E-06	.3693E-07	.2625E-08
12141		754.98	.1719E-04	.6004E-05	.1667E-05	.3407E-06	.4571E-07	.3362E-08
6044		755.03	.3930E-04	.1797E-04	.6892E-05	.2091E-05	.4596E-06	.6377E-07
12140		755.06	.1957E-04	.6934E-05	.1958E-05	.4084E-06	.5622E-07	.4275E-08
12139		755.14	.2219E-04	.7969E-05	.2287E-05	.4869E-06	.6873E-07	.5397E-08
12138		755.22	.2505E-04	.9116E-05	.2659E-05	.5771E-06	.8349E-07	.6765E-08
12137		755.30	.2814E-04	.1038E-04	.3074E-05	.6802E-06	.1008E-06	.8420E-08

TABLE XVI (Continued)

BAND	CODE	WAVE NUMBER	INTENSITY				
			T=300K	T=275K	T=250K	T=225K	T=200K
12136		755.38	.3149E-04	.1176E-04	.3536E-05	.7971E-06	.1209E-06
12135		755.45	.3506E-04	.1326E-04	.4046E-05	.9287E-06	.1440E-06
8217		755.51	.1092E-02	.6507E-03	.3427E-03	.1532E-03	.5470E-04
12134		755.52	.3887E-04	.1487E-04	.4605E-05	.1076E-05	.1705E-06
12133		755.59	.4289E-04	.1660E-04	.5213E-05	.1239E-05	.2006E-06
12132		755.66	.4710E-04	.1844E-04	.5870E-05	.1418E-05	.2344E-06
12131		755.73	.5148E-04	.2038E-04	.6572E-05	.1613E-05	.2722E-06
14219		755.77	.2395E-03	.1086E-03	.4120E-04	.1234E-04	.2669E-05
12130		755.79	.5600E-04	.2240E-04	.7318E-05	.1825E-05	.3138E-06
12129		755.85	.6062E-04	.2450E-04	.8102E-05	.2051E-05	.3595E-06
12128		755.91	.6530E-04	.2665E-04	.8920E-05	.2291E-05	.4089E-06
12127		755.97	.6998E-04	.2884E-04	.9763E-05	.2543E-05	.4620E-06
3247		756.00	.7957E-02	.4546E-02	.2278E-02	.9580E-03	.3168E-03
12126		756.03	.7461E-04	.3103E-04	.1062E-04	.2805E-05	.5182E-06
12125		756.08	.7913E-04	.3321E-04	.1149E-04	.3073E-05	.5772E-06
12124		756.13	.8347E-04	.3533E-04	.1235E-04	.3345E-05	.6382E-06
12123		756.18	.8756E-04	.3737E-04	.1319E-04	.3616E-05	.7004E-06
12122		756.23	.9134E-04	.3929E-04	.1400E-04	.3883E-05	.7629E-06
8218		756.26	.1089E-02	.6448E-03	.3371E-03	.1494E-03	.5272E-04
12121		756.27	.9471E-04	.4105E-04	.1476E-04	.4139E-05	.8246E-06
12120		756.32	.9762E-04	.4261E-04	.1546E-04	.4380E-05	.8841E-06
12119		756.36	.9997E-04	.4394E-04	.1607E-04	.4599E-05	.9402E-06
12118		756.40	.1017E-03	.4499E-04	.1658E-04	.4792E-05	.9913E-06
12117		756.43	.1027E-03	.4573E-04	.1698E-04	.4951E-05	.1036E-05
12116		756.47	.1030E-03	.4612E-04	.1725E-04	.5072E-05	.1072E-05
12115		756.50	.1025E-03	.4613E-04	.1736E-04	.5148E-05	.1099E-05
12114		756.53	.1011E-03	.4573E-04	.1732E-04	.5173E-05	.1115E-05
12113		756.56	.9875E-04	.4490E-04	.1710E-04	.5144E-05	.1119E-05
12112		756.59	.9548E-04	.4360E-04	.1670E-04	.5056E-05	.1109E-05
12111		756.61	.9124E-04	.4184E-04	.1610E-04	.4904E-05	.1084E-05
12110		756.64	.8600E-04	.3959E-04	.1530E-04	.4687E-05	.1043E-05
121 9		756.66	.7976E-04	.3684E-04	.1430E-04	.4402E-05	.9855E-06
121 8		756.68	.7251E-04	.3359E-04	.1309E-04	.4047E-05	.9112E-06
121 7		756.69	.6422E-04	.2984E-04	.1166E-04	.3621E-05	.8193E-06
121 6		756.71	.5486E-04	.2555E-04	.1001E-04	.3120E-05	.7092E-06
121 5		756.72	.4432E-04	.2068E-04	.8127E-05	.2540E-05	.5794E-06
121 4		756.73	.3233E-04	.1511E-04	.5951E-05	.1864E-05	.4267E-06
121 3		756.74	.1823E-04	.8535E-05	.3366E-05	.1057E-05	.2425E-06
6042		756.78	.5211E-04	.2455E-04	.9756E-05	.3091E-05	.7175E-06
8219		757.00	.1078E-02	.6339E-03	.3289E-03	.1443E-03	.5034E-04
14221		757.25	.2273E-03	.1016E-03	.3792E-04	.1112E-04	.2345E-05
3249		757.36	.5774E-02	.3191E-02	.1537E-02	.6156E-03	.1915E-03
8220		757.74	.1059E-02	.6186E-03	.3183E-03	.1383E-03	.4763E-04
8221		758.48	.1033E-02	.5994E-03	.3058E-03	.1315E-03	.4469E-04
6040		758.51	.6790E-04	.3290E-04	.1353E-04	.4469E-05	.1093E-05
							.1739E-06

TABLE XVI (Continued)

BAND CODE	WAVE NUMBER	INTENSITY					
		T=300K	T=275K	T=250K	T=225K	T=200K	T=175K
3251	758.72	.4120E-02	.2200E-02	.1016E-02	.3870E-03	.1130E-03	.2261E-04
14223	758.72	.2106E-03	.9270E-04	.3396E-04	.9739E-05	.1996E-05	.2531E-06
8222	759.21	.1002E-02	.5769E-03	.2916E-03	.1240E-03	.4157E-04	.9926E-05
122 3	759.87	.2617E-05	.1225E-05	.4830E-06	.1516E-06	.3478E-07	.5100E-08
8223	759.95	.9657E-03	.5515E-03	.2762E-03	.1161E-03	.3836E-04	.8991E-05
3253	760.06	.2892E-02	.1490E-02	.6591E-03	.2381E-03	.6513E-04	.1197E-04
14225	760.19	.1908E-03	.8257E-04	.2964E-04	.8294E-05	.1648E-05	.2009E-06
6038	760.24	.8692E-04	.4327E-04	.1838E-04	.6316E-05	.1622E-05	.2751E-06
122 4	760.64	.6193E-05	.2895E-05	.1140E-05	.3570E-06	.8170E-07	.1194E-07
8224	760.68	.9251E-03	.5240E-03	.2598E-03	.1079E-03	.3512E-04	.8074E-05
3255	761.40	.1996E-02	.9909E-03	.4193E-03	.1434E-03	.3664E-04	.6168E-05
8225	761.41	.8810E-03	.4948E-03	.2428E-03	.9959E-04	.3191E-04	.7189E-05
122 5	761.42	.1014E-04	.4732E-05	.1859E-05	.5809E-06	.1325E-06	.1929E-07
14227	761.64	.1691E-03	.7187E-04	.2525E-04	.6879E-05	.1322E-05	.1544E-06
6036	761.96	.1093E-03	.5582E-04	.2444E-04	.8722E-05	.2348E-05	.4230E-06
8226	762.14	.8343E-03	.4644E-03	.2255E-03	.9128E-04	.2878E-04	.6349E-05
122 6	762.19	.1418E-04	.6602E-05	.2588E-05	.8061E-06	.1832E-06	.2653E-07
3257	762.73	.1356E-02	.6475E-03	.2616E-03	.8455E-04	.2012E-04	.3093E-05
8227	762.87	.7858E-03	.4334E-03	.2081E-03	.8311E-04	.2576E-04	.5561E-05
122 7	762.96	.1815E-04	.8429E-05	.3294E-05	.1023E-05	.2314E-06	.3332E-07
14229	763.09	.1469E-03	.6121E-04	.2100E-04	.5561E-05	.1031E-05	.1150E-06
8228	763.59	.7362E-03	.4021E-03	.1909E-03	.7517E-04	.2289E-04	.4832E-05
6034	763.67	.1349E-03	.7059E-04	.3183E-04	.1177E-04	.3313E-05	.6319E-06
122 8	763.72	.2194E-04	.1016E-04	.3958E-05	.1224E-05	.2755E-06	.3942E-07
3259	764.05	.9061E-03	.4157E-03	.1601E-03	.4880E-04	.1079E-04	.1510E-05
8229	764.31	.6861E-03	.3711E-03	.1741E-03	.6755E-04	.2020E-04	.4165E-05
122 9	764.49	.2547E-04	.1176E-04	.4565E-05	.1405E-05	.3145E-06	.4468E-07
14231	764.53	.1250E-03	.5103E-04	.1708E-04	.4385E-05	.7826E-06	.8310E-07
8230	765.03	.6361E-03	.3405E-03	.1578E-03	.6032E-04	.1770E-04	.3563E-05
12210	765.25	.2871E-04	.1321E-04	.5105E-05	.1563E-05	.3478E-06	.4901E-07
3261	765.36	.5958E-03	.2622E-03	.9609E-04	.2757E-04	.5653E-05	.7174E-06
6032	765.37	.1634E-03	.8750E-04	.4055E-04	.1550E-04	.4552E-05	.9163E-06
8231	765.75	.5869E-03	.3108E-03	.1422E-03	.5352E-04	.1540E-04	.3024E-05
14233	765.96	.1044E-03	.4168E-04	.1358E-04	.3375E-05	.5782E-06	.5826E-07
12211	766.01	.3159E-04	.1448E-04	.5572E-05	.1697E-05	.3749E-06	.5236E-07
8232	766.47	.5388E-03	.2822E-03	.1274E-03	.4720E-04	.1331E-04	.2547E-05
3263	766.67	.3854E-03	.1626E-03	.5659E-04	.1525E-04	.2892E-05	.3318E-06
12212	766.77	.3410E-04	.1557E-04	.5961E-05	.1804E-05	.3956E-06	.5472E-07
6030	767.06	.1942E-03	.1063E-03	.5053E-04	.1994E-04	.6089E-05	.1290E-05
8233	767.18	.4922E-03	.2549E-03	.1136E-03	.4137E-04	.1143E-04	.2129E-05
14235	767.39	.8559E-04	.3336E-04	.1056E-04	.2536E-05	.4161E-06	.3966E-07
12213	767.52	.3623E-04	.1647E-04	.6270E-05	.1886E-05	.4100E-06	.5612E-07
8234	767.89	.4475E-03	.2291E-03	.1006E-03	.3604E-04	.9749E-05	.1767E-05
3265	767.96	.2454E-03	.9904E-04	.3270E-04	.8261E-05	.1445E-05	.1494E-06
12214	768.28	.3795E-04	.1716E-04	.6498E-05	.1941E-05	.4183E-06	.5661E-07

TABLE XVI (Continued)

BAND CODE	WAVE NUMBER	INTENSITY					
		T=300K	T=275K	T=250K	T=225K	T=200K	T=175K
8235	768.60	.4049E-03	.2048E-03	.8869E-04	.3121E-04	.8259E-05	.1455E-05
6028	768.75	.2263E-03	.1263E-03	.6154E-04	.2501E-04	.7925E-05	.1760E-05
14237	768.80	.6888E-04	.2618E-04	.8046E-05	.1862E-05	.2918E-06	.2622E-07
12215	769.03	.3927E-04	.1767E-04	.6649E-05	.1971E-05	.4208E-06	.5626E-07
3267	769.25	.1538E-03	.5930E-04	.1854E-04	.4382E-05	.7050E-06	.6552E-07
8236	769.31	.3647E-03	.1822E-03	.7774E-04	.2687E-04	.6951E-05	.1190E-05
12216	769.78	.4019E-04	.1799E-04	.6724E-05	.1977E-05	.4179E-06	.5516E-07
8237	770.02	.3269E-03	.1613E-03	.6778E-04	.2299E-04	.5813E-05	.9656E-06
14239	770.21	.5444E-04	.2015E-04	.6001E-05	.1336E-05	.1995E-06	.1684E-07
6026	770.43	.2583E-03	.1469E-03	.7320E-04	.3058E-04	.1003E-04	.2329E-05
3269	770.53	.9483E-04	.3490E-04	.1031E-04	.2276E-05	.3361E-06	.2797E-07
12217	770.53	.4074E-04	.1813E-04	.6728E-05	.1961E-05	.4102E-06	.5340E-07
8238	770.72	.2918E-03	.1421E-03	.5878E-04	.1956E-04	.4829E-05	.7780E-06
12218	771.27	.4092E-04	.1809E-04	.6666E-05	.1926E-05	.3982E-06	.5110E-07
8239	771.42	.2592E-03	.1246E-03	.5071E-04	.1655E-04	.3987E-05	.6224E-06
14241	771.61	.4227E-04	.1522E-04	.4383E-05	.9370E-06	.1330E-06	.1052E-07
3271	771.80	.5756E-04	.2018E-04	.5630E-05	.1158E-05	.1565E-06	.1163E-07
12219	772.02	.4075E-04	.1790E-04	.6545E-05	.1873E-05	.3827E-06	.4836E-07
6024	772.09	.2886E-03	.1670E-03	.8497E-04	.3642E-04	.1233E-04	.2983E-05
8240	772.12	.2292E-03	.1087E-03	.4352E-04	.1392E-04	.3270E-05	.4943E-06
12220	772.76	.4027E-04	.1757E-04	.6371E-05	.1805E-05	.3642E-06	.4528E-07
8241	772.82	.2018E-03	.9435E-04	.3715E-04	.1164E-04	.2665E-05	.3898E-06
14243	773.00	.3225E-04	.1128E-04	.3137E-05	.6426E-06	.8646E-07	.6384E-08
3273	773.07	.3438E-04	.1148E-04	.3016E-05	.5767E-06	.7121E-07	.4707E-08
12221	773.50	.3951E-04	.1711E-04	.6152E-05	.1724E-05	.3434E-06	.4198E-07
8242	773.52	.1769E-03	.8152E-04	.3155E-04	.9682E-05	.2159E-05	.3052E-06
6022	773.76	.3152E-03	.1853E-03	.9613E-04	.4218E-04	.1471E-04	.3695E-05
8243	774.21	.1544E-03	.7011E-04	.2666E-04	.8006E-05	.1738E-05	.2373E-06
12222	774.24	.3849E-04	.1655E-04	.5894E-05	.1634E-05	.3209E-06	.3854E-07
3275	774.32	.2022E-04	.6413E-05	.1586E-05	.2814E-06	.3165E-07	.1856E-08
14245	774.38	.2419E-04	.8207E-05	.2200E-05	.4309E-06	.5483E-07	.3768E-08
8244	774.90	.1342E-03	.6001E-04	.2241E-04	.6583E-05	.1390E-05	.1832E-06
12223	774.97	.3725E-04	.1589E-04	.5606E-05	.1536E-05	.2974E-06	.3506E-07
6020	775.41	.3360E-03	.2005E-03	.1058E-03	.4745E-04	.1700E-04	.4421E-05
3277	775.57	.1170E-04	.3523E-05	.8183E-06	.1345E-06	.1374E-07	.7124E-09
8245	775.59	.1161E-03	.5113E-04	.1875E-04	.5383E-05	.1105E-05	.1405E-06
12224	775.70	.3582E-04	.1515E-04	.5294E-05	.1433E-05	.2733E-06	.3160E-07
14247	775.76	.1784E-04	.5861E-05	.1512E-05	.2827E-06	.3393E-07	.2163E-08
8246	776.28	1.0000E-04	.4336E-04	.1560E-04	.4377E-05	.8731E-06	.1069E-06
12225	776.44	.3423E-04	.1436E-04	.4965E-05	.1327E-05	.2492E-06	.2824E-07
3279	776.81	.6670E-05	.1903E-05	.4144E-06	.6295E-07	.5831E-08	.2664E-09
8247	776.96	.8580E-04	.3660E-04	.1292E-04	.3540E-05	.6855E-06	.8084E-07
6018	777.05	.3489E-03	.2110E-03	.1132E-03	.5174E-04	.1899E-04	.5098E-05
14249	777.12	.1293E-04	.4110E-05	.1019E-05	.1814E-06	.2049E-07	.1208E-08
12226	777.16	.3252E-04	.1352E-04	.4625E-05	.1220E-05	.2254E-06	.2501E-07

TABLE XVI (Continued)

PASC CCCE	WAVE NUMBLR	INTENSITY					
		T=300K	T=275K	T=250K	T=225K	T=200K	T=175K
8248	777.64	.7329E-04	.3075E-04	.1064E-04	.2847E-05	.5350E-06	.6070E-07
12227	777.89	.3072E-04	.1265E-04	.4281E-05	.1114E-05	.2024E-06	.2197E-07
3281	778.04	.3742E-05	.1010E-05	.2060E-06	.2887E-07	.2417E-08	.9700E-10
8249	778.33	.6234E-04	.2572E-04	.8723E-05	.2277E-05	.4150E-06	.4526E-07
14251	778.48	.9218E-05	.2831E-05	.6733E-06	.1139E-06	.1208E-07	.6563E-09
12228	778.62	.2886E-04	.1177E-04	.3937E-05	.1011E-05	.1803E-06	.1914E-07
6016	778.69	.3520E-03	.2154E-03	.1172E-03	.5453E-04	.2046E-04	.5648E-05
8250	779.00	.5280E-04	.2142E-04	.7115E-05	.1811E-05	.3199E-06	.3351E-07
3283	779.26	.2066E-05	.5274E-06	.1005E-06	.1296E-07	.9790E-09	.3440E-10
12229	779.34	.2696E-04	.1089E-04	.3599E-05	.9105E-06	.1595E-06	.1654E-07
8251	779.68	.4453E-04	.1775E-04	.5775E-05	.1433E-05	.2451E-06	.2464E-07
14253	779.83	.6464E-05	.1915E-05	.4362E-06	.7002E-07	.6949E-08	.3469E-09
12230	780.06	.2506E-04	.1002E-04	.3270E-05	.8148E-06	.1401E-06	.1418E-07
6014	780.32	.3436E-03	.2125E-03	.1171E-03	.5533E-04	.2117E-04	.5991E-05
8252	780.36	.3740E-04	.1465E-04	.4665E-05	.1128E-05	.1867E-06	.1800E-07
3285	780.47	.1124E-05	.2707E-06	.4811E-07	.5704E-08	.3875E-09	.1188E-10
12231	780.78	.2316E-04	.9163E-05	.2953E-05	.7245E-06	.1222E-06	.1206E-07
8253	781.03	.3129E-04	.1203E-04	.3749E-05	.8826E-06	.1413E-06	.1306E-07
14255	781.17	.4458E-05	.1272E-05	.2771E-06	.4212E-07	.3903E-08	.1785E-09
12232	781.50	.2131E-04	.8336E-05	.2652E-05	.6402E-06	.1058E-06	.1018E-07
8254	781.70	.2606E-04	.9838E-05	.2999E-05	.6870E-06	.1064E-06	.9406E-08
6012	781.94	.3225E-03	.2013E-03	.1121E-03	.5372E-04	.2090E-04	.6046E-05
12233	782.21	.1950E-04	.7544E-05	.2367E-05	.5621E-06	.9099E-07	.8523E-08
8255	782.37	.2162E-04	.8009E-05	.2386E-05	.5319E-06	.7956E-07	.6731E-08
14257	782.50	.3025E-05	.8304E-06	.1727E-06	.2480E-07	.2140E-08	.8934E-10
12234	782.93	.1776E-04	.6791E-05	.2101E-05	.4905E-06	.7773E-07	.7083E-08
8256	783.04	.1786E-04	.6491E-05	.1890E-05	.4096E-06	.5915E-07	.4784E-08
6010	783.55	.2884E-03	.1814E-03	.1020E-03	.4943E-04	.1951E-04	.5749E-05
12235	783.64	.1610E-04	.6081E-05	.1855E-05	.4255E-06	.6595E-07	.5843E-08
8257	783.70	.1465E-04	.5237E-05	.1490E-05	.3138E-06	.4372E-07	.3377E-08
14259	783.83	.2019E-05	.5325E-06	.1055E-06	.1429E-07	.1146E-08	.4353E-10
12236	784.34	.1452E-04	.5418E-05	.1628E-05	.3668E-06	.5559E-07	.4784E-08
8258	784.36	.1204E-04	.4207E-05	.1169E-05	.2390E-06	.3212E-07	.2367E-08
8259	785.02	.9824E-05	.3364E-05	.9121E-06	.1812E-06	.2346E-07	.1649E-08
12237	785.05	.1304E-04	.4803E-05	.1422E-05	.3144E-06	.4655E-07	.3887E-08
14261	785.14	.1326E-05	.3355E-06	.6327E-07	.8062E-08	.5994E-09	.2064E-10
60 8	785.15	.2414E-03	.1529E-03	.8664E-04	.4238E-04	.1693E-04	.5065E-05
8260	785.68	.7985E-05	.2679E-05	.7086E-06	.1366E-06	.1703E-07	.1140E-08
12238	785.76	.1165E-04	.4236E-05	.1235E-05	.2678E-06	.3872E-07	.3136E-08
8261	786.34	.6463E-05	.2123E-05	.5478E-06	.1024E-06	.1229E-07	.7835E-09
12239	786.46	.1036E-04	.3718E-05	.1066E-05	.2268E-06	.3200E-07	.2512E-08
60 6	786.74	.1829E-03	.1164E-03	.6636E-04	.3270E-04	.1319E-04	.3993E-05
8262	786.99	.5210E-05	.1676E-05	.4215E-06	.7637E-07	.8816E-08	.5347E-09
12240	787.16	.9174E-05	.3247E-05	.9161E-06	.1910E-06	.2628E-07	.1997E-08
8263	787.64	.4183E-05	.1317E-05	.3227E-06	.5666E-07	.6287E-08	.3624E-09

TABLE XVI (Continued)

BAND CODE	WAVE NUMBER	INTENSITY					
		T=300K	T=275K	T=250K	T=225K	T=200K	T=175K
12241	787.86	.8087E-05	.2822E-05	.7829E-06	.1599E-06	.2144E-07	.1576E-08
8264	788.29	.3345E-05	.1030E-05	.2460E-06	.4181E-07	.4457E-08	.2440E-09
60 4	788.33	.1146E-03	.7320E-04	.4193E-04	.2078E-04	.8436E-05	.2577E-05
12242	788.55	.7096E-05	.2441E-05	.6656E-06	.1331E-06	.1738E-07	.1235E-08
8265	788.94	.2664E-05	.8025E-06	.1865E-06	.3069E-07	.3142E-08	.1632E-09
12243	789.25	.6199E-05	.2101E-05	.5629E-06	.1102E-06	.1400E-07	.9612E-09
6146	789.25	.1377E-05	.6100E-06	.2252E-06	.6521E-07	.1353E-07	.1744E-08
6144	789.44	.1941E-05	.8868E-06	.3398E-06	.1030E-06	.2262E-07	.3138E-08
8266	789.59	.2114E-05	.6224E-06	.1480E-06	.2241E-07	.2201E-08	.1084E-09
6142	789.62	.2695E-05	.1268E-05	.5036E-06	.1594E-06	.3699E-07	.5502E-08
6140	789.79	.3685E-05	.1784E-05	.7330E-06	.2420E-06	.5912E-07	.9404E-08
60 2	789.91	.3931E-04	.2516E-04	.1446E-04	.7188E-05	.2931E-05	.9005E-06
12244	789.94	.5391E-05	.1800E-05	.4736E-06	.9066E-07	.1121E-07	.7427E-09
6138	789.95	.4964E-05	.2469E-05	.1048E-05	.3599E-06	.9240E-07	.1566E-07
6136	790.11	.6588E-05	.3362E-05	.1471E-05	.5247E-06	.1412E-06	.2543E-07
8267	790.23	.1670E-05	.4806E-06	.1058E-06	.1628E-07	.1533E-08	.7155E-10
6134	790.25	.8612E-05	.4503E-05	.2029E-05	.7498E-06	.2110E-06	.4022E-07
6132	790.39	.1109E-04	.5935E-05	.2748E-05	.1050E-05	.3082E-06	.6202E-07
6130	790.52	.1407E-04	.7694E-05	.3657E-05	.1442E-05	.4402E-06	.9321E-07
12245	790.63	.4669E-05	.1535E-05	.3964E-06	.7419E-07	.8918E-08	.5698E-09
6128	790.64	.1760E-04	.9815E-05	.4779E-05	.1941E-05	.6149E-06	.1365E-06
6126	790.76	.2167E-04	.1232E-04	.6134E-05	.2562E-05	.8399E-06	.1949E-06
6124	790.86	.2630E-04	.1521E-04	.7735E-05	.3314E-05	.1122E-05	.2713E-06
8268	790.87	.1314E-05	.3695E-06	.7909E-07	.1177E-07	.1062E-08	.4690E-10
6122	790.96	.3145E-04	.1848E-04	.9582E-05	.4203E-05	.1465E-05	.3680E-06
6120	791.05	.3705E-04	.2210E-04	.1166E-04	.5226E-05	.1872E-05	.4867E-06
6118	791.13	.4303E-04	.2601E-04	.1394E-04	.6373E-05	.2339E-05	.6277E-06
6116	791.20	.4925E-04	.3013E-04	.1639E-04	.7622E-05	.2860E-05	.7893E-06
6114	791.26	.5558E-04	.3436E-04	.1893E-04	.8943E-05	.3421E-05	.9681E-06
6112	791.32	.6188E-04	.3861E-04	.2151E-04	.1030E-04	.4007E-05	.1159E-05
12246	791.32	.4025E-05	.1303E-05	.3301E-06	.6037E-07	.7051E-08	.4340E-09
6110	791.37	.6802E-04	.4278E-04	.2405E-04	.1165E-04	.4599E-05	.1355E-05
61 8	791.41	.7393E-04	.4680E-04	.2652E-04	.1297E-04	.5181E-05	.1550E-05
61 6	791.44	.7976E-04	.5075E-04	.2894E-04	.1426E-04	.5749E-05	.1741E-05
61 4	791.46	.8633E-04	.5513E-04	.3158E-04	.1565E-04	.6352E-05	.1941E-05
61 2	791.47	.9848E-04	.6304E-04	.3621E-04	.1801E-04	.7342E-05	.2256E-05
8269	791.51	.1030E-05	.2829E-06	.5885E-07	.8457E-08	.7308E-09	.3054E-10
12247	792.01	.3455E-05	.1101E-05	.2735E-06	.4886E-07	.5540E-08	.3283E-09
62 0	792.26	.7976E-04	.5111E-04	.2940E-04	.1464E-04	.5980E-05	.1842E-05
12248	792.69	.2954E-05	.9254E-06	.2255E-06	.3932E-07	.4326E-08	.2467E-09
12249	793.37	.2514E-05	.7745E-06	.1850E-06	.3147E-07	.3357E-08	.1840E-09
62 2	793.82	.1581E-03	.1012E-03	.5812E-04	.2890E-04	.1178E-04	.3620E-05
12250	794.05	.2130E-05	.6453E-06	.1510E-06	.2504E-07	.2590E-08	.1363E-09
12251	794.73	.1798E-05	.5351E-06	.1226E-06	.1982E-07	.1985E-08	.1003E-09
62 4	795.37	.2314E-03	.1478E-03	.8465E-04	.4194E-04	.1702E-04	.5201E-05

TABLE XVI (Continued)

BAND CODE	WAVE NUMBER	INTENSITY					
		T=300K	T=275K	T=250K	T=225K	T=200K	T=175K
12252	795.40	.1511E-05	.4418E-06	.9908E-07	.1561E-07	.1513E-08	.7327E-10
12253	796.08	.1264E-05	.3630E-06	.7967E-07	.1222E-07	.1146E-08	.5317E-10
12254	796.75	.1054E-05	.2970E-06	.6374E-07	.9516E-08	.8624E-09	.3832E-10
62 6	796.91	.2967E-03	.1887E-03	.1076E-03	.5302E-04	.2138E-04	.6472E-05
13037	797.76	.1033E-05	.3924E-06	.1205E-06	.2787E-07	.4366E-08	.3921E-09
62 8	798.44	.3513E-03	.2223E-03	.1260E-03	.6159E-04	.2460E-04	.7359E-05
13036	798.62	.1154E-05	.4439E-06	.1384E-06	.3261E-07	.5229E-08	.4838E-09
13035	799.48	.1283E-05	.4997E-06	.1581E-06	.3793E-07	.6221E-08	.5925E-09
6210	799.97	.3933E-03	.2473E-03	.1390E-03	.6733E-04	.2657E-04	.7828E-05
13034	800.34	.1420E-05	.5596E-06	.1796E-06	.4386E-07	.7352E-08	.7204E-09
13033	801.19	.1564E-05	.6235E-06	.2030E-06	.5041E-07	.8632E-08	.8692E-09
6212	801.49	.4217E-03	.2630E-03	.1465E-03	.7013E-04	.2728E-04	.7889E-05
13032	802.04	.1714E-05	.6911E-06	.2280E-06	.5757E-07	.1007E-07	.1041E-08
13031	802.89	.1869E-05	.7620E-06	.2547E-06	.6536E-07	.1166E-07	.1237E-08
6214	802.99	.4362E-03	.2696E-03	.1485E-03	.7014E-04	.2682E-04	.7590E-05
13030	803.74	.2028E-05	.8356E-06	.2829E-06	.7373E-07	.1341E-07	.1459E-08
6216	804.49	.4377E-03	.2676E-03	.1455E-03	.6767E-04	.2538E-04	.7005E-05
13029	804.58	.2189E-05	.9114E-06	.3124E-06	.8264E-07	.1532E-07	.1707E-08
13028	805.42	.2351E-05	.9885E-06	.3429E-06	.9204E-07	.1737E-07	.1982E-08
6218	805.99	.4272E-03	.2581E-03	.1383E-03	.6321E-04	.2319E-04	.6223E-05
13027	806.26	.2511E-05	.1066E-05	.3740E-06	.1018E-06	.1956E-07	.2283E-08
13026	807.10	.2668E-05	.1143E-05	.4055E-06	.1119E-06	.2186E-07	.2607E-08
6220	807.47	.4066E-03	.2424E-03	.1279E-03	.5729E-04	.2051E-04	.5333E-05
13025	807.94	.2818E-05	.1218E-05	.4368E-06	.1221E-06	.2425E-07	.2954E-08
13024	808.77	.2960E-05	.1290E-05	.4675E-06	.1323E-06	.2669E-07	.3318E-08
6222	808.94	.3781E-03	.2221E-03	.1151E-03	.5047E-04	.1759E-04	.4417E-05
13023	809.60	.3090E-05	.1358E-05	.4969E-06	.1424E-06	.2915E-07	.3694E-08
6224	810.41	.3439E-03	.1988E-03	.1010E-03	.4328E-04	.1464E-04	.3541E-05
13022	810.44	.3206E-05	.1420E-05	.5246E-06	.1520E-06	.3158E-07	.4077E-08
13021	811.26	.3305E-05	.1475E-05	.5498E-06	.1611E-06	.3393E-07	.4459E-08
6226	811.87	.3063E-03	.1740E-03	.8661E-04	.3616E-04	.1185E-04	.2750E-05
13020	812.09	.3384E-05	.1521E-05	.5718E-06	.1693E-06	.3614E-07	.4830E-08
13019	812.91	.3440E-05	.1557E-05	.5901E-06	.1765E-06	.3815E-07	.5181E-08
6228	813.32	.2674E-03	.1491E-03	.7254E-04	.2945E-04	.9327E-05	.2070E-05
13018	813.74	.3471E-05	.1581E-05	.6040E-06	.1824E-06	.3989E-07	.5501E-08
13017	814.56	.3474E-05	.1592E-05	.6127E-06	.1867E-06	.4129E-07	.5779E-08
6230	814.76	.2289E-03	.1250E-03	.5940E-04	.2341E-04	.7145E-05	.1512E-05
13016	815.37	.3447E-05	.1589E-05	.6158E-06	.1892E-06	.4230E-07	.6002E-08
13015	816.19	.3388E-05	.1571E-05	.6126E-06	.1898E-06	.4285E-07	.6158E-08
6232	816.20	.1922E-03	.1028E-03	.4758E-04	.1817E-04	.5330E-05	.1072E-05
13014	817.00	.3296E-05	.1536E-05	.6026E-06	.1881E-06	.4287E-07	.6237E-08
6234	817.62	.1585E-03	.8283E-04	.3730E-04	.1378E-04	.3874E-05	.7385E-06
13013	817.81	.3169E-05	.1484E-05	.5856E-06	.1841E-06	.4233E-07	.6227E-08
13012	818.62	.3008E-05	.1414E-05	.5612E-06	.1776E-06	.4116E-07	.6119E-08
6236	819.04	.1283E-03	.6546E-04	.2863E-04	.1020E-04	.2745E-05	.4941E-06

TABLE XVI (Continued)

BAND	CCCE	WAVE NUMBER	INTENSITY				
			T=300K	T=275K	T=250K	T=225K	T=200K
13011	819.43	.2812E-05	.1328E-05	.5294E-06	.1685E-06	.3936E-07	.5908E-08
13010	820.24	.2582E-05	.1224E-05	.4901E-06	.1569E-06	.3689E-07	.5587E-08
6238	820.45	.1021E-03	.5075E-04	.2152E-04	.7387E-05	.1896E-05	.3212E-06
130 9	821.04	.2319E-05	.1103E-05	.4436E-06	.1427E-06	.3377E-07	.5155E-08
130 8	821.84	.2026E-05	.9666E-06	.3902E-06	.1261E-06	.3001E-07	.4614E-08
6240	821.85	.7979E-04	.3860E-04	.1585E-04	.5228E-05	.1277E-05	.2030E-06
130 7	822.64	.1707E-05	.8163E-06	.3306E-06	.1072E-06	.2565E-07	.3970E-08
6242	823.25	.6129E-04	.2882E-04	.1144E-04	.3619E-05	.8390E-06	.1248E-06
130 6	823.44	.1364E-05	.6541E-06	.2656E-06	.8648E-07	.2078E-07	.3234E-08
130 5	824.23	.1006E-05	.4832E-06	.1967E-06	.6424E-07	.1549E-07	.2423E-08
6244	824.63	.4628E-04	.2112E-04	.8088E-05	.2450E-05	.5379E-06	.7457E-07
6246	826.01	.3436E-04	.1520E-04	.5607E-05	.1623E-05	.3365E-06	.4335E-07
13143	826.23	.1097E-05	.3831E-06	.1064E-06	.2177E-07	.2927E-08	.2160E-09
13142	826.32	.1260E-05	.4466E-06	.1263E-06	.2640E-07	.3646E-08	.2786E-09
13141	826.41	.1441E-05	.5183E-06	.1491E-06	.3183E-07	.4514E-08	.3567E-09
13140	826.49	.1641E-05	.5986E-06	.1751E-06	.3816E-07	.5553E-08	.4536E-09
13139	826.57	.1861E-05	.6881E-06	.2046E-06	.4550E-07	.6789E-08	.5728E-09
13138	826.65	.2101E-05	.7872E-06	.2378E-06	.5394E-07	.8247E-08	.7181E-09
13137	826.73	.2361E-05	.8963E-06	.2751E-06	.6358E-07	.9956E-08	.8939E-09
13136	826.81	.2642E-05	.1016E-05	.3165E-06	.7452E-07	.1194E-07	.1105E-08
13135	826.88	.2942E-05	.1145E-05	.3622E-06	.8684E-07	.1423E-07	.1356E-08
13134	826.95	.3262E-05	.1285E-05	.4122E-06	.1006E-06	.1686E-07	.1651E-08
13133	827.02	.3600E-05	.1435E-05	.4668E-06	.1159E-06	.1983E-07	.1997E-08
13132	827.09	.3955E-05	.1594E-05	.5256E-06	.1327E-06	.2318E-07	.2397E-08
13131	827.16	.4324E-05	.1762E-05	.5887E-06	.1510E-06	.2692E-07	.2856E-08
13130	827.22	.4705E-05	.1937E-05	.6556E-06	.1708E-06	.3105E-07	.3378E-08
13129	827.28	.5094E-05	.2120E-05	.7262E-06	.1920E-06	.3558E-07	.3965E-08
13128	827.34	.5489E-05	.2306E-05	.7997E-06	.2146E-06	.4048E-07	.4619E-08
6248	827.37	.2508E-04	.1074E-04	.3811E-05	.1051E-05	.2054E-06	.2451E-07
13127	827.40	.5884E-05	.2497E-05	.8756E-06	.2383E-06	.4575E-07	.5339E-08
13126	827.46	.6276E-05	.2688E-05	.9531E-06	.2629E-06	.5134E-07	.6123E-08
13125	827.51	.6660E-05	.2877E-05	.1031E-05	.2882E-06	.5721E-07	.6968E-08
13124	827.56	.7029E-05	.3063E-05	.1109E-05	.3139E-06	.6329E-07	.7865E-08
13123	827.61	.7378E-05	.3241E-05	.1185E-05	.3395E-06	.6950E-07	.8806E-08
13122	827.66	.7701E-05	.3410E-05	.1259E-05	.3648E-06	.7575E-07	.9778E-08
13121	827.70	.7991E-05	.3565E-05	.1328E-05	.3891E-06	.8194E-07	.1076E-07
13120	827.75	.8244E-05	.3704E-05	.1392E-05	.4121E-06	.8793E-07	.1175E-07
13119	827.79	.8451E-05	.3824E-05	.1449E-05	.4332E-06	.9360E-07	.1271E-07
13118	827.83	.8607E-05	.3920E-05	.1497E-05	.4519E-06	.9880E-07	.1363E-07
13117	827.86	.8708E-05	.3990E-05	.1535E-05	.4676E-06	.1034E-06	.1447E-07
13116	827.90	.8746E-05	.4031E-05	.1561E-05	.4798E-06	.1072E-06	.1521E-07
13115	827.93	.8718E-05	.4040E-05	.1575E-05	.4879E-06	.1101E-06	.1583E-07
13114	827.96	.8619E-05	.4015E-05	.1575E-05	.4916E-06	.1120E-06	.1629E-07
13113	827.99	.8447E-05	.3954E-05	.1560E-05	.4903E-06	.1127E-06	.1658E-07
13112	828.02	.8199E-05	.3854E-05	.1529E-05	.4837E-06	.1121E-06	.1667E-07

TABLE XVI (Continued)

BAND CODE	WAVE NUMBER	INTENSITY					
		T=300K	T=275K	T=250K	T=225K	T=200K	T=175K
13111	828.04	.7873E-05	.3717E-05	.1482E-05	.4715E-06	.1101E-06	.1653E-07
13110	828.07	.7469E-05	.3539E-05	.1417E-05	.4536E-06	.1067E-06	.1615E-07
131 9	828.09	.6989E-05	.3323E-05	.1336E-05	.4298E-06	.1017E-06	.1552E-07
131 8	828.11	.6432E-05	.3068E-05	.1238E-05	.4000E-06	.9519E-07	.1464E-07
131 7	828.12	.5801E-05	.2774E-05	.1123E-05	.3644E-06	.8716E-07	.1349E-07
131 6	828.14	.5098E-05	.2444E-05	.9926E-06	.3231E-06	.7762E-07	.1208E-07
131 5	828.15	.4324E-05	.2077E-05	.8457E-06	.2761E-06	.6658E-07	.1041E-07
131 4	828.16	.3477E-05	.1673E-05	.6825E-06	.2234E-06	.5404E-07	.8485E-08
131 3	828.17	.2542E-05	.1225E-05	.5005E-06	.1641E-06	.3980E-07	.6271E-08
131 2	828.17	.1469E-05	.7086E-06	.2899E-06	.9522E-07	.2313E-07	.3653E-08
6250	828.73	.1801E-04	.7456E-05	.2539E-05	.6668E-06	.1224E-06	.1349E-07
132 1	829.74	.2669E-05	.1288E-05	.5276E-06	.1735E-06	.4219E-07	.6674E-08
6252	830.09	.1272E-04	.5083E-05	.1659E-05	.4138E-06	.7123E-07	.7223E-08
132 2	830.52	.2947E-05	.1421E-05	.5815E-06	.1910E-06	.4640E-07	.7328E-08
132 3	831.30	.3281E-05	.1581E-05	.6460E-06	.2119E-06	.5137E-07	.8093E-08
6254	831.43	.8834E-05	.3404E-05	.1064E-05	.2513E-06	.4046E-07	.3764E-08
132 4	832.07	.3624E-05	.1744E-05	.7112E-06	.2328E-06	.5631E-07	.8842E-08
6256	832.77	.6037E-05	.2240E-05	.6687E-06	.1494E-06	.2244E-07	.1909E-08
132 5	832.85	.3955E-05	.1900E-05	.7733E-06	.2525E-06	.6088E-07	.9521E-08
132 6	833.62	.4266E-05	.2045E-05	.8303E-06	.2702E-06	.6491E-07	.1010E-07
6258	834.09	.4060E-05	.1448E-05	.4123E-06	.8699E-07	.1215E-07	.9423E-09
132 7	834.39	.4549E-05	.2175E-05	.8807E-06	.2856E-06	.6831E-07	.1057E-07
132 8	835.15	.4800E-05	.2289E-05	.9237E-06	.2984E-06	.7100E-07	.1092E-07
6260	835.41	.2686E-05	.9198E-06	.2494E-06	.4958E-07	.6428E-08	.4528E-09
132 9	835.92	.5016E-05	.2385E-05	.9587E-06	.3083E-06	.7295E-07	.1114E-07
13210	836.68	.5195E-05	.2461E-05	.9855E-06	.3153E-06	.7414E-07	.1123E-07
6262	836.72	.1749E-05	.5741E-06	.1480E-06	.2766E-07	.3321E-08	.2118E-09
13211	837.44	.5336E-05	.2518E-05	.1004E-05	.3194E-06	.7458E-07	.1119E-07
6264	838.02	.1120E-05	.3522E-06	.8621E-07	.1511E-07	.1675E-08	.9648E-10
13212	838.20	.5437E-05	.2556E-05	.1014E-05	.3206E-06	.7430E-07	.1104E-07
13213	838.95	.5500E-05	.2574E-05	.1015E-05	.3190E-06	.7333E-07	.1079E-07
7214	839.71	.5524E-05	.2573E-05	.1009E-05	.3148E-06	.7174E-07	.1043E-07
715	840.46	.5512E-05	.2554E-05	.9954E-06	.3083E-06	.6958E-07	.9997E-08
7216	841.21	.5464E-05	.2518E-05	.9750E-06	.2995E-06	.6693E-07	.9493E-08
13217	841.96	.5383E-05	.2466E-05	.9484E-06	.2889E-06	.6386E-07	.8935E-08
13218	842.70	.5273E-05	.2400E-05	.9163E-06	.2766E-06	.6046E-07	.8337E-08
13219	843.45	.5134E-05	.2322E-05	.8796E-06	.2630E-06	.5680E-07	.7713E-08
13220	844.19	.4972E-05	.2233E-05	.8390E-06	.2483E-06	.5297E-07	.7077E-08
13221	844.93	.4788E-05	.2135E-05	.7953E-06	.2329E-06	.4903E-07	.6441E-08
13222	845.67	.4587E-05	.2030E-05	.7493E-06	.2170E-06	.4506E-07	.5816E-08
13223	846.40	.4371E-05	.1919E-05	.7017E-06	.2009E-06	.4112E-07	.5209E-08
13224	847.13	.4144E-05	.1805E-05	.6534E-06	.1848E-06	.3726E-07	.4630E-08
13225	847.87	.3909E-05	.1688E-05	.6049E-06	.1690E-06	.3353E-07	.4083E-08
13226	848.59	.3670E-05	.1571E-05	.5568E-06	.1535E-06	.2997E-07	.3574E-08
13227	849.32	.3428E-05	.1454E-05	.5096E-06	.1386E-06	.2661E-07	.3105E-08

TABLE XVI (Concluded)

BAND CODE	WAVE NUMBER	INTENSITY					
		T=300K	T=275K	T=250K	T=225K	T=200K	T=175K
13228	850.05	.3187E-05	.1339E-05	.4639E-06	.1244E-06	.2347E-07	.2677E-08
13229	850.77	.2949E-05	.1226E-05	.4199E-06	.1110E-06	.2056E-07	.2291E-08
13230	851.49	.2716E-05	.1118E-05	.3781E-06	.9846E-07	.1789E-07	.1946E-08
13231	852.21	.2490E-05	.1014E-05	.3386E-06	.8681E-07	.1547E-07	.1641E-08
13232	852.93	.2272E-05	.9152E-06	.3016E-06	.7610E-07	.1329E-07	.1374E-08
13233	853.64	.2064E-05	.8220E-06	.2673E-06	.6632E-07	.1135E-07	.1142E-08
13234	854.36	.1866E-05	.7348E-06	.2356E-06	.5747E-07	.9627E-08	.9427E-09
13235	855.07	.1680E-05	.6537E-06	.2066E-06	.4952E-07	.8114E-08	.7725E-09
13236	855.77	.1506E-05	.5787E-06	.1802E-06	.4242E-07	.6796E-08	.6285E-09
13237	856.48	.1344E-05	.5100E-06	.1564E-06	.3614E-07	.5657E-08	.5077E-09

TABLE XVII

COMPARISON BETWEEN COMPUTED LINE POSITIONS AND
INTENSITIES AND MADDEN'S EXPERIMENTAL VALUES
(T = 300°K)

Band	Branch	J	Madden's Values		Est. Error, %	Computed	
			$\nu(\text{cm}^{-1})$	$S_{J''}$ ($\text{cm}^{-2} \text{ atm}^{-1}$)		$\nu(\text{cm}^{-1})$	$S_{J''}$ ($\text{cm}^{-2} \text{ atm}^{-1}$)
1	P	4	664.29	1.00	6	664.3	0.992
4	P	8	661.52	0.106	15	661.5	0.121
1	P	8	661.18	2.24	6	661.2	2.088
4	P	9	660.81	0.140	15	660.7	0.138
4	P	34	641.65	0.105	20	641.6	0.0846
4	P	35	641.65*	0.095	20	640.9	0.0765
1	P	50	629.46	0.143	7	629.4	0.132
2	R	13	628.91	0.0750	7	629.1	0.0707
1	P	52	627.99	0.101	7	627.9	0.0932
2	R	11	627.38	0.0695	7	627.5	0.0655
1	P	54	626.51	0.0704	7	626.4	0.0647
2	R	9	625.83	0.0613	7	625.9	0.0578
1	P	56	625.05	0.0481	7	625.0	0.0441
2	P	7	612.56	0.0565	3	612.6	0.0468
2	P	9	611.00	0.0627	3	611.0	0.0562
2	P	11	609.42	0.0682	3	609.5	0.0633
2	P	13	607.84	0.0712	3	607.9	0.0679
2	P	15	606.27	0.0715	3	606.4	0.0701
2	P	17	604.70	0.0692	3	604.8	0.0699
2	P	19	603.13	0.0656	3	603.3	0.0678
2	P	21	601.56	0.0614	3	601.8	0.0641
2	P	23	599.98	0.0568	3	600.2	0.0591
2	P	25	598.40	0.0522	3	598.7	0.0533

*Obvious misprint in Madden's paper.

REFERENCES

- Aller, L. H., 1953: Astrophysics, the atmospheres of the sun and stars. Ronald Press Company, New York, 412 pp.
- Benedict, W. S., 1962: Private communication.
- _____, R. Herman, G. E. Moore and S. Silverman, 1956: The strengths, widths and shapes of infrared lines. I. General considerations. Can. J. Phys., 34, 830-849.
- Breene, R. G., 1955: The shift and shape of spectral lines. Geophysical Res. Papers, No. 41, G.R.D., Air Force Cambridge Res. Labs.
- Burch, D. E., D. A. Gryvnak and D. Williams, 1962a: Total absorptance of carbon dioxide in the infrared. Appl Optics, 1, 759-765.
- _____, 1962b: Absorption by carbon dioxide. Infrared absorption by carbon dioxide, water vapor and minor atmospheric constituents. G.R.D. Research Report, AFCRL-62-698, Air Force Cambridge Res. Labs.
- Busbridge, I. W., 1960: The mathematics of radiative transfer. Cambridge Univ. Press, 143 pp.
- Callendar, G. S., 1941: Infrared absorption by carbon dioxide, with special reference to atmospheric radiation. Q.J.R.M.S., 67, 263-274.
- Chamberlain, J. W., 1962: Upper atmospheres of the planets. Ap. J., 136, 582-593.
- Chandrasekhar, S., 1960: Radiative transfer. Dover, New York, 393 pp.
- Curtis, A. R., 1952: Discussion of Goody's, "A statistical model for water-vapour absorption." Q.J.R.M.S. 78, 638-640.
- _____ and R. M. Goody, 1954: Spectral line shape and its effect on atmospheric transmissions. Q.J.R.M.S., 80, 58-67.
- _____ and R. M. Goody, 1956: Thermal radiation in the upper atmosphere. Proc. Roy. Soc., 236A, 193-206.
- Dennison, D. M., 1931: The infrared spectra of polyatomic molecules. Ref. Mod. Phys., 3, 280-345.

Elsasser, W. M., 1942: Heat transfer by infrared radiation in the atmosphere. Harvard Meteorological Studies, No. 6.

Faddeeva, V. N., and N. M. Terentev, 1961: Tables of the probability integral for complex argument. Pergamon Press, London, 280 pp.

Glueckauf, E., 1951: The composition of atmospheric air. Compendium of meteorology, ed. T. F. Malone, American Meteorological Society, 3-10.

Godfrey, G. H., and W. L. Price, 1937: Thermal radiation and absorption in the upper atmosphere. Proc. Roy. Soc., 163A, 228-249.

Godson, W. L., 1953: The evaluation of infrared radiative fluxes due to atmospheric water vapour. Q.J.R.M.S., 79, 367-379.

_____, 1955: The computation of infrared transmission by atmospheric water vapour. J. Met., 12, 272-284.

Gold, E., 1909: The isothermal layer of the atmosphere and atmospheric radiation. Proc. Roy. Soc., 82A, 43-70.

Goody, R. M., 1952: A statistical model for water-vapour absorption. Q.J.R.M.S., 78, 165-169.

Gowan, E. H., 1947a: Ozonosphere temperatures under radiative equilibrium. Proc. Roy. Soc., 190A, 219-226.

_____, 1947b: Night cooling of the ozonosphere. Proc. Roy. Soc., 190A, 227-231.

Harris, D. L., 1948: On the line-absorption coefficient due to the Doppler effect and damping. App. J., 108, 112-115.

Hastings, C., 1955: Approximations for digital computers. Princeton University Press, 201 pp.

Herzberg, G., 1945: Infrared and Raman spectra of polyatomic molecules. Van Nostrand, New York, 632 pp.

Herzfeld, K. F., and T. A. Litovitz, 1959: Absorption and dispersion of ultrasonic waves. Academic Press, Inc., New York, 535 pp.

Hildebrand, F. B., 1956: Introduction to numerical analysis. McGraw-Hill, New York, 511 pp.

Hitschfeld, W., and J. T. Houghton, 1961: Radiative transfer in the lower stratosphere due to the 9.6 micronband of ozone. *Q.J.R.M.S.*, 87, 562-577.

Humphreys, W. J., 1909: Vertical temperature gradient of the atmosphere, especially in the region of the upper inversion. *Ap. J.*, 29, 14-32.

Jones, L. M., J. W. Peterson, E. J. Schaefer and H. F. Schulte, 1959: Upper-air density and temperature: some variations and an abrupt warming in the mesosphere. *J. Geophys. Res.*, 64, 2331-2340.

Kaplan, L. D., 1959: A method for calculation of infrared flux for use in numerical models of atmospheric motion. *The atmosphere and sea in motion*, ed. B. Bolin. Oxford University Press, 509 pp.

_____ and D. F. Eggers, 1956: Intensity and line width of the 15-micron CO₂ band, determined by a curve of growth method. *J. Chem. Phys.*, 25, 876-883.

Kellogg, W. W., 1961: Warming of the polar mesosphere and lower ionosphere in the winter. *J. Met.*, 18, 373-381.

Kleman, B., and E. Lindholm, 1945: The broadening of Na lines by argon. *Ark. Mat. Astron. och Fys.*, 32B, No. 10.

Kindrat'yev, K. Ya., 1963: On the possibility of the direct measurement of radiative divergence. *Problems of the physics of the atmosphere*, Collection 1, Leningrad State University, NASA Technical Translation, TTF-184, 1-25.

Kopal, Z., 1961: Numerical analysis. Wiley, New York, 594 pp.

Lambert, J. D., 1962: Relaxation in gases. *Atomic and molecular processes*, ed., D. R. Bates. Academic Press, Inc., New York, 904 pp.

Lindholm, E., 1945: Pressure broadening of spectral lines. *Ark. Mat. Astron. och. Fys.* 32A, No. 17.

Madden, R. P. 1961: A high resolution study of CO₂ absorption spectra between 15- and 18-microns. *J. Chem. Phys.*, 35, 2083-2097.

Martin, P. E., and E. F. Barker, 1932: The infrared absorption spectrum of CO₂. *Phys. Rev.*, 41, 291-303,

Matossi, F., R. Mayer and E. Rauscher, 1946: Über die Gesamtaborption in linienreichen Spektren. *Naturwiss.*, 23, 219-220.

Matossi, F., R. Mayer and E. Rauscher, 1949: On total absorption in spectra with overlapping lines. *Phys. Rev.*, 76, 760-764.

_____, and E. Rauscher, 1949: Zur Druckabhängigkeit der Gesamtabsorption in ultraroten Bandenspektren. *Zeit. für Phys.*, 125, 418-422.

Milne, E. A., 1930: Thermodynamics of the stars. *Handbuch der Astrophys.*, 3, 1st half, 65-255.

Mitchell, A.C.G., and M. W. Zemansky, 1934: Resonance radiation and excited atoms. Cambridge Univ. Press, 338 pp.

Murgatroyd, R. J., and R. M. Goody, 1958: Sources and sinks of radiative energy from 30 to 90 km. *Q.J.R.M.S.*, 84, 225-234.

Murgatroyd, R. J., and F. Singleton, 1961: Possible meridional circulations in the stratosphere and mesosphere. *Q.J.R.M.S.*, 87, 125-135.

Newell, R. E., 1963: Preliminary study of quasi-horizontal eddy fluxes from meteorological rocket network data. *J. Atmos. Sci.*, 20, 213-225.

Nordberg, W., and W. Smith, 1963: Rocket measurements of the structure of the stratosphere and mesosphere. Proceedings of the international symposium on stratospheric and mesospheric circulation. *Abhandlungen Institut für Meteorologie und Geophysik der Freien Universität Berlin*, 26, 391-408.

Ohring, G., 1958: The radiation budget of the stratosphere. *J. Met.*, 15, 440-451.

Pagurova, V. J., 1961: Tables of the exponential integral. Pergamon Press, New York, 151 pp.

Penner, S. S., 1959: Quantitative molecular spectroscopy and gas emissivities. Addison-Wesley, Reading, Mass., 587 pp.

Plass, G. N., 1954: Spectral line shape and its effect on atmospheric transmissions. *Q.J.R.M.S.*, 80, 452-454.

_____, 1956a: The influence of the 9.6 micron ozone band on the atmospheric infrared cooling rate. *Q.J.R.M.S.*, 82, 30-44.

_____, 1956b: The influence of the 15 micron carbon dioxide band on the atmospheric infrared cooling rate. *Q.J.R.M.S.*, 82, 310-324.

Plass, G. N., 1958: Models for spectral band absorption. J. Opt. Soc. Am., 48, 690-703.

_____, and D. Warner, 1952: Influence of line shift and asymmetry of spectral lines on atmospheric heat transfer. J. Met., 9, 333-339.

_____, and D. I. Fivel, 1953: Influence of Doppler effect and damping on line-absorption coefficient and atmospheric radiation transfer. Ap. J., 117, 225-233.

Randall, H. M., D. M. Dennison, N. Ginsberg and L. R. Weber, 1937: The far infrared spectrum of water vapor. Phys. Rev., 52, 160-174.

Roberts, O.F.T., 1930: On radiative diffusion in the atmosphere. Proc. Roy. Soc., Edinburgh, 50, 225-242.

Rosser, J. B., 1950: Notes on zeroes of the Hermite polynomials and weights for Gauss mechanical quadrature formula. Proc. Am. Math. Soc., 1, 388-389.

Schwarz, R. N., Z. I. Slawsky and K. F. Herzfeld, 1952: Calculation of vibrational relaxation times in gases. J. Chem., Phys., 20, 1591-1599.

_____, and K. F. Herzfeld, 1954: Vibrational relaxation times in gases (three-dimensional treatment). J. Chem. Phys., 22, 767-773.

Stroud, W. G., W. Nordberg, W. R. Bandeen, F. L. Bartman and P. Titus, 1960: Rocket grenade measurements of temperature and winds in the mesosphere over Churchill, Canada. J. Geophy. Res., 65, 2307-2323.

Stull, V. P., P. J. Wyatt and G. N. Plass, 1961: The infrared absorption of carbon dioxide. Aeronutronic Division, Ford Motor Company, Report No. U-1505.

Sobolev, V. V., 1963: A treatise on radiative transfer. Van Nostrand New York, 319 pp.

Walshaw, C. D., and C. D. Rodgers, 1963: The effect of the Curtis-Godson approximation on the accuracy of radiative heating-rate calculations. Q.J.R.M.S., 89, 122-130.

Witteman, W. J., 1962: Vibrational relaxation in carbon dioxide, II, J. Chem. Phys., 37, 655-661.

Wyatt, P. J., V. R. Stull and G. N. Plass, 1962: Quasi-random model of band absorption. J. Opt. Soc. Am., 52, 1209-1217.

Yamamoto, G., and T. Sasamori, 1958: Calculations of the absorption of the 15 micron carbon dioxide band. Science Reports, Tôhoku Univ., 5th Series (Geophysics), 10, 37-57.

_____, 1961: Further studies on the absorption by the 15 micron carbon dioxide bands. Science Reports, Tôhoku Univ., 5th Series (Geophysics), 13, 1-19.

Young, C., and E. S. Epstein, 1962: Atomic oxygen in the polar winter mesosphere, J. Met., 19, 435-443.